University of Sheffield

S W Gaines

Tails of twists and turns:
Using zebrafish to unravel neutrophil chromatin remodelling

A thesis submitted in partial fulfilment of the requirements for the degree of Doctor of Philosophy

Department of Infection, Immunity and Cardiovascular Disease

2022

Tails of twists and turns:
Using zebrafish to unravel neutrophil chromatin remodelling

Stuart William Gaines

Supervised by Prof. Stephen Renshaw, Ms. Catherine Loynes, Dr. Helen Wright, and Prof. Steven Edwards

A thesis submitted in partial fulfilment of the requirements for the degree of Doctor of Philosophy

Department of Infection, Immunity and Cardiovascular Disease

December 2022

Acknowledgements

First, I would like to acknowledge my amazing supervisory team. I could not have asked for a more supportive and kinder group of bosses. Thank you to Steve R for providing constant knowledge and guidance throughout the project and for putting up with my regular crises of confidence over the past four years. Cat, thank you for constantly being there to help in the lab, teaching me all the basics and most of the complicated stuff too, putting up with annoying questions, requests to proof-read presentations, funding applications and posters, and most importantly always being the first to suggest a pint when things all go wrong (or go right!). To Helen and Steve E in Liverpool, thank you for your input on all the work and for adding a human spin to all our fishy thoughts. An especially big thank you to Helen and her lab for being so welcoming during my visit in October 2022. I will never forget the warm working environment you all created and future employers have some very large boots to fill.

Thank you to everyone in D31 past and present – especially Dave Drew for all your technical support – so many memories and friendships have been formed over the years from long working days, Friday pub trips, Saturday morning climbing trips, Christmas parties and beyond. Also, thank you to everyone else in the Bateson Centre, IICD, the BSU Aquarium, and all the core facilities that helped to make all this work possible.

Thank you to the MRC, Versus Arthritis and CIMA for funding my work and to the CIMA Centre Managers – especially Rachael Wright. Also, thank you to previous supervisors from Durham and Edinburgh and the skills (and references) you provided.

Thank you to all the close friends who have supported and shared in my PhD experiences from Norfolk, Durham, Edinburgh, Sheffield, and further afield. Your constant, and often drunken advice will always be important especially those of you who have battled through your own PhDs simultaneously.

A massive thank you to Holly Rutherford for being the best partner possible, for putting up with me and my PhD while managing her own PhD, a global pandemic, her own wacky family,

and plenty of things in between. I love you and will always treasure the support you've provided, even if it was sometimes through gritted teeth.

Finally, thank you to all my family who have supported me through the past 30 years to get here. Especially to my Mum and Dad, who may not have made it to the end of this journey but have given me the qualities to complete it.

Summary

Neutrophils are the most abundant leucocytes and the primary effector cells in innate inflammation. Because neutrophils play an important role in returning the body to homeostasis following immune challenge, neutrophil dysfunction is linked to chronic inflammatory diseases and age-related immune decline. Understanding mechanisms that control neutrophils can therefore help develop therapies for inflammatory dysfunction. The role of epigenetic modifications and specifically chromatin remodelling in neutrophils is only beginning to be explored. Recent work has shown that neutrophil response is regulated by chromatin changes, and further work has shown neutrophil function alters with ageing. We therefore, hypothesised that changes to chromatin conformation drive neutrophil dysfunction in ageing and disease. I aimed to use a zebrafish model to identify chromatin remodelling enzymes responsible for chromatin conformational changes regulating neutrophil function. Zebrafish provide an excellent model for neutrophil function as they can be easily chemically and genetically modified, have numerous transgenic reporters for immune function, and transparent larvae can be easily imaged. Here, the TLR8 agonist R848 – previously shown *in vitro* to exert its function on human neutrophils by chromatin remodelling at the *il6* locus – was first shown to manipulate neutrophil function by promoting inflammation resolution in a tailfin injury model. R848 also promoted expression of the pro-inflammatory transcription factor NF-κB and cytokine TNFα. This provided evidence that zebrafish neutrophils could be manipulated by similar pathways to human neutrophils. CRISPR/Cas9 was then used to knockdown chromatin remodelling enzymes *kdm6b* and *ezh2*. In the tailfin injury model, knockdown of *kdm6b* resulted in a delay to inflammation resolution, while knockdown of *ezh2* increased recruitment of neutrophils and delayed inflammation resolution. RNA sequencing was then performed following *kdm6b* knockdown. In the injury model, *kdm6b* knockdown showed a reduction in pro-inflammatory pathways and specifically reduction in expression of *il1b* and *tnf.* These data presented in this thesis suggest that Kdm6b plays a role in neutrophil response to injury and provides a target for exploration in neutrophil samples from aged individuals and chronic inflammatory disease patients for potential drivers of neutrophil dysfunction.

Table of Contents

Acknowledgements **2**

Summary **4**

Table of Contents **5**

Table of Figures **16**

Chapter 1: Introduction **20**

1.1. The immune system **20**

1.1.1. The Inflammatory response **20**

1.1.1.a. Innate immunity *21*

1.1.1.b. A brief introduction to the neutrophil *22*

1.1.1.c. Adaptive immunity *22*

1.1.1.c.i. Major histocompatibility complexes 23

1.1.1.c.ii. T lymphocytes 23

1.1.1.c.iii. B lymphocytes and antibody production 24

1.1.2. Acute vs. chronic inflammation **25**

1.2. The Neutrophil **27**

1.2.1. The neutrophil response to infection and tissue damage **27**

1.2.1.a. Neutrophil recruitment to sites of infection/damage *28*

1.2.1.b. Neutrophil effector mechanisms at sites of infection and damage *28*

1.2.1.b.i. Neutrophil granules and degranulation 29

1.2.1.b.ii. Phagocytosis 29

1.2.1.b.iii. Neutrophil extracellular trap formation 30

1.2.1.c. Resolution of neutrophil inflammation and interactions with other immune cells *30*

1.2.2. The effect of increased neutrophilic activity in chronic inflammation **32**

1.2.3. Neutrophil subtypes **33**

1.2.3.a. Neutrophil subtypes in action *36*

1.2.4. Models of neutrophil function **37**

1.2.4.a. Primary human neutrophils *38*

1.2.4.b. Cell culture *38*

1.2.4.c. Murine models *38*

1.2.4.d. Zebrafish as a model to study neutrophil function. *39*

1.3. Chromatin and the epigenetic regulation of gene expression **42**

1.3.1. Chromatin structure **42**

1.3.2. Types of Epigenetic regulation **42**

1.3.2.a. DNA Methylation *43*

1.3.2.b. Post translational histone modifications *43*

1.3.2.c. Non-coding RNAs *44*

1.3.3. A brief overview of how chromatin remodelling regulates the innate immune system. **45**

1.4. Neutrophil chromatin remodelling **46**

1.4.1. The current picture of neutrophil chromatin remodelling **46**

1.4.2. Trained neutrophil immunity: Reprogramming of neutrophils following infection and vaccination. **48**

1.5. Ageing, functional decline and the epigenome **50**

1.5.1. Defining ageing **50**

1.5.2. Age-related functional decline and changes to cells and tissues **51**

1.5.2.a. Defining functional decline. *51*

1.5.2.b. The Hallmarks of ageing: age-related cellular changes that drive functional decline. *51*

1.5.2.b.i. Telomere attrition 51

1.5.2.b.ii. Mitochondrial dysfunction 52

1.5.2.b.iii. Genomic instability 53

1.5.2.b.iv. Loss of Proteostasis 53

1.5.2.b.v. Deregulation of nutrient sensing 54

1.5.2.b.vi. Cellular Senescence 54

1.5.2.b.vii. Stem cell exhaustion 55

1.5.2.b.viii. Alterations in intercellular communication 56

1.5.2.b.ix. Dysbiosis 56

1.5.2.b.x. Disabled macroautophagy 57

1.5.2.b.xi. Chronic inflammation 57
1.5.2.b.xii. Epigenetic alterations 58
1.5.2.b.xiii. Overview of the hallmarks of ageing 58

1.5.3. Chromatin remodelling in ageing. 60

1.5.3.a. Global age-related chromatin remodelling 60

1.5.3.b. Tissue specific age-related chromatin remodelling 62

1.5.4. Considering epigenetics changes in immune ageing 62

1.6. Ageing in the immune system 63

1.6.1. Immunosenescence and inflammageing 63

1.6.1.a. Immunosenescence is a loss of immune cell homeostasis. 63

1.6.1.b. Inflammageing is a global, low-grade chronic inflammation. 64

1.6.1c. The effects of ageing on the inflammatory response 64

1.6.2. Inflammageing and immunosenescence in age-related decline disease 66

1.6.3. How innate immune epigenetics change with age 67

1.7. Age-related changes to neutrophil function 69

1.7.1. Changes to neutrophil migration 69

1.7.2. Changes to neutrophil effector mechanisms 70

1.7.3. Changes to neutrophil inflammation resolution and apoptosis 72

1.7.4. How age-related changes to neutrophil function drive age-related decline and disease. 73

1.7.5. Studying age-related chromatin remodelling in neutrophils 74

1.8. Aims and Objectives 75

Chapter 2. Materials and Methods 77

2.1. General materials and methods used across all chapters 77

2.1.1 Zebrafish Husbandry 77

2.1.2. Zebrafish tailfin injury 77

2.1.3. PCR Primer design **77**

2.1.4. Genomic DNA extraction **79**

2.1.5. TRIzol based RNA extraction **79**

2.1.6. First strand cDNA synthesis **80**

2.1.7. RT-PCR **80**

2.1.8 qRT-PCR **81**

2.1.9 qRT-PCR Analysis **82**

2.1.10. Sample size and statistics **82**

2.2. Materials and Methods for Chapter 3 **83**

2.2.1 Drug preparation **83**

2.2.1.a. R848 *83*

2.2.1.b. C646 *83*

2.2.1.c. EX527 *83*

2.2.2. R848 toxicity test **83**

2.2.3. Neutrophil distribution assays in the presence of R848 **83**

2.2.4. Neutrophil recruitment assay following tailfin transection. **84**

2.2.5. Neutrophil counts during inflammation resolution following tail fin transection and R848 incubation. **84**

2.2.6. Calculation of percentage change in neutrophil number **85**

2.2.7. Quantification of caudal fin specific reporter expression **85**

2.2.7.a. tnfa *85*

2.2.7.b. Il1b *86*

2.2.8. Quantification of neutrophil specific reporter expression **86**

2.2.8.a. NF-κB *86*

2.2.8.b. tnfa *87*

2.2.9. qRT-PCR for *il6* following R848 treatment. **87**

2.2.9.a. Sample preparation and snap freezing for RNA extraction *87*

2.2.9.b. Primer optimisation *88*

2.2.9.b.i. RT-PCR 88

2.2.9.b.ii. qRT-PCR 88

2.2.9.c. Whole body qRT-PCR to detect changes in il6 expression following R848 incubation. *89*

2.2.10. *myd88* Morpholino injection optimisation **89**

2.2.11. Neutrophil inflammation resolution following *myd88* morpholino injection and R848 incubation. **91**

2.2.12. Neutrophil counts during inflammation resolution following incubation with C646 and R848 **91**

2.3. Materials and Methods for Chapter 4 **93**

2.3.1. RNAseq analysis **93**

2.3.1.a. Human datasets *93*

2.3.1.b. Zebrafish datasets *93*

2.3.2. CRISPR RNA design **93**

2.3.3. crRNA optimisation and diagnostic digests **94**

2.3.4. Single cell injection of crRNAs **95**

2.3.5. Neutrophil counts following single cell injection and tailfin transection. **95**

2.3.6. Analysis of gene expression following whole body knockdown of *kdm6ba/b* **95**

2.3.6.a. RT-PCR *95*

2.3.6.b. qRT-PCR *96*

2.3.7. Neutrophil specific CRISPR/Cas9 plasmid creation **96**

2.3.7.a. Transgenic construct for Cas9 expression *96*

2.3.7.b. Design of neutrophil specific chromatin remodelling sgRNA primers for constructs *96*

2.3.7.c. Digestion of p3E-U6-U6c-Rac2 for preparation of 3.5 kb and 0.5 kb fragments for cloning *96*

2.3.7.d. Optimisation of primers insertion of guide RNAs into the 3' entry clone *97*

2.3.7.e. Insertion of chromatin remodelling sgRNAs into U6a/U6c 3' entry clone *98*

2.3.7.e.i. RT-PCR 98

2.3.7.e.ii. DpnI digest to remove non-amplified template. 98
2.3.7.e.iii. PCR purification of amplified fragments. 98
2.3.7.e.iv. In-Fusion HD Cloning of 3.5 kb and 0.5 kb *kdm6ba/b* guide RNA plasmid. 98
2.3.7.e.v.Transformation of InFusion HD Product 99
2.3.7.e.vi. Midi-prep of transformed InFusion HD colonies 99
2.3.7e.vii. Confirmation of successful reaction to form p3E-U6a-kdm6bg1-U6c-kdm6bg2. 99
2.3.7.f. Gateway Cloning by LR Reaction to make the full sgRNA insertion plasmid. *100*
2.3.7.g. Digest to confirm successful LR reaction. *101*
2.3.8. Micro-injection of pDest-LyzC-EGFP-U6akdm6bg1-U6c-kdm6bg2-Tol2-pA2 into single-cell zebrafish embryos **102**
2.4. Materials and Methods for Chapter 5 **103**
2.4.1. Preparation of zebrafish embryos **103**
2.4.1.a. Single cell injection and tailfin injury *103*
2.4.1.b. Homogenisation of zebrafish larvae *103*
2.4.2. Preparation of streptavidin beads **104**
2.4.3. Nuclei isolation by INTACT BirA/streptavidin pulldown **104**
2.4.4. Extraction of RNA **105**
2.4.4.a. TRIzol *105*
2.4.4.b. Preparation of nuclei suspensions for Qiagen RNeasy Micro Kit RNA extraction *105*
2.4.4.b.ii. Flow-through nuclei 105
2.4.4.b.ii. Neutrophil nuclei 105
2.4.4.c. Qiagen RNeasy Micro Kit RNA extraction *106*
2.4.5. Quality control of isolated nuclei **106**
2.4.5.a. cDNA synthesis *106*
2.4.5.b. RT-PCR *107*
2.4.5.c. Agilent 2100 Bioanalyzer *107*
2.4.6. Analysis of isolated nuclei **108**
2.4.6.a. Library preparation and RNA sequencing *108*
2.4.6.b. Bioinformatics analysis *108*

Chapter 3: The TLR8 agonist R848 alters neutrophil activity *in vivo* using a zebrafish tailfin injury model. 109

3.1. Introduction 109

3.2. Aims and hypothesis. 111

3.3. Results 113

3.3.1. The TLR7/8 agonist R848 is not toxic to larval zebrafish with or without caudal fin injury. 113

3.3.2. R848 does not alter neutrophil number or distribution in larval zebrafish. 115

3.3.3. Incubation with R848 at the time of caudal fin injury has no effect on neutrophil recruitment to the wound site 117

3.3.4. R848 significantly increases inflammation resolution following caudal fin injury. 120

3.3.5. Pre-incubation prior to caudal-fin injury significantly alters the neutrophilic kinetics by 3 hpi but has no effect on neutrophil number. 122

3.3.6. Extended pre-incubation with R848 does not significantly alter neutrophil numbers at the wound site. 124

3.3.7. R848 significantly increases whole tissue and neutrophil-specific activation of NF-κB. 126

3.3.8. R848 has no effect on IL-1β expression at the wound site. 129

3.3.9. R848 significantly increases TNFα expression in caudal fin injury of larval zebrafish. 131

3.3.10. 16-hour incubation with R848 has no effect on TNFα expression at the wound site or in neutrophils 134

3.3.11. Whole-body qRT-PCR shows an R848 dependent significant increase in IL-6 expression that is not observed following tailfin injury. 137

3.3.12. R848-dependent changes in neutrophil inflammation resolution are lost in knockdown of *myd88* by morpholino injection 139

3.4. Discussion 143

Chapter 4: Knockdown of chromatin remodelling enzymes using CRISPR/Cas9 technology and assessment of neutrophil activity in zebrafish. 150

4.1. Introduction 150

4.2. Aims and hypothesis. **152**

4.3. Results **153**

4.3.1.a. Identification of initial CRISPR/Cas9 targets using a bioinformatic approach **153**

4.3.1.b. Refinement of the chromatin remodelling enzyme Cas9 knockdown candidate list *157*

4.3.2. Design and testing of Cas9 crRNAs for *kdm6b*, *ezh2* and *dot1l*. **161**

4.3.3 Creation of *kdm6ba/b* crRNA constructs for neutrophil-specific knockdown **164**

4.3.3.a. Optimisation of primers and DNA polymerase for insertion of crRNAs into 3' entry clone *164*

4.3.3.b. RT-PCR to insert fragment into 3'Entry Clone *166*

4.3.3.c. Confirmation of correct In-Fusion reaction product. *167*

4.3.3.d. Confirmation of correct LR Clonase Reaction product *170*

4.3.3.e. Injection of pDest-Lyz-EGFP-U6akdm6bg1-U6c-kdm6bg2-Tol2-pA2 into Tg(lyz:nfsβ-mCherry)sh260 embryos *174*

4.3.4. RT-PCR and qRT-PCR does not clearly show *kdm6b* transcript knockdown by 5'UTR guides. **176**

4.3.5. Design and optimisation of crRNAs targeting the coding sequence of *kdm6ba* and *kdm6bb*. **179**

4.3.6. Whole-body knockdown of *kdm6ba* and *kdm6bb* using coding sequence targeting CRISPR/Cas9 results in decreased neutrophil inflammation resolution following tailfin injury **184**

4.3.7. Whole-body CRISPR/Cas9 knockdown targeting the coding sequence of *kdm6ba/b* causes a 1.58-fold increase in *hif1a* expression **186**

4.3.8. Design and optimisation of crRNAs targeting the coding sequence of *dot1l* and *ezh2* **188**

4.3.9. Whole-body knockdown of *ezh2* leads to increased neutrophil recruitment 6 hpi and decreased neutrophil inflammation resolution 24 hpi. **191**

4.4. Discussion **193**

Chapter 5: INTACT BirA/streptavidin pulldown of zebrafish neutrophils to understand how kdm6b regulates the neutrophil transcriptome. **200**

5.1. Introduction **200**

5.2. Aims and hypothesis. **202**

5.3. Results **204**

5.3.1. INTACT BirA/streptavidin pulldown extracts show enrichment for neutrophil nuclear RNA based on RT-PCR for neutrophil genes and adequate RNA quality using Agilent Bioanalyzer 2100 readouts. **204**

5.3.2. Quality control of INTACT pulldown *kdm6b* knockdown RNA sent for sequencing. **208**

5.3.3. Post-sequencing bioinformatics report for the *kdm6b* knockdown RNAseq dataset shows the data set to be of sufficient quality for analysis. **210**

5.3.4. PCA plots and mean difference plots show the clustering and spread of the *kdm6b* knockdown RNAseq dataset. **213**

5.3.4.a. PCA plots show clustering of groups based on knockdown/injury condition. *213*

5.3.4.b. Mean difference plots show a different distribution of differentially expressed genes depending on the knockdown/injury comparison. *215*

5.3.5. *kdm6b* knockdown shows a different pattern of differentially expressed genes compared to the *tyr* control. **217**

5.3.5.a. Top 10 DEGs for tyr injected and injured vs. tyr injected and uninjured. *217*

5.3.5.b. Top 10 DEGs for kdm6b injected and uninjured vs. tyr injected and uninjured. *218*

5.3.5.c. Top 10 DEGs for kdm6b injected and injured vs. kdm6b injected and uninjured. *218*

5.3.5.d. Top 10 DEGs for kdm6b injected and injured vs. tyr injected and injured. *219*

5.3.5.e. Differentially expressed genes Top 10 summary. *220*

5.5.6 Ingenuity pathway analysis (IPA) shows trends toward down regulation of inflammatory canonical pathways following *kdm6b* knockout and injury **221**

5.5.6.a. IPA analysis of tyr injected and injured vs. tyr injected and uninjured *221*

5.5.6.b. IPA analysis of kdm6b injected and uninjured vs. tyr injected and uninjured *223*

5.5.6.c. IPA analysis of kdm6b injected and injured vs. kdm6b injected and uninjured. *225*

5.5.6.d. IPA analysis of kdm6b injected and injured vs. tyr injected and injured. *227*

5.5.6.e. Summary of IPA analysis *227*

5.3.7. IPA upstream analysis shows *kdm6b* knockdown significantly reduces trends in activation of pro-inflammatory pathways with and without injury. **230**

5.3.8. Genes shown to be up regulated in neutrophil activation trend toward differential expressed in kdm6b knockouts. *232*

5.3.8.a. Expression of genes regulating neutrophil maturation do not change in kdm6b knockdown. *232*

5.3.8.b. Genes regulating neutrophil activation present a varied expression pattern following kdm6b knockdown. *232*

5.3.8.c. Expression of genes regulating neutrophil survival is altered in kdm6b knockdown. *233*

5.3.8.d. Expression of genes upregulated with open chromatin in neutrophil activation show trends towards reduction in kdm6b knockdown. *233*

5.3.8.e. Genes downregulated with closed chromatin in neutrophil activation show trends of differential regulated in kdm6b knockdown. *234*

5.3.8.f. Summary: Genes associated with neutrophil activation show trends towards downregulated following kdm6b knockdown and tailfin injury. *234*

5.3.9. Transcription factors up regulated following bacterial exposure may also be up-regulated following injury following *kdm6b* knockdown. **237**

5.3.10. Genes associated with R848 treatment of neutrophils show some trends in differential regulation following *kdm6b* knockdown. **239**

5.3.10.a. Expression of receptors agonised by R848 does not change or genes are not detectable in the kdm6b dataset. *239*

5.3.10.b. Expression of several cytokines linked to R848 activation of TLR8 are altered by kdm6b knockdown. *240*

5.3.10.c. Expression of transcription factors activated by R848 binding TLR8 are trend towards reduction following kdm6b knockdown. *240*

5.3.10.d. Expression of the chromatin remodelling enzyme brd4 is altered by kdm6b knockdown. *240*

5.3.10.e. Summary: Genes involved in the R848 driven activation of neutrophils may be dysregulated by kdm6b knockdown. *241*

5.4. Discussion **244**

Chapter 6. General Discussion and Future Work **251**

6.1. Summary of the major findings of this work **251**

6.2. Implications for the understanding of neutrophil chromatin remodelling *in vivo*. **253**

6.3. Future work **255**

6.4. New research questions **256**

7. References **260**

8. Appendix **287**

8.1. Chapter 3 Appendix **287**

Appendix 3.1. Optimisation of IL-6 RT-qPCR primers by gradient PCR, efficiency curve and melt curve analysis **287**

Appendix 3.2. Incubation with C646 and R848 in combination significantly reduces inflammation resolution **290**

Appendix 3.3. SIRT1 inhibition significantly increases neutrophil recruitment to the tailfin 3 hpi **292**

Appendix 3.4. R848/C646 Discussion **294**

Appendix 3.5. Sirt1 discussion **295**

8.2. Chapter 4 Appendix **296**

Appendix 4.1. CRISPR/Cas9 targeting chromatin remodelling enzymes in the R848 pathway **296**

Appendix 4.2. Single-cell injection of CRISPR targeting the R848 chromatin remodelling enzymes *crebbpa*, *ep300a* and *brd4* **298**

Appendix 4.3. Optimisation of CRISPR/Cas9 guides for newly selected chromatin remodelling enzymes **300**

8.3. Chapter 5 Appendix **308**

Table of Figures

Table 1.1: Types of innate and adaptive immune cells **25**

Table 2.1. Sequences for PCR primers **79**

Table 2.2. RT-PCR cycles used for standard experiments. **81**

Figure 2.1. qRT-PCR cycler programme for standard experiments **81**

Table 2.3. Treatment conditions of *TgBAC(tnfa:GFP)pd1028* larval zebrafish for tailfin injury and expression analysis **85**

Table 2.4. Snap freeze groups for qPCR analysis of *il6* gene expression in larval zebrafish. **88**

Table 2.5. Treatment groups for *myd88* morpholino injection and R848 treatment **91**

Table 2.6. crRNAs used for CRISPR/Cas9 mediated knockdown experiments. **94**

Figure 2.3. Diagnostic digest for p3e-U6akdm6bg1-U6c-kdm6bg2 guide RNA plasmid **100**

Table 2.8. Vectors used for LR cloning reaction to make pDest-LyzC-EGFP-U6akdm6bg1-U6c-kdm6bg2-Tol2-pA2 **101**

Figure 2.4. Diagnostic digest for successful LR reaction to make the pDest-LyzC-EGFP-U6akdm6bg1-U6c-kdm6bg2-Tol2-pA2 vector **102**

Figure 2.5. Example bioanalyzer plots for INTACT pulldown samples with whole embryo for comparison **107**

Figure 3.1: 39-hour treatment with R848 is not toxic to larval zebrafish. **114**

Figure 3.2: R848 treatment for 19 hours does not alter whole body counts of neutrophils or neutrophil distribution in uninjured zebrafish larvae **116**

Figure 3.3: Treatment with R848 at time of injury does not increase the number neutrophils recruited to the wound site. **118**

Figure 3.4: Treatment with R848 4 hpi significantly increases inflammation resolution following caudal fin injury **121**

Figure 3.5: Treatment with R848 4 h before caudal fin injury significantly decreases percentage change in neutrophils at the wound between 1 and 3 hpi. **123**

Figure 3.6: Treatment with R848 16 h before caudal fin injury does not alter the number of neutrophils recruited to the wound site 125

Figure 3.7: Incubation in R848 significantly increases whole tissue activation of NF-κB and activation of NF-κB in neutrophils in caudal fin injury. 128

Figure 3.8: R848 does not affect whole tissue activation of IL-1β in caudal fin injury. 130

Figure 3.9: R848 significantly increases expression of TNFα in caudal fin injury. 132

Figure 3.11. 16-hour incubation with R848 has no effect on *tnfa* expression at the wound site or in neutrophils 8 hpi 136

Figure 3.13. MyD88 morpholino injection significantly reduces neutrophil inflammation resolution when incubated with R848. 141

Figure 4.1. Flow chart for determining which chromatin remodelling enzymes to investigate. 156

Figure 4.2. Enhancer/promoter enrichment for Top 6 ranked chromatin remodelling enzymes 160

Figure 4.3. Diagnostic digest of larval gDNA injected with crRNAs targeting the 5'UTRs of *kdm6ba, kdm6bb, dot1l* and *ezh2.* 163

Figure 4.4. Testing DNA polymerase for neutrophil-specific knockdown guide RNA constructs 165

Figure 4.5. Confirmation of correct RT-PCR product following addition of *kdm6b* crRNA to 3'Entry clone 166

Figure 4.6. Digest of In-Fusion HD reaction product to confirm correct product. 168

Figure 4.7. Confirmation of the correct LR reaction product by diagnostic digests 172

Figure 4.8. Plasmid of the *kdm6ba/b* guide RNA construct 173

Figure 4.9. Injection of *kdm6b* crRNA construct to *Tg(lyz:nfsβ-mCherry)sh260* zebrafish embryos produce GFP+ neutrophils. 175

Figure 4.10. PCR for *kdm6ba/b* expression following CRISPR/Cas9 targeting the 5'UTR 179

Figure 4.11. Optimisation of injection of crRNAs for *kdm6ba* and *kdm6bb* coding sequences 183

Figure 4.12. Whole-body knockdown of *kdm6ba* and *kdm6bb* targeting the coding sequence with CRISPR/Cas9 results in a significant reduction in inflammation resolution 185

Figure 4.13. Whole-body knockdown of *kdm6ba/b* by CRISPR/Cas9 targeting the coding sequences causes a 1.58-fold increase in *hif1a* expression following tailfin injury 187

Figure 4.14. *dot1l* and *ezh2* coding sequence targeting crRNAs and primer optimisation. 189

Figure 4.15. Whole-body CRISPR/Cas9 knockdown of *ezh2* results in a significant increase in neutrophils 6 hpi and 24 hpi 192

Figure 5.1. INTACT BirA/Streptavidin pulldown as a method for isolation of zebrafish neutrophil nuclei. 206

Figure 5.2. Analysis of INTACT extracted nuclear RNA samples shows enrichment for neutrophil genes and adequate RNA quality based on Agilent Bioanalyzer 2100 readouts. 207

Figure 5.3. Quality control report from Source Biosciences 209

Figure 5.4. Bioinformatics Report from Source Biosciences 211

Figure 5.5. PCA plots show some clustering of groups based on sample type. 214

Figure 5.6. Mean difference plots show *kdm6b* knockdown and tailfin injury result in a different distribution of differentially expressed genes. 216

Table 5.1. Top 10 DEGs for *tyr* injected and injured vs. *tyr* injected and uninjured. 217

Table 5.2. Top 10 DEGs for *kdm6b* injected and uninjured vs. *tyr* injected and uninjured. 218

Table 5.3. Top 10 DEGs for *kdm6b* injected and injured vs. *kdm6b* injected and uninjured. 219

Table 5.4. Top 10 DEGs for *kdm6b* injected and injured vs. *tyr* injected and injured. 219

Figure 5.7. Ingenuity pathway analysis (IPA) shows trends in upregulation of pro-inflammatory pathways in *tyr* knockout control samples following and injury. 222

Figure 5.8. IPA shows trends of downregulation in inflammatory pathways in kdm6b knockout samples without injury relative to tyr control. 224

Figure 5.9. IPA shows trends of upregulation in pro-inflammatory pathways in *kdm6b* knockout samples with injury relative to *kdm6b* knockdown without injury. 226

Figure 5.10. IPA shows trends in downregulation of pro-inflammatory pathways in *kdm6b* knockout samples with injury relative to *tyr* knockdown with injury. 228

Table 5.5. IPA Upstream pathways shows trends of inhibition in pro-inflammatory pathways in *kdm6b* knockdown and injury. 231

Figure 5.11. Genes shown to be up regulated with open chromatin during the neutrophil life cycle and activation trend towards differential expression following *kdm6b* knockdown and tailfin injury. 235

Figure 5.12. Transcription factors up-regulated following bacterial exposure may also be up-regulated following injury following *kdm6b* knockdown. 238

Figure 5.13. Expression of genes in *kdm6b* knockdown RNAseq previously shown by Zimmerman *et al.,* (2015) to be involved in neutrophil activation of R848. 243

Appendix Figure 3.1: Optimisation of IL-6 qPCR primers pairs for quantification of IL-6 expression 288

Appendix Figure 3.2. In combination with R848, inhibition of EP300 and CREBBP by C646 significantly reduces neutrophil inflammation resolution and neutrophil kinetics 24 hpi 291

Appendix Figure 3.3. The SIRT1 inhibitor, EX527, significantly increases the recruitment of neutrophils to the injured zebrafish tailfin, 3 hpi 293

Appendix Figure 4.1. Sequences and primer tests for R848 pathway associated chromatin remodelling enzymes 297

Appendix Figure 4.2. Diagnostic digest for efficiency of crRNAs for chromatin remodelling enzymes implemented in the R848 pathways 299

Appendix Figure 4.3. crRNA target sites for promoters or 5'UTRs of chromatin remodelling enzymes and testing of primers 301

Appendix Figure 4.4. Diagnostic digest of PCR product from gDNA of embryos injected with 5'UTR/promoter crRNAs 302

Appendix Figure 4.5. crRNA target sites for 5'UTRs of chromatin remodelling enzymes and testing of primers 303

Appendix Figure 4.6. Optimising a diagnostic digest for the *kdm6ba* 5'UTR crRNA 305

Appendix Figure 4.7. kdm6ba and kdm6bb coding sequence targeting crRNAs and primer optimisation 306

Appendix Figure 5.1. Optimisation of primers for analysis of INTACT pulldown products 308

Appendix Figure 5.2. Missed reads in bioinformatics. 309

Chapter 1: Introduction

1.1. The immune system

Ageing arguably presents the greatest risk to health in the developed world. While people are living longer, they are not living healthier lives (Drew, Wilson and Sapey, 2018). Multimorbidity – the co-existence of multiple disorders– is a key factor in this reduction in health in old age (Barnett *et al.*, 2012). Socioeconomic hardship, especially during development, further compounds these issues, with those from disadvantaged backgrounds seeing earlier onset of multimorbidity and age-related decline (Schrempft and Stringhini, 2023). Many age-related diseases have inflammatory components and there are global changes to immune function with age. The two major changes in immunity with age are immunosenescence – the dysregulation of immune cell function with age – and inflammageing – a whole-body, non-specific, and low-grade chronic inflammation (Santoro, Bientinesi and Monti, 2021). Both immunosenescence and inflammageing can promote damage to host tissues and alter responses to pathogenic infection or removal of damaged tissue (Santoro, Bientinesi and Monti, 2021). Expanding our understanding of how the immune system changes with age can help us treat age-related diseases and increase healthy lifespan. Targeting specific cells of the immune system provides one of these potential treatments. As the most abundant immune cell and first responder of the immune system, the neutrophil, is an important target for further examination. However, before examining the functions and the roles of neutrophils, it is important to introduce the immune system to provide an understanding of how neutrophils sit within it and how the healthy immune system functions in response to challenges to use that information to analyse age-related changes.

1.1.1. The Inflammatory response

To maintain homeostasis, the body must be able to defend and kill invasive pathogens, and remove and repair damaged tissue to return the body to a healthy state (Hato and Dagher, 2015). The immune system plays a role in how the body maintains this homeostasis, with a healthy immune system being essential to a healthy life. The immune system is often divided for convenience into two classes of inflammatory response - the innate immune response and the adaptive immune response. Both involve specialised leukocytes which respond to danger

signals to remove threats and play an important role in the cascade that leads to tissue repair. Innate immunity provides immediate responses regardless of prior exposure, whereas adaptive immunity responds to infection or damage, using memory of previous exposures for rapid and targeted removal of threats. Working in combination, the innate and adaptive immune systems aim to rapidly return the body to immune homeostasis (Sun *et al.*, 2020). However, inflammation can become chronic and can cause serious health complications. For example, when there is an overload of pathogen or excess tissue damage. Better understanding of the pathways that drive chronic inflammation should allow for the development of new therapies to treat chronic inflammatory conditions.

1.1.1.a. Innate immunity

The innate immune system is the first line of immune defence for the body. Cells of the innate immune system, predominantly neutrophils and macrophages, respond directly and indirectly to pathogenic or damaged cells (Table 1.1.). The initial response is triggered by recognition of threats by toll-like receptors (TLRs), recognition of antibodies or complement bound to antigens, to mount a response to infection. The complement system consists of proteins that are processed and released by cells on detection of threats that then opsonise antigens that can be detected by receptors found on immune cells and then activate pro-inflammatory pathways (Lo and Woodruff, 2020). TLRs are found on leukocytes and non-immune cells and can be found either on the cell surface or in endosomes within cells. There are 10 types of human TLRs, each specialising in detecting specific molecules, including host proteins, bacterial DNA, and viral RNA (Kawai and Akira, 2010). On detection of a TLR ligand, receptors complex and a signalling cascade is triggered, where signal transduction through MyD88 (apart from TLR3 which uses TRIF) leads to NF-κB activation and the gene transcription of proinflammatory cytokines (Futosi, Fodor and Mócsai, 2013). These cytokines can drive inflammatory behaviour in leukocytes directly and create signalling gradients that promote the recruitment of further immune cells to the site of infection/damage.

On detection of proinflammatory cytokines or activation via TLR signalling, leukocytes of the innate immune system work to remove the detected threat (Brubaker *et al.*, 2015). Innate immune cells can phagocytose pathogenic cells, damaged host cells and foreign particles in a non-specific manner, processing the contents of the phagosome to break down the pathogen

into constituent parts for recycling. Innate immune cells also release proteins and extracellular structures to break down threats, including metalloproteases, neutrophil extracellular traps (NETs), and reactive oxygen species. These processes are essential as they fight the infection and remove damaged tissue, but they are also non-specific, especially the release of proteins and extracellular structures such as NETs (Brinkmann *et al.*, 2004). As a result, healthy tissue can be damaged if the innate response persists. Innate immunity, therefore, must be tightly controlled and other mechanisms need to be employed to target infection and return the body to homeostasis. This project will focus on innate immunity and its primary effector cell, the neutrophil.

1.1.1.b. A brief introduction to the neutrophil

The innate immune response is performed by several specialist immune cells (Table 1.1) The most abundant and primary effector is the neutrophil. Neutrophils are professional phagocytes that have a multi-lobed nucleus and are rich in granules filled with cytotoxic proteins. They mature within the bone marrow and migrate into the circulation where they patrol for threats (Ballesteros *et al.*, 2020). On detection of immune challenge by cell-surface receptors for pro-inflammatory cytokines and chemokines, neutrophils will migrate to the source of the pro-inflammatory signal (Ravetch and Bolland, 2003). The neutrophils will move from the circulation and into the tissue and perform effector functions to remove the threat including phagocytosis, release of granular contents, and NETosis (Hidalgo *et al.*, 2019). Once the threat is cleared, anti-inflammatory cytokine signalling causes neutrophils to either migrate out of the tissue and return to the circulation, or undergo apoptosis, where the neutrophil is then removed by macrophages (Savill *et al.*, 1989; Woodfin *et al.*, 2011). Because neutrophil effector functions are so potent and therefore have the potential to harm host tissue if not properly regulated, control of neutrophil function is highly important to inflammation and homeostasis.

1.1.1.c. Adaptive immunity

Adaptive immunity specifically targets pathogens using specialist immune cells that contain memory of previous infections over the individual's lifetime thereby allowing for a rapid response for future infection.

1.1.1.c.i. Major histocompatibility complexes

Recruitment of adaptive immune cells occurs via communication with the innate immune system and surrounding tissues through major histocompatibility complexes. All nucleated human cells possess the type I major histocompatibility complex (MHC-I) (Neefjes *et al.*, 2011). Proteins within MHC-I cells are processed by the proteasome and fragments are trafficked and presented on the MHC-I cell surface protein, while some of the antigens presented are self-antigens, intracellular pathogen antigens are also presented in this way meaning it is a valuable part of defence against pathogens. Antigen presenting cells (APCs) of the innate immune system such as macrophages and dendritic cells also possess type II MHC (Yatim and Lakkis, 2015). These cells phagocytose foreign material and through a series of processing events within the phagosome, produce antigens that are trafficked to the cell surface and presented on type II major histocompatibility complexes (MHC-II) (Neefjes *et al.*, 2011).

1.1.1.c.ii. T lymphocytes

T lymphocyte subtypes have receptors for MHC complexes that will only recognise specific antigens in combination with T cell receptors (TCRs) leading to activation of the T-cells. MHC-I complexes are detected by $CD8^+$ T killer cells. CD8 receptors combine with TCRs to recognise antigens and on detection of the correct epitope are activated causing apoptosis of the APC. MHC-II complexes present to the naïve $CD4^+$ T helper cell. A correct CD4/TCR interaction with the MHC-II/antigen complex leads to polarisation of the naïve cell into a memory or effector T-cell (Brummelman, Pilipow and Lugli, 2018). The effector cells are largely T_h1 cells, that recruit macrophages and T-killer cells to fight the infection, and T_h2 cells that recruit and activate B cells to induce antibody class switching and production to further recognise antigens and fight infection. Memory T cells are an expandable population of T-cells specific to the antigen that activated the naïve cell, creating a reserve of cells that can be quickly expanded into active effector cells on a repeat infection. There are also T_h17 cells and other subtypes of effector that aid in controlling the adaptive response (Kumar, Connors and Farber, 2018; Lee, 2018).

1.1.1.c.iii. B lymphocytes and antibody production

Antibodies – also known as immunoglobulins – play an essential part of adaptive immunity and the development of immune memory to fight repeated infection. B lymphocytes produce antibodies that recognise and bind antigens on pathogenic cells allowing the pathogen to be recognised by other immune cells and to prevent pathogenic functions (Parker, 1993). Antibodies initially form as B cell receptors (BCRs), found on the naïve B lymphocyte plasma membrane and are specific to one antigen due to a complex molecular process known as V(D)J recombination modifying the binding site to recognise specific molecular patterns (Borghesi and Milcarek, 2006). When the BCR is presented with the correct antigen, the naïve cell is activated and divides and differentiates. B lymphocytes can differentiate into plasma cells that secrete antibody into the plasma, and memory cells that retain memory of the specific antigen and can be activated at a repeat infection (Cancro and Tomayko, 2021). Antibodies are divided into four classes: IgA, IgD, IgE, IgG, and IgM, each of which have a specific function (Schroeder and Cavacini, 2010). When activated, a B lymphocyte will perform class switching to produce a specific antibody class depending on the cytokine environment. Antibodies act as the main link between the adaptive and innate immune system as when antibodies bind an antigen, they promote recruitment and activation of innate immune cells by recognition of the antibody via Fc receptors on the immune cell surface (Bournazos *et al.*, 2017). Cells that can bind antibodies include neutrophils and macrophages and on binding, phagocytosis and effector functions are triggered to remove the infection. Antibodies can also interact with complement, when an antibody binds an antigen, complement can bind the antibody, which will then recruit innate immune cells such as neutrophils to remove the threat (Ravetch and Bolland, 2003). While the focus of this work is on innate immunity, it is important to understand the interplay between the innate and adaptive immune system and the role innate immune cells play in antigen presentation to adaptive immune cells and how antibody recognition of antigens can recruit innate immune cells to fight reoccurring infection.

Innate immune cells	Adaptive immune cells
Neutrophils	T lymphocytes CD8+ T cells (killer cells) CD4 + T cells (helper cells) T_h1 cells T_h2 cells Gamma delta T cells Follicular helper T cells T-helper 17 cells Tissue resident memory T cells
Monocytes/Macrophages	
Dendritic cells	
Basophils	B lymphocytes Naïve B cells Plasma B cells Memory B cells
Eosinophils	
Natural killer cells	
Innate lymphoid cells	
Mast cells	

Table 1.1: Types of innate and adaptive immune cells

(Brubaker *et al.*, 2015; Yatim and Lakkis, 2015; Kumar, Connors and Farber, 2018; Cancro and Tomayko, 2021)

1.1.2. Acute vs. chronic inflammation

Acute inflammation is the rapid response to infection or wounding to return the body to homeostasis. There are four cardinal signs of acute inflammation caused by the initiation of protective mechanisms against invasion – *rubor et tumor cum calore et dolore* (Aulus Cornelius Celsus (25 BC-50 AD)), or redness and swelling with heat and pain (Freire and Van Dyke, 2013). For inflammation to completely return the body to homeostasis, it can require the innate and adaptive responses of the immune system working together to remove any pathogens and damaged tissue and then trigger repair processes to return the body to normal (Sun *et al.*, 2020). Sections 1.1.1.a. and 1.1.1.c. detail how the innate and adaptive responses of the immune system interplay to resolve inflammation and retain an immunological memory of the threat.

Chronic inflammation is a response that often persists long after infection or injury, when the processes that normally resolve an incident of acute inflammation are not in place or the source of inflammation cannot be cleared such as tuberculosis infection or foreign materials such as surgical suture (Kotas and Medzhitov, 2015). Instead, a pro-inflammatory state dominates and either exacerbates existing damage or causes new long-term damage that can result in loss of quality of life and eventual mortality. As the primary effector cell in inflammation, neutrophils can drive non-specific chronic inflammation and so it is a process of particular interest here. During chronic inflammation, innate immune cells, such as neutrophils and macrophages, are recruited to the site of inflammation and persist in an activated state. An increased release of pro-inflammatory cytokines and chemokines from both immune cells and endogenous cells, such as endothelial cells, and release of DAMPs maintains a pro-inflammatory environment (Nathan and Ding, 2003). The constant activation of innate immune cells leads to non-specific release of cytotoxic molecules by processes such as NETosis, respiratory bursts, and neutrophil degranulation and increased phagocytosis from professional phagocytes. This environment of cytotoxicity damages endogenous tissues and can lead to loss of tissue function and disease. The dominant inflammatory state prevents damaged tissues from being repaired, leading to scarring or remodelling of the tissue in a way that leads to a loss of function. This can be seen in atherosclerosis, where the recruitment of immune cells to atherosclerotic plaques increases blockage of the vasculature, and chronic obstructive pulmonary disease (COPD), where scarring and remodelling to the lungs and airway leads to a reduction in respiratory function (Galkina and Ley, 2009; Rabe and Watz, 2017).

Secondary pathologies can arise from chronic inflammation. Chronic inflammation can lead to an inflammatory state that masks other infections. These infections have the potential to overcome the host and cause serious illness that is very difficult to manage. An example of this is infection of chronic wounds due to persistent pro-inflammatory states, reduced bacterial killing, and reduced inflammation resolution in diabetes patients that prevents removal of pathogens or repair of tissue due to dysfunctional immune cells including macrophages and neutrophils (Wong *et al.*, 2015; Aitcheson *et al.*, 2021).

The onset of non-infectious diseases can also be driven by chronic inflammation. Chronic inflammation can promote cancer development by allowing the tumour microenvironment to develop (Coussens and Werb, 2002). The cellular stress brought on by chronic inflammation such as the release of reactive oxygen species can drive oncogenic changes in cells leading to mutations that allow cancerous cells to be able to avoid immune checkpoints and continue to proliferate. The inflammatory environment can also aid tumour growth and metastasis by utilising chemokines and cytokines that can drive proliferation and migration of tumour cells. Because of this benefit of chronic inflammation to cancer progression, tumours can then further promote immune cell to maintain a pro-inflammatory state (Coussens and Werb, 2002).

Chronic inflammation is therefore an important target for inflammatory research. The examples above show why finding ways to control chronic inflammation will not only have an impact on chronic inflammatory diseases, but also have an impact on the treatment of secondary pathologies. Finding drivers of chronic inflammation may therefore lead to therapy development for many diseases as a result.

1.2. The Neutrophil

1.2.1. The neutrophil response to infection and tissue damage

Neutrophils are the most abundant circulating leukocyte and the first responders of the innate immune system, acting as one of the main effector cells at sites of inflammation (Schultze, 1865; de Oliveira *et al.*, 2013). Mature neutrophils are short-lived, terminally differentiated myeloid cells that originate from a common myeloid progenitor pool within the bone marrow. The differentiation process begins with committed myelocytes, differentiating into post-mitotic banded neutrophils and, finally, mature neutrophils that can be found in either the bone marrow, circulation, or tissues (Hidalgo *et al.*, 2019). It was initially thought that active neutrophils had a short half-life of 7-10 hours, however evidence is beginning to suggest that active neutrophils are much more heterogeneous and can survive for longer, probably several days, though many of these observations are hard to repeat (Hidalgo *et al.*, 2019). Inactive neutrophils die rapidly by spontaneously triggered apoptosis and are removed

by macrophages, but if they are activated, they migrate to sites of infection based on pro-inflammatory chemokine gradients where they can employ effector mechanisms such as phagocytosis to remove pathogens (Amulic *et al.*, 2012). Activated neutrophils are then removed either by migration away from the site of infection or apoptosis and subsequent phagocytosis by macrophages (Savill *et al.*, 1989; Nourshargh, Renshaw and Imhof, 2016).

1.2.1.a. Neutrophil recruitment to sites of infection/damage

The cell surface of inactive neutrophils is coated with a variety of receptors able to detect pathogens, cytokines and chemokines, and host cells (Futosi, Fodor and Mócsai, 2013). Direct activation of neutrophils can occur by sensing of pathogens by TLRs, or detecting pathogenic molecules opsonised with antibodies or complement. Indirect activation of neutrophils can occur by detecting proinflammatory cytokines and chemokines released by epithelial cells. At a site of tissue damage or infection, endothelial cells and tissue resident leukocytes sense changes to the microenvironment and begin to release inflammatory mediators to recruit neutrophils to migrate to the site (Mócsai, Walzog and Lowell, 2015). When neutrophils sense such factors, signalling cascades activate the neutrophils leading to a phenotypic change, allowing for migration and antimicrobial killing. Changes to cytoskeletal dynamics such as actin organisation within the activated neutrophil allow it to move along the chemokine gradient and transcriptional changes to drive expression of antimicrobial agents (Servant *et al.*, 2000). Neutrophils use cell-surface integrins. like MAC1, to bind intercellular adhesion molecules (ICAMs) on the endothelial cell and migrate using an actin cascade to the site of attack in a rolling motion following a gradient of chemokines, including IL-8 and N-formyl-methionyl-leucyl-phenylalanine (fMLP). When the neutrophils reach the site of infection, they transmigrate through the endothelium and basement membrane and into the tissue, where they can employ effector mechanisms to return the body to immune homeostasis (Liew and Kubes, 2019).

1.2.1.b. Neutrophil effector mechanisms at sites of infection and damage

On arrival at the site of infection, neutrophils rely on three main mechanisms to deal with microbes and damaged host cells. These mechanisms are used in combination with multiple neutrophils working together, with evidence that neutrophils form coordinated swarms when

they recruit into pro-inflammatory tissue for more efficient clearing, mediated by LTB4 signalling (Lämmermann *et al.*, 2013).

1.2.1.b.i. Neutrophil granules and degranulation

Granules are involved in several processes during the inflammatory response as they can release their contents into both phagosomes and the extracellular space. Neutrophils can also release granular contents into the surrounding tissue to directly attack microbes and break down damaged tissue for phagocytosis (Lacy, 2006; Liew and Kubes, 2019). These granules are pre-packaged following activation and release, which requires binding of microbial peptides and formation of phagosomes, which trigger specific signalling cascades for trafficking, binding, and release of granules at the cell membrane. There are four subtypes of granule: Azurophilic granules contain proteins that function to breakdown pathogenic cells; these include enzymes that produce reactive oxygen species and aid in oxidative killing, such as myeloperoxidase (MPO), and the protein complex NAPDH oxidase that assembles on the membrane, proteolytic enzymes, such as cathepsins and proteinases, and the enzymes lysozyme and defensins to break down cell membranes (Rørvig *et al.*, 2013). There are also secondary, tertiary, and secretory granules. Secondary granules contain lactoferrin to sequester iron and copper away from microbes and prevent the use of these essential metal ions in microbial functions. Tertiary granules contain gelatinase-based metalloproteinases to break down extracellular matrix to better aid neutrophils in moving around the site of infection or damage. The final granule type is secretory granules that contain pre-packed cytokines that are released to recruit more neutrophils and other immune cells. Degranulation needs to be tightly regulated as the release of granular proteins into the extracellular matrix risks damaging healthy host tissue.

1.2.1.b.ii. Phagocytosis

Neutrophils are termed professional phagocytes. Receptors on the neutrophil surface such as CD32, CD16 and CD64 recognise pathogenic material and facilitate the formation of a phagosome from a section of the plasma membrane. CD32, CD16 and CD64 are all examples of Fc receptors (reviewed by Wang and Jönsson, 2019). These Fc receptors are a prime example of how neutrophils interact with the adaptive immune system (Section 1.1.1.c) as

they allow for the phagocytosis of pathogens opsonised by IgG molecules that have recognised and bound specific antigens. Activation of Fc receptors trigger a signalling cascade driven by Src-family kinase activity to activate neutrophils and promote phagocytosis. The phagosome envelopes the pathogenic material and keeps it within the phagosome that forms a membrane bound vesicle that exists within the neutrophil. When surface receptors are triggered by the formation of a phagosome, neutrophils traffic membrane bound azurophilic granules to the phagosome to release their granular contents into the phagosome and break down the pathogen within the phagosome by the release of proteolytic enzymes, and reactive oxygen species production by the respiratory burst. Granules are trafficked using the cytoskeleton and fuse to the phagosome to release granular material into the phagosome (Nordenfelt and Tapper, 2011).

1.2.1.b.iii. Neutrophil extracellular trap formation

Neutrophils can release DNA and proteins into a web-like structure to trap microbes to aid with killing and returning to immune homoeostasis (Brinkmann *et al.*, 2004). These DNA webs are referred to as neutrophil extracellular traps and released by a multistep process called NETosis in a ROS dependent manner (Burgener and Schroder, 2020). NETosis is a form of programmed cell death with distinct steps (Fuchs *et al.*, 2007). First, the nuclear membrane shape is lost leading to the formation of nuclear vesicles, and chromatin structure is decondensed. Nuclear and granule membranes are then broken down and effector proteins for targeting pathogens such as neutrophil elastases – a serine protease with anti-microbial abilities – associate with the decondensed chromatin strands (Brinkmann *et al.*, 2004). These structures are then released from the neutrophil into the extracellular space. The proteins associated with the chromatin strands then perform microbial killing when microbes become entangled in the NETs.

1.2.1.c. Resolution of neutrophil inflammation and interactions with other immune cells

Controlling neutrophil action is an important part of inflammation. If neutrophils persist at the site of infection host tissues can be damaged. Before they are removed, neutrophils must work with other immune cells to clear the infection or tissue debris. This removal therefore must be finely controlled to allow the beneficial work of the neutrophil to be carried out

without their detrimental effect ensuing. This balance is key to establishing homeostasis following tissue injury or infection.

Neutrophils interact with a variety of leukocytes from both innate and adaptive immunity through cytokines and chemokines, and cell surface receptors. Macrophage interactions with neutrophils play a vital role in driving the progression of the inflammatory process, as NETs and signalling molecules, such as MIP-1 and mCRAMP, promote macrophage recruitment, activity, and cytokine release (Lapinet *et al.*, 2000; Kumar and Sharma, 2010; Peiró *et al.*, 2018). Neutrophils also play a part in antigen presentation to adaptive immune cells. Neutrophils can recruit dendritic cells both directly and indirectly through cell-cell contact or cytokine release and promote the migration of dendritic cells to lymph nodes for antigen presentation to T-cells (Weber *et al.*, 2015; Krishnamoorthy *et al.*, 2018). There is also evidence that neutrophils can migrate to the lymph nodes themselves and interact with T and B cells, driving proliferation of both adaptive immune cell lineages, though further work is required to better understand how these processes are regulated (Vono *et al.*, 2017; Burn *et al.*, 2021).

A change in the inflammatory microenvironment drives resolution of inflammation. Anti-inflammatory cytokines IL-10 and IL-4 and proinflammatory receptor agonists, such as IL-1R, are released and pro-inflammatory cytokines are downregulated to promote a reduction in neutrophils and recruit macrophages (Liew and Kubes, 2019). Neutrophil removal occurs via two pathways. The first is by caspase-dependent apoptosis at the site of infection leading to engulfment by macrophages, a process known as efferocytosis (Savill *et al.*, 1989; Grigg *et al.*, 1991; Loynes *et al.*, 2010). During efferocytosis, engulfment of the dying neutrophils triggers the release of anti-inflammatory cytokines from the macrophages to drive a positive feedback loop that promotes further inflammation resolution and polarisation of macrophages with an M2 anti-inflammatory phenotype (Fadok *et al.*, 1998; Filardy *et al.*, 2010). Second, is reverse migration, where neutrophils retreat from the site of inflammation and return to the circulation or other organs (Nourshargh, Renshaw and Imhof, 2016).The phenomenon of reverse migration has been observed in both zebrafish and murine models, but the overall fate of these neutrophils is unclear (Woodfin *et al.*, 2011; Robertson *et al.*, 2014; Loynes *et al.*, 2018). There is evidence that reverse migratory neutrophils up-regulate CXCR4 to drive

homing to the bone marrow where they undergo apoptosis (Wang *et al.*, 2017). Interestingly, neutrophils that have reverse migrated in zebrafish can continue to phagocytose bacteria (Ellett *et al.*, 2015). Discovering what happens to these neutrophils will greatly expand our understanding of neutrophil function and lifecycle.

1.2.2. The effect of increased neutrophilic activity in chronic inflammation

Neutrophils have been linked to many chronic inflammatory diseases, including rheumatoid and juvenile idiopathic arthritis, and chronic obstructive pulmonary disease (Wright *et al.*, 2017; Ramanathan *et al.*, 2018; Hidalgo *et al.*, 2019). Neutrophil dysregulation, persistence and altered function are often key to disease pathogenesis.

Several disorders are characterised by neutrophil subtypes that appear to drive the disease phenotype. An example of such a disease is acute respiratory distress syndrome (ARDS), where neutrophils have distinct phenotypes depending on whether they are found in the circulation or within the lung alveoli, and relative to healthy controls (Juss *et al.*, 2016) Patient neutrophils have decreased apoptosis and increased priming for NADPH oxidative bursts suggesting increased inflammation, driving the disease phenotype and lung tissue damage due to ROS production. The environment within these patients' lungs is high in inflammatory cytokines such as IL-6, IL-8 and TNFα, further promoting inflammation and host tissue damage. Low density granulocytes (LDGs) are immature neutrophils like those seen in ARDS but are present in rheumatoid arthritis (Wright *et al.*, 2017). LDGs are more resistant to apoptosis, less responsive to TNFα, and more likely to form NETs. LDGs also produce more ROS, while showing similar migration and phagocytosis to neutrophils from RA patients. There has been no crossover work to see if these ARDS neutrophils are LDGs, but it presents an interesting area of investigation.

Chronic obstructive pulmonary disease (COPD) is an umbrella term for disorders characterised by chronic inflammation, tissue remodelling, tissue damage to the airway and lungs. Patients with COPD suffer from reduced airflow due to constant damage and remodelling in the lungs (Rabe and Watz, 2017). It is the third largest cause of death worldwide. COPD is caused by environmental exposure to hazards such as the harmful chemicals found in tobacco smoke and air pollutants. Exposure of the airway to these

chemicals causes damage to epithelial cells and triggers the release of endogenous pro-inflammatory signals that when detected by TLR2 and 4 on other epithelial cells, drives the release of pro-inflammatory cytokines to recruit innate immune cells via TLR signalling. As exposure to the chemical agents continue, this damage escalates, causing the chronic inflammation associated with the disease. This chronic inflammation is characterised by chronic neutrophilia with activated neutrophils driving disease progression (Jasper *et al.*, 2019). Neutrophil elastase is the causative enzyme in COPD and is a serine protease released from neutrophils in NETs and found in neutrophil granules (Voynow and Shinbashi, 2021). When neutrophil elastase is released into the COPD pro-inflammatory environment, matrix metalloproteases (MMPs) are first activated, and MMP levels are sustained as neutrophil elastase degrades MMP inhibitors leading to break down of endogenous tissue. To further drive disease progression, hydrogen peroxide, a component of tobacco smoke and a ROS generated by MPO inhibits α_1-antitrypsin, an inhibitor of neutrophil elastase (Taggart *et al.*, 2000). Increase neutrophil elastase can then promote NETosis and granulation causing further damage and increased neutrophil recruitment (Voynow and Shinbashi, 2021). As the inflammatory behaviour of neutrophils is non-specific, phagocytosis, NETosis, and degranulation not only attempts to remove the damaged epithelial cells but drives damage of healthy epithelial cells causing build-up of inflammatory material and restriction of airflow in the airway. These factors all contribute to the idea that neutrophils are the main driver in the pathology of COPD with evidence pointing to COPD neutrophils showing altered phenotypes compared to age-matched controls (Jasper *et al.*, 2019). Understanding the core mechanisms of neutrophil function such as recruitment, pathogenic killing and inflammation resolution can increase understanding of these abnormal cells and overall disease pathogenesis, leading to the development of better therapies.

1.2.3. Neutrophil subtypes

The traditional model of neutrophils describes a homogeneous population of terminally differentiated cells, pre-programmed to respond to immune challenge. Recent advances are beginning to challenge that notion, describing subtypes of neutrophils dedicated to specific tissues, roles, and disease pathologies (Wright *et al.*, 2017; Evrard *et al.*, 2018; Ballesteros *et al.*, 2020). The concept of neutrophil subtypes in disease was briefly described in Section 1.2.2 discussing the specific phenotype of neutrophils in ARDS and LDLs in rheumatoid arthritis

(Juss *et al.*, 2016; Wright *et al.*, 2017). Genome sequencing has been able to greatly increase our understanding of neutrophil heterogeneity in core functions. As neutrophils proliferate and mature in the bone marrow, specific transcriptional programmes can be identified based on developmental stage (Evrard *et al.*, 2018). Further work has refined this idea and characterised eight sub-populations across the potential lifespan of a neutrophil, encompassing stage of maturation, cell function and fate using single-cell RNA sequencing (Xie *et al.*, 2020). These subtypes encompass five stages of neutrophil lifespan, named G0-G5 and overlap with those discovered by Evrard *et al.,* (2018). G0-2 neutrophils are precursor neutrophils capable of mitotic division and are found in the bone marrow. G3 and 4 cells are still post-mitotic premature neutrophils capable of differentiating into further G5 cells in the bone marrow. The mature G5 neutrophils are split into a further three subtypes and predominately exist in the peripheral blood and spleen but can be found in the bone marrow. G5 neutrophils show upregulation of genes associated with migration and immune responses, as well as a specific population in the spleen that show increased expression associated with interactions with adaptive immune cells such as antigen presentation. G5a neutrophils appear to mature from only the G3 population, whereas G5b can come from either G3 or G4. The G5c population are the final stage of the neutrophil subtypes and show high expression of ageing and apoptosis markers. Three distinct populations of intravascular neutrophils have also been observed using 4D imaging but without sequencing an overlap is unconfirmed (Crainiciuc *et al.*, 2022). 4D imaging using intravital microscopy with antibody labelled neutrophils across multiple time points. When exposed to bacterial challenge, all subtypes were able to show upregulation of genes and functions associated with bacterial clearance relative to the subtype, for example, G4 and G5 subtypes show increased expression of pro-inflammatory cytokines, whereas the G1 subtype showed an increase in proliferation.

Neutrophils are not only defined by their stage of maturity or how they can respond to infection. While neutrophils are mainly considered to mature in the bone marrow and then migrate into the peripheral blood where they perform pathogen sensing roles, neutrophils are adapted to reside in specific tissues (Ballesteros *et al.*, 2020). Neutrophils from the bone marrow, blood, spleen, intestine, lung, and skin were analysed to examine specific profiles. Transcriptional and epigenetic landscapes were examined, and specific profiles were found depending on the site the neutrophil was taken from with new functions arising depending

on the tissue. Imprinting of these profiles was found to occur within the resident tissues, with neutrophils of the peripheral blood failing to show any tissue specific markers and transplanted bone marrow neutrophils taking on the phenotype associated with the site of injection. These data further challenge the notion of neutrophils as a homogenous population and present possible areas for treatment of diseases. Either targeting or inducing specific neutrophil sub-types by altering transcriptional patterns may allow for treatment of specific diseases, for example targeting lung-specific neutrophils in COPD.

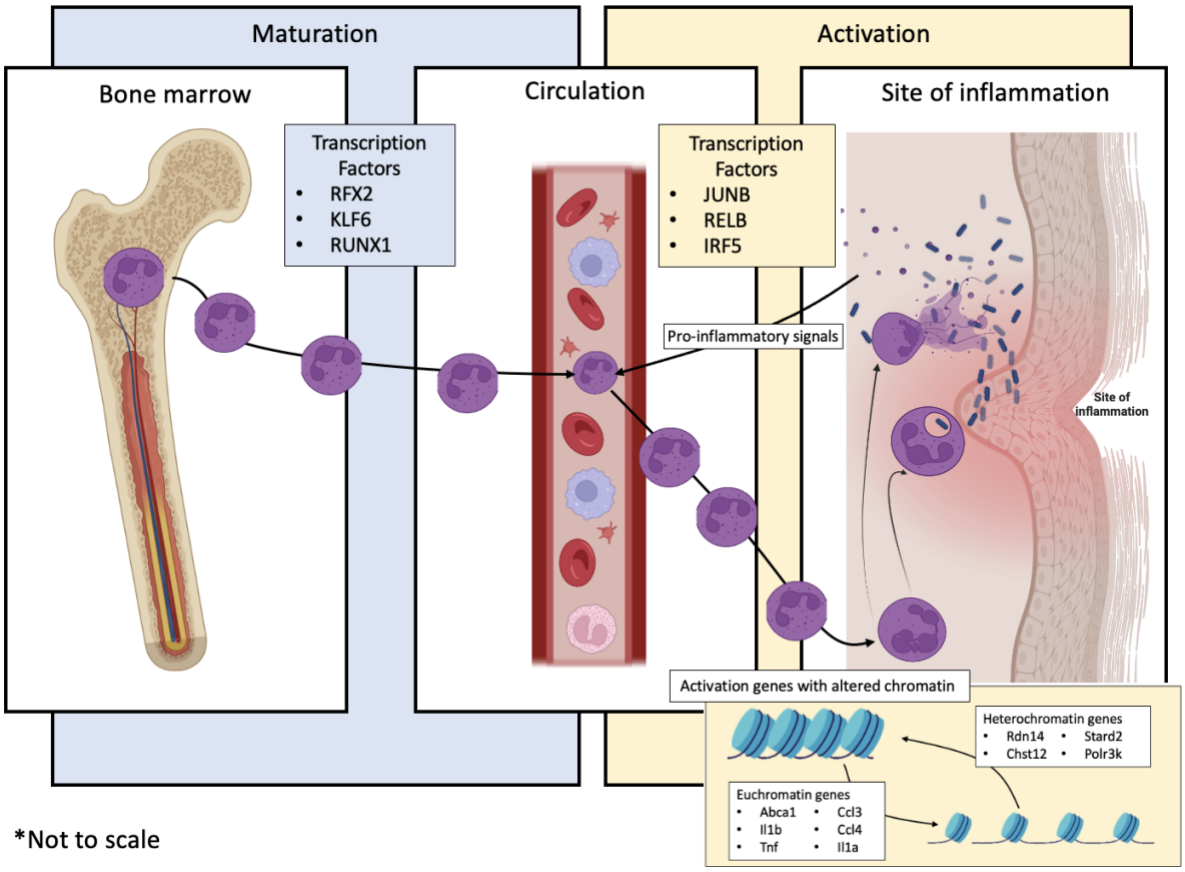

Figure 1.1. Summary of the role of transcription factors in neutrophil maturation

Diagram showing the role distinct transcription factors play in neutrophil maturation from the bone marrow to the circulation (blue boxes), in activation following sensing of proinflammatory signals causing migration from the circulation to the site of inflammation (yellow boxes) and how chromatin is opened and closed during activation at key effector genes (Khoyratty *et al.*, 2021). Figure created using premade assets from BioRender in PowerPoint.

For neutrophils to be able to present these subtypes, large scale changes occur in transcription factor networks and gene expression. For these changes to occur, there must be regulation of transcription factor and gene expression. Identifying the changes in gene expression that promote differentiation into specific subtype will improve our understanding of neutrophils as a heterogenous population.

1.2.3.a. Neutrophil subtypes in action

The above work shows the classification of neutrophil subtypes by transcriptional programme and by the niche the cells are found in (Evrard *et al.*, 2018; Khoyratty *et al.*, 2021; Crainiciuc *et al.*, 2022). However, identifying the role these subtypes play in neutrophil effector functions is just as important and may allow for manipulation of phenotype for the development of novel therapies. Section 1.2.2. describes how some diseases are associated with specific neutrophil subtypes such as low-density granulocytes in rheumatoid arthritis (Wright *et al.*, 2017). Furthermore, in tumour microenvironments two populations of neutrophils exist, a pro-inflammation, anti-tumour N1 neutrophils and a pro-angiogenesis, pro-tumour N2-neutrophil (Kubes, 2018). However, questions remain about subtypes in homeostatic functions.

In neutrophil recruitment, pro-inflammatory neutrophils and pro-angiogenic neutrophils like those in cancer have been observed in local tissue but not blood in specific experimental conditions in mice with much more work required to identify whether these neutrophils are an effect of a specific experimental treatment. Furthermore, specific bacterial stimuli have been shown to potentially promote effector functions (Kubes, 2018). *S. aureus* stimulation can drive NET formation in 25% of neutrophils in *in vivo* mouse and human *in vitro* models and $CD177^{+}$ neutrophils an example of a subtype that on detection of bacterial stimuli is better suited to bacterial killing (Pilsczek *et al.*, 2010; Christoffersson *et al.*, 2012; Yipp *et al.*, 2012; Wu *et al.*, 2016; Zhou and Liu, 2017). Work has also demonstrated how stimuli can alter neutrophil response pathways to give what may be thought of as subtypes by altering epigenetic programming to deal with specific pathogens and this will be discussed in more detail later in this introduction (Denholtz *et al.*, 2020)

One concept is that of the anti-inflammatory neutrophil, a subtype of neutrophil that aids in the promotion of inflammation resolution and recruitment of other immune cells (reviewed in Loh and Vermeren, 2022). Specific forms of neutrophil apoptosis are examples of how neutrophils may undergo transcriptional reprogramming to carry out specific functions. Phagocytosis of opsonised pathogens can trigger neutrophil differentiation leading to phagocytosis induced cell death (PICD). In sterile inflammation, insoluble and pro-inflammatory immune complexes are also taken up by neutrophils and cell death pathways are induced. In both cases, pro-inflammatory complexes are removed from the affected tissue reducing local inflammation. In these scenarios, neutrophils undergo apoptosis – a form of cell death that is part of the normal neutrophil life cycle. Relative to other forms of neutrophil death such as NETosis, because neutrophil apoptosis maintains plasma membrane integrity, pro-inflammatory agents are not released into the tissue as the cell dies. Furthermore, PICD or immune complex induced neutrophil apoptosis both trigger an anti-inflammatory cascade by recruiting macrophages that engulf the neutrophils via efferocytosis and induces macrophage polarisation to the pro-resolution M2 phenotype aiding in repair and a return to homeostasis.

These present examples of what were previously thought to be terminally differentiated neutrophils undergoing specific transcriptional reprogramming to have new functions – what can therefore be seen as a subtype. An important question however is whether these are true subtypes of neutrophils or just stages in the neutrophil life cycle defined by changes in transcriptional networks and response to stimuli such as cytokines or pathogenic material. As part of the functional lifespan of a neutrophil it matures, activates, and dies like many cells in the body. In fact, plenty of cells go through this pathway, but are not defined by subtypes. Developing a true definition of subtype versus stage of the lifecycle would greatly aid in answering this question and furthering our understanding of neutrophil behaviour.

1.2.4. Models of neutrophil function

As mature neutrophils are very short-lived cells, it is technically challenging to directly assess human neutrophil function direct from patient blood samples. There are several models of neutrophil function that can be used each with their own pros and cons.

1.2.4.a. Primary human neutrophils

Human neutrophils can be cultured *in vitro* following isolation from human blood samples (Sabroe *et al.*, 2004). As these are human cells, they contain identical genetic pathways to human cells *in vivo* and provide the best percentage genetic homology compared to any model. However, they are short-lived cells that can go through activation and apoptosis very easily either naturally or due to improper or aggressive handling and cannot be genetically altered using technologies such as CRISPR/Cas9 (Henry *et al.*, 2013). *In vitro* primary human cell culture can also never fully replicate the tissue microenvironment and therefore important regulatory factors may always be missed, altering function accordingly.

1.2.4.b. Cell culture

Neutrophil-like cell lines were developed with the aim of minimising some of the limitations of primary cells. Two commonly used cell lines were developed from acute myeloid leukaemia (AML) patients (Rincón, Rocha-Gregg and Collins, 2018). HL-60 cells are a myeloblast-stage cell line that, when exposed to retinoic acid, can differentiate into a neutrophil-like state (Manda-Handzlik *et al.*, 2018). When differentiation is induced, HL-60 cells display nuclear chromatin condensation and segmentation, as well as gene and protein expression profiles like human primary neutrophils. These are often used for studies of phagocytosis and chemotaxis. PLB-985 cells were developed from a different AML patient. Again, these have similar gene expression profiles to human primary neutrophils but have different properties to HL-60 cells and are used to study ROS production and chemotaxis. Much like primary cell lines, there are questions behind their function and activity, relative to human primary cells. There are also questions behind the differentiation protocols used with no gold-standard protocol, however studies have attempted to develop a better protocol (Rincón, Rocha-Gregg and Collins, 2018).

1.2.4.c. Murine models

Robust *in vivo* models are required to overcome *in vitro* difficulties discussed above and would be a valuable tool in the laboratory for studying homeostasis and disease.

Mouse (*Mus musculus*) models can be used for both tracking and/or depletion of neutrophils (reviewed by Stackowicz, Jönsson and Reber, 2019). Depletion of neutrophils is beneficial for

studying a system when neutrophils are absent and identifying key pathways accordingly. Ablation of neutrophils can be achieved by genetic or chemical methods to gain either constitutive or inducible neutropenia. Chemical approaches include drugs such as cyclophosphamide that ablate the native haematopoietic stem cell population and neutrophils as a result. Genetic approaches involve the knockdown of genes essential to neutrophil function such as CXCR2 or myeloperoxidase (MPO). However, there are limitations to these methods, as many do not completely ablate the neutrophil population and many of the chemical methods require repeated administration that may stress the mouse and alter its immune pathways. Secondly, ablation of neutrophils can have off target effects that will significantly alter the health of the mouse. For *in vivo* tracking, luminol can be administered to mice. The luminol is taken up by neutrophils and is oxidised by ROS generated within phagosomes by MPO. When the luminol is oxidised, it generates a luminescent signal allowing for the neutrophil to be traced. However, luminol tracing also has its limitations. First, MPO is not specific to murine neutrophils and is expressed in macrophages meaning the wrong cells may be observed. An alternative is to use intravital technologies to trace pre-stained neutrophils deep in mouse tissues. Intravital imaging can examine neutrophils kinetics and neutrophilic responses to inflammation. There are also limitations to intravital imaging. First, any of the processes intravital imaging observes requires the repeated administration of tracking or labelling molecules, such as antibodies or transplant of pre-labelled cells. Second, the imaging is more complicated relative to that of other models. Both limitations raise concerns when it comes to the wellbeing of the animal, for example, stressing the animal, which has the potential to alter responses of neutrophils as a side effect.

1.2.4.d. Zebrafish as a model to study neutrophil function.

Zebrafish (*Danio rerio*) provide a valuable model for the *in vivo* study of immune function (Henry *et al.*, 2013). The mammalian immune system has rapidly developed in complexity from an evolutionary standpoint in a relatively short period of time (Renshaw and Trede, 2012). The zebrafish immune system provides a simpler evolutionary model for understanding the core functions of immunity while retaining many key features (Table 1.2). While the early immune system in mammals develops *in utero*, providing several challenges for live study, the zebrafish system develops following external fertilisation and so can be observed using live imaging (Traver *et al.*, 2003). Zebrafish larvae are especially well-suited

for studying innate immunity. Firstly, larvae do not develop adaptive immunity until 4 weeks post-fertilisation, so innate immunity can be studied in isolation (Henry *et al.*, 2013). Secondly, the larvae are transparent allowing for easy *in vivo* imaging, so the blood circulation and fluorescent transgenic labelling can be observed readily using microscopy, allowing for the monitoring of leucocyte behaviour in detail. Thirdly, they are relatively easy to genetically modify to create transgenic lines. Finally, zebrafish also have high conservation with the human genome, providing a robust homolog for *in vivo* study without the increased resource impact of using murine or other mammalian models as more zebrafish can be housed and maintained relative to the same resources for a mammalian *in vivo* model.

Feature	**Zebrafish**
Immune development	Following external fertilisation
Isolated Innate immune system	For 4 weeks post fertilisation
Major blood cell linages	All
Neutrophil response to chemokines	Yes
Neutrophil killing mechanisms	Degranulation, NETosis, phagocytosis
Neutrophil apoptosis	Yes
Neutrophil inflammation resolution	Yes
Fluorescent imaging	Yes
Genetic manipulation	Yes

Table 2.2. Key examples of why zebrafish are a suitable model for live study of neutrophils.

Examples of characteristics which make zebrafish a suitable model for neutrophil study, especially in the context of this project. (Traver *et al.*, 2003; Renshaw and Trede, 2012; Henry *et al.*, 2013)

Over the past 15 years, the Renshaw group have taken advantage of the above properties to develop many zebrafish transgenic and mutant lines for observing neutrophil and overall immune system behaviour, both during homeostasis and dysregulation (Renshaw *et al.*, 2006). Perhaps the most useful tool and assay for neutrophil function is tail fin transection using the *Tg(mpx:GFP)i114* reporter line which specifically labels neutrophils with green

fluorescent protein (GFP). For this assay, the larval tail fin is amputated posterior to the circulatory loop and neutrophil function is monitored over time (Renshaw *et al*., 2006). The properties that can be observed include migration to the wound site, ROS production, apoptosis, and reverse migration (Renshaw *et al.*, 2006; Ellett *et al.*, 2015; Robertson *et al.*, 2016). Regeneration of the tailfin itself can also be monitored and therefore potential disruption to regenerative pathways can be evaluated easily. Techniques such as fluorescent labelling of neutrophil-specific gene expression allow for these observations to be made. Genetic manipulation by knockout can be easily performed and knock-in of genes is possible though more complicated. In the past, modified Morpholino oligomers (Morpholino/MOs) were used for this but it is commonplace now for CRISPR techniques to be used, as they are generally efficient and specific with fewer off target effects relative to MOs. Chemical and pharmacological manipulation can easily be performed by adding compounds to the fish media and observing how neutrophil function is altered (Robertson *et al.*, 2014). Alternatively, compounds can be injected directly into the larval circulation. Genetic and chemical manipulation can be used either separately or in combination. Zebrafish models still have limitations when it comes to the effects of stress on the animal. Stress responses are evolutionarily conserved and this needs to be considered when designing experiments to ensure that pathways are not negatively affected and results skewed due to stress responses (Chin *et al.*, 2019). Examples of factors that alter zebrafish stress levels include holding densities in tanks and there are examples of stress going on to alter sperm quality and gene expression in progeny (Andersson *et al.*, 2022; Valcarce *et al.*, 2023).

Zebrafish provide a robust *in vivo* model for understanding sensitive, short-lived activated neutrophils. Zebrafish transparency, the ease at which larvae can be manipulated and their high fecundity provides a great opportunity for modelling changes at the molecular level. Not only do the tools already exist for analysing immune cell function, such as the *Tg(mpx:GFP)i114* line, but the short development period and small size make them an excellent tool for analysis of genetic and chemical manipulation.

1.3. Chromatin and the epigenetic regulation of gene expression

1.3.1. Chromatin structure

Each human cell contains about three metres of genomic DNA if it was laid out end to end. Every nucleated cell contains that entire length of DNA yet is microns in size (Chen *et al.*, 2017). For DNA to fit into the nucleus, it must be tightly packaged and not every gene can be readily available for transcriptional machinery to access it. DNA strands are packaged around protein cores that allow for tight packaging of DNA into chromosomes. This nucleoprotein complex is known as chromatin.

Histones form the protein core that DNA is wrapped around to form chromatin. Histones form specific structures with DNA with each collection of eight histones – two copies of H2A, H2B, H3 and H4 – occupied by 146-147 bp of DNA to form a 10 nm nucleosome. To package the entire length of DNA, each nucleosome is linked by a variable length of DNA and H1 linker histone (Mariño-Ramírez *et al.*, 2005). Further packaging then structures nucleosomes into 30 nm chromatin fibres, that are again packaged to form chromosomes. Various modifications to amino acids and histones allow for interactions to form between the stands and alter conformation (Luger, Dechassa and Tremethick, 2012). Once genomic DNA is packaged, specific modifications are required to switch genes on and off depending on which are needed, at that is where epigenetics comes in.

1.3.2. Types of Epigenetic regulation

Within the 3 metres of genomic DNA in every nucleated cell there are ~20,000 genes coded within it (Chen *et al.*, 2017). Cells are specifically regulated to express specific genes to define and control cellular function and one of the methods of regulation is epigenetic modifications, regulation of gene expression by heritable modifications beyond the DNA coding level. An individual's collection of epigenetic modifications is referred to as the epigenome and can be split into three types of modification: DNA methylation, post-translational modifications, and non-coding RNAs.

1.3.2.a. DNA Methylation

The most common epigenetic modification in mammalian cells is DNA methylation and involves chemical alterations directly at base sequences. DNA is methylated at three base pair CpG sites, where a methyl group is attached to the C5 position of the cytosine residue of the CpG (Bird, 1986). The methylation process is carried out by DNA methyltransferases (DNMTs) and can be reversed. Hypermethylation leads to transcriptional repression by preventing the recognition of DNA by transcription factors or promoting the binding of transcriptional repressors leading to a down-regulation of a gene (Portela *et al.*, 2013). Methylation is a heritable process as is maintained during cell replication to conserve epigenetic regulation and subsequent phenotype throughout multiple generations (Handy, Castro and Loscalzo, 2011).

1.3.2.b. Post translational histone modifications

Chromatin conformation can be altered to dictate gene expression. Chromatin can be arranged in two ways, with properties associated with function. Heterochromatin is tightly-packed chromatin that represses transcription as the conformation prevents the binding of transcriptional machinery and association of enhancers and promoters with coding sequences. In contrast euchromatin is loosely packed and promotes transcription by allowing transcriptional machinery to bind coding regions and bring promoters and enhancers closer together using proteins such as cohesins. There are many ways that the histone core can be modified, and these accumulate to give the “Histone Code Hypothesis” (Jenuwein and Allis, 2001). The hypothesis states that different combinations of modifications such as phosphorylation, acetylation, and methylation, lead to reversible and heritable regulation of chromatin structure and transcription by driving repression or promotion of gene expression. One example of modifications that promote transcription is acetylation of H3 and H4 lysine. Acetylation is carried out by histone acetyl transferases (HATs) such as CREB binding protein (CBP) and EP300. When gene transcription is needed these HATs recognise transcription factors that bind specific DNA sequences and are recruited to histones to catalyse the addition of acetyl groups to the correct lysine residue and conversion of heterochromatin to euchromatin. These acetylated lysine residues can then be recognised by bromodomain containing factors such as BRD4, which then mediate formation of complexes that activate transcription (Wu and Chiang, 2007). When the gene associated with the acetylated lysine

residue is no longer required, signals from DNA binding proteins and repressor complexes, recruit histone deacetylases (HDACs) to remove the acetyl group and return the section of chromatin to heterochromatin (Kao *et al.*, 2000). Lysine residues can also be methylated by chromatin remodelling enzymes. Lysine methylation is more complex modification as it can promote both formation of euchromatin or heterochromatin depending on the site of methylation. The addition of methyl groups is carried out by histone lysine methyltransferases which can add multiple methyl groups to a single lysine to give varying effects depending on the need for repression or promotion of expression. Examples of modifications are tri-methylation of lysine 27 in H3 (H3K27me3) which is repressive, whereas trimethylation of H3K4 promotes transcription. Addition of modifications promote the recruitment of complexes that alter chromatin dynamics leading to open or closed structures. When that confirmation needs to be altered, methyl groups can be removed by lysine demethylases (Handy, Castro and Loscalzo, 2011).

1.3.2.c. Non-coding RNAs

The third mechanism of epigenetic modification bis by binding of non-coding RNAs that are sub-categorised into long non-coding and small non-coding RNAs. Long non-coding RNAs (lncRNAs) recruit remodelling complexes that can alter histone modification pathways such as methylation and deacetylation. Small non-coding RNAs (sncRNAs) are further split into microRNAs, small inhibitory RNAs (siRNAs), and piRNAs that can associate with RNA silencing argonaute proteins and recruit complexes that can epigenetically modify DNA and histones (Kim *et al.*, 2006, 2008; Hawkins *et al.*, 2009).

The three methods above show the basis by which epigenetic changes control gene expression. These mechanisms are heritable and dynamic and can be altered by many different factors altering cell phenotype across the body. The focus here is on post-translational histone modifications and chromatin remodelling.

1.3.3. A brief overview of how chromatin remodelling regulates the innate immune system.

Understanding how immune cells are epigenetically regulated can help unravel the transcriptional pathways that drive cell function. In many immune cells this is poorly characterised but presents the opportunity to discover druggable targets for regulating immune function.

Epigenetic sequencing of immune cells has identified that cells have specific chromatin profiles associated with cell function and activity. Analysis of histone modifications of neutrophils and monocytes from the innate immune response and $CD4^+$ naïve T cells from the adaptive immune response from healthy donors with a mean age 55 were performed (Chen *et al.*, 2016). Genome, DNA methylation and histone modifications were analysed, and the focus here will be on the neutrophil and macrophage chromatin remodelling data. ChiP-seq used antibodies for H3K4me1 and H3K27ac to profile poised enhancers and active enhancers and promoters. Specific profiles were found for each type of cell by coordinating the genetic and chromatin profile. The chromatin profile was associated with the function of the cell, for example, monocytes had active chromatin marks for inflammasome formation and signalling such as NF-κB. Assessment of human foetal chromatin accessibility expanded the knowledge of chromatin profiles for innate immune cells (Domcke *et al.*, 2020). Analysis of blood cells using single cell ATAC-seq found specific profiles for dendritic cells, NK cells and macrophages, with the macrophages further split into tissue-specific macrophages and phagocytic macrophages in line with mouse data previously produced (Cusanovich *et al.*, 2018). However, other innate cell types such as neutrophils are missing and no further information into the profiles are provided. On the other hand, the data produced by Domcke *et al.,* (2020) has been made publicly available as a searchable database (https://descartes.brotmanbaty.org/bbi/human-chromatin-during-development/).

In terms of performing deep dives into these chromatin events, work is mostly limited to macrophages. Chromatin remodelling enzymes such as members of the KDM family, SETD methyltransferase, HDACs, HATs and p300 have been implemented in the macrophages behaviour such as the antiviral response, responses to LPS such as cytokine production, transcription of secondary response genes and inflammation resolution (reviewed by Zhang and Cao, 2019). As many of the genes involved in macrophage function such as cytokines and

pro-inflammatory transcription factors are also present in neutrophils and other innate immune cells, a question is whether there is conservation in the regulatory processes or if regulation of chromatin at specific loci are cell specific.

1.4. Neutrophil chromatin remodelling

1.4.1. The current picture of neutrophil chromatin remodelling

Due to the sensitivity of neutrophils, profiling of the neutrophil epigenetic and transcriptional landscape is limited. However, over the past 5-10 years, groups have begun to develop a basic understanding of neutrophil chromatin remodelling during maturation and activation by using more refined techniques for sample preparation such as sequencing library preparation suited to sensitive and low concentrations of material, and prevention of spontaneous apoptosis by working at low temperatures allowing for detailed sequencing (Kenyon *et al.*, 2017; Denholtz *et al.*, 2020; Khoyratty *et al.*, 2021). While many of these preparations require expensive kits and a high throughput of animals/cells, they begin to shed new light on neutrophil biology.

Perhaps the most interesting discovery in neutrophil epigenetics is the role chromatin remodelling plays in neutrophil maturation and activation. Work has analysed how chromatin is remodelled following pro-inflammatory stimuli (Denholtz *et al.*, 2020). *In vitro* neutrophils were treated with PMA – a neutrophil activating protein kinase C – and microbially challenged using *E.coli,* changes to nuclear architecture were then observed and transcription factor binding analysed (Denholtz *et al.*, 2020). On treatment with either PMA or exposure to *E*. *coli*, the neutrophils showed a shift in chromatin folding dependent on the treatment. PMA treatment did not result in large-scale changes from heterochromatin to euchromatin but did increase interchromosomal interactions and an increase in euchromatin structure within already formed euchromatin, most notably in complement receptors, cell migration and lysosomal pH. *E. coli* treatment showed a similar chromatin architecture to PMA in terms of a lack of euchromatin/heterochromatin switching or chromosomal association, but an increase in euchromatin formation within euchromatin compartments. This included in genes for cytokines, chemokines, degranulation, and the inflammatory response. Comparing the two data sets showed only partial overlap between the sites of rearrangement in the

euchromatin showing euchromatin rearrangement is specific to the stimuli. Further analysis of specific loci post-*E.coli* exposure found an increase in the euchromatin characteristics of the chemokine (C-X-C motif) ligand (CXCL) locus with increased interactions, CCCTC-binding factor (CTCF) occupancy (transcription factor binding), cohesin occupancy (mediation of DNA looping), and increased gene expression. It was also shown that areas that undergo euchromatin changes are associated with neighbouring areas that are altered. Enhancer binding was then analysed using H3K27ac deposition (chromatin mark for active enhancers), cohesin binding, and SMC3 (mediation of DNA looping) and CTCF occupancy. Active enhancers were found to be associated to genes that correlated with earlier findings such as cytokines, chemotaxis, and degranulation. These data show that upon stimuli, neutrophils undergo extensive remodelling and enhancer activation to drive removal of pathogens by activated neutrophils.

Work has also looked at maturation and activation of neutrophils in mammalian systems. As neutrophils mature, they migrate from the bone marrow and into the circulation and on sensing of threats migrate further into inflamed tissue. These two key transition points have been profiled for changes in the chromatin landscape using a model of acute inflammation in the murine lung (Khoyratty *et al.*, 2021). It was found that during neutrophil activation that both bone marrow-blood and blood-inflamed tissue are accompanied by chromatin remodelling, consisting of a mixture of opening, and closing of chromatin peaks as profiled by ATAC-seq. When analysing the genes associated with these remodelling events, the bone marrow-blood events showed increased accessibility at genes associated with antigen presentation and metabolic activity, whereas the blood-tissue transition showed increased accessibility at genes associated with the inflammatory response and signalling pathways. Transcription factors associated with these two transition points were identified based on the clusters of differentially accessible chromatin peaks – mainly at transcription factor loci. Bone-blood was regulated by RFX2, KLF6 and RUNX1, whereas blood-tissue was regulated by JUNB, RELB and IRF5. *In vitro* Clustered Regularly Interspaced Short Palindromic Repeats (CRISPR)/CRISPR associated protein-9 (Cas9) knockdown of these transcription factors in HoxB8 neutrophil progenitors further validated the transcriptional pathways in the transition steps. In the bone marrow-blood transition, the transcription factors Krueppel-like factor 6 (KLF6) and runt-related transcription factor 1 (RUNX1) regulate neutrophil maturation and

migration, with maturation associated reduction in *Mpo* expression not seen and heightened mitochondrial activity relative to control maturing cells and a significant reduction in Cas9 knockdown cell migration relative to WT controls. Comparison of RNAseq and ATAC-seq following knockdown of transcription factors RELB, IRF5 and JUNB found the pathways essential to blood-tissue transition. Neutrophil adhesion and transendothelial migration genes were affected by knockdown and further analysis of phenotype of the knockdown cells showed that neutrophil effector mechanisms such as ROS production, phagocytosis and NETosis were all reduced, as was associated gene expression. Pro-inflammatory cytokine expression was also decreased following knockdown of transcription factors, particularly *Il1b*. Transplantation of transcription factor knockdown neutrophils into murine lung pouches and subsequent analysis of activity mirrored what was seen *in vitro* for both bone marrow-blood and blood-tissue neutrophils. Taken together, these data show how essential chromatin remodelling is at key neutrophil checkpoints to drive activity and identified essential transcription factors and the pathways they regulate in response to inflammatory signals.

These data discussed above show how chromatin remodelling events are essential to regulating neutrophil function (Denholtz *et al.*, 2020; Khoyratty *et al.*, 2021). At specific stages in neutrophil activity, remodelling events increase accessibility of chromatin at key genes for the function that needs to be carried out and specific transcription factors are involved, further events then remodel the chromatin for the next stage in neutrophil maturation and drive effector mechanisms. However, there are many questions still to be answered. The role specific chromatin marks play in driving confirmational changes is largely unknown and the chromatin remodelling enzymes required are therefore unknown. The role these events play in disease is also largely unidentified. Finding regulators of these events presents potential druggable targets for treating disease and inflammatory dysfunction.

1.4.2. Trained neutrophil immunity: Reprogramming of neutrophils following infection and vaccination.

There is evidence that infection can alter the neutrophil epigenome (Moorlag *et al.*, 2020). Exposure to pathogens has been shown to provide trained immunity to neutrophils as seen by response to secondary infection. Trained immunity has been shown following bacille Calmette-Guérin (BCG) vaccination, shigella infection and mathematically modelling following

Lipopolysaccharide (LPS) exposure, with chromatin remodelling implicated in BCG vaccination exposure (Willis *et al.*, 2018; Moorlag *et al.*, 2020; Ciupe *et al.*, 2021).

The BCG vaccine against tuberculosis has been shown to impart trained immunity onto macrophages and NK cells for up to one year, which allows for better protection against non-related infections. This information was lacking for other innate immune cells. Therefore, mature neutrophil function following administration of the BCG vaccine was analysed and provided a first look at the remodelling events that drive trained immunity in neutrophils (Moorlag *et al.*, 2020). Blood from BCG treated individuals was shown to have higher total neutrophil number from 2 weeks to 3 months with flow cytometry identifying a specific subgroup that dominates over that period. When exposed to secondary stimuli *ex vivo*, these neutrophils showed changes to phenotype. Bacterial or fungal infection, led to increased degranulation, release of pro-inflammatory cytokines, ROS production and phagocytosis. Analysis of the reasons for these changes found that trained neutrophils had an increase in H3K4me3 – a mark for increased transcription – at JAK-STAT signalling promoters such as those found in pro-inflammatory signalling. H3K4me3 is also increased at promoters for metabolic processes. They hypothesise that the targeting of specific promoters is driven by lncRNA interactions, but this hypothesis requires further work to confirm anything more than correlative association. Developing therapies to target specific chromatin marks may provide advances in understanding trained immunity and altering immune function to fight disease. However, base knowledge of what marks do is essential to developing these treatments, as unknown secondary changes may result in unwanted side effects. Furthermore, treatments must be specific as the role of chromatin marks at specific loci is not universal in all cell types. Deposition and removal of chromatin marks must be specific to target cell types to prevent alteration of gene expression in other, healthy cell types. Several compounds are in various stages of pre-clinical and clinical trials for use as chromatin remodelling agents, particularly in cancer therapy, however time will tell if these are options for treatments in the future and whether they may be repurposed for other conditions (Kaur, Daoud and Eblen, 2019).

These data show how environmental exposure and not just neutrophil genetics are essential to cellular function and can drive responses to inflammation and driving a return to immune homeostasis. While previous examples have looked at negative influences, this shows positive

changes that aid neutrophil function (Moorlag *et al.*, 2020). Understanding how environment alters neutrophil function through chromatin remodelling is another strategy in finding preventative strategies for inflammatory diseases and infection as this trained immunity may be able to be used in a healthcare setting.

1.5. Ageing, functional decline and the epigenome

1.5.1. Defining ageing

Ageing is defined as the progressive loss of cellular homeostasis leading to whole body functional decline (Benayoun *et al.*, 2019). Ageing occurs in almost all species, but happens at different rates, suggesting that the ageing timeline is not universal and involves multiple factors and triggers. These factors can include genetics and environment (Benayoun, Pollina and Brunet, 2015). The evolutionary reason for ageing is highly debated and several ideas have been posed over time. The key question surrounds the fact that much of the ageing process occurs after reproductive maturity, ruling out selective pressure on the ageing process. Three major theories pose an answer to this question.

Mutation accumulation theory suggests that ageing is caused by accumulation of damage that only manifests later in life and so is not seen during an organism's reproductive prime (Gavrilov and Gavrilova, 2002). Antagonistic pleiotropy suggests that mechanisms of ageing have a benefit to reproductive viability early in life, hence they have remained in the gene pool (Williams, 1957). Finally, disposable soma theory posits that an organism has a finite number of resources to maintain homeostasis and as these resources decline, ageing becomes more pronounced (Kirkwood, 1977). But while the evolutionary theory will likely be debated for years to come, the mechanisms that drive ageing can be identified and many have been outlined as the Hallmarks of Ageing, an evolving list of key drivers of ageing (López-Otín *et al.*, 2013, 2023).

1.5.2. Age-related functional decline and changes to cells and tissues

1.5.2.a. Defining functional decline.

Functional decline is driven by age-related loss of physical and cognitive ability leading to reduction in a person's ability to perform activities of daily living (ADLs) (Hastings and Heflin, 2005). ADLs are activities a person relies on for independence and include walking, washing, grocery shopping, and preparing food, and socialising (Abdulaziz *et al.*, 2016). As functional decline sets in and the ability to perform ADLs reduces, quality of life is subsequently reduced, and individuals see a significant decline in both physical and mental health. Onset and severity of functional decline is a predictor for hospitalisation with severity linked to length of stay and risk of mortality and is driven by both natural ageing and age-related disease (Sutton, Grimmer-Somers and Jeffries, 2008). Preventative interventions to address functional decline can increase the time a person can live unassisted (Hébert, 1997). Understanding the cellular drivers of functional decline will help to target tissue and system-specific areas of functional decline.

1.5.2.b. The Hallmarks of ageing: age-related cellular changes that drive functional decline.

Cellular homeostasis is maintained by many pathways that incorporate all organelles. As we age, some of these processes decline either due to signalling changes or alterations to organelle structure driving cellular dysfunction, senescence, or death. These processes are defined as the hallmarks of ageing (López-Otín *et al.*, 2013, 2023). Classification of the hallmarks of ageing are based on three criteria: first, that the change is seen during normal ageing, second, that by experimentally inducing the change, the model sees a decline in lifespan, and third, that by reversing the change, the model sees an increase in lifespan.

1.5.2.b.i. Telomere attrition

One element of cellular decline in ageing is telomere shortening. Telomeres are nucleotide tandem repeats found at the end of chromosomes that stretch up to 15 kb in humans (Srinivas, Rachakonda and Kumar, 2020). Telomeres and their associated proteins help to protect genomic DNA during replication. With each division an estimated 250 bp fragment of telomere DNA is lost in a process called "the end replication problem" – though this can vary

in cell type and under specific conditions such as rapid telomere attrition. Telomerase attempts to patch some of the lost DNA in a highly regulated process, but telomerase is found in very few mammalian somatic cells and the end of telomeres are protected from DNA break repair by proteins called shelterins to prevent chromosomal fusion (López-Otín *et al.*, 2013). Over time telomeres become too short due to the reduction or lack of telomerase action and the end replication problem and trigger cellular senescence – known as replicative senescence. High levels of replicative senescence in a tissue will lead to dysfunction and disrupt homeostasis, increasing the risk of morbidity (Liu *et al.*, 2019). As immune cells come from a highly replicative pool, this could be an important factor in age-related decline of neutrophils.

1.5.2.b.ii. Mitochondrial dysfunction

The mitochondria play a crucial part in maintaining cellular function, generating ATP for energy rich processes, and contributing mitochondrial DNA to the genome. Mitochondrial processes are reduced with age, reducing metabolic capacity and increasing harmful reactive oxygen species production (Sun, Youle and Finkel, 2016). Mitochondria generate ATP through the electron transport chain, a process that requires several enzyme complexes, integrity in the mitochondrial membrane and mitochondrial DNA. Over time, the components required for ATP generation in mitochondria are damaged and function is lost meaning respiration is reduced and therefore the amount of ATP available for cellular processes declines. Second, biogenesis and recycling of faulty mitochondria by mitophagy is altered leading to a reduction in new mitochondria and increase in dysfunctional mitochondria (López-Otín *et al.*, 2013; Palikaras, Lionaki and Tavernarakis, 2015). Another major factor associated with ageing and mitochondria is the generation of reactive oxygen species (ROS). While evidence has shown that ROS build up can be protective as seen in yeast and *C. elegans* build-up of dysfunctional mitochondria drives increased ROS production to a harmful level and promotes cellular decline (López-Otín *et al.*, 2013). At a whole tissue level this mitochondrial decline promotes reduced tissue function and low-grade chronic inflammation from ROS production. This phenomenon is particularly prominent in energy demanding tissues like the musculoskeletal system, brain, and central nervous system, as well as immune cells such as neutrophils as they require large amounts of ATP to maintain homeostasis (Grimm and Eckert, 2017; Gonzalez-Freire *et al.*, 2018).

1.5.2.b.iii. Genomic instability

During the ageing process there is a loss of genomic stability leading to DNA degradation. DNA is constantly exposed to both external and internal genotoxic factors such as endogenous ROS, infection, chemicals, DNA replication errors, and radiation. These assaults cause mutations to the genome that alter gene expression. While many of these changes are typically associated with development of cancers, they also promote cellular changes that promote senescence or apoptosis to drive tissue decline. Whereas in cancer development DNA damage response elements such as p53 are mutated leading to repeated replication of a damaged cell and tumour formation. In ageing, DNA damage response proteins are still functional and promote cell cycle arrest to prevent tumour formation and instead promote tissue function decline (Ou and Schumacher, 2018).Changes can also occur to the scaffolding that supports DNA within the nucleus. Changes to nuclear laminin alter the support for both chromatin and protein complexes that regulate genome stability leading to changes in nuclear architecture (López-Otín *et al.*, 2013). Neutrophils are transcriptionally active to respond to specific threats, if there is DNA degradation in key genes, it may hinder the response to infection and damage.

1.5.2.b.iv. Loss of Proteostasis

Proteostasis is the term used for maintenance of protein homeostasis. Processes of proteostasis maintain the stability of folded proteins and allow for the degradation and recycling of proteins that are no longer needed. Proteostasis is disrupted with ageing leading to an accumulation of misfolded and damaged proteins within ageing cells (Vilchez, Saez and Dillin, 2014). Folded proteins are often associated with chaperones that maintain structural integrity, in ageing the synthesis of these chaperones is reduced leading to a decline in protein structure and reduction in function that leads to reduced lifespan in both worm and fly experimental models (López-Otín *et al.*, 2013). As part of proteostasis, proteins that are damaged or no longer needed are ubiquitinated and degraded in the proteasome or taken up into an autolysosome and recycled through autophagy. These processes are disrupted in ageing either due to global reductions in transcription or specific mutations in crucial proteostasis genes (López-Otín *et al.*, 2013). Build-up and aggregation of damaged proteins

causes cellular senescence and promotes loss of tissue function with senescence able to promote inflammation (Sonninen *et al.*, 2020). Neutrophils synthesise and recycle a lot of proteins as part of their effector mechanisms and as such are susceptible to damage due to changes in proteostasis.

1.5.2.b.v. Deregulation of nutrient sensing

Nutrient sensing via the somatotropic axis allows cells to detect levels of glucose within the body using growth hormone (GH), insulin-like growth factor (IGF-1) and insulin known as the insulin and IGF-1 signalling pathway (IIS) (López-Otín *et al.*, 2013). The somatotropic axis is essential to cellular function as many processes require glucose for ATP generation and therefore situations must be tightly monitored to prevent nutrient starvation. In times of low nutrients, the IIS can reduce cell growth and metabolism, whereas in times of high nutrients the IIS promotes cell growth and metabolism. Early in life, components of the IIS are high, which promotes growth and development but decline into adulthood and later life and appear to have a protective effect (López-Otín *et al.*, 2023). While this process is normally protective, there is an argument that prolonged reduction may lead to damage as lost cells are not replaced and metabolism does not generate the energy for essential processes (López-Otín *et al.*, 2013). Conversely to this, increase IIS signalling can promote cell growth and increase processes such as telomere shortening and DNA damage that can in turn promote ageing (López-Otín *et al.*, 2023). Within the IIS pathway, several targets present options for therapies such as the mammalian target of rapamycin (mTOR) pathway, FOXO signalling and Sirtuin deacetylases which are all pathways with readily available pharmaceuticals that may be repurposed for preventing age-related changes in nutrient sensing. Another therapeutic option is regulating nutritional uptake through processes such as dietary restriction which have shown promise in invertebrate and mouse models for sustained reduction in IIS signalling (López-Otín *et al.*, 2023).

1.5.2.b.vi. Cellular Senescence

Cellular senescence is triggered by specific stimuli and causes the cessation of cellular reproduction combined with specific phenotypic changes (López-Otín *et al.*, 2013). The first example of observed senescence was due to telomere shortening brought on by repeated

passage of human fibroblasts in culture (Hayflick and Moorhead, 1961). The role of senescence is to prevent the replication of damaged cells – which may lead to cancer – and alert the immune system to recycle the damaged cell. Over time, other stimuli have been observed to trigger cellular senescence – many of which are hallmarks of ageing themselves – including DNA damage, bacterial or viral infection, mechanical stress, nutrient imbalance, mitochondrial damage and increased mitogenic signalling. Phenotypic changes include lysosomal expansion – which can be measured using staining for beta-galactosidase – increased reactive oxygen species, changes to the nuclear envelope, increased cyclin-dependent kinase inhibition, increased p21 and/or p16 expression, and the senescence-associated secretory phenotype (SASP) (López-Otín *et al.*, 2023). The SASP is a change in cellular transcriptional behaviour to increase the release of pro-inflammatory cytokines and promote immune clearance of senescence cells and promote tissue remodelling (López-Otín *et al.*, 2023). Like many hallmarks of ageing, cellular senescence is a protective process, but in ageing increased senescence causes problems (López-Otín *et al.*, 2013). An increase in senescent cells associated with ageing results in a lack of clearance that allows for inflammation to dominate and fibrosis to occur due the effect the SASP has on the microenvironment. Much like changes to nutrient sensing, senescence provides a potential therapeutic target to delay the onset of ageing using a family of pharmaceuticals referred to as senolytics. Senolytics kill senescent cells and recover the immune processes required to return tissue to homeostasis, a process that in mouse studies has increased life span and many of these compounds are now entering clinical trials (López-Otín *et al.*, 2023).

1.5.2.b.vii. Stem cell exhaustion

Stem cells provide a population of highly proliferative and differentially immature cells to repopulate microenvironments following tissue damage and cell death. Stem cell populations are often specific to the tissue and require a series of triggers to proliferate and differentiate to maintain homeostasis including immune cell populations from haematopoietic pools (López-Otín *et al.*, 2013). Across the lifespan, these populations of stem cells reduce and as a result the body's ability to repair after damage and normal cell turnover reduces (López-Otín *et al.*, 2013). The exhaustion of the stem cell pool can come from sustained proliferative signalling, such as increase IIS pathway factors and as a knock-on effect off telomere attrition and other hallmarks in stem cells leading to senescence (López-Otín *et al.*, 2023). Much effort

has gone into attempting to reprogramme old stem cells to be able to repopulate niches following damage in ageing models including mice, being able to transiently recover stemness may present a target to prevent age-related tissue decline (López-Otín *et al.*, 2023).

1.5.2.b.viii. Alterations in intercellular communication

Cells within the body are constantly communicating to maintain homeostasis. Cells do this by the release of signalling molecules such as growth factors, cytokines, and hormones (López-Otín *et al.*, 2013). Most notably in ageing is perhaps changes to immune communication in the form of inflammageing and that is explored in more detail below. There are other examples, with contagious ageing being the idea that changes in one tissue can cause changes in the other due to bystander effects of senescent cells acting through gap junctions (López-Otín *et al.*, 2013). Also, there are several changes in endocrine axes, with reductions in certain hormones altering cellular function such as the changes to the IIS discussed above (Section 1.5.2.b.v). Changes in release of neurotransmitters can alter nervous communication and as a result alter cognition and behaviour and ECM changes are also seen with changes to matrix proteins altering tissue structure (López-Otín *et al.*, 2023).

1.5.2.b.ix. Dysbiosis

In 2023, López-Otín *et al.*, further expanded on the hallmarks of ageing based on the outlines set out in their 2013 review. Dysbiosis was added as a new hallmark. Over the past decade, our understanding of the importance of the microbiota in health and disease has greatly increased. Not only does the microbiota communicate internally, but it also communicates with cells of the body to maintain homeostasis. Our microbiota is established in childhood based on a mixture of genetic and environmental factors, once established it remains relatively unchanged until later in life, when diversity is reduced (López-Otín *et al.*, 2023). However, there is debate over what the microbiota for healthy ageing looks like, with long lived and healthy individuals showing unique microbiota relative to those of people of advanced age and ill health, who show more characteristic microbiota. Identifying the microbiomes associated with healthy ageing and maintain specific systems may provide potential anti-ageing therapies using treatments such as pre- and probiotics and faecal transplants (López-Otín *et al.*, 2023). Of relevant interest to this project may be finding

associations between the crosstalk of the microbiome and the immune system, how that may alter the immune epigenome, and how that can be altered to improve lifespan.

1.5.2.b.x. Disabled macroautophagy

Another new addition to the hallmarks of ageing, disabled macroautophagy involves the process by which cellular material is recycled for making new organelles called autophagy (López-Otín *et al.*, 2023). During autophagy, cytoplasmic material is taken up by membrane bound autophagosomes and fused to lysosomes where the vesicle contents are broken down. The contents of these vesicles can be entire organelles or components such as proteins, lipids, or DNA from either the host or pathogens. Cells from ageing patients show decreased autophagy and this can lead into many of the other hallmarks of ageing due to build-up of protein aggregates, inability to dispose of faulty organelles such as mitochondria, and build-up of pro-inflammatory proteins and the inflammasome (López-Otín *et al.*, 2023). Targeting autophagy has shown promising improvements to lifespan in mouse models particularly using spermidine (López-Otín *et al.*, 2023).

1.5.2.b.xi. Chronic inflammation

Chronic inflammation is another newly added hallmark of ageing (López-Otín *et al.*, 2023). Inflammageing is the term for a low-grade chronic inflammation associated with ageing (Franceschi *et al.*, 2000). There is a predominance of pro-inflammatory cytokines, particularly IL-6 and IL-1β, leading to constant inflammatory conditions that can damage surrounding tissue and make it difficult for the immune system to respond to threats such as infection and tissue damage (López-Otín *et al.*, 2023). The triggers for inflammageing are a combination of many of the other hallmarks of ageing such as exhaustion of haematopoietic stem cell populations, genetic instability and epigenetic alterations causing the cells to behave differently (López-Otín *et al.*, 2023). Chronic inflammation is a potential therapeutic target for anti-ageing therapies as many anti-inflammatory agents are already used in the clinic to treat chronic and acute inflammatory conditions. The focus of this thesis is to find potential chromatin remodelling enzymes to target in neutrophils that may be used in the future to protect from the neutrophilic contribution to inflammageing.

1.5.2.b.xii. Epigenetic alterations

The epigenome of a cell is the collection of DNA coding altering modifications beyond the DNA coding level. These modifications are introduced in Section 1.3.2 and can be altered as part of the hallmarks of ageing. DNA methylation is one of the of the three main classes of epigenetic marks and studies have shown hypermethylation at specific sites associated with ageing (López-Otín *et al.*, 2013). Furthermore, ageing clocks have been generated based on individuals' methylation status with reversal of these modifications able to reduce individuals' epigenetic age (Fahy *et al.*, 2019; Lu *et al.*, 2019). However a causative link is yet to be made and more research is needed into the role of DNA methylation in age-related decline (López-Otín *et al.*, 2023). Non-coding RNAs (ncRNAs) are another form of epigenetic modification that bind coding RNA and alter transcription that show links to ageing (López-Otín *et al.*, 2023). There are several families of ncRNAs and much of the work in the ageing field focus on long non-coding RNAs (lncRNAs). Several mouse studies have shown evidence for both gain and loss of specific lncRNAs resulting in changes to lifespan (López-Otín *et al.*, 2023). Further work is needed to look at the role other ncRNAs play in ageing and provides an exciting area of exploration in the field. The final modification type is histone modifications and chromatin remodelling and these are heavily implemented in the ageing process with specific histone modifications associated with ageing as well as changes to chromatin architecture and the ratio between heterochromatin and euchromatin associated with ageing (López-Otín *et al.*, 2023). These histone modifications and alterations to chromatin remodelling will be the focus of this thesis and will be expanded on greatly throughout this introduction. Unlike DNA mutations, epigenetic alterations are reversible, they present a possible target for pharmaceutical interventions to prevent ageing and prolong healthy lifespan.

1.5.2.b.xiii. Overview of the hallmarks of ageing

The above cellular hallmarks of ageing combine to cause whole tissue functional decline. Specific tissues show hallmarks that either drive whole-body ageing or promote age-related diseases. The more of these changes a person accumulates, the more difficult it is for them to perform ADLs which in turn promotes further functional decline. Decline in specific tissues has more of an effect on the individual than other tissues in the way that may affect quality of life. Most notably, decline in function of the musculoskeletal system, brain, and nervous system all significantly alter the independence of a person and can increase their risk of

morbidity and mortality. Figure 1.B Shows how many of the hallmarks of ageing are connected and fall under certain categories. It demonstrates that potentially by treating one hallmark, there is potential to treat multiple hallmarks by association and have a profound effect on healthy lifespan.

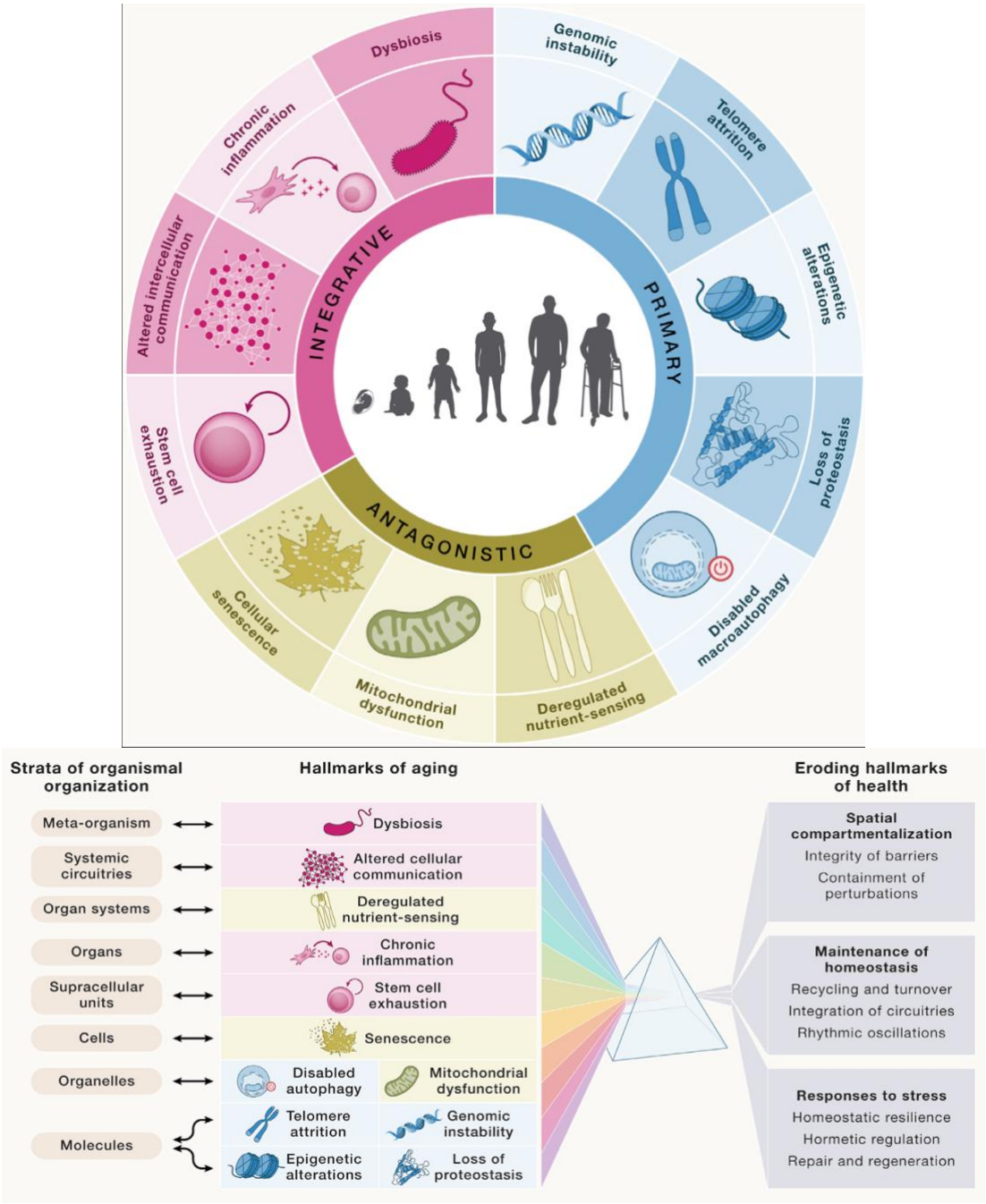

Figure 1.2. Hallmarks of ageing

(A) The 12 hallmarks of ageing and their subcategories (B) How the hallmarks of ageing are connected and categorised. Both taken from López-Otín *et al.*, (2023)

1.5.3. Chromatin remodelling in ageing.

1.5.3.a. Global age-related chromatin remodelling

Global chromatin structural changes have been identified in cell lines generated from old patient samples and animal models (Haithcock *et al.*, 2005; Scaffidi and Misteli, 2006; Larson *et al.*, 2012). The changes observed largely involve changes in the amount of heterochromatin in a cell. The heterochromatin loss model of ageing shows that progressive decline in heterochromatin structure leads to cellular senescence (Villeponteau, 1997). This loss of heterochromatin has been shown to be due to the age-related loss of chromatin proteins such as histones and associated chaperones (O'Sullivan *et al.*, 2010). The loss of heterochromatin removes transcription repression and promotes gene transcription as chromatin has a more open confirmation, deregulating cellular function as shown in yeast (Hu *et al.*, 2014). The specific changes to the transcriptional landscape and gene expression of cells due to this change in heterochromatin are unknown and more work is needed to identify changes to chromatin marks that are promoting more specific changes in chromatin confirmation.

Looking at specific modifications, knockout or overexpression of chromatin remodelling enzymes in model organisms have shown specific marks regulate lifespan but evidence in aged animals and patients is lacking.

Histone acetylation is a mark for active transcription. Inhibition of histone acetyltransferases (HATs) – the enzymes that catalyse addition of acetyl groups to histones – by addition of spermidine has been shown in yeast, flies, mice, worms, and an *in vitro* human peripheral blood mononuclear cell to increased lifespan (Eisenberg *et al.*, 2009). Addition of spermidine prevented cell death, reduced ROS, promoted autophagy, and saw a reduction in H3 acetylation. While no direct link was made, endogenous spermidine polyamine declines in humans and model organisms with age, and therefore has the potential to drive age-related chromatin remodelling (Scalabrino and Ferioli, 1984). Histone deacetylases (HDACs) work inverse of HATs to remove acetyl groups and reduce gene expression. In yeast, the HDAC Sir2 reduces in aged cells and these cells show increased pro-transcriptional marks and reduction in gene silencing analogous to a reduction in heterochromatin in higher organisms (Dang *et*

al., 2009). Knockdown of HDAC expression in yeast has also been shown to drive accelerated ageing by promoting the retention of pro-transcriptional marks (Feser *et al.*, 2010). While this work is all in lower organisms such as yeast, it demonstrates how altering histone acetylation can alter lifespan.

Histone methylation can be both a mark for transcriptional repression and transcriptional activation depending on the histone/lysine residue that is modified. As specific enzymes target specific modifications, genetic manipulation of enzymes can still tell us a lot about if they can regulate lifespan. H3K4me3 is an activator of gene transcription. Work in *C. elegans* has shown that manipulation of H3K4me3 regulates lifespan (Greer *et al.*, 2010). Knockdown of the methyltransferase SET-2 by RNA interference prolongs lifespan by preventing addition of the active H3K4me3 mark while knockdown of RBR-2 (homologous to human KDM5A), the demethylase that removes H3K4me3 to promote heterochromatin formation led to decreased lifespan. Conversely, H3K27me3 is an example of a methylation mark that represses transcription. Knockdown of the demethylase LSD-1 prolongs lifespan, likely because LSD-1 removes the repressive H3K27me3 mark (McColl *et al.*, 2008). This is further confirmed by the overexpression of the demethylase UTX-1 reducing lifespan in worms and that forced removal of H3K27me3 reduces lifespan (Jin *et al.*, 2011; Maures *et al.*, 2011). These data show that specific regulation of chromatin remodelling enzymes and the subsequent alteration of histone marks and chromatin conformation can drive ageing. However, it needs to be confirmed if these changes are seen during natural ageing.

Overall, previous research suggests that maintenance of gene repression and heterochromatin promote extended life span. However, study of these changes is limited to animal models and human cell lines using genetic or chemical manipulation to artificially induce changes to lifespan rather than longitudinal studies of endogenous changes. To really understand age-related changes, mapping of human chromatin landscapes is required to observe global changes associated with ageing using biopsies from various tissues throughout the life course. The changes seen could then be cross referenced to the studies described above and expression levels of chromatin remodelling enzymes compared between old and young samples.

1.5.3.b. Tissue specific age-related chromatin remodelling

While tissue specific profiling of age-related changes to human chromatin remodelling are not available, progress has been made using murine models. Analysis of heart, liver, cerebellum and olfactory bulb mouse tissue and neural stem cells cultured from mice aimed to produce tissue specific chromatin maps (Benayoun *et al.*, 2019). Tissue was taken from early-, mid- and late- stage mice and markers for active chromatin, H3K4me3 and H3K27ac, were used to produce these tissue specific maps of chromatin peaks. Maps showed global changes in active chromatin states between young and old tissues and led to investigation into the actual pathways where these changes were seen. Across all tissues processes dysregulated at the chromatin level include upregulation of protein homeostasis and immune responses, while mitochondrial function was downregulated. The pathways highly altered by ageing were immune response pathways and in particular interferon response signalling. Benayoun *et al.,* (2019) state that findings here correlate with previous work using other tissues and cell types such as kidney, astrocytes and choroid plexus and species such as humans, mice, rats, and killifish. The main takeaway from these data is the increase in pro-inflammatory signalling suggesting increased inflammation is a downstream consequence of age-related chromatin remodelling as samples taken across multiple tissues from aged mice showed increased pro-inflammatory pathways relative to young mouse samples.

1.5.4. Considering epigenetics changes in immune ageing

Making a link between specific epigenetic changes associated with ageing and cell, tissue and system decline could drive preventative therapies for ageing. Cellular and tissue specific decline drive whole-body functional decline and age-related morbidity and mortality. These changes are accompanied by epigenetic changes that have the potential to alter transcriptional networks. A common factor in both cellular and tissue specific decline is the presence of chronic inflammation due to factors such as the build-up of ROS due to mitochondrial decline and pro-inflammatory signalling such as that created by infiltration of adipose tissue into sarcopenic muscle. However, it is unclear how the hallmarks of ageing contribute to overall ageing, with hallmarks connected in bidirectional networks. Epigenetics changes also show marks associated with increased immune activity. During this build-up of inflammation, leukocytes are also going through cellular ageing and therefore present dysfunction that can drive ageing rather than returning the body back to homeostasis.

Investigating this age-related immune function may offer a systemic approach to treating ageing, rather than a tissue specific approach.

1.6. Ageing in the immune system

1.6.1. Immunosenescence and inflammageing

During ageing, cellular decline (Section 1.5.2.b) results in changes to the immune system both due to changes to the microenvironment and changes within the immune cells themselves. Identifying these changes can provide therapeutic targets for preventative strategies against age-related immune decline. The two major ways in which the immune system changes are inflammageing and immunosenescence, but the relationship between the two is debated.

1.6.1.a. Immunosenescence is a loss of immune cell homeostasis.

The age-related changes within leukocytes need to be identified to understand immune ageing. The general term for the age-related decline of immune cells is immunosenescence and sees a multifaceted and dynamic alteration to both cell function and regulatory pathways (Franceschi *et al.*, 2000). When age-related changes to the immune system are discussed in the literature, they are often split into innate or adaptive immune changes and analysed at a cell-specific level (Santoro, Bientinesi and Monti, 2021). There are many signalling pathways, genes and processes involved such as heat shock proteins, protein folding and NF-κB regulation. It is also important to establish that immunosenescence is not necessarily cellular senescence (section 1.5.2.b.vi) and there is debate about how the two forms of senescence overlap and interact (Covre *et al.*, 2020). Immune cells can display senescent-like traits during normal function such as T lymphocytes which are constitutively non-proliferative and have a secretory phenotype (Covre *et al.*, 2020) – arguably activated neutrophils fit this description too. In fact, effector T cells show many of the hallmarks of senescent cells such as short telomeres, DNA damage and kinase signalling . While these T cells are not directly pathogenic, it is proposed that with ageing they can accumulate due to low-grade viral infection and escape apoptosis, move toward an innate immune cell phenotype, and may cause systemic inflammation (Covre *et al.*, 2020; Laphanuwat, Gomes and Akbar, 2023). Classification of when and how these effector T cells go from effector to senescent cells is therefore important to understanding the process and how it relates to more general cellular senescence. Further

work can also aim to make similar observations in other immune cell types that are terminally differentiated and highly secretory, especially in the innate immune system, as currently, much of this work focuses on the adaptive system.

As immunosenescence is evolutionary conserved, there is some argument that it has protective benefits, but we are interested in the negative impact, with age-related diseases linked to immunosenescence (Fulop *et al.*, 2020). The focus here will be on innate immune changes and later how neutrophils are altered.

1.6.1.b. Inflammageing is a global, low-grade chronic inflammation.

Inflammageing is defined as a whole body, low-grade, sterile, chronic inflammation that can alter the maintenance of homeostasis in the body (Franceschi *et al.*, 2000). The link to immunosenescence is unclear, with questions remaining whether inflammageing drives immunosenescence or *vice versa.* On-set of inflammageing is multifaceted and linked to an increase in cellular stress from the microenvironment on immune cells. Cells in the body decline with age and present a senescent phenotype due to DNA damage, changes to mitochondrial function, and protein misfolding altering gene expression, increasing ROS release, and changing cell function (Section 1.5.2.b). These changes increase the release of age-related damage associated molecular patterns (DAMPs) that activate innate immune cells (Feldman, Rotter-Maskowitz and Okun, 2015). The activation of immune cells due to these non-specific damage signals drives whole-body inflammation in a feed-forward loop that can cause damage to host tissue. Damaged tissues may not be repaired correctly causing remodelling and scarring that can result in a loss of function and increase the risk of age-related multi-morbidity as the body cannot return to homeostasis (Fabbri *et al.*, 2016; Blaes *et al.*, 2017).

1.6.1c. The effects of ageing on the inflammatory response

Immunosenescence and inflammageing result in changes to the inflammatory environment of the body and has consequential effects on how the body deals with inflammatory stimuli. One of the largest changes is to the cytokine environment, with a rise in pro-inflammatory (IL-1, IL-6, TNFα and IFN-γ) and decline in anti-inflammatory (IL-1Ra, IL-10 and TGF-β1) cytokines seen during ageing, with further imbalance in accelerated ageing and sarcopenic

obesity (Fagiolo *et al.*, 1993; Minciullo *et al.*, 2016). The larger the imbalance between pro-inflammatory and anti-inflammatory cytokines, the more severe the chronic inflammation is, with a higher risk of morbidity and mortality (Gomez, Boehmer and Kovacs, 2005; Newman *et al.*, 2016). While many changes in the cytokine environment have been studied extensively in isolation, developing an understanding of what cytokines are contributing at high levels is unclear. An immune clock to track how these cytokine changes correlate to age-related decline was created using deep-learning analysis of blood samples from 1,001 8 to 96-year-olds (Sayed *et al.*, 2021). This study found that while many of the cytokines described above were differentially expressed in older adults, CXCL9 was the highest predictor for immune ageing. CXCL9 was shown in induced pluripotent stem cell lines to induce cellular senescence but no direct mechanistic link has been made outside of a cell culture system (Sayed *et al.*, 2021).

I propose that changes to the whole-body signalling environment as reviewed by Miniciullo *et al.,* (2016), results in an increased cytokine release from both endogenous tissues and circulatory leukocytes. While the increase in cytokines initially recruits more leukocytes such as neutrophils, macrophages, B cells and T cells to sites of inflammation, the constant bombardment of cytokines alters signalling cascades within these cells leading to chromatin remodelling within the epigenome. If these changes can be inherited from proliferative precursors whole scale changes can be seen in leukocyte populations, causing immunosenescence across the body and contributing to ageing. Epigenetic inheritance of immune traits is an understudied concept with some literature suggesting inheritance of autoimmune promoting modifications between generations in type 1 diabetes clinical trials and maternal immune inheritance of non-coding modifications in drosophila, however these are between generations, rather than lifespan (Todd, 2010; Grentzinger *et al.*, 2012). There is certainly evidence for ageing acting on the bone marrow to alter haematopoiesis and altering counts of mature immune cells due to increased myelopoiesis and decreased lymphopoiesis (Kim, Moon and Spangrude, 2003; Rossi *et al.*, 2005). This swing towards myelopoiesis will lead to an increase in innate immune responses and a decline in adaptive immunity, increasing the risk of chronic inflammation.

1.6.2. Inflammageing and immunosenescence in age-related decline disease

An inflammageing environment can promote a more general ageing environment leading to decline in tissue function. Sarcopenia is the age-related progressive loss of muscle strength and mass. The loss of muscle function associated with function is a major driver of functional decline and reduction in ability to perform ADLs (Section 1.5.2.c.). Sarcopenia can be driven by lifestyle factors, ageing, and age-related changes to the immune system creating a feedback loop that results in a progressive decline of the musculoskeletal (MSK) system (Abete *et al.*, 2019). During general activity and training, muscle acquires damage that must be repaired and remodelled to maintain MSK homeostasis. Part of the signalling for this damage is inflammatory pathways and recognition of DAMPs. Immune cells remove damaged tissues and recruit satellite cells – the stem-like cell of muscle – to repair fibres and cause hypertrophy. In states of chronic inflammation, these pro-repair signals are masked by systemic inflammation (Section 1.6.1.c) and muscle damage is not repaired altering MSK composition by promoting atrophy and the infiltration of adipose tissue (Chazaud, 2016). This damage is further compounded by the progressive decline in type II muscle fibre satellite cells seen in ageing patients meaning there are fewer cells to promote repair (Verdijk *et al.*, 2014). Increased infiltration of the muscle with adipose tissue could also further recruit immune cells. Crosstalk between adipocytes and neutrophils have shown in murine models to drive neutrophilic inflammation in healthy white adipose tissue (Watanabe *et al.*, 2019). If adipose tissue in sarcopenia can recruit neutrophils that have been activated due to inflammageing, they risk further damage to the muscle tissue and further progression of the sarcopenic phenotype. This may be because the aged neutrophils can damage healthy muscle as they are non-specifically releasing cytotoxic compounds that can attack endogenous tissue and cause functional decline (Wilson *et al.*, 2017). Increased inflammation combined with loss of satellite cells is therefore a potential major driver of sarcopenia and inflammageing in the MSK system.

Osteoarthritis (OA) is another example of how inflammageing can drive an age-related disease. OA is a disease of the joints where a combination of mechanical use and inflammation causes multi-tissue remodelling causing a loss of mobility and joint pain (Millerand, Berenbaum and Jacques, 2019). Much like in sarcopenia, the presence of systematic inflammageing and the associated pro-inflammatory cytokines such as IL-6 and IL-

1β and release of DAMPs from endogenous tissue can promote over activation of immune cells and damage at the joint. The damage creates further cytokine and DAMP release that in turn causes more damage causing extensive remodelling and breakdown of the cartilage within a joint. Therefore, the more prevalent the inflammageing phenotype is, the more damage will be seen at the joint.

In fact, the idea of how inflammageing links to many chronic inflammatory diseases is like that described in sarcopenia and OA. The basic idea being that an influx in pro-inflammatory cytokines recruits excess immune cells that through their effector mechanisms damage host tissue and allow disease pathologies to spread by preventing resolution of inflammation due to a lack of anti-inflammatory signals. Understanding how to alter these signals can help treat these diseases and the use of anti-inflammatory drugs to treat conditions such as arthritis by inhibition of IL-1 and TNF-α provide examples of this in action (Abbasi *et al.*, 2019).

1.6.3. How innate immune epigenetics change with age

Within the immune system, the role of chromatin remodelling in regulating function is becoming apparent (Section 1.3.3). Epigenetic regulation of gene expression by chromatin organisation is dynamic and altered throughout the lifespan by environmental influences. Using epigenetic sequencing to analyse innate immune cell age-related chromatin remodelling presents a powerful tool in ageing research. Understanding age-related changes to chromatin conformation in immune cells can help us understand the transcriptional networks that are altered in inflammageing and immunosenescence.

High-throughput analysis of age-related immune cell chromatin modifications was first achieved in 2018. Single-cell profiling of immune cell chromatin remodelling identified that different immune cells have specific chromatin modification profiles that vary with age (Cheung *et al.*, 2018). Both innate and adaptive immune cells were analysed and here the focus was on the innate immune cell data. Samples were taken from healthy individuals <25 years old and >65 years old. Distinct chromatin profiles were first generated for immune cell types. These profiles were then compared in samples from young and old individual's and 29/30 tests showed high cell-cell variability with age. While analysis of specific chromatin marks focused on T cells of the adaptive immune system and no connections were made

between the different cell types analysed, cells in the monocyte lineage were included in parts of the analysis and variation were seen though not described in detail. Analysis of genes associated with these marks by single cell RNA sequencing (scRNA-seq) showed that expression was highly variable in aged samples. The factors behind the epigenetic variability were also analysed and the variation was largely shown to be down to environmental factors, not genetics, as shown by comparing genetically identical twins. Analysis of the pathways associated with these epigenetic changes and genes would be major guide to age-related immunological changes at a cell specific level. While detail is lacking in this dataset for innate immune cells, the presence of specific epigenetic profiles for immune cells subtypes and the variation seen here with age would suggest that all immune cells are susceptible to epigenetic remodelling throughout the lifespan. Further analysis is required to find whether the changes observed between the old and young patient samples reflect detrimental changes to chromatin that lead to immunosenescence and inflammageing. Induction of these changes in animal models would help to identify whether over and under enrichment of these marks leads to detrimental changes, showing causation and not just correlation.

Analysis of circulating immune cells in aged vs young people was again performed in 2020 with the aim of making more connections between different cell types and to look at epigenetic effects of COVID-19 infection (Zheng *et al.*, 2020). Data was produced comparing healthy aged and young individuals and specifically the innate population of monocytes and dendritic cells. Analysis of differential gene expression within the monocyte population showed ageing patient cells had an upregulation of pro-inflammatory genes such as *NFKB, IL1B, TNF* and *CXCL8* and when looking at chromatin accessibility at transcription factor binding sites associated with these genes, a more open confirmation was seen. These data show how chromatin rearrangements associated with ageing can promote an inflammageing phenotype by driving pro-inflammatory behaviour in monocytes. A dataset of this type for neutrophils is required to look at wholescale innate immune changes. Much like the Cheung *et al.* (2018) data above, the observations of Zheng *et al.* (2020) need to be confirmed as causative and not correlative when it comes to the age-related decline of immune cells. Again, induced specific marks in animal models and analysing the ageing phenotype would aid in drawing these conclusions.

The two datasets discussed above show that within the limited pool of datasets on chromatin remodelling in innate immune ageing, monocytes and macrophages dominate the analysis. The skew towards monocyte lineages is likely because they are easier cells to sequence compared to neutrophils and provide more general interest to the inflammation community than basophils, eosinophils, and other innate immune cells. Creating more comprehensive profiles are key to advancing our knowledge of age-related chromatin remodelling in the immune system.

1.7. Age-related changes to neutrophil function

Throughout this introduction, the concept that changes to neutrophil function may be driving inflammageing have been hypothesised. However, evidence for these changes has not been discussed. This final section will look at how neutrophil phenotype changes with age and the genetic and epigenetic evidence for these changes.

1.7.1. Changes to neutrophil migration

Elderly patients show increased rate of chronic wounds and impaired wound healing. Using a mouse model of cutaneous lesions and bacterial infection, young and old mouse wound healing and bacterial clearance was compared (Brubaker *et al.*, 2013). The older mice showed reduced wound healing and maintenance of infection relative to young mice. This was found to not be due to a reduction in cytotoxic activity in wound neutrophils, but a reduction in chemotaxis. The subcutaneous injection of the murine homolog to interleukin-8 (IL8) – KC – into old mice lead to reduced neutrophil recruitment. However, analysis of the cytokine environment at the wounds showed increases in pro-inflammatory chemokines. Furthermore, analysis of *Cxcr2* expression on circulating neutrophils – a receptor for KC that drives migration and transmigration to wounds – was found to be increased in old mouse neutrophils suggesting another factor is altered that can inhibit neutrophil migration.

Work using *in vitro* neutrophil culture comparing neutrophils from aged and young donors may help answer what is driving changes to chemotaxis. Sapey *et al.*, (2014) found that neutrophil response to chemoattractants IL-8, fMLP, leukotriene B4, C5a, and CXCL1 declined *in vitro* with age. Chemokinesis between young and old patient neutrophils remained constant relative to untreated controls, but the accuracy of migration in exposed older patient

cells declined significantly. This was not down to changes in receptor expression: instead, older patient neutrophils had increased constituent phosphatidylinositol 3-kinase (PI3K) activation by hyperphosphorylation. Recovery of the phenotype in older patient neutrophils towards that of a young patient neutrophil was possible using inhibitors of PI3K class I γ and δ isoforms. These data suggest alteration in the loci for either PI3K class I γ and δ isoforms, or the kinases responsible for hyperphosphorylation and activation. These alterations may be epigenetic and caused by age-related decline in function, leading to this immunosenescent phenotype. *In vivo* data would help to confirm these findings and allow exploration of potential epigenetic drivers of these changes.

1.7.2. Changes to neutrophil effector mechanisms

The ability of neutrophils to kill pathogens is greatly reduced during ageing as shown by increases in rates of chronic infection in the elderly. Various elements of neutrophil activity are altered in the elderly including phagocytosis, NET production, degranulation, and the oxidative burst.

Further to the analysis of neutrophil migration and accuracy, Sapey *et al*., (2014) also showed alterations to degranulation by donated aged patient neutrophils by analysing plasma. Neutrophils from elderly donors showed increased neutrophil elastase activity based on concentration of fibrinogen cleavage product in the plasma relative to younger donors. When analysing cell surface expression of CD63, a marker for degranulation, unstimulated elderly donor neutrophils showed increased expression relative to younger donors.

An analysis of neutrophil phagocytosis and ROS production was performed using neutrophils donated from three age groups, 21-36, 38-56, and 62-83, and exposed to *E. coli* and *S. aureus* (Wenisch *et al.*, 2000). To prevent spontaneous apoptosis, the neutrophils were first isolated from the blood samples before being pre-treated in Hanks' buffer to maintain cell state. Before imaging experiments, ice-cold buffer washes were performed aiming to prevent cell loss. High numbers of neutrophils were also used. Since this work was carried out, techniques have advanced to further attempt to prevent these issues. In the analysis, phagocytosis of opsonised and fluorescently tagged *E. coli* and *S. aureus* was reduced in an age-dependent manner analysed using a fluorescent microscope. Bacterial killing as measured using acridine

orange staining of *E. coli* was also reduced in the aged donor neutrophils. Specific to *S. aureus* treatment, a reduction in intracellular ROS production was also seen in the aged neutrophils. Aged neutrophils also saw an increase in intracellular calcium in a resting state but activation with fMLP lead to decreased calcium concentration. These data show that in the presence of opsonised bacteria, neutrophil ability to phagocytose and kill bacteria are reduced, though certain processes are specific to the bacteria causing the infection. Earlier work showed that unopsonised bacteria are phagocytosed at the same rate, independent of the age of the neutrophil donor, yet serum exposed bacteria were phagocytosed less by aged donor neutrophils (Emanuelli *et al.*, 1986). These works suggest that it is not bacterial recognition that is altered, but instead recognition of innate immune tags such as complement, and immunoglobulin receptors are altered with age. CD16 is the Fcγ receptor and was shown to have reduced expression in neutrophils from elderly donors, leading to a reduction in phagocytosis when exposed to opsonised *E. coli* (Butcher *et al.*, 2001).

The oxidative burst is also altered in aged patient neutrophils. This was briefly described above when referencing the analysis carried out by Wenisch *et al.*, (2000) and was also seen in the work carried out by Butcher *et al.*, (2001). Both showed a reduction in respiratory burst in aged donor neutrophils. Lack of release of ROS will inhibit bacterial killing. One possible answer to the reduction to the oxidative burst is again changes to the Fcγ receptor in old donor neutrophils as opsonised fungi do not trigger the respiratory burst relative to young donor neutrophils though this has not been further validated since it was observed (Fülöp *et al.*, 1985). There is also debate whether bacterial formyl peptide (fMLP) recognition changes during ageing influence this reduction in respiratory burst, though observations are mixed across several groups with some showing no change and others showing initial decreases that eventually significantly increase compared to young donor neutrophils (Fulop *et al.*, 2004). More recently, specific immune subsets have been linked to oxidative burst reduction. Aged donor samples were found to contain an immunosuppressive subpopulation of $CD16^{high}/CD62L^{low}$ population that showed lower ROS production and phagocytic index (Sauce *et al.*, 2017). With increased evidence for neutrophil subsets, the role they play in ageing phenotypes provides an exciting area of study. However, many of these suggested subsets may provide anti-inflammatory effects, going against my hypothesis and the idea of neutrophils driving age-related chronic inflammation.

Production of NETs is also altered in neutrophils from healthy aged donors (Hazeldine *et al.*, 2014). Donor neutrophils *in vitro* were primed with TNFα and then treated with PMA, IL-8 and LPS. Aged donor neutrophils were shown to produced fewer NETs relative to the activated young donor control when treated with IL-8 and LPS but not PMA. The aged donor neutrophils also produced less ROS compared to young donor controls following IL-8 and LPS treatment. This was shown to not be dependent on an age-related decline in CXCR1, CXCR2, or TLR4 expression, or age-dependent changes to TNFα priming. Therefore, more work is required to find the trigger for changes in NET formation with age.

These changes result in reductions to the removal of infection but allow for non-specific chronic inflammation that damages host tissue to dominate due to factors such as increased degranulation. The work above suggests that neutrophil function is reduced and that may have anti-inflammatory consequences but when combined with observations on migration described in Section 1.7.1 and alterations to inflammation resolution described below, dysfunctional, activated neutrophils may be found away from a site of immune challenge and instead release cytotoxic substances due to increased degranulation that may damage healthy tissue, especially when combined with ineffective clearance of infection.

1.7.3. Changes to neutrophil inflammation resolution and apoptosis

Section 1.2.1.c. describes how specific triggers within the site of inflammation drive reverse migration of neutrophils out of the tissue and back into the circulation as a form of inflammation resolution. By confocal intravital microscopy comparing old and young mice, fluorescent tagging of neutrophils showed this process to be poorly regulated in aged mice (Barkaway *et al.*, 2021). IL-1β was injected into cremaster muscle and neutrophil behaviour observed. Fewer neutrophils were recruited to the injection site, and this was attributed to reverse transendothelial migration (rTEM), where activated neutrophils prematurely migrate back into the circulation. The neutrophil chemoattractant CXCL1 was found to be the driver of rTEM with aged mice showing an increase in expression relative to young mice following IL-1β injection. This CXCL1 was produced by mast cells, with an increase in senescence mast cells seen at the site of injection. The CXCL1 localised to endothelial cell junctions by atypical chemokine receptor 1 (ACKR1). CXCR2 is the receptor for CXCL1 found on neutrophils, aged

mouse neutrophils had reduced cell surface CXCR2 due to an increase in CXCL1-ACKR1 binding events as shown by a reduction in rTEM in mutants for CXCR2 downstream signalling. Once these neutrophils entered the circulation, they migrated to the lungs and as they were activated, caused damaged to respiratory tissue. If this phenotype is seen in neutrophils from human donors, it has implications to inflammageing and chronic inflammatory diseases as following infection or wounding, these neutrophils can enter the circulation and damage tissues.

Apoptosis of aged patient neutrophils is a relatively understudied area relative to effector mechanisms, potentially due to spontaneous death *in vitro*. A clinical trial exposing young and aged donor neutrophils to a panel of pro-inflammatory agents showed that GM-CSF, LPS and IL-2 delay neutrophil apoptosis in young donor neutrophils relative to unstimulated cells. However, in the aged donor neutrophils apoptosis was only seen with GM-CSF and the unstimulated aged donor neutrophils showed increased apoptosis relative to the young donor neutrophils (Fülöp *et al.*, 1997). Further analysis of aged and young donor neutrophils exposed donor neutrophils to GM-CSF to investigate changes to the JAK/STAT pathway (Fortin *et al.*, 2007). This work showed that GM-CSF rescued young donor neutrophils from apoptosis and prolonged survival, however in aged donor neutrophils this recovery was lost. It was deemed that this was caspase-3 dependent apoptosis and aged donor neutrophils showed increased caspase-3 activity. However, GM-CSF isn't the only cytokine that acts on neutrophils and ageing leads to a whole scale increase in pro-inflammatory cytokine expression (Minciullo *et al.*, 2016). Another factor to consider is how apoptotic neutrophils are cleared from a site of inflammation and how macrophage efferocytosis may be influenced by both age-related changes to the signalling environment and macrophage immunosenescence. Persistence of uncleared apoptotic neutrophils could promote inflammation and drive tissue damage.

1.7.4. How age-related changes to neutrophil function drive age-related decline and disease.

Sections 1.7.1-3 have briefly discussed how elements of neutrophil function can drive disease. One major defect of neutrophils in the ageing individual is the reduction in phagocytic activity and cellular killing. This will obviously limit how the elderly can deal with infection and cause chronic and long-term infections that may overwhelm the host. Dealing with infection and

damage is then further inhibited by changes to receptors on the cell surface that may alter pathogen sensing. Another change is the migratory phenotype associated with ageing in neutrophils and this presents the most danger to endogenous tissues. Neutrophil chemotaxis to infection and recruitment to wounds have been shown to be altered in an ageing patient neutrophil. Delayed recruitment of neutrophils and a loss of sensitivity to chemoattractants causes inefficient migration of activated neutrophils. These activated neutrophils can release granules and NETs and phagocytose incorrect tissue causing damage to sites as they migrate, contributing to low-grade chronic inflammation such as that seen in inflammageing (Sapey *et al.*, 2014). In a condition such as sarcopenia, this fault in neutrophil migration to wounds may prevent muscle repair and drive frailty as neutrophils are required for removal of necrotic tissues before macrophage driven remodelling of the muscle following use associated damage (Teixeira *et al.*, 2005). Not only will neutrophils not perform clearance, but the change in neutrophil phenotype may damage healthy muscle and drive sarcopenia even further (reviewed in Wilson *et al.*, 2017). Further work aimed to confirm this hypothesis using patient samples from 40–77-year-olds (Wilson *et al.*, 2020). Wilson *et al*. (2020) found that increased age-related frailty was associated with impaired neutrophil function including reduced chemotaxis. Furthermore, the reduction in human neutrophil chemotaxis could be recovered with PI3K inhibitors *in vitro* presenting a potential therapeutic target. These examples present how loss of neutrophil homeostasis in ageing may contribute to an environment when inflammation damages host tissue but fails to prevent infection, reducing quality of life and increasing the risk of morbidity and mortality. Wilson *et al.* (2020) also demonstrates the potential for therapeutics to target neutrophil activity and potentially protect against ageing, though further research is required to show recovery from the ageing phenotype *in vivo*.

1.7.5. Studying age-related chromatin remodelling in neutrophils

Sections 1.4.1. and 1.4.2. describe how it is becoming increasingly evident that chromatin remodelling plays an extensive role in the maturation, activation, and training of neutrophils to fight infection and prevent disease. It would therefore be reasonable to hypothesise that changes to neutrophil chromatin can drive neutrophil dysfunction in disease as described in Section 1.2.2. and neutrophil specific decline as seen in ageing detailed in Section 1.7.1-3. However, datasets unravelling the role chromatin remodelling plays in regulating age-related

changes in neutrophil function are non-existent. Section 1.6.3. shows evidence of changes in innate immune chromatin remodelling with age but also shows how neutrophils are excluded from these analyses. The evidence presented discussed in this introductory review shows that this needs to change and that an extensive mapping of an ageing neutrophil chromatin structure could be a key driver in developing therapies in preventing age-related inflammatory diseases. Chromatin remodelling enzymes provide druggable targets – as shown by the onset of promising clinical trials (Kaur, Daoud and Eblen, 2019) – and induction of pro-inflammatory changes such as those seen in trained neutrophil immunity may help alleviate some age associated neutrophil decline though specificity needs to be better understood to prevent detrimental changes in other cells. Developing profiles of age-related changes to neutrophil chromatin remodelling will help identify those potential targets and secondary targets in the form of downstream genes.

1.8. Aims and Objectives

We hypothesise that changes to chromatin remodelling in neutrophils dictates neutrophil response and that in ageing and disease, a change in these chromatin remodelling events drives disease progression. More work is needed to understand what these changes are and the mechanisms by which they may drive ageing. Current neutrophil models do not allow for *in vivo* tracking of epigenetic changes. Cell culture and murine assays often require neutrophils to be studied in isolation or for neutrophil lysates to be taken. These factors create the need for a model system that traces real-time epigenetic changes in neutrophils *in vivo*. This project aims to investigate chromatin remodelling enzymes responsible for neutrophil function using an *in vivo* zebrafish model.

Various compounds have been shown to alter human neutrophil chromatin remodelling *in vitro* (Zimmerman et al., 2015, Visnes et al., 2018). The action of one of these chromatin remodelling compounds, R848, has been well characterised using human neutrophils *in vitro* (Zimmermann *et al.*, 2015, 2016). The effects of, R848, will be tested in the well-validated *in vivo* zebrafish inflammation models available to the Renshaw group. I will investigate the inflammatory activity of neutrophils by designing experiments to look at their activation state, recruitment to wounding, gene expression profiles and removal of neutrophils after tail fin

injury in the presence or absence of R848. This will test that *in vivo* zebrafish neutrophils can be modified in a similar way to *in vitro* human neutrophils.

Second, CRISPR/Cas9 technology will be used to knockout chromatin remodelling enzymes firstly in the whole fish then using innovative, rapid, neutrophil-specific CRISPR approaches (Wang *et al.*, 2021). CRISPR/Cas9 knockdown will allow identification of chromatin remodelling enzymes that are key in influencing neutrophil responses to inflammatory stimuli *in vivo.* The successful CRISPR knockdown of chromatin remodelling enzyme target genes will be confirmed by RT-PCR and restriction digest, and neutrophil phenotype following tailfin injury and knockdown will be observed. This will then be repeated in the neutrophil specific-system. This aims to further strengthen our understanding of the chromatin remodelling modifications and associated enzymes in neutrophil regulation.

Following the identification of key enzymes that regulate neutrophil function using CRISPR/Cas9 technology, I will set about investigating how these enzymes regulate neutrophil gene expression. I will do this by utilising the INTACT method of BirA/Strepatavidin pulldown to extract neutrophil nuclei from zebrafish (Deal and Henikoff, 2011; Kenyon *et al.*, 2017; Trinh *et al.*, 2017). These extracted neutrophil nuclei will then be RNA sequenced and differential gene expression analysis performed to understand the role the chromatin remodelling enzymes in regulating neutrophil phenotype. Differentially expressed genes will then be validated by qRT-PCR.

The information obtained from this project has the potential to significantly increase our understanding of neutrophil regulation. Knowing the chromatin modifications to target to control neutrophil function could one day prove useful not only in preventing harmful ageing, but also treating various chronic inflammatory disorders. Successful completion of the project will therefore provide a useful tool for the study of neutrophil chromatin remodelling.

Chapter 2. Materials and Methods

2.1. General materials and methods used across all chapters

2.1.1 Zebrafish Husbandry

All zebrafish were kept and raised according to UK Home Office guidelines in the approved biological services aquaria at the University of Sheffield. Tanks were maintained at 28^{O}C with continuous recirculating water supply and a daily light/dark cycle of 14/10h. Most procedures were performed on embryos or larvae <5 days post-fertilisation (dpf), meaning these procedures were not regulated by the Animals (Scientific Procedures) Act. All regulated procedures were performed under PPL P5983040C and PIL I43237193 in line with Animals (Scientific Procedures) Act.

2.1.2. Zebrafish tailfin injury

To perform the tail fin injury, larvae were anesthetised in 0.168 mg/ml tricaine (Sigma-Aldrich, Cat #E10521) + E3 embryo medium + 1% methylene blue (Williams and Renquist, 2016) and the caudal fin removed posterior to the circulatory loop using a Swann Morton scalpel blade under a dissection microscope. The injured fish was then returned to fresh E3 using a P200 pipette with the end cut off the tip.

2.1.3. PCR Primer design

RT-PCR and qRT-PCR primers were both designed using primer-BLAST (www.ncbi.nlm.nih.gov/tools/primer-blast/index.cgi?LINK_LOC=BlastHome) when published primers were not available. The DNA sequence or gene of choice was entered and a product size of 50-150 bps (qRT-PCR) and 100-250 bps (RT-PCR) and primer size of 20 bps specified, annealing temperature was prioritised as 58-60^{O}C. Off-target binding was confirmed by comparison with *Danio rario* against the Refseq mRNA database. Primers designed for mRNA amplification such as those for qRT-PCR were designed spanning exon-exon junctions. Primers were ordered from eu.idtdna.com.

Gene and Primer name	**Forward primer**	**Reverse Primer**
ef1a qPCR (Hamilton *et al.*, 2020)	CAGCTGATCGTTGGAGTCAA	TGTATGCGCTGACTTCCTTG
rsp29 qPCR	TTTGCTCAAACCGTCACGGA	ACTCGTTTAATCCAGCTTGACG
mpx qPCR (Ferrari *et al.*, 2019)	GCTGCTTACAAGTATTCTCG	ACGGCCTCCCGTGTCTTTCG
ece2b	AACACACAGAGCAGAGGACG	CTCCTCCTCAAACGTTGCAC
mitfa	GAAGTCAGAGCCCTGGCAAA	GCTTTCAGGATGGTGCCTTT
fastkd2	GCTTTAGGGTTGCGTCTGAA	TCTGCCAACGACAGAGTCTT
numa1	AGACGAAGGCCTCGATCAAT	GAGAGCTGTCTGAGCTGGAA
itga2b (Zhu *et al.*, 2017)	TTCTTCACTCCACGGCTCAC	ATAGAAGCAGTCCAGCGACG
il6 qPCR	TCCGCTCAGAAAACAGTGCTAT	CCCCATACTGCTGAACACGG
myd88 (Bates *et al.*, 2007)	TCTTGACGGACTGGGAAACTCG	GATTTGTAGACGACAGGGATTAGCC
hif1a qPCR	AGATCCTGTTCTCACGCTGG	ATTTAGAGAGGAGCACGGGG
kdm6ba qPCR	GAGCCGAGATTTGACCGAAC	AAAACTCGTTCAGCTTGCGT
kdm6bb qPCR	AGCAAGCTGGACTCTGAACT	ACCTGCCCTAACTTTCTCCC
kdm6ba crRNA 5'UTR	CAGAGTGCAGAAGCATTAAACG	ACTTTCACCTCTTCTCTTCCCC
kdm6bb crRNA 5'UTR – attempt 2	CCTAAACTCAGGGCTTCAGAGA	GGGTAAACTGGAGTTGGAACAG
kdm6ba coding seq crRNA	GGTTTGCCTTGACAACTAACTG	GGTCTTGCTTATCCCCTCGA
kdm6bb coding seq crRNA	GAGATCTGCAGTGGAGGGTT	TGGCATGCTGTAATGGGAGA
kdm6ba/b neutrophil specific g1	TGTATGACCTGCTGGACATGTTTAAGAGCTATGCTGGAAACAGCATAGC	CCGAGTCAATCCTGTCGCCCGAACTAGGAGCCTGGAGAACTGC
kdm6ba/b neutrophil specific g2	CAGGATTGACTCGGGGTTTAAGAGCTATGCTGGAAACAGCATAGC	CCAGCAGGTCATACACGAACCAAGAGCTGGAGGGAGA
Neut specific scaffold g1 (Zhou *et al.*, 2018)	GTTTAAGAGCTATGCTGGAAACAGCATAGC	CGAACTAGGAGCCTGGAGAACTGC

Neut specific scaffold g2 (Zhou *et al.*, 2018)	GTTTAAGAGCTATGCTGGAAAC AGCATAGC	CGAACCAAGAGCTGGAGGGAG A
dot1l crRNA 5'utr – attempt 2	GGTACCAGGCAACACAAGAAAT	TTCTGCATAGGTAGCTGGAATG
dot1l crRNA coding seq	GTACAGACTTTGAAGCGCAATG	CTTCCTCCATCATCTCCATCTC
ezh2 crRNA 5'UTR	CAAAGTCAAAAGGAAAACCACC	CACCAAACTCTACACAAGCAGC
ezh2 crRNA coding seq	CAAAGTCAAAAGGAAAACCACC	CACCAAACTCTACACAAGCAGC
brd4 promoter crRNA	CAGAGCGGCTTTAAGTGATCTT	GCTGGCACCGTTAGTAAGAAAT
crebbpa 5'UTR crRNA	TTCACAAGAAGCCAGAGGATTT	ATTCACCCCATGATAATCCAAC
ep300a promoter crRNA	TAAAGAACAAATATCGGGCTGG	GGGATGAGAGTTTAGGCCTCTT
brd2a crRNA	CTCTGAGCTGGAGGATAGAGG A	AATTCCAAAAGATGCCGAATTA
brd2b crRNA	GGACGAATTCTGATTGGTCAGT	CCACACGCAGGATTAGTTTACA
hdac6 crRNA	AACCAAAAGGCAAATGTACACC	AGGGTTGAGTTTTAGGGGTGAT
sirt6 crRNA	GCAAACTCTCTGACGTAATCCC	GAAGCTATTTTTGCTAGCAGGC
dot1l crRNA 5'UTR – attempt 1	GGTACCAGGCAACACAAGAAAT	GGTAGCTGGAATGTCTGCTTTC
kdm6bb crRNA 5'UTR– attempt 1	CCCTTCTCCTTTCTCTCTCCAG	TCAGCTTCATTTCAATTAGCCA

Table 2.1. Sequences for PCR primers

2.1.4. Genomic DNA extraction

A single embryo was pipetted into a 0.2 ml PCR tube, excess E3 was removed before adding 100 µl 50 mM NaOH (Sigma-Aldrich, Cat #S5881). The tube was then vortexed and incubated at 95^{O}C for 20 minutes. 10 µl 1 M Tris-HCl pH 8 (Sigma, Cat #T-2694) was added and the tube was vortexed for 10 s and then centrifuged briefly to pellet the debris. Samples were stored at -20^{O}C.

2.1.5. TRIzol based RNA extraction

Samples were homogenised in 500 µl TRIzol (Invitrogen, Cat #15596026) for 20s at room temperature in a biological safety cabinet. 100 µl of chloroform (Fisher scientific, Cat #C/4920/08) was added, the sample vortexed for 15 s and then left at room temperature for

3 minutes. Samples were centrifuged at maximum speed at 4^{O}C for 10 mins and the upper aqueous phase removed to an RNAse free 1.5 ml tube. 250 ml isopropanol (Thermo Scientific, Cat #42385000) was added to the tube and vortexed for 15 s then left at room temperature for 10 mins. Samples were centrifuged at maximum speed at 4^{O}C for 10 mins, to pellet the RNA, and the supernatant removed. The pellet was washed in 1 ml chilled 75% ethanol (Fisher Scientific, Cat #E/0665DF/17) by centrifugation at 7,500 x g for 5 mins at 4^{O}C. The supernatant was removed, and the pellet was left to air dry for 2-5 mins before addition of 20 µl nuclease free water (Qiagen, Cat #129114) and quantification on a Thermo Scientific Nanodrop 2000 and stored at -80^{O}C.

2.1.6. First strand cDNA synthesis

cDNA synthesis was performed using a Superscript II RT kit (Invitrogen Cat, #18064022). A reaction mixture of 1 µL Oligo(dT)12-18 (500 µg/mL), 2 µg total RNA, 1 µL dNTP Mix (10 mM each) and distilled water to 12 µL was made and incubated at 65^{O}C for 5 mins. 4 µL 5X First-Strand Buffer, 2 µL 0.1 M DTT, 1 µL RNaseOUT (Invitrogen, Cat #10777019) and 1 µL (200 units) of SuperScript™ II RT were added to the reaction mixture and incubated at 42^{O}C for 50 mins before the reaction was inactivated by incubation at 70^{O}C for 15 mins. cDNA was stored at -20^{O}C.

2.1.7. RT-PCR

Unless stated, RT-PCR was performed using 5x FIREPol DNA Polymerase master mix (Solis BioDyne, Cat #04-12-00125) in 10 µl reactions on a BioRad C1000 Touch or T1000 thermocycler. Reactions used 2 µl 5x FIREPol Master Mix, 0.5 µl 10 µM primer (forward and reverse), 1 µl cDNA and 6 µl nuclease free water. Any larger volume RT-PCR reactions were scaled accordingly. RT-PCR cycles were as listed in Table 2.2. unless stated with variable cycle numbers specific to the experiment and annealing temperatures specific to the primers listed in Table 2.1.

Initial Denaturation	98 ^{O}C	5 min
Variable cycles	95 ^{O}C denaturation Variable ^{O}C annealing 72 ^{O}C Extension	30 s 30s 20 s
Final Extension	72 ^{O}C	5 mins
Storage	4^{O}C	Hold

Table 2.2. RT-PCR cycles used for standard experiments.

2.1.8 qRT-PCR

qRT-PCR was performed using 2x SYBR Green master mix (Applied Biosystems, Cat #4309155) with a 20 µl reaction on a Biorad CFX96 Touch Thermocycler. 10 µl 2x SYBR Green Master Mix, 1 µl 10 µM primer (forward and reverse), 1 µl cDNA and 7 µl nuclease-free water. Unless stated, cycles followed Figure 2.1. with annealing temperatures specific to the primer pair in Table 2.1. Three technical replicates were used for each sample with a no cDNA control for each primer pair used and a technical replicate of three nuclease free water only wells per plate.

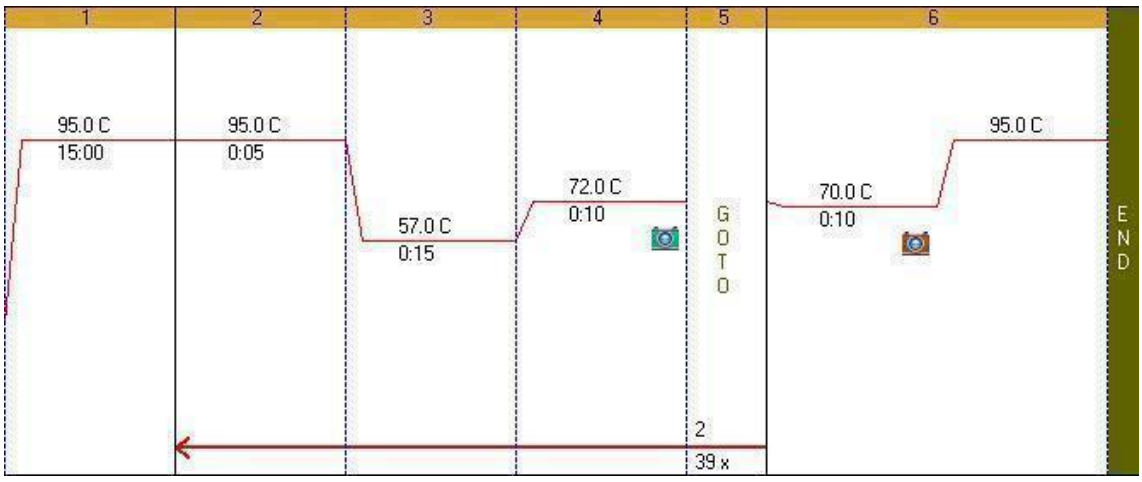

Figure 2.1. qRT-PCR cycler programme for standard experiments

(1) initial denaturation. (2-5) 39 cycles of denaturation, annealing, extension, and recording. (6) Melt curve analysis and final hold.

2.1.9 qRT-PCR Analysis

Ct values were analysed and technical replicates outside of the 0.5 standard deviation range were removed for calculation of ΔCt and ΔΔCt. ΔCt scores were calculated from the housekeeping gene and ΔΔCt calculated for comparison of gene expression and statistics performed on this value. $2^{-\Delta\Delta Ct}$ scores were then calculated for presentation of the data.

2.1.10. Sample size and statistics

Sample sizes and experimental power were selected based on previous experiments using zebrafish tailfin injury and the observation of neutrophil phenotype published by the Renshaw group (Renshaw *et al.*, 2006; Ogryzko *et al.*, 2014; Robertson *et al.*, 2014; Isles *et al.*, 2019).

Statistics were carried out using GraphPad Prism 9. All data was tested to confirm it fit a normal distribution using a Shapiro-Wilk test. Experiments comparing a single variable used a two-tailed student t-test. Multiple variable comparisons used ANOVA with multiple comparisons or a mixed-effects analysis with multiple variables when there were missed values. Single-variable data comparisons that did not fit a normal distribution were analysed using a Mann-Whitney test.

2.2. Materials and Methods for Chapter 3

2.2.1 Drug preparation

2.2.1.a. R848

R848 (Invivogen, Cat #tlrl-r848) was supplied lyophilised as 500 ug. 1mg/µl was prepared as a stock solution of 2.85 mM in endotoxin-free water supplied with the kit. Stock solution was made into 50 µl aliquots and stored at -20^{O}C.

2.2.1.b. C646

C646 (MCE, Cat #HY-13823)) was supplied as a 1 mg (molecular weight 445.43 g/mol) powder soluble in DMSO. 25 mM stock was made by addition of 89.8 µl of DMSO (Sigma-Aldrich, Cat #276855). 10 µl aliquots were made and stored at -20^{O}C.

2.2.1.c. EX527

EX527 (Santa Cruz Biotechnology, Cat #sc-203044) was provided as a 50 mM stock from the Lynne Prince group and stored at -20^{O}C.

2.2.2. R848 toxicity test

Dechorionated 2 dpf *Tg(mpx:GFP)i114* zebrafish were added to a well of a 6 well plate containing 0, 1, 5 or 50 µM of R848 in 3 ml of E3 and incubated for 16 h at 28^{O}C. Larvae either underwent tailfin transection (Materials and Methods 2.1.2) or were left uninjured. Injured fish were returned to the appropriate R848 concentration immediately following tail transection. Larvae were observed for anatomical and behavioural abnormalities 16 hours post-incubation and then 1-, 3-, 6-, 8- and 24-hours post-injury (hpi) in line with key inflammatory time points in caudal fin injury. Any fish deemed too unwell to continue the experiment were euthanised.

2.2.3. Neutrophil distribution assays in the presence of R848

Dechorionated 2 dpf *Tg(mpx:GFP)i114* zebrafish were added to a well of a 6 well plate containing 0, 1 and 5 µM of R848 in 3 ml of E3 and incubated overnight for 16 h at 28^{O}C. 17.5 hours after incubation the fish were embedded in 0.8% Low Melting Point (LMP)-Agarose (Sigma, Cat #A9414) containing 0.168 mg/ml tricaine. Fish were imaged using a wild-field Nikon microscope taking vertical Z-stacks at 18 hours after incubation. Maximum intensity

projections (MaxIP) were created using NIS elements and the fish separated into four regions of interest, head, caudal haematopoietic tissue (CHT), somites and tail, with neutrophil numbers in each region assessed. The sum of neutrophils in each region indicated total neutrophil numbers in the whole organism.

2.2.4. Neutrophil recruitment assay following tailfin transection.

Neutrophil recruitment was assessed in larvae incubated immediately with R848 following tailfin transection or following 16 hours pre-incubation prior to transection. 2 or 3 dpf *Tg(mpx:GFP)i114* zebrafish were anaesthetised in 0.168 mg/ml tricaine, the caudal fin removed (Materials and Methods 2.1.2) and added to a 24 well plate containing a range of R848 (0-50uM) in 500 µl of E3, time points of incubation and injury specific to experiment. At 1-, 3-, 6-, and 24-hours post injury, the number of neutrophils posterior to the circulatory loop were counted under a wide-field fluorescent microscope and percentage changes in neutrophils calculated between timepoints indicated in the results, with one fish kept per well to ensure percentages calculated applied to individual fish.

2.2.5. Neutrophil counts during inflammation resolution following tail fin transection and R848 incubation.

3 dpf *Tg(mpx:GFP)i114* zebrafish were anaesthetised in 0.168 mg/ml tricaine and the caudal fin removed (Materials and Methods 2.1.2). At 3.5 hpi injured fish were screened under a Leica fluorescent microscope for non-responders and over-responders (fish that display abnormally high or low numbers of neutrophils at the site of injury), and these were removed from the experiment. At 4 hpi single injured fish were added to each well of a 24 well plate containing 0, 5 or 50 µM R848 in 500 µl E3 giving 6 fish for each concentration. At 8 and 24 hpi, the number of neutrophils posterior to the circulatory loop were counted under a wide-field fluorescent microscope and percentage changes in neutrophils calculated.

2.2.6. Calculation of percentage change in neutrophil number

Percentage change in number of neutrophils between specific time points where *x* is the earlier time point and *y* is the later, was calculated as follows:

$$\%\ increase\ in\ neutrophils\ = 100(\frac{\#\ neutrophils\ at\ y - \#\ neutrophils\ at\ x}{\#\ neutrophils\ at\ x})$$

$$\%\ decrease\ in\ neutrophils\ = 100(\frac{\#\ neutrophils\ at\ x - \#\ neutrophils\ at\ y}{\#\ neutrophils\ at\ x})$$

2.2.7. Quantification of caudal fin specific reporter expression

2.2.7.a. *tnfa*

Adapted from Lewis and Elks, (2019). Dechorionated 2 dpf *TgBAC(tnfa:GFP)pd1028* zebrafish – a line containing a single copy of the *tnfa:GFP* transgene confirmed by Catherine Loynes, though it is unclear whether these were homozygous or heterozygous carriers of the transgene – were incubated for 4 h in a 6 well plate with 4 wells containing 0 or 5 µM R848 in 3 ml E3 (15 fish per well, 2 wells per concentration). Each larva from one of the treated and untreated wells were anaesthetised in 0.168 mg/ml tricaine, the caudal fin removed (Materials and Methods 2.1.2) and returned to the well. This gave 4 groups (Table 2.3).

Well #	Larvae condition
1	Untreated and uninjured
2	5 µM R848 and uninjured
3	Untreated and injured
4	5 µM R848 and injured

Table 2.3. Treatment conditions of *TgBAC(tnfa:GFP)pd1028* larval zebrafish for tailfin injury and expression analysis

At 15.5 hpi, fish were mounted in 0.8% low-melting point agarose and at 16 hpi vertical z-stacks were taken using a Perkin Elmer spinning disk confocal microscope. Using Volocity, MaxIP were created, and ROIs drawn around the caudal fin posterior to the circulatory loop. Mean GFP intensity within the ROI was then recorded.

2.2.7.b. *Il1b*

Adapted from Ogryzko *et al.*, (2014). Dechorionated 2 dpf *TgBAC(il1b-GFP)sh445* zebrafish – a homozygous transgenic reporter line containing a single copy of the *il1b-GFP* transgene confirmed by Catherine Loynes – were incubated for 16 h in a 6 well plate containing 0 or 5 µM R848 in 3 ml E3. Each fish was anaesthetised in 0.168 mg/ml tricaine, and the caudal fin removed (Materials and Methods 2.1.2) and returned to the 6 well plate. At 5.5 hpi, fish were mounted in 0.8% low-melting point agarose and at 6 hpi vertical z-stacks were taken using a Perkin Elmer spinning disk confocal microscope. Using Velocity, MaxIP were created, and an ROI drawn around the caudal fin posterior to the circulatory loop. Mean GFP intensity within the ROI was then recorded.

2.2.8. Quantification of neutrophil specific reporter expression

2.2.8.a. NF-κB

Adapted from Ogryzko *et al.*, (2014). For specific quantification of GFP intensity within the neutrophils, *Tg(pnfκB:EGFP)sh235* – confirmed as containing a single, heterozygous copy of the transgenic insert by Catherine Loynes – were crossed to *Tg(LyzC:ntr-mCherry)sh260* zebrafish. Larvae were incubated in R848, anaesthetised in 0.168 mg/ml tricaine, the caudal fin removed (Materials and Methods 2.1.2). At 7.5 hpi, fish were mounted in 0.8% low-melting point agarose and at 8 hpi vertical z-stacks were taken using a wide-field Nikon microscope. Using NIS Elements, MaxIP were created. Within the MaxIP images two regions of interest (ROI) were drawn posterior to the circulatory loop; one ROI dorsal to the notochord and one ROI lateral to the neuroblasts. These 2 regions have endogenous NF-κB expression and therefore GFP expression and were subsequently removed from the analysis. To detect and count neutrophils, the autodetect ROI function in NIS elements was used to highlight all mCherry labelled cells posterior to the circulatory loop. Any neutrophils overlapping with the notochord and neuromasts were removed for the reasons stated above (Materials and Methods 2.2.7.a). The mean value of GFP was recorded within the neutrophils.

2.2.8.b. *tnfa*

To observe GFP intensity in neutrophils specifically and at neutrophil specific time points of resolution, *TgBAC(tnfa:GFP)pd1028* were crossed with *Tg(lyz:nfsβ-mCherry)sh260* – this ensured any fish contained single copies of the *tnfa:GFP* transgene as any positive fish would be heterozygous. 2 dpf larvae were dechorionated and incubated in R848 for 16 h in 6 well plates (as in Materials and Methods 2.2.7.b). After the 16 h incubation larvae were anaesthetised in 0.168 mg/ml tricaine, and the caudal fin removed (Materials and Methods 2.1.2). At 7.5 hpi, fish were mounted in 0.8% low-melting point agarose and at 8 hpi vertical z-stacks were taken using a Perkin Elmer spinning disk confocal microscope. Using Volocity, MaxIP were created, and ROIs drawn around the caudal fin posterior to the circulatory loop. Mean GFP intensity within the ROI was then recorded. Using the detect object tool cropped to the ROI, mCherry labelled neutrophils were highlighted and mean GFP recorded. Neutrophil numbers were also recorded.

2.2.9. qRT-PCR for *il6* following R848 treatment.

2.2.9.a. Sample preparation and snap freezing for RNA extraction

2 dpf *Tg(mpx:GFP)i114* zebrafish were treated with 0 and 5 µM R848 in 3 ml E3 in a 6 well plate with 15 fish in each well for 16 hours. Groups were created as shown in Table 2.4. The injury groups were anaesthetised in 0.168 mg/ml tricaine, and the caudal fin removed (Materials and Methods 2.1.2) . At the time points listed, all the fish in a designated well were anaesthetised in 0.168 mg/ml tricaine and pipetted into a 1.5 ml tube and excess E3 removed. Samples were snap frozen in a methanol dry-ice bath and stored at -80^{O}C for RNA extraction (Materials and Methods 2.1.5).

Snap-freeze timepoint	Plate 1 – Untreated and Uninjured	Plate 2 – Untreated and injured	Plate 3 – 5 µM R848 and Uninjured	Plate 4 - 5 µM R848 and injured
0 hpi	Well 1	Well 1	Well 1	Well 1
1 hpi	Well 2	Well 2	Well 2	Well 2
3 hpi	Well 3	Well 3	Well 3	Well 3
6 hpi	Well 4	Well 4	Well 4	Well 4
8 hpi	Well 5	Well 5	Well 5	Well 5
24 hpi	Well 6	Well 6	Well 6	Well 6

Table 2.4. Snap freeze groups for qPCR analysis of *il6* gene expression in larval zebrafish. 15 fish per well, 0 hpi denotes injury following 16 h R848 incubation.

2.2.9.b. Primer optimisation

2.2.9.b.i. RT-PCR

il6 Primers were designed as described in method 2.1.3 spanning exon-exon junctions for qRT-PCR. Primers were first tested using RT-PCR with a gradient of temperatures ranging ±5^{O}C from the suggested primer T_m (Table 2.1) with cDNA from the untreated and uninjured group described in method 2.2.9i. RT-PCR cycles and reaction mix for 10 µl reaction were as described in Materials and Methods 2.1.7 and Table 2.2. 10 µl PCR product and 5 µl 50 bp ladder was run for 45 minutes at 100 V on a 2% agarose gel (SLS, Cat #BIO41025) in TAE and imaged using a Syngene U:Genius gel dock. The annealing temperature with the clearest band was selected to be used for qRT-PCR.

2.2.9.b.ii. qRT-PCR

Primer efficiency was optimised by using serial dilutions of cDNA from 1:5, 1:10, 1:20, 1:50 to 1:100 with *il6* primers or *rsp29* primers as a housekeeping gene. Melt curve analysis was also performed to check for non-specific amplification. 20 µl reactions were set up for each dilution and run as described in Materials and Methods 2.1.8 and Figure 2.1 using a 57^{o}C annealing temperature. Ct values for each dilution for the primers were then plotted against Log_{10}(dilution) to assess the efficiency of the primers.

2.2.9.c. Whole body qRT-PCR to detect changes in *il6* expression following R848 incubation.

cDNA generated from the samples described in Table 2.4 were amplified with primers for *il6* and *rsp29* (Table 2.1) as a housekeeping gene using the reaction mixes and protocol described in method 2.1.8 and Figure 2.1 respectively. Annealing temperatures were 57^{O}C. Comparison of *il6* expression was then compared between groups injured and treated with R848 using ΔΔCt values calculated from Ct values as described in Materials and Methods 2.1.9.

2.2.10. *myd88* Morpholino injection optimisation

myd88 e2i2 splice-blocking morpholino-oligonucleotide (MO) (Bates *et al.*, 2007) 5'-GTTAAACACTGACCCTGTGGATCAT-3' was injected into *TgBAC(mpx:GFP)i114* embryos at the single cell stage. 0.5 mM and 1 mM were injected at 0.5, 1 and 2 nl volumes. At 3 dpf, embryos were euthanised by overdose of tricaine and RNA extracted by TRIzol (Materials and Methods 2.1.5) and converted to cDNA using First strand synthesis with Superscript II (Materials and Methods 2.1.6). Successful knockdown was confirmed by RT-PCR using published primers (Table 2.1) (Bates *et al.*, 2007) using standard RT-PCR protocols as described in Materials and Methods 2.1.7 and Table 2.2. A no cDNA and uninjected controls were also added. Samples were run on a 2% agarose gel at 100 V for 45 mins with a NEB 50 bp ladder. Successful MO knockdown was shown by a 598 bp band, compared to a 543 bp wildtype (WT) band. Figure 2.2A shows how the morpholino alters the MyD88 sequence. The MO (magenta) blocks intron splicing between exon 2 and 3 (grey) by blocking the splice site at the 3' end of exon 2. This incorporates intron 2 (green) into the mRNA sequence creating a new exon 2 that combines exon 2, intron 2 and exon 3 (cyan). RT-PCR of cDNA synthesised from the RNA of MO injected larvae will therefore produce a 598 bp band that incorporates this larger exon 2, while the RT-PCR amplification of cDNA from wildtype RNA will produce a 543 bp band as the amplicon spans the wildtype exon 2-3 junction (Figure 2.2B).

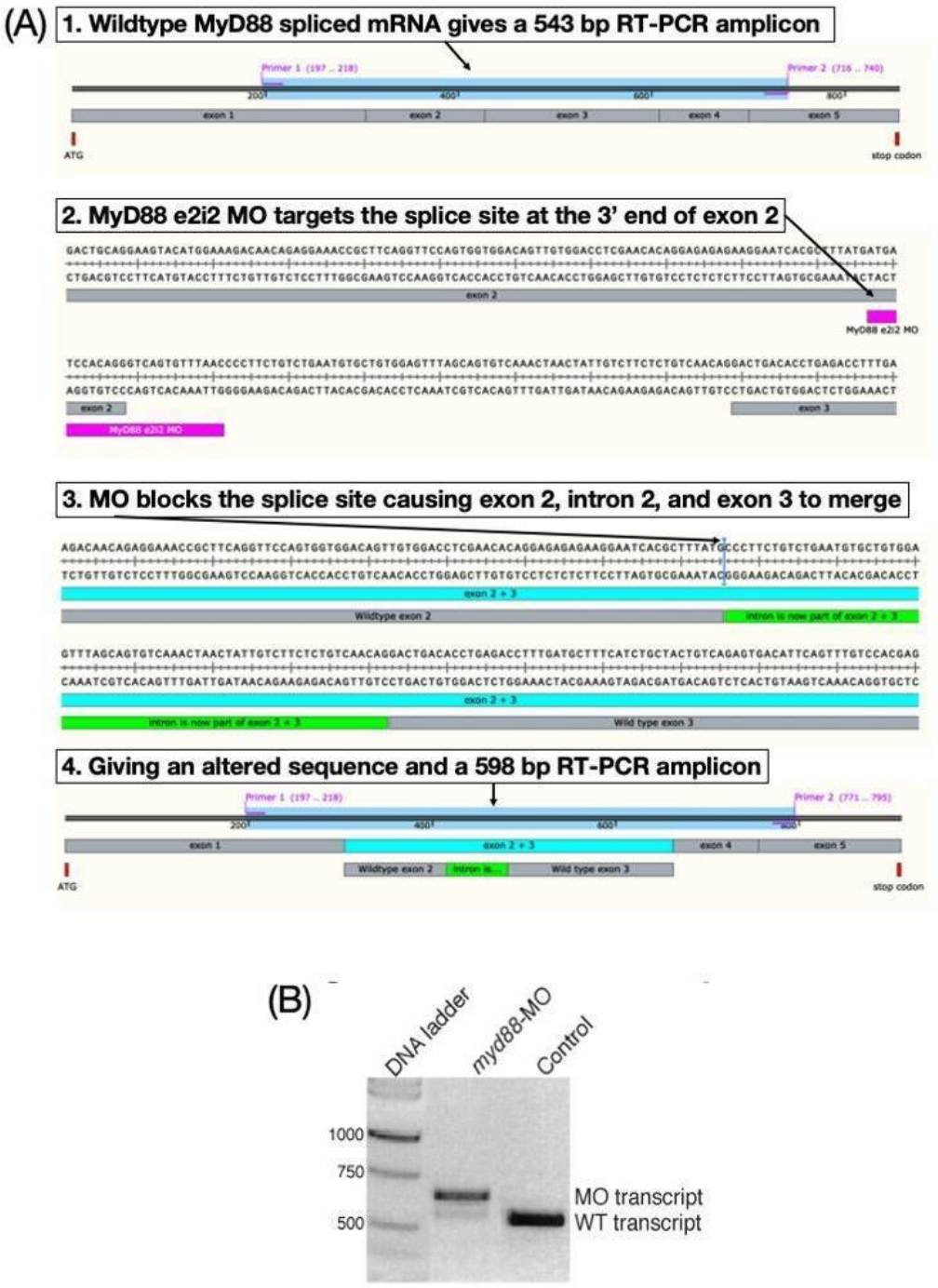

Figure 2.2. MyD88 morpholino expected band size.

(A) SnapGene created schematic of how the MyD88 e2i2 splice-site blocking morpholino (magenta) alters the wild type MyD88 sequence (grey) to change structure and function by combining exon 2 and 3 by blocking splicing when the 3' end of exon 2 meets intron 2 (cyan and green) (B) Example gel for transcript size of *myD88* mRNA fragment following injection of *myd88* MO and RT-PCR using primers in A (Bates *et al.*, 2007)

2.2.11. Neutrophil inflammation resolution following *myd88* morpholino injection and R848 incubation.

2 nl, 1 mM MyD88 e2i2 morpholino or a scramble control MO were injected into 50 *TgBAC(mpx:GFP)i114* embryos at the single cell stage. Injected plates were screened for survival daily. 6 treatment groups were needed for analysis with 6 embryos per group (Table 2.5).

Group	Morpholino	5 µM R848
1	-	-
2	-	+
3	Control	-
4	Control	+
5	MyD88	-
6	MyD88	+

Table 2.5. Treatment groups for *myd88* morpholino injection and R848 treatment

Each treatment group was prepared in a labelled universal tube in E3 with methylene blue. 3 dpf, embryos were anaesthetised in 0.168 mg/ml tricaine, the caudal fin removed (Materials and Methods 2.1.2), and the embryo transferred to clean E3 for 4 hours. 4 hpi, embryos were transferred to a 24 well plate in 20 µl E3, each row represented a treatment group and containing 480 µl of media. Neutrophils were counted at 8 and 24 hpi under a Leica fluorescent microscope.

2.2.12. Neutrophil counts during inflammation resolution following incubation with C646 and R848

3 dpf *TgBAC(mpx:GFP)i114* zebrafish were anaesthetised in 0.168 mg/ml tricaine, the caudal fin removed (Materials and Methods 2.1.2), and larvae transferred to clean E3 to recover. At 4 hpi single injured fish were added to each well of a 24 well plate containing E3 + methylene blue, an E3 + DMSO control, 5 µM R848, 5 µM C646 and 5 µM R848 + 5 µM C646 giving 6 fish for each concentration. At 8 and 24 hpi, the number of neutrophils posterior to the circulatory loop were counted under a wide-field fluorescent microscope and percentage changes in neutrophils calculated (Materials and Methods 2.2.6).

2.2.13. Neutrophil recruitment in the presence of the SIRT1 inhibitor EX527

3 dpf *TgBAC(mpx:GFP)i114* zebrafish were anaesthetised in 0.168 mg/ml tricaine, the caudal fin removed (Materials and Methods 2.1.2) and added to a 24 well. Each well was prepared containing 480 µl of 50 µM Sirt1 inhibitor EX527. At 3 and 6 hpi the number of neutrophils posterior to the circulatory loop were counted under a Leica wide-field fluorescent microscope and percentage changes in neutrophils calculated between timepoints (Materials and Methods 2.2.6).

2.3. Materials and Methods for Chapter 4

2.3.1. RNAseq analysis

2.3.1.a. Human datasets

Chromatin remodelling enzyme lists were compiled from the literature (Keppler and Archer, 2008; Zhang *et al.*, 2016). These enzymes were identified in two datasets. First, a human neutrophil RNAseq dataset measuring expression of genes in human *in vitro* neutrophils treated with a range of pro-inflammatory cytokines (G-CSF, GM-CSF, IL-1β, IL-6, IFNγ, IFNα, IL-8 and TNFα) (Wright *et al.*, 2013). Second, a dataset of human *in vitro* neutrophils stimulated with either PMA or *E. coli* (Denholtz *et al.*, 2020). RPKM values below 0.3 were removed from both datasets as potential false positives. Chromatin remodelling enzymes RPKM values were compiled from both datasets and analysed separately.

2.3.1.b. Zebrafish datasets

Chromatin remodelling enzyme expression was analysed in zebrafish neutrophils. The dataset compiled RPKM values for genes in cells sorted for *mpx*- or *mpx*+, with *mpx*+ denoting the neutrophil population (Rougeot *et al.*, 2019). RPKM values below 0.3 were removed as potential false positives and chromatin remodelling enzyme RPKM values compiled.

2.3.2. CRISPR RNA design

Guide RNA targeting within either the 5'-UTR, promoter or coding sequence region of each protein were designed using CHOPCHOP (https://chopchop.cbu.uib.no/) (Table 2.6). Guides were ordered as CRISPR RNAs (crRNAs), guides that are synthesised to better form the guide RNA-tracrRNA-Cas9 complex that cleaves DNA (Karvelis *et al.*, 2013). RT-PCR primers either side of the target Cas9 region were selected, along with restriction enzymes to identify successful Cas9 activity by diagnostic digest.

Target gene/guide name	Target site	5'-3' Sequence inc. 3'PAM
brd4	Promoter	GGTGACGTCATGCAGCGCGGAGG
crebbpa	5'UTR	GCGTTGAATTCGCGGAAAGGAGG
ep300a	Promoter	GGCTTATGTGCCTATCTCCGAGG
kdm6bb guide 1	5' UTR	AAGGCCACTCACCAAAACGGAGG
dot1l guide 1	5" UTR	CTGACCGACCCCTGCAAAGGAGG
hdac6	5' UTR	CGGCTTCGATGAGCTCACTGCGG
brd2a	5' UTR	CGGATCCATCCCGATGGAAACGG
brd2b	5' UTR	GCGATACATCCGGATGGAGGCGG
sirt6	5' UTR	ATGTCGGTGAATTACGCCGCAGG
tyr	Coding sequence	GGACTGGAGGACTTCTGGGGAG G
kdm6ba	5'UTR	TTGTATGACCTGCTGGACATTGG
kdm6bb guide 2	5'UTR	GGCGACAGGATTGACTCGGGAG G
***kdm6ba* exon 5**	Coding sequence	CACACGGGACCCTTTTCCTCTGG
***kdm6ba* exon 6**	Coding sequence	CCATTGTTCAAGAATTTACTAGG
***kdm6bb* exon 3.1**	Coding sequence	GTATTCTGGACGTAACTCGTTGG
***kdm6ba* exon 3.2**	Coding sequence	CCCCAGGCAACAACCGGCACTGG
dot1l guide 2	5'UTR	CTTTGCAGGGGTCGGTCAGGTGG
dot1l	Coding sequence	TTTCCGGGTCGGTGACAGAGTGG
ezh2	Coding sequence	CTCGGACAGCCAGGTAGCACGGG
ezh2	5'UTR	TCTGTCTATAGGGAAACCATGGG

Table 2.6. crRNAs used for CRISPR/Cas9 mediated knockdown experiments.

Guides in bold show those selected for CRISPR/Cas9 experiments

2.3.3. crRNA optimisation and diagnostic digests

Primers were tested on genomic DNA from 3 dpf *TgBAC(mpx:GFP)i114*. A 20 µl reaction mixture was made scaled to the mixture described in Materials and Methods 2.1.7 with a programme as described in Table 2.2. with annealing temperatures specific to the primer.

Following PCR, 10 µl of reaction mixture was run on a 2% agarose TAE gel for 45-60 mins at 100 V and imaged using a Syngene U:Genius gel dock to confirm the presence of the correct size amplicon. 1 µl restriction enzyme – enzyme specific to the sgRNA cut site – was added to the remaining 10 µl of PCR product and incubated for 4 h at the correct temperature specific to each restriction enzyme.

2.3.4. Single cell injection of crRNAs

crRNA guides for chromatin remodelling enzymes (Table 2.6) were injected into the yolk of *TgBAC(mpx:GFP)i114* embryos at the one cell stage. Injection mixture contained 1 µl crRNA 20 µM, 1 µl Tracr 20 µM, 1 µl Cas9 protein (Invitrogen Cat #A36496) and 0.2 µl phenol red. crRNA guide for *tyr* (tyrosinase) was used as a control. 2 nl was injected using a graticule to confirm correct volume was injected. Larvae were checked daily, and unfertilised eggs/dead embryos removed. 3 dpf embryos were dechorionated and genomic DNA was extracted (Materials and Methods 2.1.4). PCR and diagnostic digests (Materials and Methods 2.3.3) were performed to check Cas9 activity and efficiency.

2.3.5. Neutrophil counts following single cell injection and tailfin transection.

Single cell injection was performed as described in method 2.2.4. At 3 dpf, the larvae were anaesthetised in 0.168 mg/ml tricaine, the caudal fin removed (Materials and Methods 2.1.2) and each larva placed into single wells of a 24 well plate containing 480 µl of E3. At 3 hpi, larvae were anaesthetised in 0.168 mg/ml tricaine, and neutrophils counted at the tailfin using a Leica fluorescent microscope. Larvae were then transferred to a new 24 well plate containing fresh E3. The anaesthetic, counting and recovery steps were repeated at 6 and 24 hpi. Following counting at 24 hpi, larvae were placed into labelled 8-strip PCR tubes and gDNA extracted for genotyping to confirm successful knockdown (Materials and Methods 2.1.4).

2.3.6. Analysis of gene expression following whole body knockdown of *kdm6ba/b*

2.3.6.a. RT-PCR

RT-PCR was used to confirm reduction in expression of *kdm6ba* and *kdm6bb* following CRISPR/Cas9 mediated knockdown. Primers used were for *ef1a* as a housekeeping gene – replacing *rsp29* as members of the laboratory showed *ef1a* produced more consistent and reliable Ct values (Hamilton *et al.*, 2020), *kdm6ba* mRNA, *kdm6bb* mRNA and *hif1a* – a gene linked to *kdm6b* – as listed in Table 2.1 with an annealing temperature of 58^{O}C. 10 µl reactions

were used and standard cycles (Materials and Methods 2.1.7 and Table 2.2). Samples were run on a 1% agarose TAE gel with NEB low molecular weight ladder and imaged using a Syngene U:Genius gel dock.

2.3.6.b. qRT-PCR

qRT-PCR was used to look at expression changes following CRISPR/Cas9 knockdown of *kdm6ba* and *b*. As in method 2.2.6.i. primers for *ef1a, kdm6ba* mRNA, *kdm6bb* mRNA and *hif1a* were used. 20 µl reaction mix with 1:10 cDNA was used and standard cycles at 58^{O}C (Materials and Methods 2.1.8 and Figure 2.1). Analysis was performed as described in Materials and Methods 2.1.9.

2.3.7. Neutrophil specific CRISPR/Cas9 plasmid creation

2.3.7.a. Transgenic construct for Cas9 expression

Plasmids for neutrophil specific knockdown of chromatin remodelling enzymes were adapted from published methods (Zhou *et al.*, 2018). Cas9 protein expression was driven within the zebrafish using a neutrophil specific promoter within the following vector lyz:cas9-pA-Cry-GFP and a stable line generated *Tg(lyz:cas9;cry:GFP)* by Catherine Loynes.

2.3.7.b. Design of neutrophil specific chromatin remodelling sgRNA primers for constructs

Guide RNAs specific to chromatin remodelling enzymes were generated using the protocol for cloning two sgRNAs into one plasmid by replacement of Rac2 sgRNAs supplied by the Deng group (Zhou *et al.*, 2018). Guide RNAs were chosen from crRNAs that showed successful whole-body knockdown combined with priority lists (Chapter 4). Guides *kdm6ba* and *kdm6bb* 2 (Table 2.6) were chosen and primers designed based on the Zhou *et al.*, (2018). protocol, giving four primer sequences called *kdm6ba/b* neutrophil specific g1 and g2 forward and reverse (Table 2.1).

2.3.7.c. Digestion of p3E-U6-U6c-Rac2 for preparation of 3.5 kb and 0.5 kb fragments for cloning

10 ug of Midi prepped p3E-U6-U6c-Rac2 – prepared by Catherine Loynes – was digested using SalI (NEB, Cat #R0138) in a reaction mixture of 12.5 µl p3E-U6-U6c-Rac2, 2 µl SalI, 10 µl of NEB

rCutSmart buffer and 75.5 µl of nuclease free water and left at 37^{O}C overnight. 6x loading buffer (NEB, Cat #B7024) was added to the reaction mix and samples run on a 1% agarose TAE gel with a Bioline 1 kb ladder. 3.5 kb and 0.5 kb bands were cut out under blue light and kept in separate Eppendorf tubes. Gel extraction was performed using Qiagen MinElute gel extraction kit (Qiagen Cat No. 28604) using the standard instructions.

2.3.7.d. Optimisation of primers insertion of guide RNAs into the 3' entry clone

Platinum SuperFi II DNA polymerase (Invitrogen, Cat #1261010) was used with the reaction mixture of 4 µl Platinum SuperFi II buffer, 1 µl forward primer, 1 µl reverse primer, 0.4 µl 10 mM dNTPs 0.4 µl Platinum Superfi II DNA polymerase, 1 µl cut plasmid template, 12.2 µl nuclear free water.

Plasmid template was specific to the primer pair, for *kdm6ba* and *kdm6bb* knockdown the following was required:

- 0.5 kb fragment kdm6ba/b neutrophil specific g1 forward and g1 reverse
- 3.5 kb fragment kdm6ba/b neutrophil specific g2 forward and g2 reverse

RT-PCR was performed according to the Table 2.7 and successful amplification was confirmed using a 1% agarose TAE gel run for 30-45 mins at 100 V and imaged on a Syngene U:Genius gel dock.

Step	**Platinum SuperFi II DNA polymerase**
Denaturation	98^{O}C for 5 mins
35 cycles Denaturation Annealing Elongation	35 cycles 98^{O}C for 10 s 68^{O}C for 30 s 72^{O}C - 30 s for 0.5 kb, 2 min for 3.5 kb
Final Elongation	72^{O}C for 5 mins

Table 2.7. RT-PCR cycles for optimisation of primers for cloning of specific guide RNA fragments into the U6a/U6c backbone for neutrophil specific knockdown

2.3.7.e. Insertion of chromatin remodelling sgRNAs into U6a/U6c 3' entry clone

2.3.7.e.i. RT-PCR

kdm6ba and *b* guide RNA primers were cloned into the 0.5 kb and the 3.5 kb fragments of the backbone using the RT-PCR cycles for Platinum Superfi II DNA polymerase described above (Materials and Methods 2.3.7.d, Table 2.7.) The reaction mixture was increased to 50 µl and made up of 10 µl Platinum SuperFi II buffer, 2.5 µl forward primer, 2.5 µl reverse primer, 1 µl 10 mM dNTPs, 1 µl Platinum Superfi II DNA polymerase, 1 µl 3.5 kb plasmid template or 2 µl 0.5 kb plasmid template, 32 µl or 31 µl nuclear free water. The 50 µl reaction was split across two PCR tubes into 2 x 25 µl.

2.3.7.e.ii. DpnI digest to remove non-amplified template.

Following the RT-PCR, reaction mixes were treated with 1 µl of Dpn1 restriction enzyme (NEB, Cat # R0176) overnight at 37^{O}C to remove any non-amplified template. The 25 µl reactions were then recombined and 5 µl of each reaction was diluted with 6X loading buffer and run on a 1% agarose TAE gel with a 1 kb Hyperladder to confirm the presence of the correct bands and the presence of single bands.

2.3.7.e.iii. PCR purification of amplified fragments.

On confirmation of single bands in both the 0.5 kb and 3.5 kb amplified fragments, PCR purification was performed. Purification was performed using the standard instructions for NucleoSpin Gel and PCR Clean-up Kit (Cat #740609.10). Concentration was confirmed using a Thermo Scientific Nanodrop 2000.

2.3.7.e.iv. In-Fusion HD Cloning of 3.5 kb and 0.5 kb *kdm6ba/b* guide RNA plasmid.

In-Fusion HD Cloning Plus Kit (Takara Cat# 638909), following the standard instructions. Based on the concentration of the fragments obtained by PCR and purification, the following reaction mixtures was used 2 µl 5x In-Fusion HD enzyme mix, 2 µl 3.5 kb fragment, 1 µl 0.5 kb fragment, 5.14 µl dH_2O. Negative and positive control reactions were set up according to the instructions. Reactions were incubated at 50^{O}C for 15 mins and stored at -20^{O}C.

2.3.7.e.v.Transformation of InFusion HD Product

The 4 kb fragment created by the InFusion HD reaction was transformed into Top 10 competent cells to obtain a higher volume of plasmid. 50 µl of cells were used per reaction. 2.5 µl reaction was added to the cells, mixed gently with a pipette tip, and placed on ice for 30 mins. Tubes were heat shocked in a 42^{O}C water bath for 45 s and placed back on ice for 2 mins. Final volume was brought up to 500 µl with 37^{O}C SOC medium (Takara, Cat #636763) and incubated at 37 ^{O}C in a shaking incubator at 200 rpm for 90 mins. 1:5, 1:10, 1:50 and 1:100 dilutions and the remaining reactions – 5 plates per reaction – were then spread on antibiotic selection LB agar (Sigma-Aldrich, #05039) plates (control vector 100 ug/µl ampicillin (Sigma, Cat #A9393), kdm6b 50 ug/µl kanamycin (Sigma, Cat #K0254) and incubated at 37^{O}C overnight. Plates were checked for colonies the next morning and single colonies were picked and grown in 5 ml LB broth (Sigma, Cat #L7275) in the correct selection antibiotic in 14 ml culture tubes in a 37^{O}C shaking incubator overnight at 200 rpm.

2.3.7.e.vi. Midi-prep of transformed InFusion HD colonies

Cultures that showed successful growth – a cloudy culture, not clear – were prepared by Nucleobond P100 Midiprep (Macherey-Nagel, Cat #740573) for High copy plasmids using the standard instructions. Concentration was confirmed using a Thermo Scientific Nanodrop 2000.

2.3.7e.vii. Confirmation of successful reaction to form p3E-U6a-kdm6bg1-U6c-kdm6bg2.

Restriction digest was performed to confirm the presence of a successful product. PstI (NEB, Cat #R0140) was used as suggested in the original method for making the plasmid to give a single cut to linearise the circular plasmid (Zhou *et al.*, 2018). AvaI (NEB, Cat #R0152) was added as an enzyme that makes several cuts. Expected band sizes are shown in Figure 2.3

using a Bioline 1 kb Hyperladder. The reaction mixture containing 1 µl plasmid DNA, 5 µl NEB buffer, 1 µl enzyme and 43 µl nuclease free water. Both reactions were left overnight at 37^{O}C.

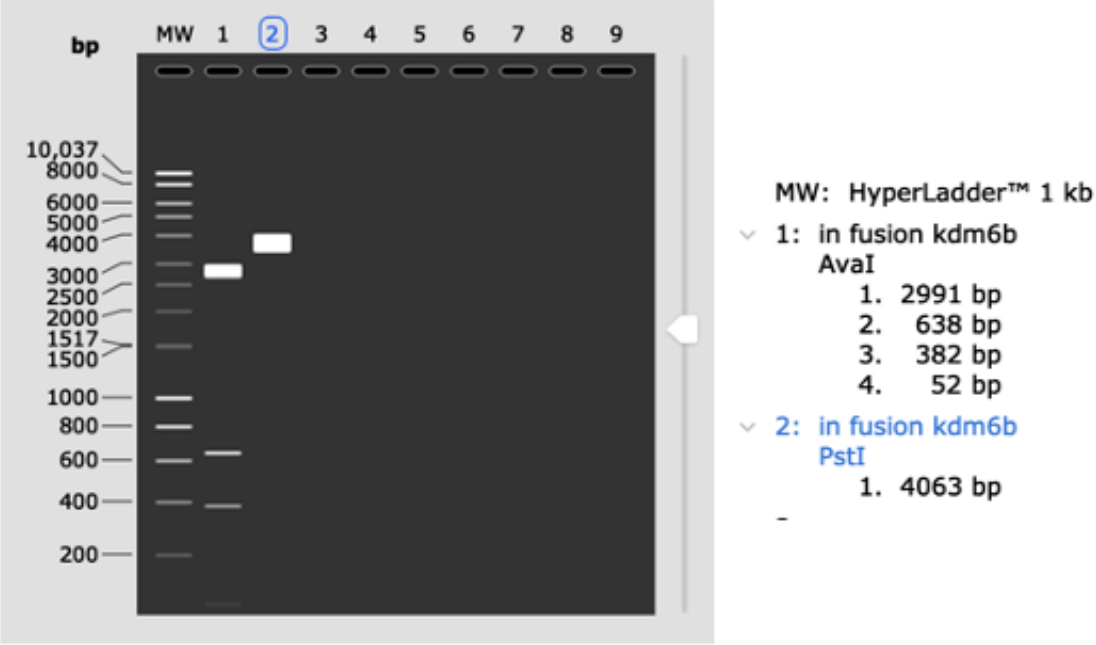

Figure 2.3. Diagnostic digest for p3e-U6akdm6bg1-U6c-kdm6bg2 guide RNA plasmid

Screenshot from simulated restriction digest with Pst1 (lane 1) and AvaI (lane 2) digests of the p3e-U6akdm6bg1-U6c-kdm6bg2 guide RNA plasmid created using Snapgene.

2.3.7.f. Gateway Cloning by LR Reaction to make the full sgRNA insertion plasmid.

Materials and Methods 2.3.7.e described how the 3' entry clone was made for incorporation into a larger plasmid for injection into zebrafish embryos. The larger plasmid is made up of four components and the specific concentrations and volumes required are listed in Table 2.8. 1 µl LR Clonase II Plus (Invitrogen, Cat #1179110) and 6.9 µl ddH_2O was added to make a 10 µl reaction mix and incubated at 25 ^{O}C for 16 hours. 3 µl Proteinase K (Invitrogen Cat #25530049) was then added for 10 mins at 37^{O}C. Reaction mixture was then transformed into Top 10 competent cells as described in Materials and Methods 2.3.7.e.v, except the entire reaction mix was added to one selection plate, rather than serial dilutions. The selection antibiotic was 50 ug/µl carbenicillin disodium (Biovision, Cat #2485). DNA was extracted from LB broth overnight selection cultures using Nucleobond P100 Midiprep kit (Materials and Methods 2.3.7.e.vi). Concentration was measured using a Thermo Scientific Nanodrop 2000.

Clone/vector	Components	Size	Stock concentration	Concentration required	Volume required
5' entry clone	p5E-LyzC-TOBIN	9270 bp	50 ng/µl	10 fmol	0.61 µl
Middle Entry clone	pME-EGFP	3327 bp	25 ng/µl	10 fmol	0.44 µl
3' Entry clone	p3e-U6akdm6bg1-U6c-kdm6bg2	4063 bp	50 ng/µl	10 fmol	0.27 µl
Destination vector	pDest-Tol2-pA2	5883 bp	50 ng/µl	20 fmol	0.77 µl

Table 2.8. Vectors used for LR cloning reaction to make pDest-LyzC-EGFP-U6akdm6bg1-U6c-kdm6bg2-Tol2-pA2

2.3.7.g. Digest to confirm successful LR reaction.

Successful LR reaction was confirmed by restriction digest. Four different reactions were set up. Expected digest and bands sizes are shown in Figure 2.4. 25 µl reactions were set up with 3 µl of rCutSmart buffer (NEB, Cat #B6004), 1 µl of each enzyme, 2 µl vector DNA and made up to 25 µl with nuclease free water. Digest was performed overnight at the temperatures required for each set of enzymes.

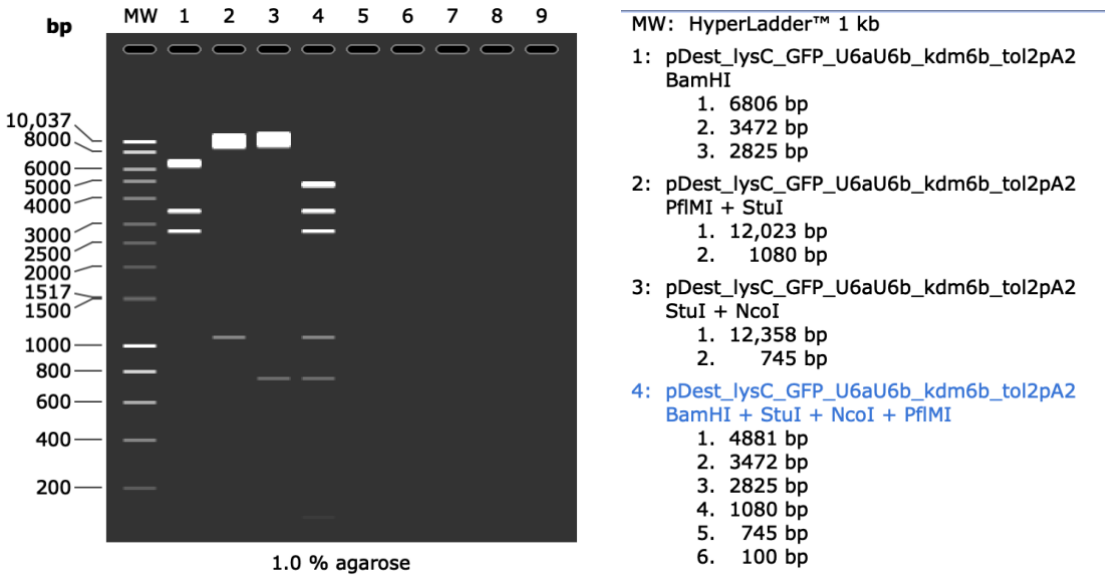

Figure 2.4. Diagnostic digest for successful LR reaction to make the pDest-LyzC-EGFP-U6akdm6bg1-U6c-kdm6bg2-Tol2-pA2 vector

Screenshot from simulated digest using SnapGene for pDest-LyzC-EGFP-U6akdm6bg1-U6c-kdm6bg2-Tol2-pA2 vector with BamHI, PflMI, StuI and NcoI (All NEB Cat #R0136, R0509, R0187 and R0193)

2.3.8. Micro-injection of pDest-LyzC-EGFP-U6akdm6bg1-U6c-kdm6bg2-Tol2-pA2 into single-cell zebrafish embryos

An injection mixture of 1 µl vector, 2 µl DEPC-Tris and 0.5 µl phenol red was made and 2 nl was injected into single-cell *Tg(lyz:nfsβ-mCherry)sh260* embryos. Survival was checked daily. 3 dpf larvae were anaesthetised in 0.168 mg/ml tricaine, and the caudal fin removed (Materials and Methods 2.1.2). 4 hpi larvae were mounted in 0.8% LMW agarose and imaged at 20 x magnification in vertical Z-stacks in the brightfield, GFP and mCherry channels on a wide-field Nikon microscope. MaxIP were made using NIS Elements software and colocalization of red and green signal used as confirmation of successful insertion in the zebrafish genome and expression in neutrophils.

2.4. Materials and Methods for Chapter 5

2.4.1. Preparation of zebrafish embryos

2.4.1.a. Single cell injection and tailfin injury

When required, single cell stage injection into *TgBAC*(*mpx:BirA-2A-Citrine*)*ox121* x *Tg*(*βactin:Avi-Cerulean-RanGap*)*ct700a* embryos was performed as described in method 2.2.4 using the crRNAs for the coding sequence of *kdm6ba* and *kdm6bb* and a *tyr* control (Table 2.5) (Kenyon *et al.*, 2017). 3 dpf, tailfin injury was performed as described in Materials and Methods 2.1.2.

2.4.1.b. Homogenisation of zebrafish larvae

The method was adapted from Trinh *et al.*, (2017). Volumes apply to a single sample/treatment group, scale up for more e.g., injured vs. non-injured. *TgBAC*(*mpx:BirA-2A-Citrine*)*ox121* x *Tg*(*βactin:Avi-Cerulean-RanGap*)*ct700a* larvae were euthanised by overdose of tricaine and 15-20 embryos added to RNAse free Eppendorfs, the E3 removed, and samples moved to a 4^{O}C coldroom. Per treatment group, 100-150 embryos were used, giving 6-8 Eppendorfs per group. Larvae were washed with 300 µl hypotonic buffer H (20mM HEPES (pH 7.4) (Sigma, Cat #83264), 1.5mM $MgCl_2$ (Sigma-Aldrich, Cat #208337), 10mM KCl (Sigma-Aldrich, Cat #P9333), 1mM DTT (Sigma, Cat #43816) and 1X cOmplete™ protease inhibitor (Roche, Cat #05892791001), supplemented with 0.01% Tricaine) per Eppendorf on a rocker for 3 mins and the buffer was removed. Larvae were then resuspended in 700 µl Buffer H and homogenised for 20 s using a Stuart SHM homogeniser and incubated on ice for 15 mins. Treatment group Eppendorfs were then pooled into a 7 ml Dounce homogeniser mortar (Kimble cat #432-0251) and dissociated for 3 x 20 strokes with the A pestle – pausing for 5 mins between strokes and covered with RNAseZap (Invitrogen, Cat #AM9780) treated aluminium foil – and for 3 x 20 strokes with the B pestle, again pausing for 5 mins and covering in foil between strokes. The dissociated cell mix was moved to a clean 50 µl falcon tube and centrifugated for 10 mins at 2,000 x g and 4^{O}C. The supernatant was removed and replaced with the 1 ml of streptavidin bead/NPB solution prepared below (Materials and Methods 2.4.2). The bead-nuclei mix was then incubated at 4 ^{O}C for 30 mins on rotation.

2.4.2. Preparation of streptavidin beads

The method was adapted from Trinh et al., 2017. Volumes apply to a single sample/treatment group, scale up for more e.g., injured vs. non-injured. Preparation was carried out in a 4^{O}C coldroom. 50 ug (50 µl) Dynabead M-280 Streptavidin (Invitrogen, Cat #11205D) were transferred to a 14 ml culture tube and separated from the supernatant using a 14 ml "Big Easy" EasySep magnet (Stemcell Technologies cat #18001). The beads were washed with 1 ml of solution A (DEPC-treated 0.1M NaOH (Sigma-Aldrich, Cat #S5881), DEPC-treated 0.05M NaCl (Sigma, Cat #S3014) on a rocker for 3 mins, left to stand on the magnet for 3 mins, the supernatant removed, and the solution A wash repeated. On removal of solution A, the beads were resuspended and washed with 1 ml solution b (DEPC-treated 0.01 M NaCl) on a rocker for 3 mins, left to stand on the magnet for 3 mins and the supernatant removed. The beads were resuspended in 1 ml NPB (10mM HEPES (pH 7.4), 40mM NaCl, 90mM KCl, 0.5mM EDTA (PanReac AppliChem, Cat #A4892), 0.5mM spermidine (Sigma, Cat #S2626), 0.15mM spermine (Sigma, Cat #S1141), 1mM DTT (Sigma, Cat #43816) and 1X cOmplete™ protease inhibitor (Roche, Cat #05892791001) and kept on ice until ready to be added to the dissociated zebrafish larvae nuclei prepared above (Materials and Methods 2.4.1.b.)

2.4.3. Nuclei isolation by INTACT BirA/streptavidin pulldown

The method was adapted from Trinh et al., 2017. Volumes apply to a single sample/treatment group, scale up for more e.g., injured vs. non-injured. Preparation was carried out in a 4^{O}C coldroom. The 1 ml streptavidin bead-nuclei mix was further diluted with 19 ml NPBt (NPB + 0.1% Triton X-100 (Sigma. Cat #X100) to give 20 ml bead-nuclei suspension. 10 ml of the bead-nuclei suspension was poured into a 14 ml culture tube that had been pre-treated for 10 mins with 10 ml NPBb (NPB + 1% BSA (Sigma-Aldrich, Cat #A8577)) and the culture tube placed on the "Big Easy" Easysep magnet for 5 mins. After 5 mins, that 10 ml was poured to an unopened 50 ml falcon tube labelled 'flow-through 1' and the remaining 10 ml of bead-nuclei suspension poured to the 14 ml culture tube and left on the magnet for 5 mins. The 10 ml was then poured into flow-through 1. 10 ml of flow-through 1 was then poured back into the 14 ml culture tube on the magnet and left to stand for 5 mins. These 10 ml was then poured to a new unopened 50 ml falcon labelled 'flow-through 2' and the remaining 10 ml of flow-through 1 poured into the 14 ml culture tube on the magnet and left to stand for 5 mins. The 10 ml were then poured to flow-through 2, using a P1000 pipette tip to remove the remaining liquid

from the nuclei-bead solution. The 14 ml culture tube should contain neutrophil nuclei and beads bound to the wall of the tube only. The nuclei-bead solution was resuspended in 1 ml NPBt, removed from the magnet, washed on a rocker for 3 mins and then returned to the magnet for 3 mins and the supernatant removed. This NPBt wash was performed 5 times in total before the bead-nuclei mix were resuspended in 500 µl NPBt. 5 µl of DNase I (Invitrogen, Cat #EN0521) was added to the suspension and incubated at 37^{O}C for 15 mins. The content of the flow-through 2 50 ml falcon was kept for analysis as it should contain nuclei from all non-neutrophil cells so can be used for quality control of the process, this was referred to as flow-through nuclei.

2.4.4. Extraction of RNA

2.4.4.a. TRIzol

Early attempts at using the INTACT method used a TRIzol based RNA extraction method for flow-through nuclear RNA. This allowed the RNA to be analysed by RT-PCR during optimisation of the INTACT method. Flow-through was not retained during RNAseq sample preparation. The flow-through 2 50 ml falcon was centrifuged for 10 mins at 2000xg at 4^{O}C and the supernatant removed. The pellet was resuspended by vigorous pipetting with 500 µl TRIzol and RNA extraction performed as described in Materials and Methods 2.1.5, concentration measured using a Thermo Scientific Nanodrop 2000 and stored at -80^{O}C.

2.4.4.b. Preparation of nuclei suspensions for Qiagen RNeasy Micro Kit RNA extraction

2.4.4.b.ii. Flow-through nuclei

1 ml of the contents of flow-through 2 was transferred to an RNAse free Eppendorf and centrifuged for 10 mins at 2000xg at 4^{O}C and the supernatant removed. The pellet was then resuspended in 350 µl buffer RLT from the Qiagen RNeasy kit (Cat # 74004), vortexed for 2 mins and incubated for 10 mins at room temperature. The mix was then transferred to an RNAse free 1.5 ml Eppendorf.

2.4.4.b.ii. Neutrophil nuclei

Following DNAse I treatment, the neutrophil nuclei-bead suspension was placed on the magnet at 4^{O}C for 3 mins and the supernatant removed. The nuclei-bead mix was

resuspended in 350 µl Buffer RLT and vortexed for 2 mins and incubated for 10 mins at room temperature – the final 3 mins, the 14 ml culture tube was placed on the magnet. The supernatant was then transferred to an RNAse free 1.5 ml Eppendorf.

2.4.4.c. Qiagen RNeasy Micro Kit RNA extraction

Qiagen RNeasy kit (Cat # 74004) MinElute spin columns were used to extract RNA from the nuclear samples using an adaptation of the standard instructions. 350 µl 70% DEPC-ethanol was added to the Buffer RLT/nuclei mix and vortexed. The lysates/ethanol mixture was then pipetted into the spin column and centrifuged at room temperature for 15 s at 8000xg. The collection tube was emptied and 350 µl buffer RW1 added to the column and centrifuged at room temperature for 15 s at 8000xg. The collection tube was emptied and 500 µl buffer RPE added to the column and centrifuged at room temperature for 15 s at 8000xg. The collection tube was emptied and 500 µl 80% DEPC-ethanol added to the column and centrifuged at room temperature for 15 s at 8000xg. The collection tube was then emptied, and the spin column returned and centrifuged for 5 mins at 16000xg at room temperature to remove excess ethanol. The collection tube was then disposed of and replaced with a labelled RNase free 1.5 ml Eppendorf. 14 µl nuclease free water was added to the membrane of the column and left to stand for 1 min. The column was then centrifuged for 1 min at 16000xg at room temperature and the column disposed of. The RNA concentration was then recorded using a Nanodrop 2000.

2.4.5. Quality control of isolated nuclei

2.4.5.a. cDNA synthesis

cDNA was synthesised using First strand superscript II (Materials and Methods 2.1.6). An amendment was made as the required 2 g of RNA listed in the kit was not always possible. Instead, the RNA sample with the lowest concentration was converted to cDNA using 10 µl of RNA. The concentration of RNA that this totalled with then matched with the other samples, made up to 10 µl with nuclease free water. This ensured a consistent concentration across the samples.

2.4.5.b. RT-PCR

RT-PCR was performed to confirm distinct populations were found within the neutrophil nuclei and the flow-through nuclei samples. Primers used were for *ef1a* – as the house keeping gene, *mpx* – as a neutrophil specific gene, and combinations of *ece2b*, *mitfa*, *fastkd2*, *numa1* and *itga2b* as low/non-neutrophil genes (Table 2.1). 10 µl reaction mixtures were used as described in Materials and Methods 2.1.8 and cycles described in Table 2.2 with 30-40 cycles depending on the input RNA concentration and an annealing temperature of 58 ^{O}C.

2.4.5.c. Agilent 2100 Bioanalyzer

Samples were further analysed for quality using the Agilent 2100 Bioanalyzer at the SITraN Multiomics Facility, University of Sheffield. 5 µl of RNA was sent for analysis. Expected peaks are shown in Figure 2.5.

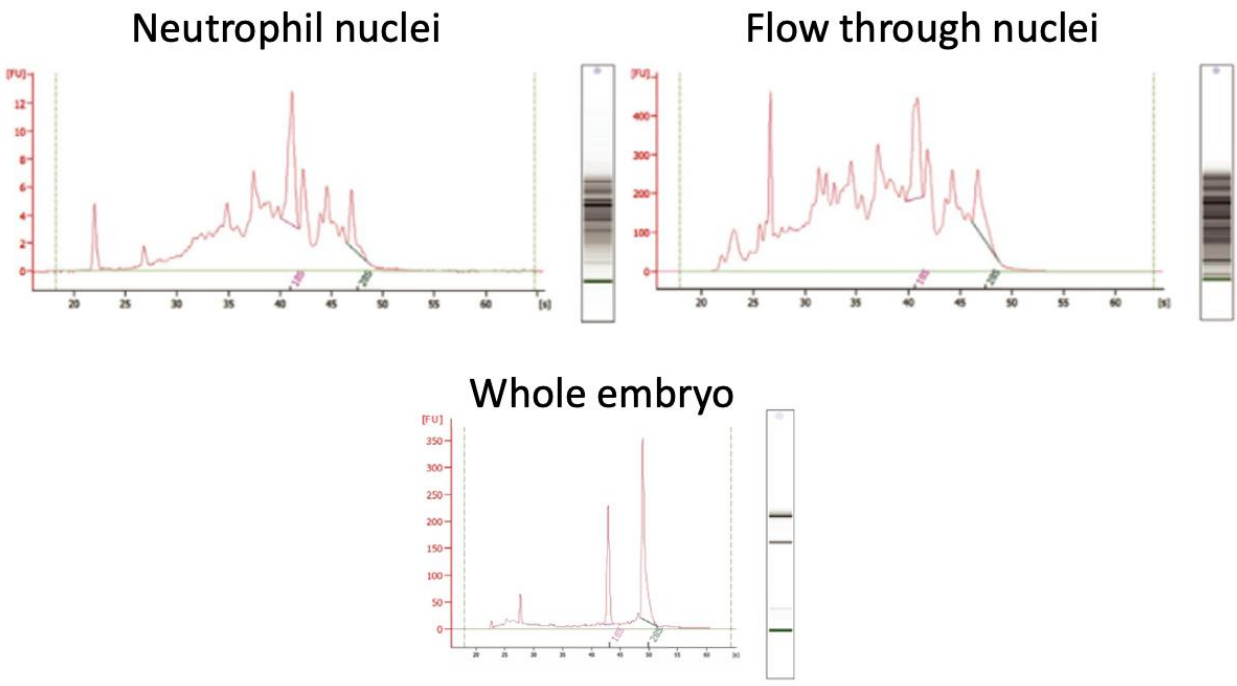

Figure 2.5. Example bioanalyzer plots for INTACT pulldown samples with whole embryo for comparison

(Adapted from Trinh *et al.*, (2017)).

2.4.6. Analysis of isolated nuclei

2.4.6.a. Library preparation and RNA sequencing

Total RNA was enriched for mRNA using poly-A selection. Libraries were prepared using NEBNext® Ultra™ II Directional RNA Library Prep Kit for Illumina and sequenced on the Illumina NovaSeq 6000 platform by Source Biosciences. Reads were mapped to the UCSC build of the Danio rerio genome (danRer10) using HISAT2 (D. Kim *et al.*, 2019) . Read counts were generated using featureCounts which is part of the Rsubread package (v2.0.1, Liao, Smyth and Shi, 2019) for R (v3.6.3). This was undertaken on Barkla, part of the High-Performance Computing facilities at the University of Liverpool, UK by Helen Wright. Statistical analysis of gene counts was carried out using edgeR (v3.28.1, Robinson, McCarthy and Smyth, 2009) in R (v4.02), applying TMM normalisation and a 0.05 false-discovery rate p-value adjustment with support from Helen Wright.

2.4.6.b. Bioinformatics analysis

Gene symbols were converted from *Danio rerio* to *Homo sapiens* using the R package babelgene (Dolgalev, 2022). Canonical pathway and up-stream regulator analysis was carried out using Ingenuity Pathway Analysis (IPA) applying a 1.5-fold change in gene expression cut-off – a chosen value equivalent to a 50% change in expression – and a Benjamini-Hochberg correction to p-values for canonical pathway and upstream regulator analysis (Krämer *et al.*, 2014).

Chapter 3: The TLR8 agonist R848 alters neutrophil activity *in vivo* using a zebrafish tailfin injury model.

3.1. Introduction

Understanding the chromatin remodelling process is an essential part of understanding how the transcriptional responses of every cell of the body are managed and regulated. Developing an atlas of these changes for every cell would be a useful tool for research scientists across the world to advance understanding of transcriptional regulation and networks. The development of such a tool has progressed in many cell types, but the neutrophil has so far been left behind (Cheung *et al.*, 2018; Domcke *et al.*, 2020).

Neutrophils are sensitive cells to work with. Spontaneous apoptosis can easily be triggered before experimental observations can be made. This sensitivity has made neutrophil research challenging, especially for the monitoring of lengthy processes such as response to an injury or infection, and particularly at a molecular level (reviewed in Henry *et al.*, 2013). Using an *in vivo* model for neutrophil study is therefore an excellent tool for answering many research questions including those about chromatin remodelling events. While a murine model can be genetically modified or given chemical treatments to alter neutrophil function, imaging and cell tracing is often complicated and invasive, increasing the risk of stressing the animal. Therefore, for the aims of this project, a more tractable system is required.

Neutrophils must be under tight transcriptional control to prevent unnecessary activation and damage to healthy tissue. Specific genes must be switched on and off for neutrophils to be able to deal with specific immune challenges. Opening and closing of chromatin structures by the addition of chemical modifications to histones by chromatin remodelling enzymes is one way in which gene transcription can be tightly controlled. Chromatin remodelling within neutrophils is understudied. Work is beginning to highlight some of the basic reprogramming that underpins the definition of specific neutrophil subtypes and some basic responses (Denholtz *et al.*, 2020; Khoyratty *et al.*, 2021). This work uses either *in vitro* or mouse models, using the zebrafish offers different ways to explore neutrophil chromatin dynamics. By using well established transgenic zebrafish reporter lines for neutrophils and neutrophil-associated

cytokines, chemical or genetic manipulation of chromatin remodelling is possible and easy to observe by fluorescent imaging. This can begin to shed light on how chromatin remodelling dictates neutrophil core functions, especially the rapid responses of neutrophils to injury.

A zebrafish model allows for a robust and traceable study of neutrophils *in vivo* (Renshaw *et al.*, 2006). Neutrophils are constantly responding to the microenvironment to maintain homeostasis by releasing cytokines, compounds such as neutrophil elastases, and structures such as NETs (Brinkmann *et al.*, 2004; Harbort *et al.*, 2015; Coombs *et al.*, 2019; Ballesteros *et al.*, 2020). A potentially major factor in regulating these changes is chromatin remodelling to change the conformation of DNA at key enhancer, promoter, and gene coding regions to turn transcription on and off. A model is required that allows for these rapid events to be traced using live imaging and following chemical or genetic manipulation, and the use of a zebrafish model allows for these events to be traced. Within an *in vitro* system, chemical or genetic alterations and artificial changes to the microenvironment often stress the neutrophils and result in spontaneous activation and premature apoptosis before meaningful measurements can be recorded (Henry *et al.*, 2013). An *in vivo* neutrophil model on the other hand, can withstand these stresses and generate essential data (Isles *et al.*, 2019).

Several chemical compounds available can alter chromatin remodelling (Zhang, Pilko and Wollman, 2020; Shait Mohammed *et al.*, 2022). These compounds operate by directly or indirectly promoting or inhibiting the action of chromatin remodelling enzymes. Chromatin remodelling enzymes catalyse the addition or removal of chemical groups such as methyl and acetyl groups on histone proteins. DNA is wrapped around histone proteins to package it into the nucleus in chromatin strands. Combinations of modifications to the histones lead to either open, transcriptionally active euchromatin or closed, transcriptionally repressed heterochromatin. When a neutrophil – or any nucleated cell – is responding to its microenvironment and various stimuli, chromatin is regularly being opened and closed to alter the transcriptome of the cell to maintain homeostasis (reviewed in Keppler and Archer, 2008). So, addition of chemical compounds that affect chromatin remodelling enzymes can alter the chromatin conformation of a neutrophil and potentially lead to changes in neutrophil phenotype when exposed to a stimulus such as an injury.

Use of a chemical approach – rather than a genetic one – allows easy testing of whether zebrafish neutrophils can be altered at an epigenetic level in the same way as human neutrophils *in vitro*. The drug of interest can be added to the zebrafish larval media and neutrophil kinetics can easily be observed using a fluorescent microscope, with changes in gene expression observed by PCR amplification. Several drugs have been shown to alter neutrophil chromatin remodelling (Visnes *et al.*, 2018; Moorlag *et al.*, 2020). A well studied example is the TLR7/8 agonist, R848 (Zimmermann *et al.*, 2015, 2016). In human neutrophils *in vitro*, R848 binds TLR8 and causes a canonical activation of MyD88 and subsequent activation of NF-κB. A secondary effect of R848 exposure is the remodelling of the chromatin at several pro-inflammatory cytokine loci that promote NF-κB binding and promote increased expression of the associated cytokine, in particular IL-6. It does this by driving the action of two chromatin remodelling enzymes, EP300 and CREBBP that promote changes at specific histone marks at the *IL-6* locus, shown by changes in mark enrichment. The *IL-6* locus showed increased histone 3 lysine 4 mono-methylation (H3K4me1) and H3K4me3 enrichment for active promoters and increased H3K27Ac and H4Ac enrichment for both active enhancers and promoters. These new modifications lead to increased binding of transcription factors C/EBPβ, NF-κBp50, NF-κBp65 and subsequent increased transcription and translation of IL-6. Zimmerman *et al., (*2015) used C646 and histone acetyltransferase II inhibitor to inhibit EP300 and CREBBP and show that these R848-dependent increases in IL-6 mRNA expression were lost when chromatin remodelling was inhibited. This suggested that changes in IL-6 expression were due to the secondary effects of R848 and not MyD88, though inhibition of MyD88 would further strengthen this hypothesis. Addition of R848 to the larval media can therefore be used to attempt to mimic these chromatin changes in the zebrafish model.

3.2. Aims and hypothesis.

We hypothesise that the effects seen exposing human neutrophils *in vitro* to R848 can be mimicked in zebrafish neutrophils *in vivo* (Zimmermann *et al.*, 2015). The aim of this chapter is to understand whether zebrafish neutrophils can be manipulated by the same pathways as *in vitro* human neutrophils by exposing zebrafish neutrophils to R848. This would provide a proof of concept that zebrafish neutrophils can be regulated by the same epigenetic processes seen in humans. The main aims are to:

- Test whether R848 is not toxic to zebrafish.
- Monitor neutrophil responses to wounding, including neutrophil recruitment and inflammation resolution following R848 exposure.
- Examine downstream signalling changes following R848 treatment such as pro-inflammatory cytokine expression - including IL-1β, NF-κB, TNFα and IL-6
- Inhibit processes known to be part of R848's method of action such a TLR signalling and the chromatin remodelling enzymes Ep300 and Crebbp to distinguish between canonical and chromatin remodelling related effects of the R848.

Chromatin remodelling enzymes identified to play important roles in neutrophil function, will be altered genetically in future experiments.

3.3. Results

3.3.1. The TLR7/8 agonist R848 is not toxic to larval zebrafish with or without caudal fin injury.

To investigate the role of chromatin remodelling on neutrophil function *in vivo*, the Toll-like receptor (TLR) 7/8 agonist R848 was chosen (also known as Resiquimod, Figure 3.1A). R848 has been shown *in vitro* to alter neutrophil chromatin structure by histone remodelling via the enzymes EP300 and cyclic adenosine monophosphate response element binding protein binding protein (CREBBP), which in turn, alters IL-6 cytokine expression (Zimmermann *et al.*, 2015). Published data on treatment of zebrafish with R848 is limited and there is no literature on treating zebrafish at the larval stage (Muire *et al.*, 2017; Progatzky *et al.*, 2019). To test whether R848 was safe, i.e. not toxic, to larval zebrafish, 2 dpf zebrafish were treated with R848 at varying concentrations (0 – 50 µM), with and without caudal fin injury (injury performed 16 hours post incubation) over a 39-hour incubation period and observed for abnormalities at 0-, 1-, 3-, 6-, 8- and 24-hpi (Figure 3.1B). Anaesthetised larvae were embedded in 0.8% low-melting point agarose and imaged using a wide-field microscope at 24 hpi and each fish was physiologically normal as shown in Figure 3.1C. No deaths were observed in either injured or uninjured fish at any concentration as shown by the 100% survival curves in Figures 3.1D and 3.1E. Taking the images and survival curves into consideration, R848 up to 50 µM was deemed suitable to be administered by incubation to larval zebrafish up to at least 4 dpf. R848 will be used in experiments to analyse *in vivo* chromatin remodelling in larval zebrafish neutrophils.

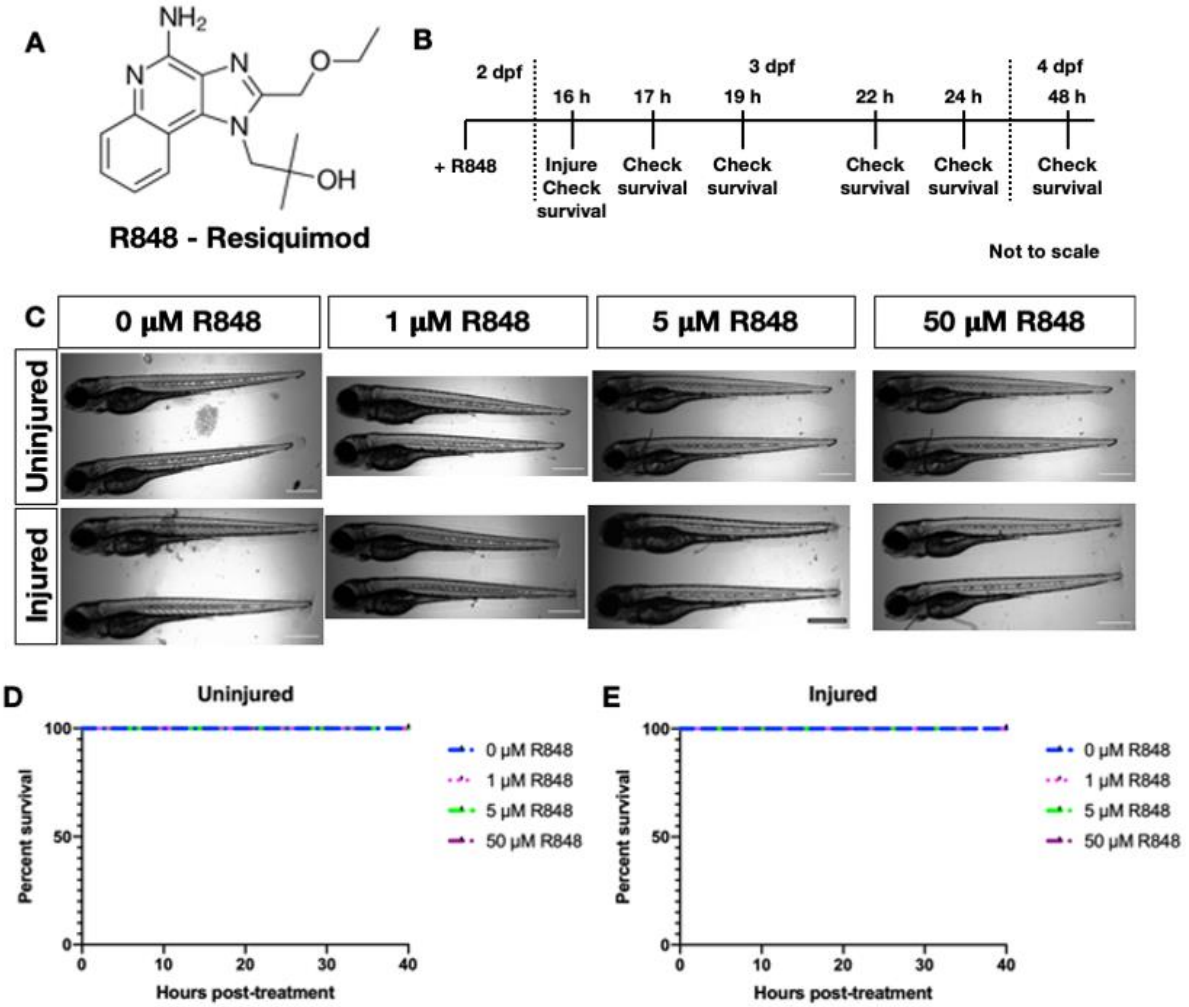

Figure 3.1: 39-hour treatment with R848 is not toxic to larval zebrafish.

(A) Chemical structure of R848. (B) Time course of the experiment (C) Images taken using wide-field bright-field microscopy (x4 magnification, scale bar 500 µm) of larval *TgBAC(mpx:EGFP)i114* zebrafish treated with varying concentrations of R848 +/- caudal fin injury. (D) Survival curve for 2 dpf zebrafish larvae treated for 39 hours with 0, 1, 5 or 50 µM R848. (E) Survival curve for 2 dpf zebrafish larvae treated for 39 hours with 0, 1, 5 or 50 µM R848. Larvae were injured after 16 hours incubation. (2 independent repeats, minimum 28 fish per concentration).

3.3.2. R848 does not alter neutrophil number or distribution in larval zebrafish.

Previous work carried out *in vitro* using R848 cannot account for the drug being able to potentially increase the production of neutrophils from haematopoietic tissue. Work has also shown that drugs can also alter neutrophil number and distribution in larval zebrafish (Candel *et al.*, 2014). To observe whether R848 could alter neutrophil number and distribution *in vivo*, larval zebrafish were treated with 1 and 5 μM R848 to match therapeutic doses. 2 dpf zebrafish were incubated in R848 for 18 hours, in line with published data on the time required for epigenetic modifications to take full effect (Makki, 2017). *TgBAC(mpx:EGFP)i114* zebrafish were used where the promoter of the neutrophil specific myeloperoxidase gene, *mpx,* drives GFP expression that allows neutrophils to be counted easily. Whole body neutrophil counts and neutrophil localisation were recorded based on four regions shown in Figure 3.2A. A change in distribution was assessed as significant increases in neutrophil numbers in regions outside of the caudal haematopoietic tissue (CHT) relative to untreated controls. Both 1 μM and 5 μM R848 did not significantly alter whole body neutrophil number or localisation across the four sites of the body (Figure 3.2C and 3.2D) suggesting R848 has no effect on neutrophil number or neutrophil distribution relative to controls.

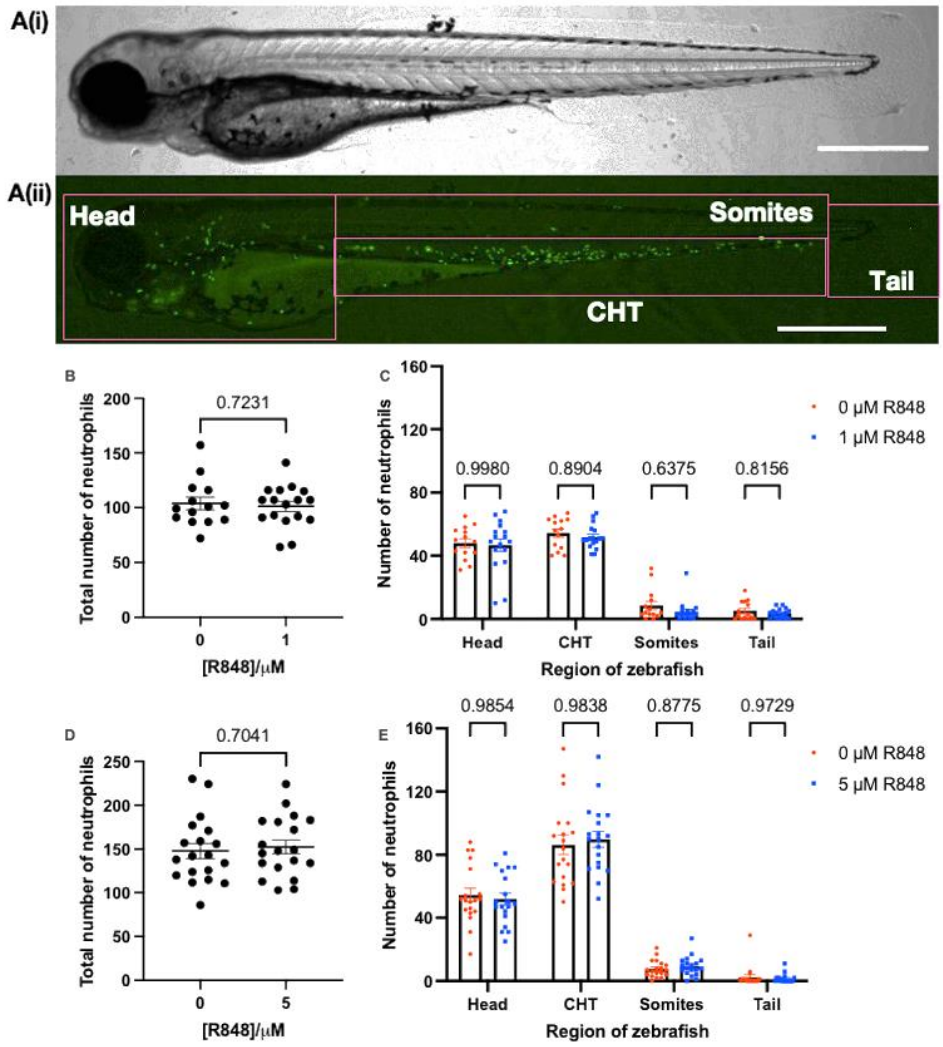

Figure 3.2: R848 treatment for 19 hours does not alter whole body counts of neutrophils or neutrophil distribution in uninjured zebrafish larvae

(Ai) Wide-field, bright-field image of 3dpf *TgBAC(mpx:EGFP)i114* and (Aii) GFP filter image with regions sectioned for the head, caudal haematopoietic tissue, somites, and tail (4x magnification, scale bar 500 μm). (B) Total number of neutrophils in the zebrafish treated with 1 μM R848 (3 independent repeats, minimum 14 larvae per treatment, ± SEM, Two-tail T-test). (C) Localisation of neutrophils based on regions in (Aii) in zebrafish treated with 1 μM R848 (3 independent repeats, minimum 14 larvae per treatment, ± SEM, Two-way ANOVA with Sidak's multiple comparisons). (D) Total number of neutrophils in the zebrafish treated with 5 μM R848 for 19 hours (3 independent repeats, 19 larvae per treatment, ± SEM, Two-tail T-test). (E) Number of neutrophils in each region in (Aii) in zebrafish treated with 5 μM R848 (3 independent repeats, 19 larvae per treatment, ± SEM, Two-way ANOVA with Sidak's multiple comparisons).

3.3.3. Incubation with R848 at the time of caudal fin injury has no effect on neutrophil recruitment to the wound site

The lack of change in neutrophil number or distribution when uninjured larval zebrafish were treated with R848, suggests that the fish may need to be immunologically challenged to detect R848-induced differences in neutrophil phenotype. To see if R848 had any effect post-injury, 3 dpf *TgBAC(mpx:EGFP)i114* larvae were exposed to 5 or 50 µM R848 immediately after caudal fin injury (Figure 3.3A). Figure 3.3B shows an example of expected neutrophil numbers at a tailfin injury from 0-48 hpi based on previous work and can be used as a guide throughout this thesis (Renshaw *et al.*, 2006). Relative to untreated controls, R848 had no significant effect on total neutrophil numbers at the wound site highlighted in Figure 3.3E at 3 and 6 hpi (Figure 3.3C). To control for variation of neutrophil numbers in each fish, percentage change was also calculated between the two time points, and this also showed no significant change relative to controls (Figure 3.3D). Taken together, these data suggest that immediate treatment with R848 has no effect on neutrophil numbers recruited to the wound site. This may be caused by a need for epigenetic modification pathways to be triggered before changes can be detected using this read out.

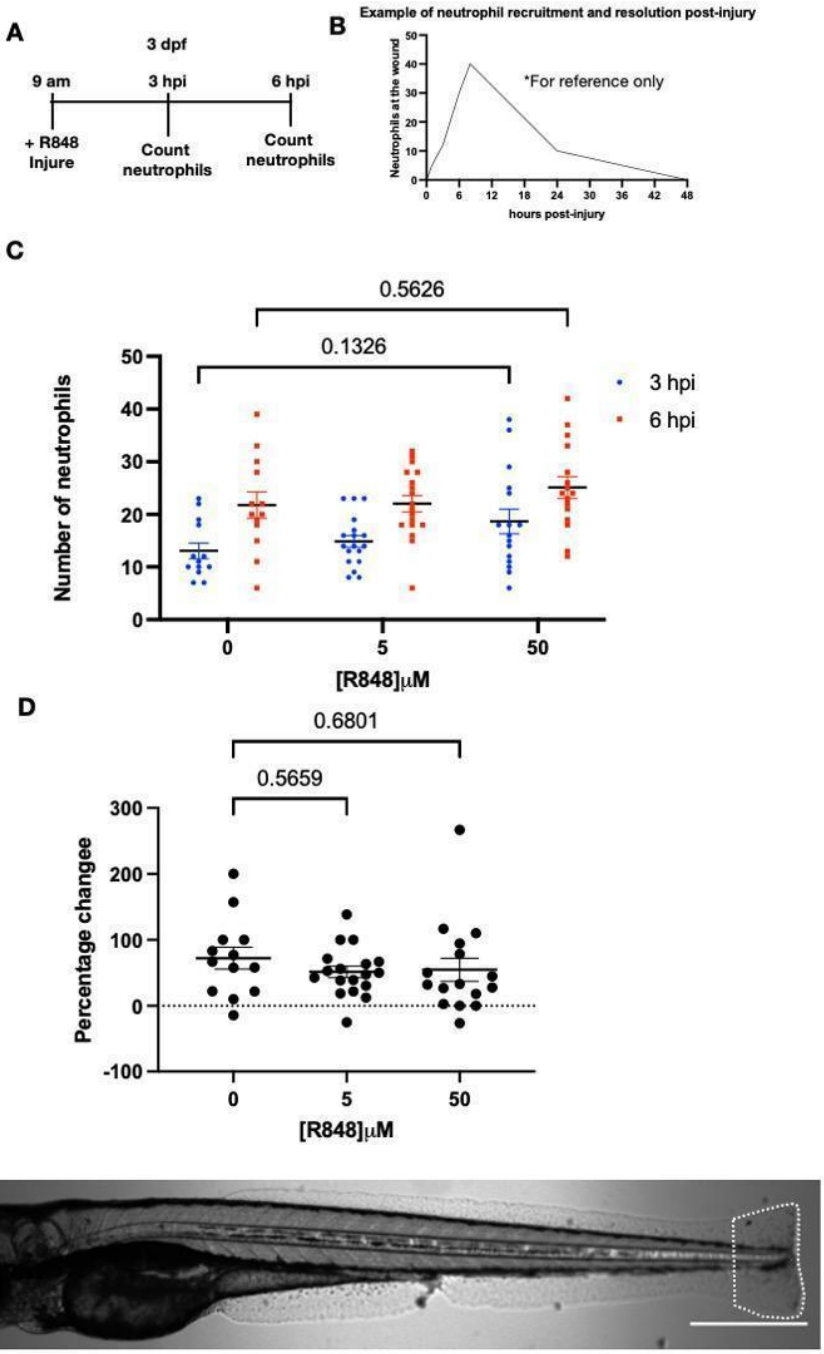

Figure 3.3: Treatment with R848 at time of injury does not increase the number neutrophils recruited to the wound site.

(A) Time course of the experiment (B) Example of expected neutrophil recruitment and resolution at a tailfin following injury - reference image (C) Total number of neutrophils at the wound site (counted posterior to the circulatory loop highlighted in Figure 3.3E) 3 and 6 hpi in 3 dpf *TgBAC(mpx:EGFP)i114* zebrafish treated with 5 and 50 µM R848 and an untreated

water control (3 independent repeats, min 13 fish per concentration, ± SEM, Two-way ANOVA with Tukey's multiple comparisons, no significance between any groups $p > 0.05$). (D) Percentage change in number of neutrophils at the wound site between 3 and 6 hpi in 3 dpf *TgBAC(mpx:EGFP)i114* zebrafish treated with 5 and 50 µM R848 and a water control (3 independent repeats, min 13 fish per concentration, ± SEM, Two-way ANOVA with Tukey's multiple comparisons). (E) Wide-field bright-field image of 3 dpf zebrafish larvae with white ROI drawn to show the area posterior to the circulatory loop where neutrophils were counted (x 4 magnification, scale bar 500 µm, adapted from Figure 3.1B)

3.3.4. R848 significantly increases inflammation resolution following caudal fin injury.

R848 did not show a significant effect on neutrophil numbers recruited to the wound site. However, an important part of the inflammatory process is inflammation resolution. Inflammation resolution is the removal of neutrophils from the wound site, either by reverse migration or apoptosis to restore tissue homeostasis (Nourshargh, Renshaw and Imhof, 2016). To test if R848 alters inflammation resolution, 3 dpf *TgBAC(mpx:EGFP)i114* zebrafish were incubated with 0, 5 or 50 µM R848 4 hpi to specifically observe the effect R848 had on neutrophil numbers following their initial recruitment, at 8 and 24 hpi, the key inflammation resolution phase (Figure 3.4A). Total neutrophil numbers were significantly lower at 24 hpi in larvae treated with 5 µM R848 than the untreated control going from 13 cells to 9 ($p = 0.0430$, Two-way ANOVA with Sidaks multiple comparisons). No significant effect was observed with 50 µM R848 – potentially due to a dose-dependent plateau which a dose response titration curve would help to answer (Figure 3.4B). This also translated into a significant increase in percentage resolution between 8-24 hpi in the larvae when treated with 5 µM R848 from 47.6% to 62.5%. R848 ($p = 0.0108$, One-way ANOVA with Dunnett's multiple comparisons), therefore alters inflammation resolution after 4 hours incubation (Figure 3.4C). This may be key in allowing epigenetic changes to take place and alter neutrophil phenotype and helps to validate the zebrafish model.

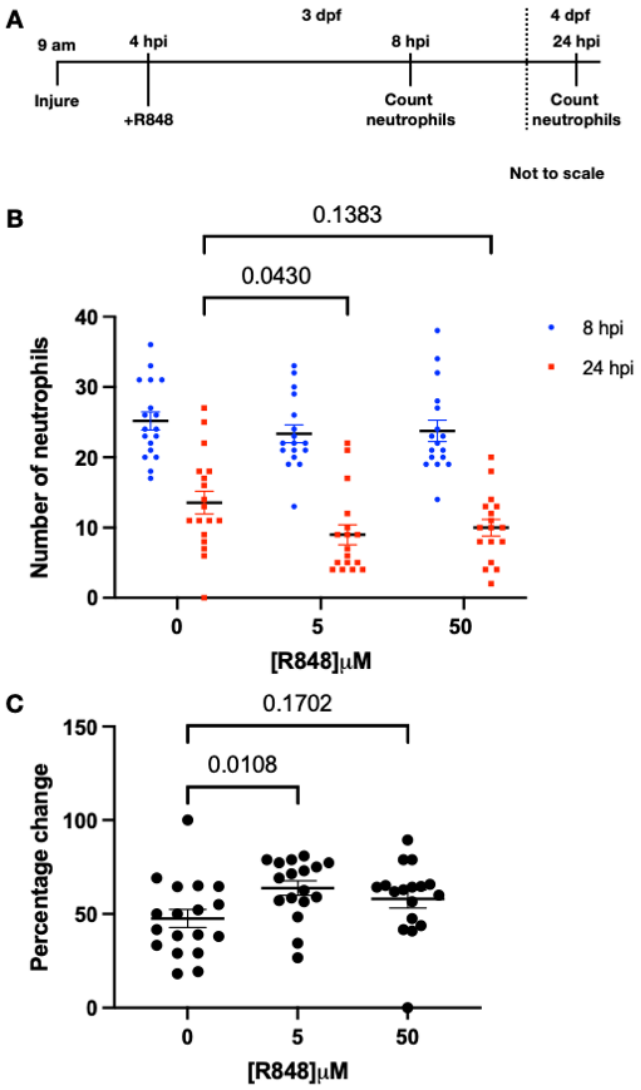

Figure 3.4: Treatment with R848 4 hpi significantly increases inflammation resolution following caudal fin injury

(A) Time course of the experiment (B)Total number of neutrophils at the wound site (counted posterior to the circulatory loop) 8 and 24 hpi in 3 dpf *TgBAC(mpx:EGFP)i114* zebrafish treated with 5 and 50 µM R848 and a water control (3 independent repeats, minimum 16 larvae per concentration, ± SEM, Two-way ANOVA with Sidaks multiple comparisons, no significance at 8 hpi $p > 0.05$). (C) Percentage change in number of neutrophils at the wound site between 8 and 24 hpi in 3 dpf *TgBAC(mpx:EGFP)i114* zebrafish treated with 5 and 50 µM R848 and a water control (3 independent repeats, minimum 16 larvae per concentration, ± SEM, One-way ANOVA with Dunnett's multiple comparisons).

3.3.5. Pre-incubation prior to caudal-fin injury significantly alters the neutrophilic kinetics by 3 hpi but has no effect on neutrophil number.

Injured 3 dpf larval zebrafish treated with R848 4-hours before inflammation resolution significantly alters neutrophil inflammation resolution. The next step was to test whether the same effect was observed at timepoints associated with neutrophil recruitment. 5 μM R848 was chosen for further experiments as it matches the published concentration used *in vitro* and due to the results of the inflammation resolution experiments (Results 3.3.4) (Zimmermann *et al.*, 2015). 3 dpf zebrafish were treated for 4-hours with R848 before caudal fin injury was performed and the fish returned to the R848 media. During the initiation of inflammation, neutrophils continue to be recruited to the wound site with a peak infiltration at 6 hpi (Renshaw *et al.*, 2006). 1-, 3- and 6-hpi were chosen, to assess neutrophil numbers. There was no significant difference relative to untreated controls (Figure 3.5B), however, neutrophil kinetics appear to have been altered. When calculating percentage change between the key timepoints, there was a significant reduction in the number of neutrophils recruited between 1-3 hpi in the treated fish relative to the untreated (Figure 3.5C). Taken together with data from Figure 3.4, these suggest that 4-hours incubation with R848 can significantly alter neutrophil kinetics at the wound site, during inflammation recruitment and inflammation resolution.

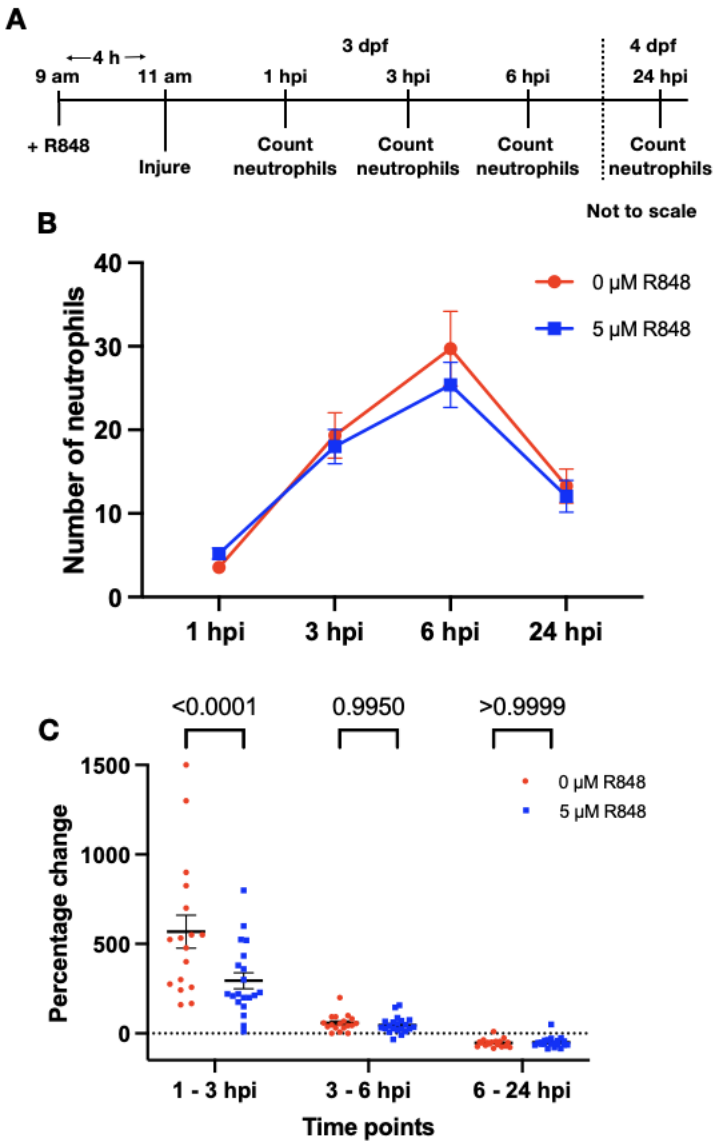

Figure 3.5: Treatment with R848 4 h before caudal fin injury significantly decreases percentage change in neutrophils at the wound between 1 and 3 hpi.

(A) Time course of the experiment (B) Total number of neutrophils at the wound site (counted posterior to the circulatory loop) between 1 and 24 hpi in 3 dpf *TgBAC(mpx:EGFP)i114* zebrafish treated with 5 µM R848 or a water control (3 independent repeats, minimum 18 fish per concentration, ± SEM, Two-way ANOVA with Sidak's multiple comparisons, no significance). (C) Percentage change in number of neutrophils at the wound site between 1-3, 3-6 and 6-24 hpi in 3 dpf *TgBAC(mpx:EGFP)i114* zebrafish treated with 5 µM R848 or a water control (3 independent repeats, 18 fish per concentration, ± SEM, Mixed effects analysis with Sidak's multiple comparisons).

3.3.6. Extended pre-incubation with R848 does not significantly alter neutrophil numbers at the wound site.

R848 can significantly alter neutrophil activity when fish are pre-incubated for 4-hours. Literature suggests that it takes up to 18 hours for the most significant epigenetic changes to occur (Zimmermann *et al.*, 2015; Makki, 2017). To see if this was the case in larval zebrafish, 2 dpf *TgBAC(mpx:EGFP)i114* were treated with 1 and 5 µM R848 for 16 hours before caudal fin injury was performed, and the fish returned to the R848 media. This aimed to observe any changes to neutrophil numbers recruited to the wound site. Neither concentration significantly altered the number of neutrophils recruited to the wound site (Figure 3.6B and 3.6D) or the percentage changes (Figures 3.6C and 3.6E).

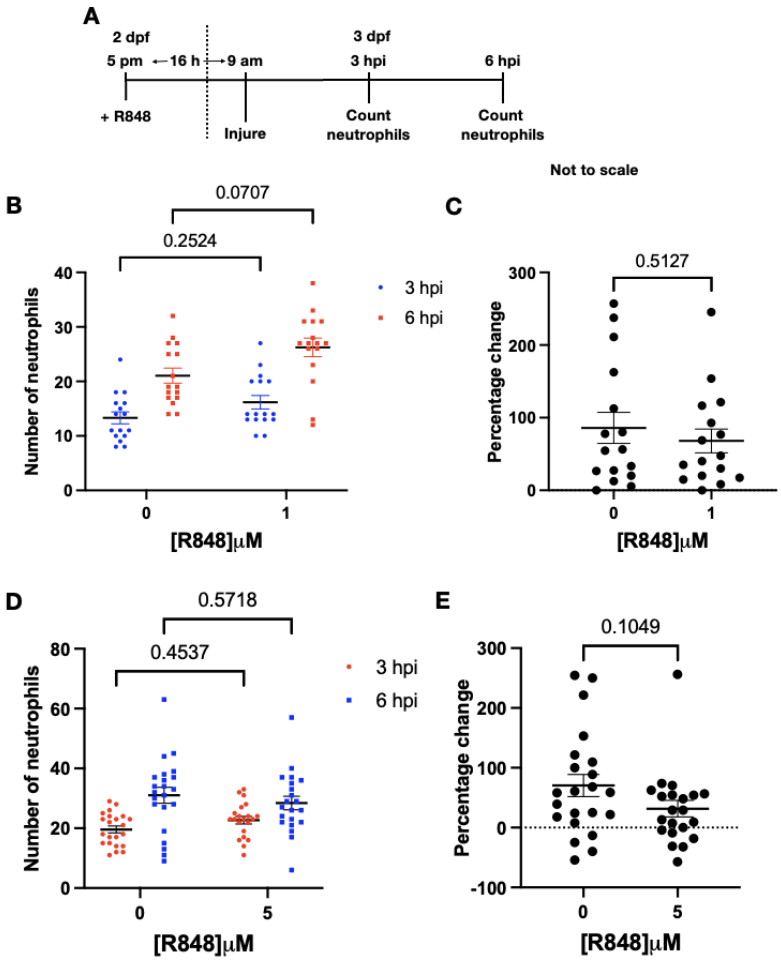

Figure 3.6: Treatment with R848 16 h before caudal fin injury does not alter the number of neutrophils recruited to the wound site

(A) Time course of the experiment (B) Total number of neutrophils at the wound site (counted posterior to the circulatory loop) between 3 and 6 in 3 dpf *TgBAC(mpx:EGFP)i114* zebrafish treated with 1 µM R848 and a water control (3 independent repeats, minimum 16 fish per concentration, ± SEM, Two-way ANOVA with multiple comparisons). (C) Percentage change in number of neutrophils at the wound site 3-6 hpi 3 dpf *TgBAC(mpx:EGFP)i114* zebrafish treated with 5 µM R848 and a water control (3 independent repeats, minimum 16 fish per concentration, ± SEM, Unpaired T-test). (D) Total number of neutrophils at the wound site between 3 and 6 hpi in 3 dpf *TgBAC(mpx:EGFP)i114* zebrafish treated with 5 µM R848 and a water control (3 independent repeats, ± SEM, Two-way ANOVA with multiple comparisons). (E) Percentage change in number of neutrophils at the wound site 3-6 hpi in 3 dpf *TgBAC(mpx:EGFP)i114* zebrafish treated with 5 µM R848 and a water control (3 independent repeats, ± SEM, Unpaired T-test).

3.3.7. R848 significantly increases whole tissue and neutrophil-specific activation of NF-κB.

It is important to try and establish the mechanism of R848 action *in vivo*. Zimmermann *et al.*, (2015) showed that *in vitro* R848 increases expression of NF-κB. Here, *Tg(pnfκb:EGFP)sh235* zebrafish that expressed the GFP gene under the control of a NF-κB recognition sequence were crossed with *Tg(lyz:nfsβ-mCherry)sh260* fish with mCherry driven by the neutrophil specific gene lysozyme-c (*lyz*) promoter (Kanther *et al.*, 2011). This assay aimed to observe NF-κB activation at the point where neutrophil recruitment stops and inflammation resolution begins, 16 hours was chosen as an incubation time based on published *in vitro* data for observing NF- κB changes (Zimmermann *et al.*, 2015). This outcross gave fish with red fluorescent neutrophils and cells that would express GFP following NF-κB activation. 2 dpf larvae were incubated for 16 h in 5 μM R848 and caudal fin injury performed (Figure 3.7A). The fish were imaged 8 hpi using a wide-field microscope to observe expression at the start of inflammation resolution. Analysis was carried out excluding the area around the notochord due to endogenous NF-κB expression – as seen in both the control and the treated fish – by drawing ROIs at the dorsal and ventral side of the notochord posterior to the circulatory loop (white boxes in Figure 3.7B). Within the ROIs, R848 significantly increased activation of NF-κB relative to controls based on mean intensity of GFP from 473 AU to 608 AU ($p=0.001$, two-tailed Mann-Whitney test) (Figure 3.7C). GFP activation within neutrophils was then measured by drawing new ROIs around red fluorescent neutrophils at the wound site – again the notochord was excluded. Mean intensity of GFP and therefore activation of NF-κB was significantly increased in the neutrophils of R848 treated larvae from 726 AU to 994 AU ($p=0.0403$, two-tailed t-test) (Figure 3.7D). To see whether the increase in GFP in neutrophils was down to an overall increase in neutrophils at the wound site, neutrophils were counted. There was no significant difference between neutrophil number in the treated or untreated larvae (Figure 3.7E). The increased activation of NF-κB in whole tissue and specifically in neutrophils suggests that R848 activates the NF-κB pathway *in vivo* as it does *in vitro* (Zimmermann *et al.*, 2015). Further evidence is required to confirm whether it is by the TLR8 pathway.

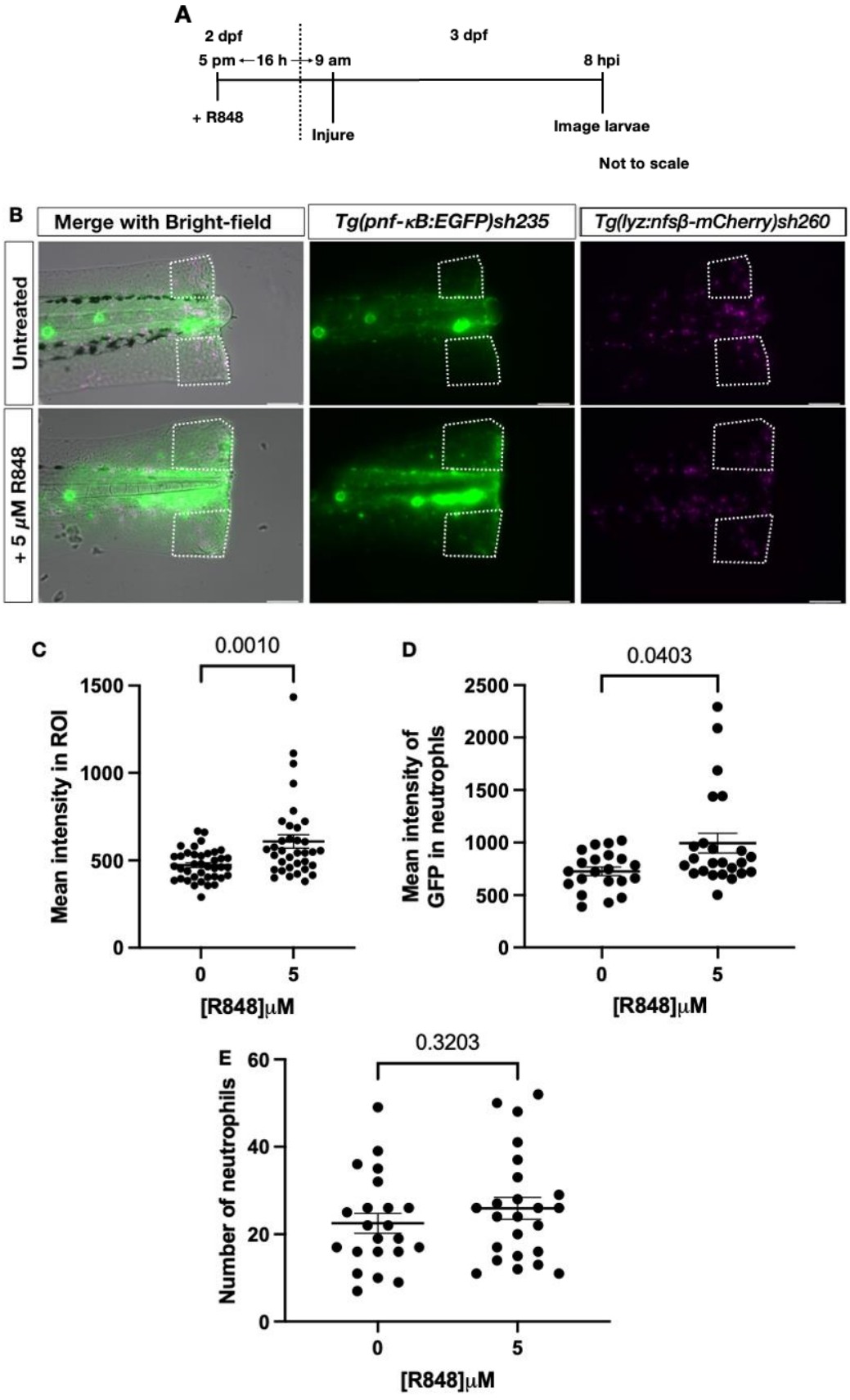
A
2 dpf
3 dpf
5 pm ←16 h→ 9 am
8 hpi
+ R848
Injure
Image larvae
Not to scale
B
Merge with Bright-field
Tg(pnf-κB:EGFP)sh235
Tg(lyz:nfsβ-mCherry)sh260
Untreated
+ 5 μM R848
C
0.0010
Mean intensity in ROI
1500
1000
500
0
0
5
[R848]μM
D
0.0403
Mean intensity of GFP in neutrophils
2500
2000
1500
1000
500
0
0
5
[R848]μM
E
0.3203
Number of neutrophils
60
40
20
0
0
5
[R848]μM

Figure 3.7: Incubation in R848 significantly increases whole tissue activation of NF-κB and activation of NF-κB in neutrophils in caudal fin injury.

(A) Time course of the experiment (B) 8 hpi wide-field microscopy images showing *Tg(pnfκb:EGFP)sh235* x *Tg(lyz:nfsβ-mCherry)sh260* (green and magenta respectively) caudal fin injury with and without 16-hour pre-injury incubation with 5 μM R848. White boxes show ROIs drawn to exclude notochord. ROI starts posterior to the circulatory loop. (10 x magnification, scale bar 100 μm). (B) Whole ROI Mean intensity of GFP pixels calculated using NIS Elements ROI analysis tool representing whole tissue activation of NF-κB (5 independent repeats, ± SEM, minimum 35 fish per concentration, Two-tailed Mann-Whitney test). (C) Mean intensity of GFP pixels specifically in mCherry labelled neutrophils highlighted using NIS Elements Auto-detect ROI tool representing neutrophil specific activation of NF-κB (4 independent repeats, minimum 35 fish per concentration, ± SEM, Two-tailed Mann-Whitney test). (D) Number of neutrophils at the wound site based on a count of mCherry labelled cells (4 independent repeats, minimum 35 fish per concentration ± SEM, two-tailed unpaired T-test)

3.3.8. R848 has no effect on IL-1β expression at the wound site.

IL-1β is a pro-inflammatory cytokine that recruits neutrophils to the site of injury. Previous work using adult zebrafish, mice and humans treated with R848 show no significant change in IL-1β mRNA levels after 8 hours of R848 exposure (Progatzky *et al.*, 2019). To analyse whether R848 influences *il1b* expression *in vivo*, 2 dpf *Tg(il1b:EGFP)sh445* zebrafish larvae were treated with 5 µM R848 for 16-hours before caudal fin injury and imaged 6 hpi on a spinning disk confocal. ROIs were drawn posterior to the circulatory loop as shown in Figure 3.8B and average GFP signal was recorded. There was no significant difference in levels of GFP expression *in vivo* between treated and untreated larvae (Figure 3.8B). These data complement previously published mRNA data (Progatzky *et al.*, 2019).

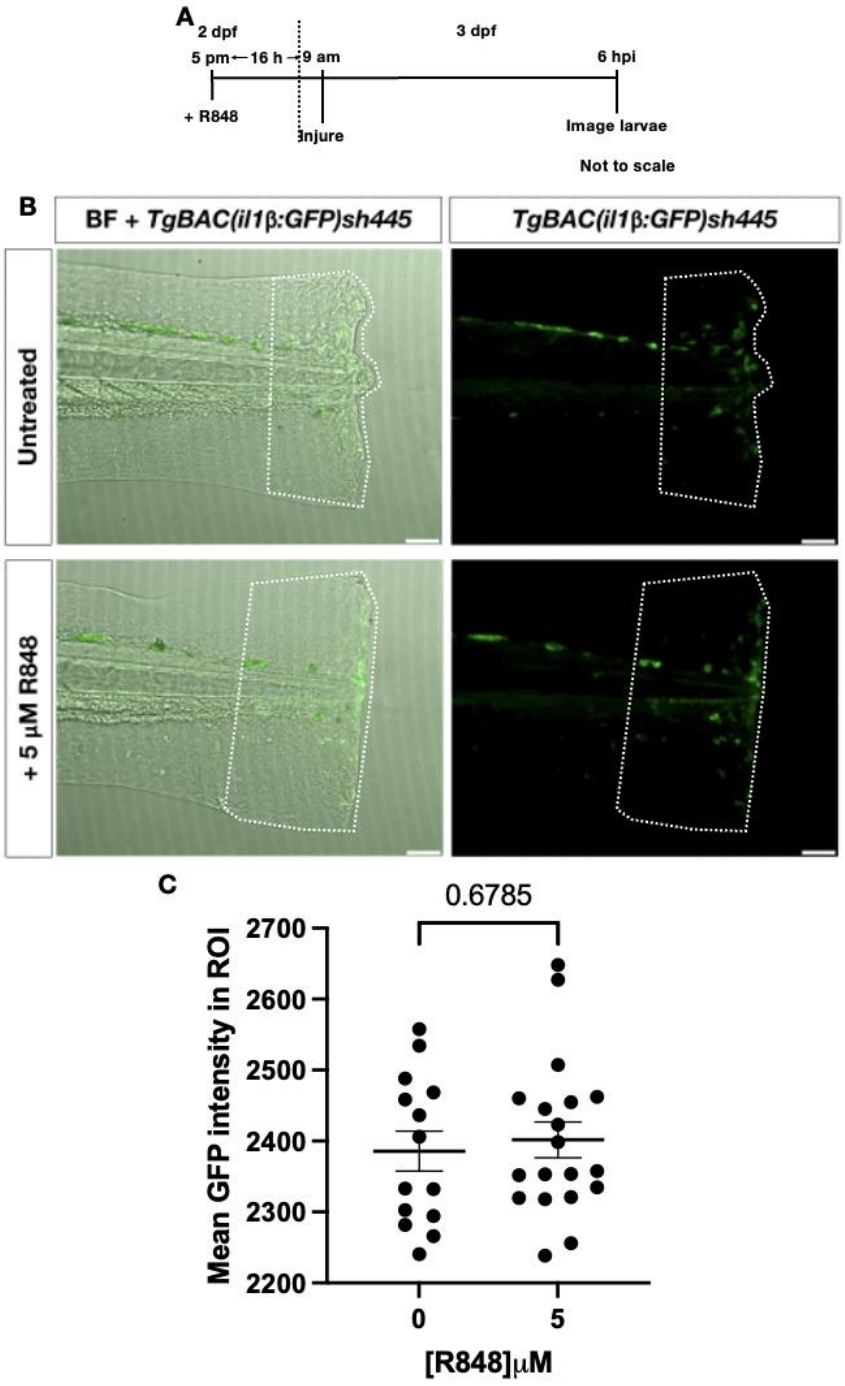

Figure 3.8: R848 does not affect whole tissue activation of IL-1β in caudal fin injury.

(A) Time course of the experiment (B) 6 hpi Spinning disk confocal microscopy images showing *Tg(il1b:GFP)sh445* caudal fin injury with and without incubation for 16 hours in 5 µM R848. White boxes show ROIs used for analysis. (10 x magnification, scale bar 60 µm). (C) Whole ROI Mean intensity of GFP pixels calculated using Volocity ROI analysis tool to show whole wound site expression of *il1b* (2 independent repeats, minimum 14 fish per concentration ±SEM, Two-tailed T-test).

3.3.9. R848 significantly increases TNFα expression in caudal fin injury of larval zebrafish.

TNFα is a potent driver of inflammation that further promotes NF-κB activation. TNFα expression was shown *in vitro* to increase in human neutrophil cultures treated with R848 for up to 20 hours (Zimmermann *et al.*, 2015). Here, a preliminary experiment was performed based on established protocols and timepoints to observe *tnfa* expression in *TgBAC(tnfa:GFP)pd1028* fish that contain a *gfp* gene driven by the *tnfa* promoter (Marjoram *et al.*, 2015; Lewis and Elks, 2019) (Figure 3.9A). 2 dpf were treated for 4 hours in 5 µM R848 before being removed for caudal fin injury and returned to the R848 bath for 16 hours. 16 hpi fish were imaged using a spinning disk confocal microscope and ROIs drawn posterior to the circulatory loop for quantification (Figure 3.9B). Uninjured fish were also added as controls to confirm effects were injury dependent. Treatment with R848 significantly increased mean GFP expression from 1368 AU to 1647 AU following R848 treatment only in injured fish (p=0.0083 Two-tailed way ANOVA with Bonferroni's multiple comparisons) (Figure 3.9C). The observation that R848 only acted on injured fish matches with Figure 3.2, confirming that immune challenge is required for R848 to act upon inflammation resolution. Overall, the increase in TNFα parallels the previously published *in vitro* data and Figure 3.4 and 3.5B shows that 4 h incubation with R848 can cause changes in the kinetics of the inflammatory time course. However, the time points here do not match previous experiments and further confirmation is needed to identify the cell type within Figure 3.9B using a neutrophil-specific reporter which was not used in this preliminary assay. Furthermore, it is unclear whether the larvae used were heterozygous or homozygous for the transgene and that may account for the differences – outcrossing the adults to wild type fish and screening for GFP positive larvae will prevent these issues arising in the future. The increase in signal could also be down to an increase in cells at the wound site and for future experiments number of neutrophils will be analysed via an outcross to a neutrophil reporter line as number of cells is difficult to observe in this assay without a co-localisation signal to confirm they are neutrophils.

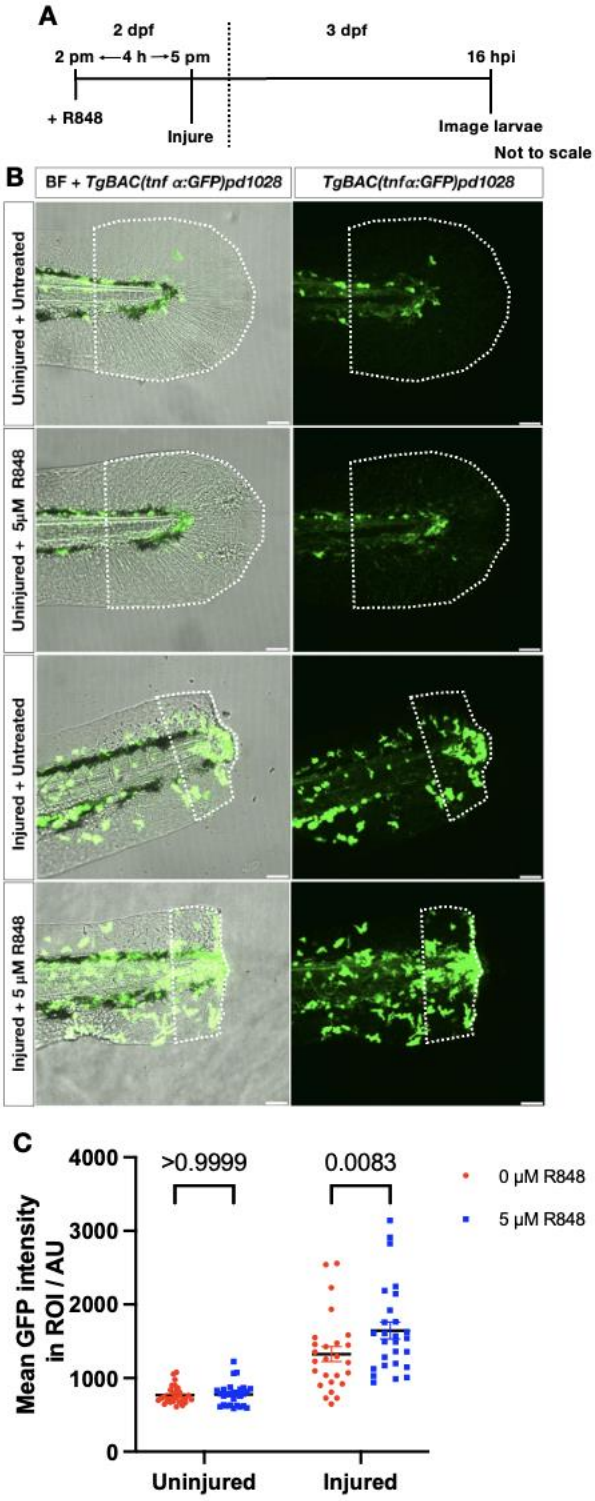

Figure 3.9: R848 significantly increases expression of TNFα in caudal fin injury.

(A) Time course for the experiment (B) Spinning disk confocal microscopy images showing *TgBAC(tnfa:GFP)pd1028* caudal fin injury with and without 5 µM R848. White boxes show ROIs used for analysis. ROIs drawn posterior to the circulatory loop. (10 x magnification, scale bar 60 µm). (C) Whole ROI mean intensity of GFP pixels calculated using Volocity ROI analysis

tool showing wound site expression of TNFα (3 independent repeats, minimum 26 fish per concentration, ±SEM, Two-tailed way ANOVA with Bonferroni's multiple comparisons)

3.3.10. 16-hour incubation with R848 has no effect on TNFα expression at the wound site or in neutrophils

To answer the questions posed by the previous TNFα experiment such as analysis of neutrophil-specific expression and number of neutrophils at the wound, the *TgBAC(tnfa:GFP)pd1028* fish were outcrossed with *Tg(lyz:nfsβ-mCherry)sh260* to allow for analysis of neutrophil specific expression of *tnfa* in the offspring. This outcross also ensured all GFP positive larvae were heterozygous carriers of the *tnfa:GFP* transgene, ensuring a single copy was present in each positive larva. Also, the time points were changed to match the NF-κB experiments described in Results 3.3.7., as TNFα and NF-κB pathways work in tandem during inflammation. 2 dpf *TgBAC(tnfa:GFP)pd1028* x *Tg(lyz:nfsβ-mCherry)sh260* larvae were treated with 5 μM R848 for 16 h before caudal fin injury was performed. Larvae were then imaged on a spinning disk confocal 8 hpi and total wound site GFP, neutrophil specific GFP and number of neutrophils at the wound site were all counted based on the ROIs shown in Figure 3.10B. Whole wound site GFP quantification shows that there is no significant increase in *tnfa* expression 8 hpi when larvae are treated with R848 (Figure 3.11A). Specific GFP expression in neutrophils suggests that TNFα production is not significantly increased in neutrophils following R848 treatment for 16 h (Figure 3.11B). At 8 hpi, the number of neutrophils at the wound site are also not significantly increased by 16-hour pre-incubation with R848 8 hpi. However, as shown in the bottom right representative image in the injury + R848 group, there is a GFP^+ $mCherry^-$ population of cells meaning they express TNFα but are not neutrophils that require more investigation (Figure 3.10B). Combined with Figure 3.9, these data suggest that 16-hour incubation with R848 has no effect on *tnfa* expression 8 hpi, but that 4-hour pre-injury incubation can increase expression at the wound site 16 hpi – a total incubation of 20 hours.

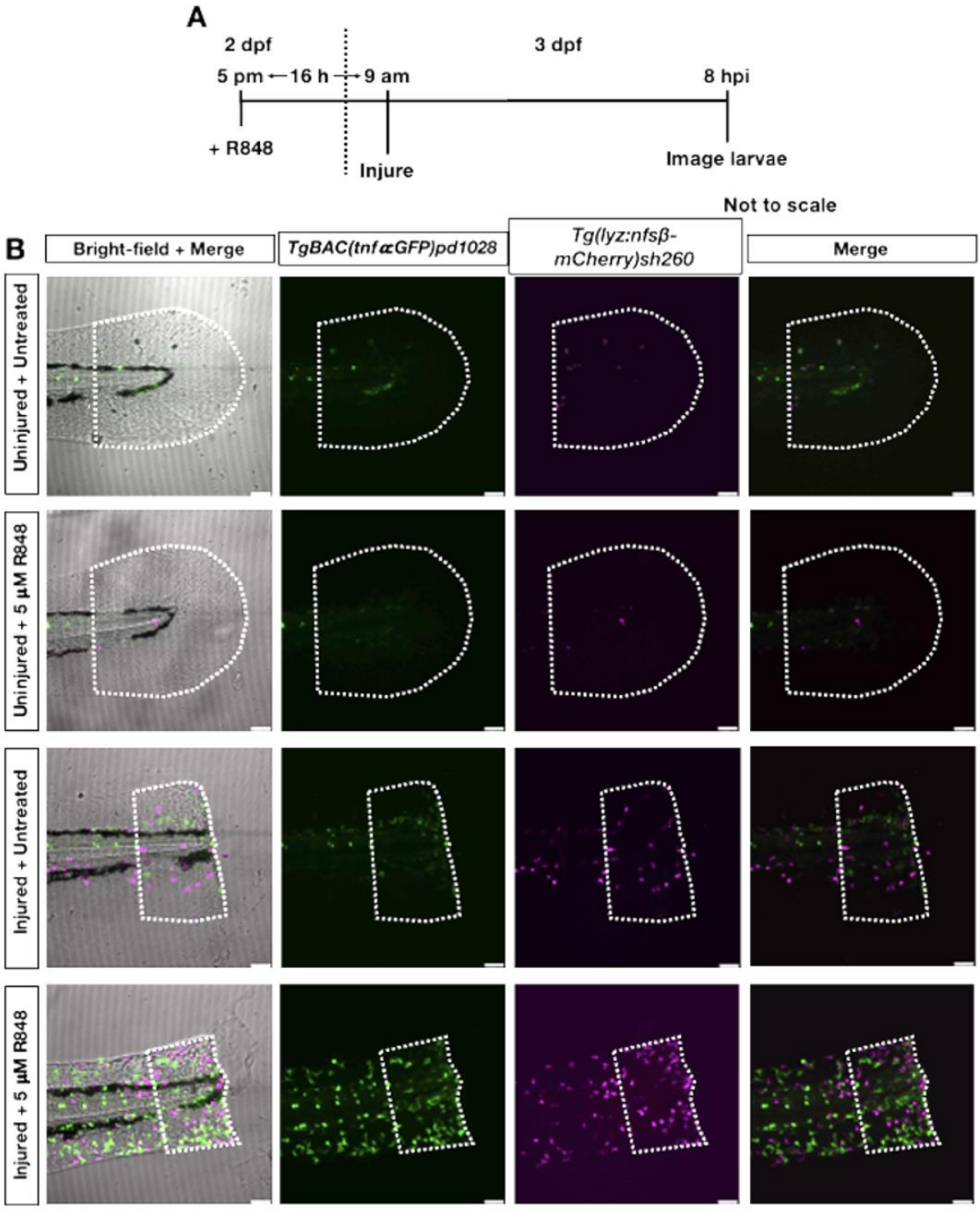

Figure 3.10: Images of the effect of 16-hour incubation with R848 on *tnfa* expression at the wound site or in neutrophils 8 hpi

(A) Spinning disk confocal microscopy images 8 hpi showing *TgBAC(tnfa:GFP)pd1028* x *Tg(lyz:nfsβ-mCherry)sh260* (green and magenta respectively) caudal fin injury with and without 16-hour incubation in 5 µM R848. White boxes show ROIs posterior to the circulatory loop. (10 x magnification, scale bar 60 µm).

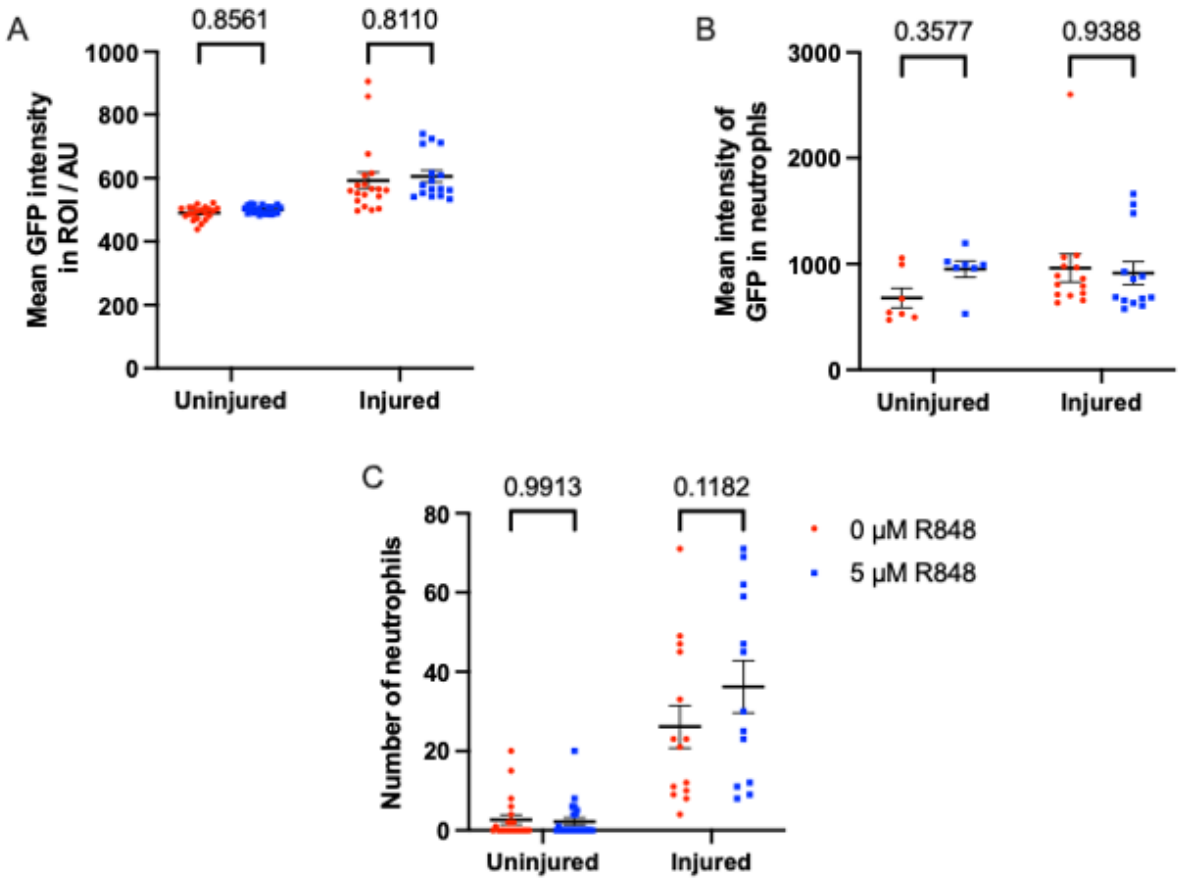

Figure 3.11. 16-hour incubation with R848 has no effect on *tnfa* expression at the wound site or in neutrophils 8 hpi

(A) Whole ROI Mean intensity of GFP pixels calculated using Volocity ROI analysis tool to show whole injury *tnfa* expression (3 independent repeats, minimum 19 larvae per concentration, ± SEM, mixed effects analysis with Sidak's multiple comparisons). (B) Mean intensity of GFP pixels specifically in mCherry labelled neutrophils highlighted using Volocity auto-detect object in ROI tool, representing neutrophil specific *tnfa* expression (3 independent repeats, minimum 7 fish per concentration, ± SEM, mixed effects analysis with Sidak's multiple comparisons).) (C) Number of neutrophils at the wound site posterior to the circulatory loop (3 independent repeats, minimum 14 larvae per concentration, ± SEM, mixed effects analysis with Sidak's multiple comparisons).

3.3.11. Whole-body qRT-PCR shows an R848 dependent significant increase in IL-6 expression that is not observed following tailfin injury.

Due to the lack of an il6 transgenic reporter zebrafish line, qRT-PCR was used to test that in zebrafish, whole larvae expression of *il6* is increased by R848 treatment, as seen *in vitro* by Zimmermann *et al.*, (2015). Two dpf zebrafish larvae were treated with 5 μM R848 for 16 hours. An untreated control was also used. Following 16 hours of incubation, a group of these larvae were removed, and the tailfin injured. Four groups were created (Materials and Methods 2.2.9 and Table 2.4). Twenty larvae were snap frozen at specific timepoints and RNA extracted and converted to cDNA for qRT-PCR. qRT-PCR was performed using primers for *rsp29* – the housekeeping gene, and *il6* – the gene of interest. ΔCt values generated by subtracting *il6* Ct from *rsp29* Ct values show relatively consistent expression of *il6* across the groups and time points, at 1 hpi –17 hours incubation – R848 treatment caused a significant decrease in ΔCt at 7.7 relative to 11.3 ($p=0.016$) and 11.25 ($p=0.023$) for the untreated and uninjured group and the R848 and injury group respectively (Two-way ANOVA with Tukey's multiple comparisons) (Figure 3.12B). ΔΔCt compares expression in the treatment groups relative to expression in the control group; across most groups there was no significant difference in relative *il6* expression (Figure 3.12C). R848 treatment alone showed a significant ΔΔCt value of -5.6, with a negative ΔΔCt representing an increase in expression relative to injury alone or combination of R848 and injury, with ΔΔCt values of -1.8 ($p=0.0017$) and -1.0 ($p<0.001$) respectively (Two-way ANOVA with Tukey's multiple comparisons). This difference in *il6* expression at 1 hpi in the R848 only group translates to an 86.2-fold increase in *il6* expression relative to the control, whereas injury alone gives a 4.6-fold increase and R848 and injury gives a 5.6-fold increase (Figure 3.12D).

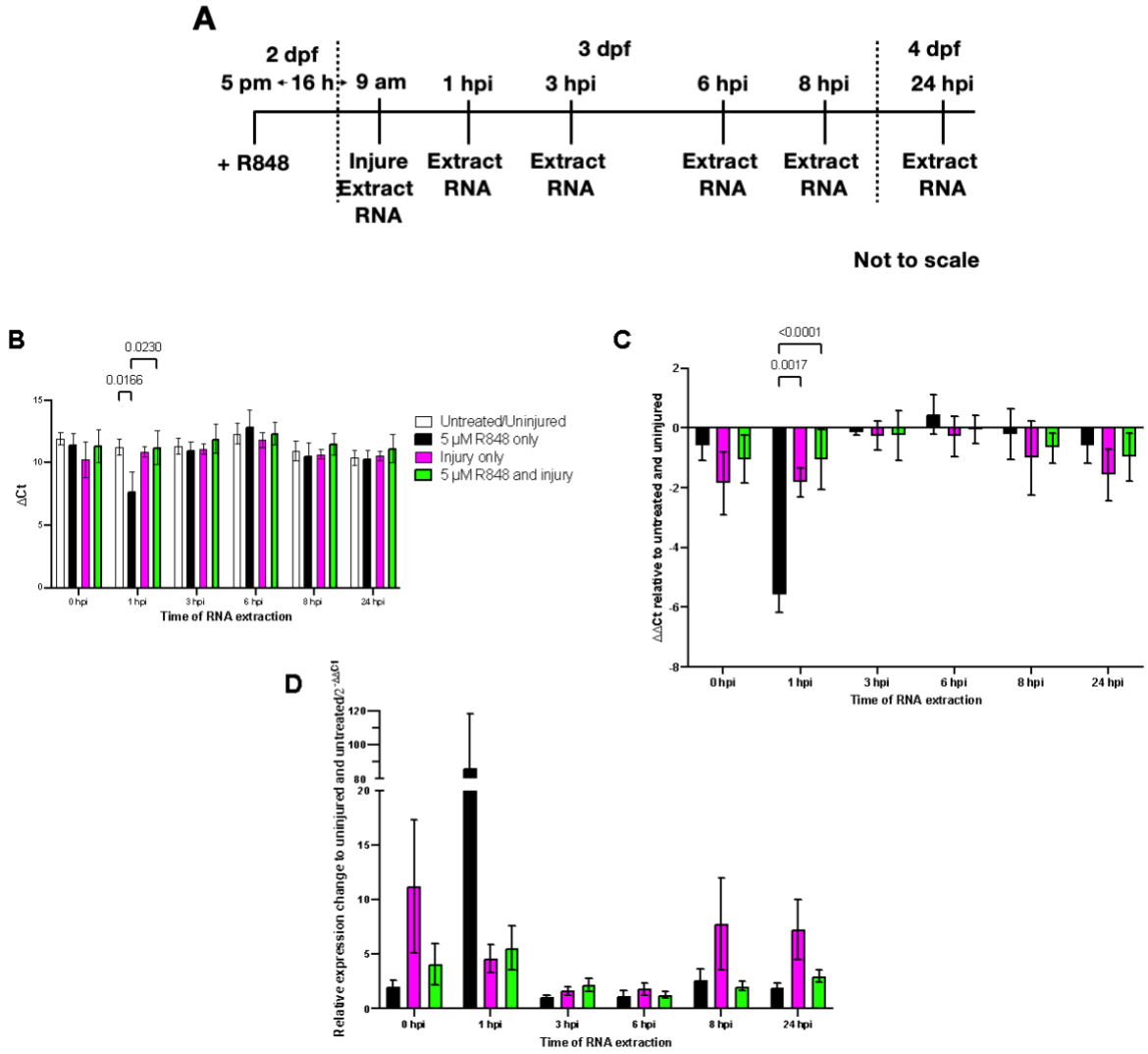

Figure 3.12. R848 treatment alone increases IL-6 expression after 1 hpi

(A) Time course of the experiment (B) ΔCt (*il6* Ct – *rsp29* Ct) for larval zebrafish comparing R848 treatment and tailfin injury at 0, 1, 3, 6, 8 and 24 hpi, colour coding in legend applies to B and C too. (C) ΔΔCt of *il6* expression (Treatment ΔCt – untreated/uninjured control ΔCt) comparing R848 treatment and tailfin injury at 0, 1, 3, 6, 8 and 24 hpi. (D) Relative expression changes of *il6* expression ($2^{-\Delta\Delta Ct}$) comparing R848 treatment and tailfin injury at 0, 1, 3, 6, 8 and 24 hpi. (3 independent biological repeats. Mean ±SEM. Statistical analysis performed on ΔCt and ΔΔCt in panels A and B using a two-way ANOVA with Tukey's multiple comparisons)

3.3.12. R848-dependent changes in neutrophil inflammation resolution are lost in knockdown of *myd88* by morpholino injection

R848 acts by the TLR7 and 8 pathways. TLR7/8 signal transduction is dependent on MyD88, a key downstream component of the protein complexes that lead to transcriptional changes in neutrophils when the toll-like receptors detect PAMPs within the endosome (Futosi, Fodor and Mócsai, 2013)(Fig 3.13B). Here, the *myd88* splice-blocking morpholino e2i2 was used to reduce *myd88* expression by single cell injection 0 dpi (Bates *et al.*, 2007) to determine if the MyD88 pathway plays a role in neutrophil regulation by R848 *in vivo*. Morpholino injected larvae were treated at 3dpf with R848, 4 hpi, to see if reduction in *myd88* expression led to a rescue of the effects on neutrophil inflammation resolution observed following R848 incubation at 8 and 24 hpi (Results 3.3.4). Successful knockdown using the morpholino was first confirmed using a range of concentrations and volumes analysed by RT-PCR products run on a 1% TAE agarose gel. Figure 2.2A explains how the MO works and why RT-PCR produces the specific bands on an agarose gel), initial attempts showed partial knockdown with 0.5 mM and 1 mM with visible 598 bp bands but also wild type 543 bp bands, though both concentrations did not show strong bands(Figure 3.13C). 1 mM was repeated and showed successful knockdown with the brightest 593 bp bands visible when 2 nl was injected (Figure 3.13D). 2 nl of 1 mM MO was used for the experiments.

R848 treatment in the absence of morpholino injection shows no significant difference in neutrophil number or kinetics between the time points (Figure 3.13F and G), with these results failing to replicate results seen in earlier experiments (Results 3.3.4). R848 treatment does, however, reproduce previous results (a reduction in neutrophils at 24 hpi) within the control morpholino group, reducing neutrophil numbers from 15 to 11 ($p=0.0367$, Two-way ANOVA with Tukey's multiple comparison test) and increasing neutrophil kinetics from 36 to 60.6% ($p=0.0014$, Two-way ANOVA with Sidak's multiple comparison test) (Figure 3.13F and G). Interestingly, R848 treatment following MyD88 knockdown mitigates this effect at 24 hpi and does not show the same reduction as in control MO larvae. This can also be seen by the significant reduction in neutrophil kinetics in the presence of R848 between control MO and MyD88 MO (Figure 3.13G), indicating that *in vivo* R848-dependent effects on neutrophils require MyD88 and may be part of canonical signalling and not chromatin remodelling events at the IL-6 locus. Knockdown of MyD88 compared to the control MO, shows a small mean reduction in neutrophil number at 24 hpi however, this is not significant in this model with

such large variation (Figure 3.13F). These results look promising however for a more definitive conclusion about MyD88 involvement, further experiments are required to ensure they are TLR8 specific – and not due to other TLRs activated by MyD88. Further experiments also need to be added using inhibitors of chromatin remodelling to confirm whether the effects seen are due to changes in canonical MyD88 signalling or secondary signalling from Ep300 and Crebbpa.

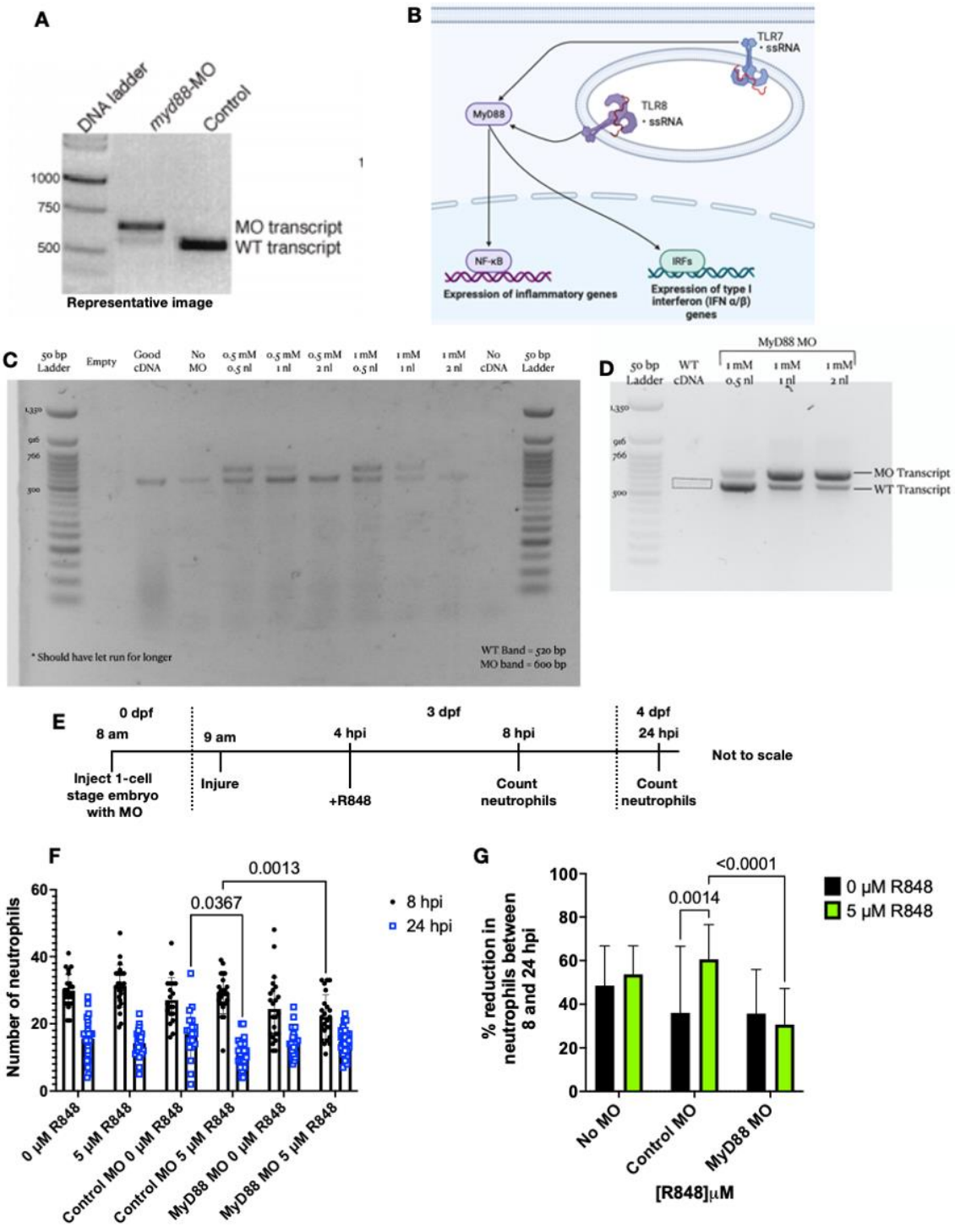

Figure 3.13. MyD88 morpholino injection significantly reduces neutrophil inflammation resolution when incubated with R848.

(A) Expected band sizes for successful and unsuccessful knockdown using the MyD88 e2i2 MO. (B) Schematic of the TLR7/8 pathways with MyD88 signalling. (C) 1% TAE agarose gel of cDNA of embryos injected with a range of concentrations and volumes of e2i2, no cDNA and

non-injected controls included (D) 1% TAE agarose gel showing cDNA from e2i2 injected embryos and a non-injected control. (E) Time course of the experiment (F) Number of neutrophils at the wound 8 and 24 hpi in injured zebrafish larvae grouped as uninjected controls, control MO, and MyD88 MO treated with or without 5 μM of R848. (3 independent repeats, ±SEM, minimum 19 fish per group, Two-way ANOVA with Tukey's multiple comparison test). (G) Percentage change in neutrophils at the wound between 8 and 24 hpi comparing larvae grouped as uninjected controls, control MO, and MyD88 MO treated with or without 5 μM of R848 (3 independent repeats, ±SEM, minimum 19 fish per group, Two-way ANOVA with Sidak's multiple comparison test)

3.4. Discussion

It has already been established that chemical compounds can be used to alter the activity of neutrophils *in vivo*, but the role chemical compounds can play on neutrophil chromatin remodelling *in vivo* remains largely unknown (Robertson *et al.*, 2014). To establish whether zebrafish provide a suitable model for studying neutrophil chromatin remodelling, R848 – a compound known to alter *in vitro* neutrophil chromatin remodelling – was added to zebrafish media and inflammatory changes observed by fluorescent microscopy and qRT-PCR (Zimmermann *et al.*, 2015).

The mechanism of R848 activity in human neutrophils is established *in vitro*, but how this relates to zebrafish remains unclear (Zimmermann *et al.*, 2015). Neutrophils in a live system behave very differently to neutrophils *in vitro* and so the effect of R848 on neutrophil number, and movement to and from wounds was explored. Incubation of unstimulated larval zebrafish with R848 had no effect on neutrophil number and immediate incubation with R848 after injury did not alter recruitment of neutrophils to the wound site. Preincubation with R848 for 4 hours was analysed and more time points were added to see if subtle changes were being missed. However, neutrophil numbers showed no significant changes at 1-, 3-, 6- or 24 hpi. A small but significant decrease in neutrophil kinetics was seen after 3 hours, but this was not seen at other time points. Incubation with R848 4 hours after injury, after the onset of the initiation of inflammation, did increase inflammation resolution. These data indicate that R848 appears to be only acting on inflammation resolution. However, for these inflammation resolution experiments, zebrafish larvae with abnormal numbers of neutrophils – very high or very low – at the wound before R848 incubation were removed and this may have altered results, future analysis retained these fish, and they were factored into statistical testing. The time taken for chromatin remodelling to alter the transcriptome within target cells may be a contributing factor, as evidence shows that *in vitro*, R848 takes up to 20 hours to cause conformational changes at target loci (Zimmermann *et al.*, 2015); a longer incubation may promote changes in neutrophil number or kinetics. 16 hours pre-injury incubation with R848 was therefore explored and this still proved insufficient to see any differences. Overall, these data disprove the hypothesis that a longer incubation will result in changes in neutrophil number, only showing early changes to kinetics. Without analysis of the conformational

changes at a chromatin level, it is unclear what the reasons for this may be. A longer incubation may also be required; more recent work has incubated human neutrophils with R848 for 48 hours before making measurements (Tamassia *et al.*, 2019). Furthermore, changes in neutrophil number or kinetics do not tell the whole story and instead signalling needs to be investigated and compared to published data on R848 action. Canonically, human neutrophil cell signalling by TLR8 – the target receptor of R848 in neutrophils – leads to MyD88 activation and NF-κB activation (Hayashi, Means and Luster, 2003; Yanagisawa *et al.*, 2009). The R848-dependend changes in zebrafish may be because of canonical MyD88 signalling and not the secondary chromatin remodelling by Ep300 and Crebbp as seen in human neutrophils *in vitro,* especially as recruitment and resolution were not analysed *in vitro* and the pathway Is therefore unknown (Zimmermann *et al.*, 2015). Repeating many of these experiments using a MyD88 inhibitor may help to answer this question. Work in adult zebrafish has shown neutrophils are recruited to the gills when R848 is present but did not investigate the TLR signalling mechanisms by which that increase occurs (Progatzky *et al.*, 2019). Zebrafish TLRs are different from human TLRs, with up to 20 different receptors discovered, including three TLR8 paralogs (Chen *et al.*, 2021). Identifying the mechanisms and pathways by which R848 operates in zebrafish may help further understand these results, as well as being essential to understand whether chromatin remodelling in zebrafish neutrophils is the same as that seen in humans. Better establishment of a working dose will also help answer many of the questions remaining from this analysis of how R848 alters neutrophil movement and kinetics. For future experiments, a dose-response titration curve should be created to establish what doses are influencing neutrophil activity. Several experiments used 50 µM R848 but this concentration was not used when looking at the effect of R848 on neutrophil number and distribution in the whole body, so it is unclear if the effects at the tailfin were due to changes in recruitment or number. Uninjured fish were also not used in any of these tailfin injury assays and while it is rare for neutrophils to be present in high numbers in the tail without injury, adding an uninjured control may shed further light on if R848 can alter neutrophil distribution.

Work *in vitro* may not have explored how R848 alters neutrophil movement and kinetics, but studies have extensively explored how R848 drives pro-inflammatory cytokine expression in human neutrophils (Zimmermann *et al.*, 2015). As mentioned above, R848 is a TLR8 agonist.

When it binds TLR8, signal transduction by MyD88 causes activation of the NF-κB transcription factor that binds pro-inflammatory genes to promote translation of multiple pro-inflammatory proteins (François *et al.*, 2005; Hattermann *et al.*, 2007; Zimmermann *et al.*, 2015). R848 treatment is associated with an increase in IL-6 and TNFα production from neutrophils. While macrophages naturally produce IL-6 in response to inflammatory stimuli, there is debate about whether human neutrophils constitutively produce IL-6 (Zimmermann *et al.*, 2015). Because of this, R848's effect on IL-6 production is of particular interest here because IL-6 increase in expression following R848 has been linked to chromatin remodelling at the IL-6 locus by the enzymes EP300 and CREBBP – rather than canonical MyD88 signalling – that allow for transcription factors such as NF-κB, PU.1 and C/EBPβ, and transcriptional machinery, to drive *il6* expression (Zimmermann *et al.*, 2015). TNFα further promotes IL-6 production by maintaining chromatin remodelling events at *il6* enhancers. The elements of this R848-dependent IL-6 production was explored in the zebrafish as a method of exploring neutrophil chromatin remodelling. As IL-6 is a potent pro-inflammatory cytokine, it may shed light on how TLR8 signalling can alter the inflammatory environment and promote chronic inflammation.

With the availability of a transgenic zebrafish reporter line for NF-κB, a 16-hour pre-incubation of R848 was performed in these larvae, resulting in a significant increase in both whole tissue and neutrophil-specific NF-κB activation 8 hpi. Interestingly, 8 hpi is associated with the inflammation resolution phase of the inflammatory response (Loynes *et al.*, 2010), a process which has been shown in this chapter to be influenced by R848. NF-κB acts as a transcription factor driving transcription and release of cytokines and chemokines in endogenous tissues and neutrophils (Vallabhapurapu and Karin, 2009). This increase in NF-κB activation may be accelerating neutrophil activity and accounting for the increased inflammation resolution, but this would rely on an attenuation of the pro-inflammatory environment allowing for inflammation resolution to occur. Assessment of neutrophil number and NF-κB activation at time points between 8 and 24 hpi would make this clearer. While these NF-κB findings start to provide insight into what may be happening downstream of R848 binding, there are some limitations. High endogenous NF-κB activation was seen in the notochord, as seen in published data using the same reporter line (Ogryzko *et al.*, 2014). Because of this signal, GFP fluorescence is very high in that region and had to be removed

from analysis. This excluded region may be masking R848 driven changes to NF-κB activity. This masking especially applies to neutrophil-specific measurements as this is the region where neutrophils migrate to the wound site, meaning cell-specific activation may be missed (Renshaw *et al.*, 2006). The use of maximum intensity projections to measure the intensity of GFP within the neutrophils also means that there may be some overlap between cell-specific activation and tissue activation, making it appear that the neutrophils have more active NF-κB. Nonetheless, these findings match those seen in *in vitro* human neutrophils, with R848 increasing activation of NF-κB components in the presence of R848 following a long incubation time (Zimmermann *et al.*, 2015) but further pathways, earlier timepoints, and the effect of R848 on epithelial cells need to be analysed to make clearer conclusions.

Another key component of the inflammatory response, the proinflammatory cytokine TNFα, is also produced by human neutrophils *in vitro*, upon 12-20 hours stimulation with R848 (Zimmermann *et al.*, 2015). During the cellular response to inflammation TNFα binds target receptors to promote further NF-κB transcription which in turn promotes pro-inflammatory gene transcription (Kalliolias and Ivashkiv, 2016). In a TNFα reporter zebrafish line, using published time points (Lewis and Elks, 2019), TNFα expression is significantly increased *in vivo* after a total of 20 h of R848 incubation – 4 hours pre-injury and 16 hpi – an effect that was not seen without injury, though earlier time points were not analysed. This mimics what was shown by Zimmerman *et al.,* (2015) with the need for injury suggesting that R848 stimulation works in synergy with caudal fin injury to drive the TNFα increase, potentially in a priming-like event (Bass *et al.*, 1986; Vogt *et al.*, 2018). Complimentary to this, it has been shown that R848-driven up-regulation of IL-6 in human neutrophils *in vitro* is increased in the presence of endogenous TNFα and with addition of IFNα for 20 hours (Zimmermann *et al.*, 2016). As TNFα promotes canonical NF-κB transcription, TNFα expression was analysed at 8 hpi following a 16-hour incubation with R848 to see if it was driving the increase in NF-κB seen *in vivo*. This did not show significant changes in TNFα at the wound or in neutrophils at the wound. Therefore, as the increase in NF-κB activation is not driven by an increase in TNFα, it could instead be driven by the activation of TLR8 or other pro-inflammatory signals. These data show that for R848 dependent changes on TNFα expression to be seen a long post-injury incubation of over 8 hours is required, and that a pre-injury incubation has little effect. Without an event to activate the neutrophils – such as caudal fin injury – an R848 dependent

change is not seen. When comparing the R848 inflammation resolution data, the NF-κB and the TNFα data, changes were only seen after 8-20 hours of post-injury incubation. This could be due to the time for activation of NF-κB and TNFα and then the time for remodelling at binding sites to occur. Another factor may be the time it takes for the drug to enter the system of the larval zebrafish. Conflicting with the data from the Cassatella group, which states that 20 hours incubation is required (Zimmermann *et al.*, 2015, 2016), Progatzky *et al.,* (2019) do show peaks in *tnfa*, *il6* and *il1b* transcript, and a significant neutrophil recruitment peak after 1-3 hours in the adult zebrafish gill when they add R848 directly onto the gill, but this difference is lost after 5-8 hours. In the larval system, the drug is added to the media and therefore may take longer to permeate the fish. Injury may even increase access as the drug may enter at the wound site. A longer time lapse of pro-inflammatory cytokine expression comparing injection of R848 and incubation with R848 may help answer some of these questions. Furthermore, the TNFα population of cells contains a non-neutrophil population shown by GFP^+ $mCherry^-$ signal. Morphologically these cells resemble macrophages, and the time frame represents a point where neutrophils begin to die by apoptosis and require removal by macrophages (Ellett *et al.*, 2011, 2015). These cells may be present either due to signalling factors released by R848 stimulated neutrophils or due to R848 acting directly on this macrophage-like population. Zimmerman *et al.,* (2015) briefly discuss the effects of R848 on monocytes and show that changes in transcription are less pronounced than in neutrophils and that epigenetic changes occur more transiently and at different loci – partly because macrophages naturally produce IL-6 – perhaps explaining why this population is altered whereas the neutrophil population is not and that more time is required for changes to be seen in neutrophils. Defining the population will be the first step in addressing these questions.

Zimmerman *et al.,* (2015) identify the IL-6 loci as the main target for remodelling following the addition of R848 to *in vitro* human neutrophils. Remodelling events occur to allow binding of NF-κB family members p50 and p65, as well as C/EBPβ. While the IL-6 gene expression changes in R848 only treated larvae at 1 hpi are statistically significant, it is unclear whether it is biologically significant. The rest of the non-significant changes throughout the time course are supported by Progatzky et al., (2019) showing a consistent pattern on *in vivo* activity. There is large variation in the data points, as shown by the large SEM error bars. As previously

mentioned, the effect of R848 on different zebrafish cell types is unclear and while the focus here is on neutrophils, the qRT-PCR was performed on cDNA from whole body RNA. This means that any changes in the neutrophil transcriptome are unlikely to be detected by this method as changes in 100-200 cells would be diluted by the remaining cells of the zebrafish larvae. So, while a change has been detected that does not fit with the above hypothesis that prolonged exposure to R848 following injury is required to see detectable changes in activity, it is difficult to confidently conclude that it is due to transcriptional changes in neutrophils. Further qRT-PCR using purified neutrophils sorted by FACS or INTACT BirA/Streptavidin pulldown is needed for further assessment.

Across the fluorescent reporter assays and IL-6 qRT-PCR, long incubations with R848 were used to attempt to trigger maximum chromatin remodelling and elicit a measurable response based on published literature on incubation times *in vitro* (Zimmermann *et al.*, 2015). Several of these assays showed some form of significant response, but the time scales used do not align with those that showed significant responses in neutrophil kinetics, most notably in inflammation resolution. Further work should use the time scale of that inflammation resolution experiment to increase the understanding of R848 action in zebrafish.

To further explore the pathways that R848 acts on in neutrophils, morpholino injection to inhibit the action of MyD88 – the downstream effector of TLR8 signalling – was performed in the neutrophil reporter line and inflammation resolution analysed. Use of the MyD88 MO alone did not show significant changes in neutrophil number or kinetics. This was unexpected as MyD88 is the downstream effector for many TLRs in both fish and humans and so deletion of its function might be expected to give some reduction in response to inflammation as seen in TLR2/MyD88 knockout studies in zebrafish (Chen *et al.*, 2021; Hu *et al.*, 2021). The previous findings in inflammation resolution using R848 were only replicated in the control MO + R848 group and not the R848 only group. A genome duplication in zebrafish makes pathway analysis more complicated due to multiple paralogs of many of the genes. The relationship between R848 and the three zebrafish paralogs of TLR8 are unknown and could account for why some effects are not always replicated across experiments as inhibitors may only be altering one out of three possible pathways and the others still functioning as normal. MyD88 morpholino injection combined with R848 showed a significant decrease in neutrophils

recruited to the wound at 8 hpi and reduced kinetics between 8 and 24 hpi relative to control MO + R848. This suggests that R848 action is dependent on MyD88 signal transduction, especially as inhibiting MyD88 alone showed no significant effect despite the multiple TLRs that function by MyD88 (Chen *et al.*, 2021). Using specific inhibitors of TLRs 7 and 8 would further confirm that this action is as seen in *in vitro* neutrophils but due to differences between zebrafish TLRs and mammalian TLRs, they may not function as predicted and have off-target effects.

A further limitation of these experiments is the lack of appropriate power calculations. Sample sizes were based on numbers of larvae used in previous zebrafish tailfin injury experiments by the Renshaw group and over time, samples sizes increased as I became more familiar with techniques (Renshaw *et al.*, 2006; Ogryzko *et al.*, 2014; Robertson *et al.*, 2014; Isles *et al.*, 2019). However, samples should have been decided based on standard deviations observed in trial experiments. This would provide increased confidence in whether statistically significant results are biologically significant. In any future R848 work, this should be rectified.

Overall, this chapter shows that chromatin remodelling compounds can alter the activity of zebrafish neutrophils. While questions remain about how R848 activity is driving the changes – particularly due to the lack of characterisation of TLR8 in zebrafish and its homology to human TLR8 – similar pathways have been shown to be up regulated in the zebrafish complimentary to *in vitro* studies, including NF-κB, TNFα and IL-6 and that neutrophil activity under R848 is dependent on MyD88 signalling. Further evidence for the role of chromatin remodelling in the R848 pathway in zebrafish neutrophils is the time taken for changes to be seen, which mirror much of the *in vitro* data produced by the Cassatella group (Zimmermann *et al.*, 2015, 2016; Tamassia *et al.*, 2021). However, heterogeneity between larvae did make some significant results hard to reproduce, though trends were seen. Further analysis of zebrafish neutrophils in isolation is required to further understand how chromatin remodelling dictates neutrophil function. Processes such as CRISPR/Cas9 knockdown and neutrophil-specific transcriptome sequencing can help further that understanding.

Chapter 4: Knockdown of chromatin remodelling enzymes using CRISPR/Cas9 technology and assessment of neutrophil activity in zebrafish.

4.1. Introduction

Targeted manipulation of gene function is a useful tool for discovering the role genes and their respective proteins play in cellular or whole system function. Zebrafish are an excellent model for this form of analysis, allowing for quick and high throughput knockdown in a traceable model relative to other vertebrate alternatives (Lieschke and Currie, 2007). Chapter 3 showed how chemical manipulation of gene function is possible in a zebrafish model. Moving forward, genetic manipulation was used to complement initial chemical work in order to specifically target and study neutrophil function.

CRISPR/Cas9 technology is now the gold standard for gene knockdown due to its efficiency, ease of use and the speed at which it can be employed. In zebrafish, CRISPR/Cas9 mediated knockdown has superseded processes such as TALENs and morpholinos to become an invaluable laboratory tool (Nasevicius and Ekker, 2000; Sander *et al.*, 2011; Hwang *et al.*, 2013). CRISPR utilises part of the bacterial *Streptococcus pyogenes* immune system to knockdown target sequences of DNA such as coding sequences, promoters, and enhancers (O'Connell *et al.*, 2014). CRISPR technology uses a custom designed template short guide RNA (crRNA) targeted to a 3' protospacer adjacent motif (3'PAM) sequences to target specific sequences of DNA for cutting by the Cas9 endonuclease protein. Following excision of the target sequence by the Cas9 endonuclease, endogenous double-strand break repair seals the gap, causing frame shifts and alterations to the coding sequence resulting in a mutation (Doudna and Charpentier, 2014). Therefore, CRISPR/Cas9 can be used in the laboratory to target genes for knockdown for downstream analysis of cell, tissue, system, or whole-animal analysis.

Using CRISPR/Cas9 for a whole-body knockdown in zebrafish is a relatively simple process (Shah *et al.*, 2015; Varshney *et al.*, 2015). A reaction mixture of a modified guide RNA called a crRNA, Cas9 endonuclease and tracrRNA – an essential RNA that anchors the crRNA to the

Cas9 to drive cleavage of target sites using the crRNA specific modifications – are microinjected into single-cell stage embryos (Hoshijima *et al.*, 2019). Many studies have shown that these whole-body knockdowns – not knockouts – give a suitable knockdown for analysis of cell phenotype and changes to gene expression, and CRISPR/Cas9 has become a regular process used for analysis of neutrophil function following gene knockdown (Varshney *et al.*, 2015; Loynes *et al.*, 2018; Isles *et al.*, 2019; Rahman *et al.*, 2019). The process, however, has its limitations. Whole-body knockdown rarely achieves 100% efficiency due to the decreased likelihood of biallelic knockdown due to potential in-frame deletions, compensation, and the chance that double-strand break repair can make a functional repair, rather than repair the target site in a way which results in a mutation (Gagnon *et al.*, 2014; Burger *et al.*, 2016; El-Brolosy *et al.*, 2019). These factors lead to a mosaic pattern of knockdown that will result in a reduction in expression of your target gene, but not full, whole-body knockout (Jao, Wente and Chen, 2013). Stable lines can be made by selectively breeding embryos with specific mutations; however, this creates a time-consuming process relative to analysing the effect of somatic knockdown in microinjected F0 embryos (Hruscha *et al.*, 2013; Varshney *et al.*, 2015). Whole-body knockdown of a gene may also hide effects seen in single cell populations due to alterations to other cells in the microenvironment caused by the knockdown or result in embryonic death, making it hard to narrow down changes to your population of interest or observe the population all together (Ablain *et al.*, 2015; Isiaku *et al.*, 2021). Overall, whole-body knockdown is a valuable tool allowing for initial observations to be made, but for further study, other forms of knockdown may be required that can target either specific regions of the body, or specific cell populations.

Cell-specific CRISPR/Cas9 knockdown allows for the study of gene knockdown on a single cell population in the zebrafish model. Neutrophil specific knockdown has been developed using a zebrafish model (Isiaku *et al.*, 2021; Wang *et al.*, 2021). This allows for analysis of knockdown specifically in neutrophils. Neutrophil specific knockdown is driven by microinjection of specific genetic constructs using transposon (Tol2) enzymes to insert into the zebrafish genome. Wang *et al.,* (2021), microinjected a plasmid into single-cell stage zebrafish embryos with the Tol2 transposase mRNA to drive *cas9* gene expression by the promoter for the neutrophil specific gene lysozyme C (*lyz*) to establish a stable zebrafish line. Gene-specific crRNAs can then be expressed in the offspring of the Cas9 zebrafish line by microinjecting

plasmids that drive crRNA expression by the ubiquitous U6a and U6c promoters. Knockdown will only occur in the cells that express both the crRNA and the Cas9 protein, in this case, neutrophils. This cell-specific system can be utilised to look at the effect of knockdown of chromatin remodelling enzymes in neutrophils.

The combination of whole-body and cell-specific knockdown of chromatin remodelling enzymes allows for a detailed and robust study of enzyme function in zebrafish neutrophils. Initial observations can be made using the whole-body knockdown method in multiple transgenic reporter lines including neutrophil reporters and pro-inflammatory cytokine and transcription factor reporters with a relatively short time scale and easy protocol (Loynes *et al.*, 2018; Isles *et al.*, 2019; Rahman *et al.*, 2019). Based on these observations, more detailed analysis into cell function can be carried out using the neutrophil specific knockdown. Neutrophil phenotype can be observed directly and the Cas9 line can be outcrossed to other reporter lines to look at the downstream effects of knockdown on neutrophil related processes (Isiaku *et al.*, 2021; Wang *et al.*, 2021). The data produced from this work can give a detailed picture of the role chromatin remodelling enzymes play in neutrophil function.

4.2. Aims and hypothesis.

We hypothesise that knockdown of chromatin remodelling enzymes will alter neutrophil function in a zebrafish tailfin injury model. The primary aim of this chapter is to identify chromatin remodelling enzymes responsible for regulating neutrophil function:

- First, neutrophil RNA sequencing data will be analysed based on differential expression following activation by different compounds and cytokines to identify potential chromatin remodelling enzymes responsible for regulating neutrophil function to narrow down a list of 150+ enzymes to a more manageable number.
- The selected enzymes will then be knocked down by zebrafish whole-body CRISPR/Cas9 and neutrophil phenotype observed following tailfin injury.
- A neutrophil-specific Cas9 knockdown system will be developed for knockdown of genes that show changes to phenotype in the whole-body CRISPR/Cas9 system

Identification of chromatin remodelling enzymes that alter neutrophil function will then be used for further sequencing experiments as part of later aims.

4.3. Results

4.3.1.a. Identification of initial CRISPR/Cas9 targets using a bioinformatic approach

I aimed to identify chromatin remodelling enzymes for further study in a zebrafish model of inflammation. A search for a panel of chromatin remodelling enzymes to target was designed based on readily available neutrophil RNA sequencing data. The initial aim was to identify a list of enzymes for a large-scale screen of genes, but this was later refined to a priority-based list due to COVID-19 lockdown. The first question to address was what are the genes that may be regulated by pro-inflammatory stimuli *in vitro*. The search began using the RNA sequencing data from human neutrophils treated with a panel of eight pro-inflammatory cytokines – GM-CSF, G-CSF, IL-1β, IFNγ, IFNα, IL-8, IL-6 and TNFα (Wright *et al.*, 2013). A literature search for chromatin remodelling enzymes identified 150+ enzymes (Keppler and Archer, 2008; Zhang *et al.*, 2016) and these were highlighted in the Wright *et al.,* (2013) data set and differential expression compared to untreated neutrophils calculated from **r**eads **p**er **k**ilobase of transcript, per million **m**apped reads (RPKM) values to find enzymes that may regulate neutrophil activation in these conditions. I calculated average differential expression change across all eight treatments and chromatin remodelling enzymes ranked to produce a top 20 – selected as a starting number of genes for knockdown within the project timescale (Figure 4.1 - orange). To confirm a potential role in neutrophil activity, these 20 enzymes were then cross referenced with another RNAseq dataset, activating human *in vitro* neutrophils with either PMA or *E. coli* (Denholtz *et al.*, 2020). Again, I calculated differential expression values from provided RPKM values and ranked the top 20 chromatin remodelling enzymes based on average expression change and combined these with the Wright *et al.,* (2013) analysis to give the first list of enzymes (Figure 4.1 – orange box). Overall expression within human neutrophils *in vitro* was then analysed for each gene to ensure expression was at detectable levels, deemed to be an RPKM above 1 – deemed an appropriate cut off above noise – in the Wright *et al.,* (2013) dataset (Figure 4.1. – blue "Yes" box). Then, for these enzymes to be suitable for the Cas9 screen, it was confirmed that the enzymes were expressed in zebrafish neutrophils using RNAseq of *mpx*$^{+}$ cells as a zebrafish neutrophil marker (Rougeot *et al.*, 2019) (Figure 4.1 – pink "Yes" box). If the RPKM value for the target gene was below 1, it was excluded from the screen (Figure 4.1 – blue "No" box). This resulted in an initial list of 10

enzymes (Figure 4.1 – yellow “Yes” box) and six enzymes were used for initial Cas9 attempts (Appendix Figure 4.2).

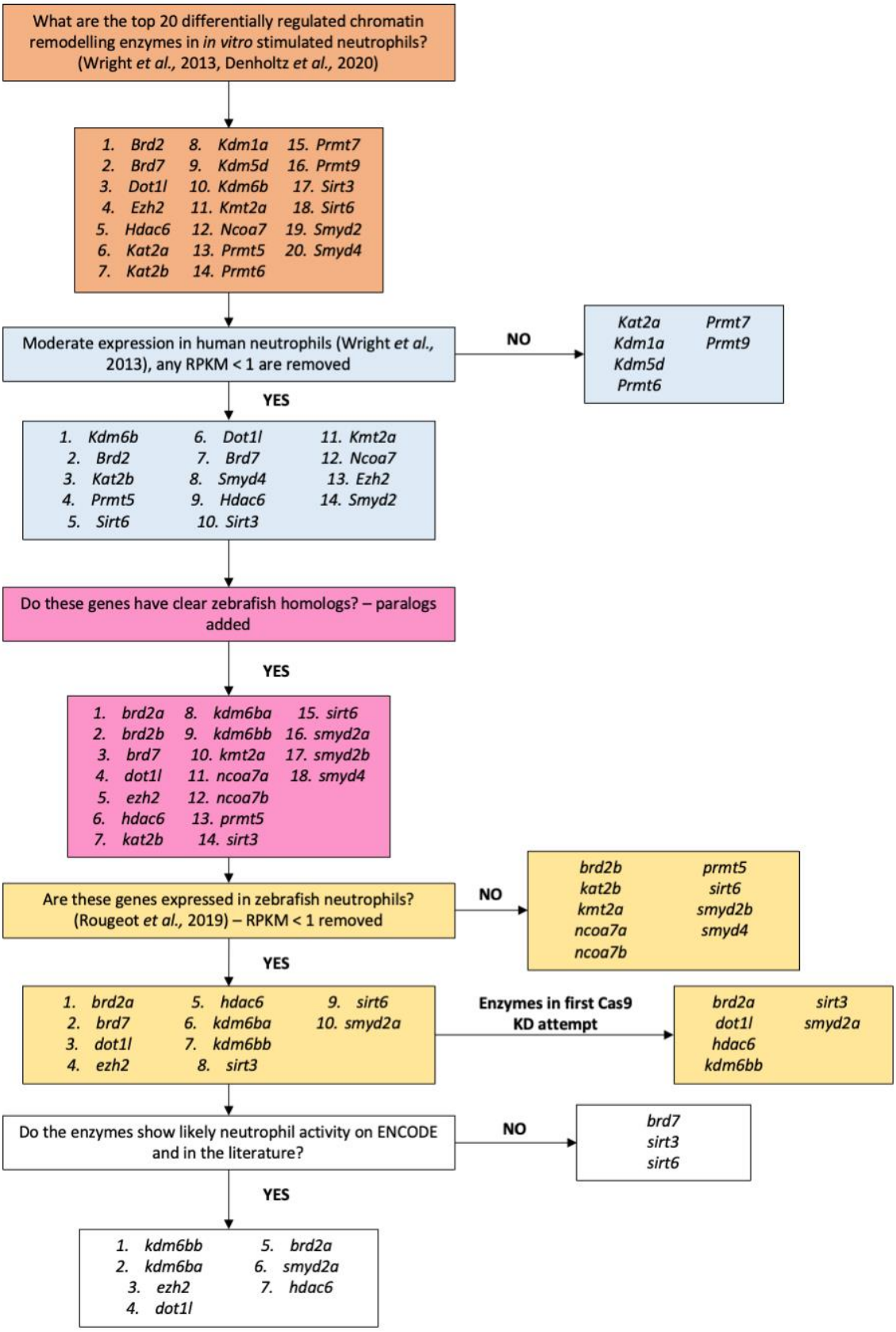
What are the top 20 differentially regulated chromatin remodelling enzymes in *in vitro* stimulated neutrophils? (Wright *et al.*, 2013, Denholtz *et al.*, 2020)
1. Brd2
2. Brd7
3. Dot1l
4. Ezh2
5. Hdac6
6. Kat2a
7. Kat2b
8. Kdm1a
9. Kdm5d
10. Kdm6b
11. Kmt2a
12. Ncoa7
13. Prmt5
14. Prmt6
15. Prmt7
16. Prmt9
17. Sirt3
18. Sirt6
19. Smyd2
20. Smyd4
Moderate expression in human neutrophils (Wright *et al.*, 2013), any RPKM < 1 are removed
NO
Kat2a
Kdm1a
Kdm5d
Prmt6
Prmt7
Prmt9
YES
1. Kdm6b
2. Brd2
3. Kat2b
4. Prmt5
5. Sirt6
6. Dot1l
7. Brd7
8. Smyd4
9. Hdac6
10. Sirt3
11. Kmt2a
12. Ncoa7
13. Ezh2
14. Smyd2
Do these genes have clear zebrafish homologs? – paralogs added
YES
1. brd2a
2. brd2b
3. brd7
4. dot1l
5. ezh2
6. hdac6
7. kat2b
8. kdm6ba
9. kdm6bb
10. kmt2a
11. ncoa7a
12. ncoa7b
13. prmt5
14. sirt3
15. sirt6
16. smyd2a
17. smyd2b
18. smyd4
Are these genes expressed in zebrafish neutrophils? (Rougeot *et al.*, 2019) – RPKM < 1 removed
NO
brd2b
kat2b
kmt2a
ncoa7a
ncoa7b
prmt5
sirt6
smyd2b
smyd4
YES
1. brd2a
2. brd7
3. dot1l
4. ezh2
5. hdac6
6. kdm6ba
7. kdm6bb
8. sirt3
9. sirt6
10. smyd2a
Enzymes in first Cas9 KD attempt
brd2a
dot1l
hdac6
kdm6bb
sirt3
smyd2a
Do the enzymes show likely neutrophil activity on ENCODE and in the literature?
NO
brd7
sirt3
sirt6
YES
1. kdm6bb
2. kdm6ba
3. ezh2
4. dot1l
5. brd2a
6. smyd2a
7. hdac6

Figure 4.1. Flow chart for determining which chromatin remodelling enzymes to investigate. Workflow of how chromatin remodelling enzymes for CRISPR/Cas9 knockdown were chosen. Analysis of Wright *et al.* (2013) dataset looking at human neutrophils treated with pro-inflammatory cytokines in vitro and analysis of Denholtz *et al.* (2019) dataset of human neutrophils activated with PMA or E. coli *in vitro* produced list of human genes. Rougeot *et al.*, (2019) dataset of zebrafish cells sorted for mpx expression – a key neutrophil specific gene was used to cross-reference human neutrophil genes to zebrafish neutrophils. Final list was produced using ENCODE and PubMed literature searches following initial attempts at a CRISPR/Cas9 screen targeting *brd2, dot1l, kdm6b, hdac6, sitr6* and *smyd2*.

4.3.1.b. Refinement of the chromatin remodelling enzyme Cas9 knockdown candidate list

Initial attempts to knockdown six of the nine enzymes by CRISPR/Cas9 proved unsuccessful as designed guides failed to give a successful knockdown (Appendix 4.1 and Appendix Figure 4.1 and 2) and the decision was subsequently made to further narrow down the screen to a priority-based knockdown (Figure 4.1 – white boxes). The chromatin remodelling list was refined and worked through in order, rather than a full screen of a wider panel. The initial list of nine enzymes was reassessed based on enrichment of gene enhancers and promoters using ENCODE. Representative examples of these enrichment graphs are shown in Figure 4.2. Higher peaks show higher levels of enrichment, suggesting increased chromatin marks. The chromatin marks selected were yellow peaks for H3K27ac – an active enhancer mark associated with higher transcription, red peaks for H3K4me3 – a mark for active promoters and transcriptional start sites and blue peaks for CTCF sites, a protein binding region that allows for chromatin loops to form (Kim, Yu and Kaang, 2015). Marks were analysed specifically in neutrophils. *kdm6b* showed consistently high peaks at enhancers, promoters, and the transcriptional start site; the same marks are seen in *dot1l* and *brd2*. *ezh2* showed consistent levels of low to medium enrichment across all marks, with more peaks in H3K4me3. *smyd2* showed some peaks in H3K4me3, but very little in other markers. *Hdac6* showed medium peaks in all three marks, but no high peaks. Overall, these peaks rank the enzymes in the order of *kdm6b, brd2, dot1l, ezh2, hdac6* and *smyd2* in levels of interest based on enrichment peaks. A literature search was then performed to look at evidence for involvement in neutrophils. Literature searches showed little to no involvement of *hdac6, smyd2* and *brd2* in inflammation and in combination with the chromatin mark enrichment, these were put to be lower priority. Work using an HDAC6 deficient mouse model has shown that knockdown of HDAC6 has no observable effect on neutrophil function (Yan *et al.*, 2018). While there is little research on the role of the remaining enzymes on neutrophil activity, KDM6B has roles in inflammation including macrophage polarisation and is linked to HIF-1α and HIF-2α, with HIF signalling playing a major role in neutrophil function (Walmsley *et al.*, 2005; Guo *et al.*, 2015; Yildirim-Buharalioğlu *et al.*, 2017; Shait Mohammed *et al.*, 2022). DOT1L is also linked to adaptive immune cell differentiation and macrophage cytokine release (Chen *et al.*, 2020; Scheer *et al.*, 2020; Aslam *et al.*, 2021). Cell differentiation/polarisation and cytokine release are vital for neutrophils to function, so there may be some crossover. Finally, EZH2 function has been linked to neutrophil related pathways such as HIF-1α in

inflammation associated with spinal cord injury and the senescence-associated secretory phenotype – a secretory phenotype linked to immune ageing (Introduction 1.5.2.b.vi) - in cancer associated fibroblasts (Ni *et al.*, 2021; Yasuda *et al.*, 2021). Yasuda *et al.,* (2021) used this cancer-associated fibroblast model to show that secretion of pro-inflammatory cytokines downregulates EZH2 expression in fibroblasts, preventing EZH2 from methylating SASP genes with H3K27me3 repressive marks. This change in chromatin state promotes SASP gene expression. Loss of EZH2 in ageing may prevent onset of the SASP and allow dysfunctional neutrophils to be retained, rather than removed from the circulation. Furthermore, unobserved SASP changes could be acting on neutrophils in the spinal cord model, as the spinal cord is deprived of neutrophils, a similar effect could be occurring on neutrophils in other tissues that wasn't detected in the Ni *et al.,* (2021) study. In atherosclerosis mouse models, *ezh2* deletion led to reduced neutrophil migration, though the focus of the study was macrophage activity (Neele *et al.*, 2021). Taken as a whole, the ENCODE analysis and literature search suggest that *kdm6b, dot1l* and *ezh2* may provide the most interesting data from Cas9-mediated knockdowns and subsequent analysis. ENCODE was used to look at chromatin accessibility at gene enhancers and promoters in neutrophils and PubMed literature was searched for evidence of involvement in neutrophil function.

(A) *kdm6b*

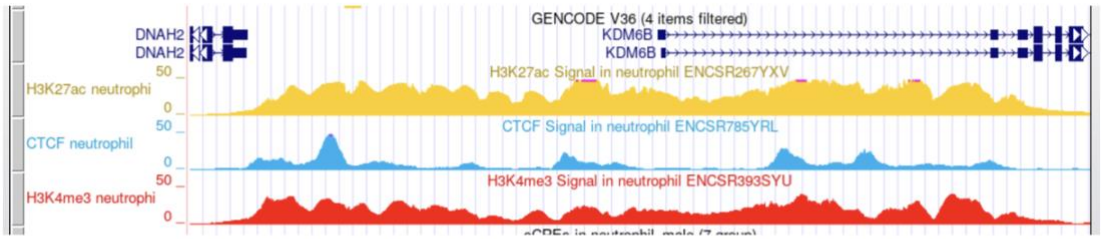

(B) *ezh2*

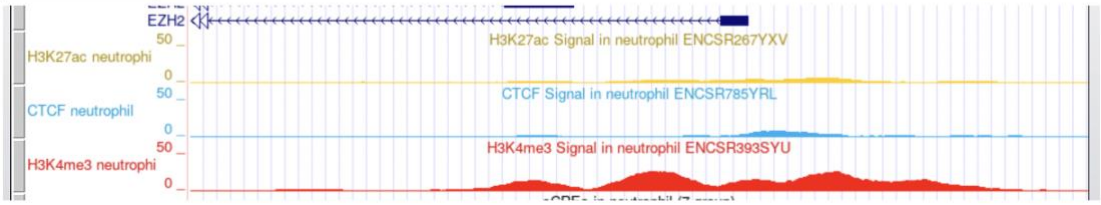

(C) *dot1l*

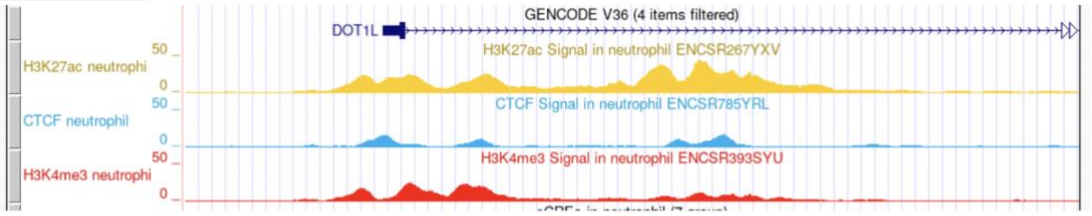

(D) *brd2*

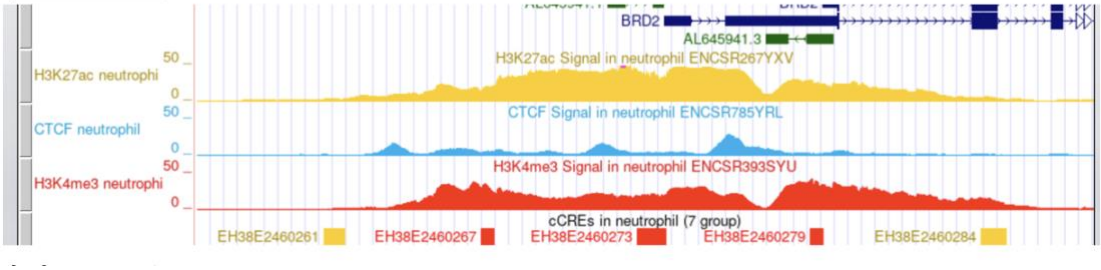

(E) *smyd2*

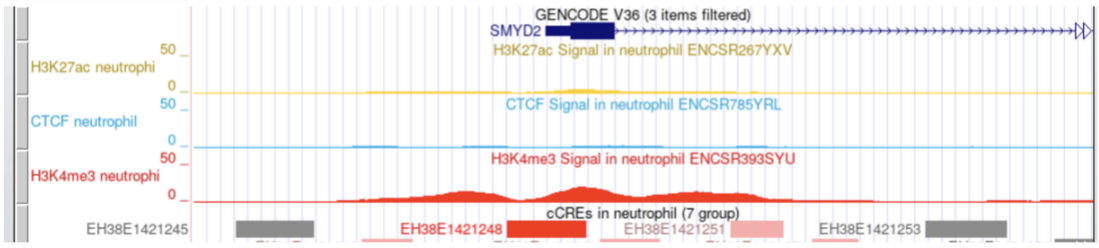

(F) *hdac6*

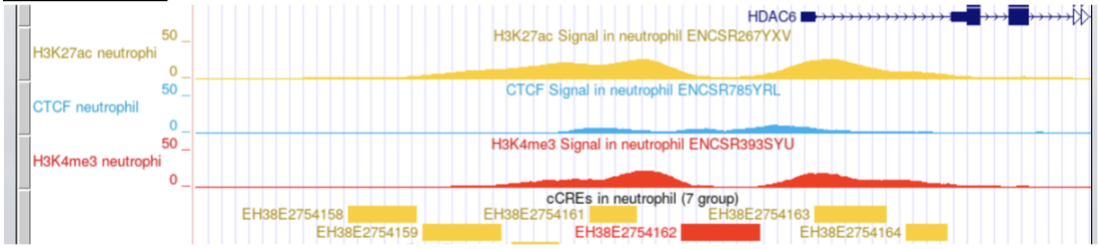

Figure 4.2. Enhancer/promoter enrichment for Top 6 ranked chromatin remodelling enzymes

Representative examples of enrichment peaks taken from ENCODE for enhancer or promoters for the top 6 enzymes identified from the refined analysis of published neutrophil RNAseq data shown in the workflow in Figure 4.3. Enzymes chosen are *kdm6b, ezh2, dot1l, brd2, smyd2* and *hdac6*. Yellow peaks are H3K27ac, blue peaks are CTCF binding, red peaks are H3K4me3. All readings are neutrophil specific analysis.

4.3.2. Design and testing of Cas9 crRNAs for *kdm6b*, *ezh2* and *dot1l*.

Guide RNAs were initially designed in the 5'UTR using CHOPCHOP to assign primer pairs and restriction enzymes for diagnostic digestion. Figure 4.3.A explains how to interpret these Cas9 diagnostic digests going forward throughout this thesis, the sequence for the *kdm6ba* 5'UTR guide RNA was used as a representative example. For this designed set of crRNAs, *kdm6ba* and *kdm6bb* were chosen, as well as *dot1l* and *ezh2* (Appendix Figure 4.3A-D). Due to the duplication in the zebrafish genome *kdm6b* has two paralogs that without targeted knockdown of both, there is a risk of compensation masking any knockdown effects. Gradient temperature RT-PCR was used to optimise the primers on uninjected larval gDNA with the annealing temperatures set around the manufacturers recommended $T_{m.}$ Initially, *kdm6ba* primers and restriction enzyme digest produced unexpected bands (Appendix Figure 4.3E-G). Issues with *kdm6ba* PCR and digest were rectified by optimising the use of a new restriction enzyme as shown in Appendix Figure 4.4. 2 nl crRNA mix was microinjected at the single cell stage. At 3 dpf, gDNA was extracted, target fragments amplified by RT-PCR, and restriction enzyme digestion performed overnight. All crRNAs showed incomplete digestion in most samples, suggesting successful mosaic knockdown by all crRNAs tested. *Kdm6ba* PCR product showed incomplete digestion in 8/8 samples, (Figure 4.3B), *kdm6bb* had 4/6 larvae with partial digestion (Figure 4.3C), *ezh2* with 7/8 samples showing some knockdown, as well as some non-specific bands (Figure 4.3D) and *dot1l* showed 6/8 larvae with successful knockdown (Figure 4.3E) . These data show that each crRNA causes mutation of the target site and can potentially trigger gene knockdown, though more analysis at the transcript level is required to confirm gene knockdown as they target the 5'UTR to enable for use with CRISPR interference if necessary. 5'UTR knockdown does not directly alter the coding region of a gene and instead disrupts the sequence before the ATG transcriptional start site. This means that deletion in the 5'UTR does not directly alter the coding sequence and instead increases the chance of upstream disruption, therefore further analysis such as qRT-PCR is required to confirm gene expression is reduced.

(A) How a diagnostic digest is performed to confirm CRISPR/Cas9 knockdown

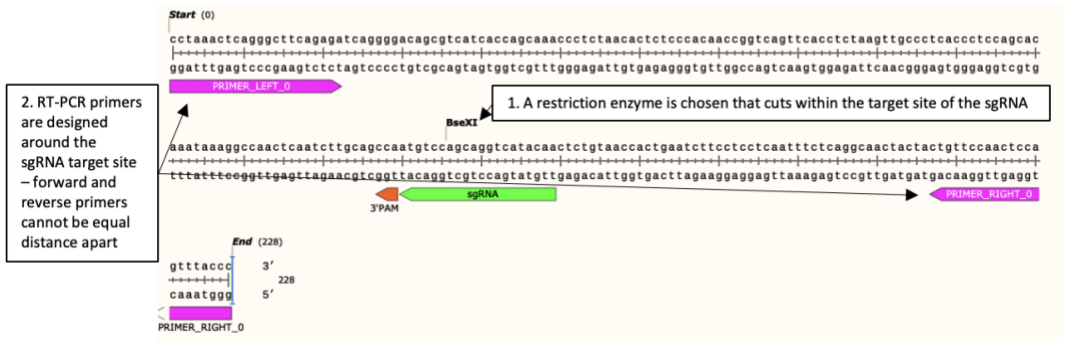

2. RT-PCR primers are designed around the sgRNA target site – forward and reverse primers cannot be equal distance apart

1. A restriction enzyme is chosen that cuts within the target site of the sgRNA

3. sgRNA + Cas9 injected larvae gDNA is amplified by RT-PCR using those primers

4. Restriction digest is performed and run on a 2% agarose + TAE gel

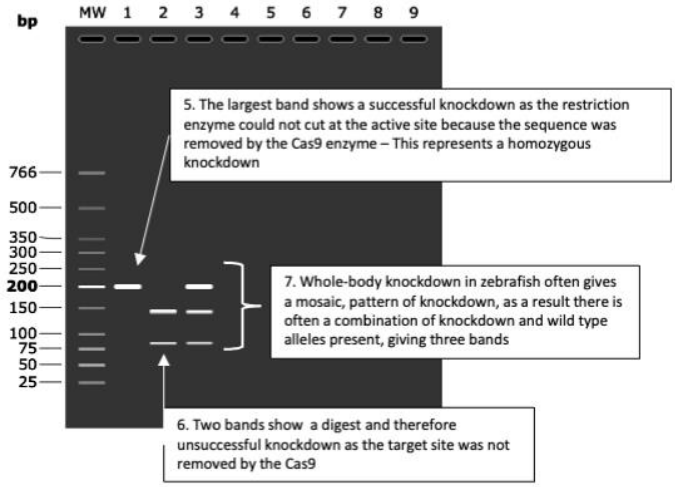

5. The largest band shows a successful knockdown as the restriction enzyme could not cut at the active site because the sequence was removed by the Cas9 enzyme – This represents a homozygous knockdown

7. Whole-body knockdown in zebrafish often gives a mosaic, pattern of knockdown, as a result there is often a combination of knockdown and wild type alleles present, giving three bands

6. Two bands show a digest and therefore unsuccessful knockdown as the target site was not removed by the Cas9

(B)

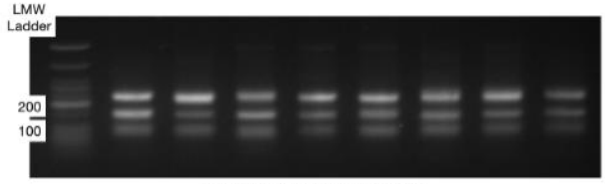

224 band = Successful knockdown
145 and 83 band = Unsuccessful knockdown

(C)

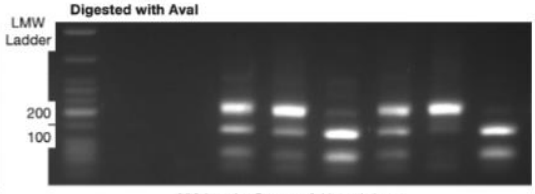

230 band = Successful knockdown
149 and 81 band = Unsuccessful knockdown

(D)

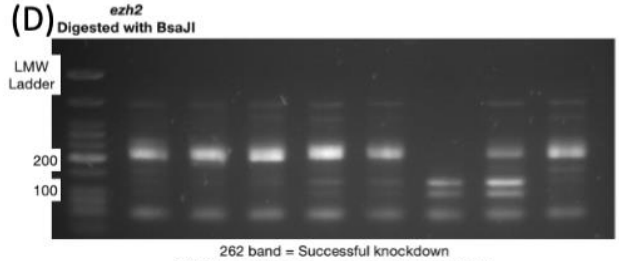

262 band = Successful knockdown
124, 94 and 47 band = Unsuccessful knockdown

(E)

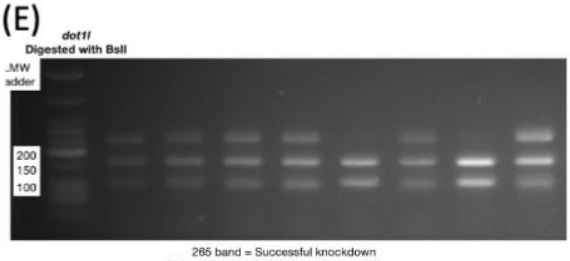

265 band = Successful knockdown
165 and 97 band = Unsuccessful knockdown

Figure 4.3. Diagnostic digest of larval gDNA injected with crRNAs targeting the 5'UTRs of *kdm6ba, kdm6bb, dot1l* and *ezh2.*

(A) Step by step guide of how the diagnostic digest is performed and how to interpret the resulting TAE/agarose gel images. Sequence is of *kdm6ba* 5'UTR amplified sequence, primers in magenta, sgRNA cut site in green, presented 5'-3', copied from SnapGene and representative gel simulated using SnapGene's restriction digest function with an NEB Low molecular weight ladder and edited to show heterozygous knockdown in lane 3 (B-D) 2% Agarose gels of digested PCR product from 8 individual embryos injected with 2 nl crRNA mixture. crRNA target and enzyme listed above each gel. Expected band sizes shown below each gel. All ladders are NEB Quick-load low molecular weight DNA ladder, necessary bands annotated.

4.3.3 Creation of *kdm6ba/b* crRNA constructs for neutrophil-specific knockdown

Transgenic constructs for the Cas9 driven knockdown of *kdm6ba* and *kdm6bb* were made based on protocols designed by the Deng group (Zhou *et al.*, 2018; Wang *et al.*, 2021) for neutrophil specific CRISPR/Cas9 knockdown. Materials and Methods 2.3.7.b. describes how the crRNA primer guides were created based on established protocols and Materials and Methods 2.3.7.c. describes how the control backbone was digested for insertion of the crRNA sequences. The following section will describe how the full crRNA construct was made from 4 fragments to make a full plasmid.

4.3.3.a. Optimisation of primers and DNA polymerase for insertion of crRNAs into 3' entry clone

Insertion of primers into the 3'entry clone was performed by RT-PCR of the linearised control plasmid. Reaction mixtures are described in Materials and Methods 2.3.7.d. Primers containing the sgRNA sequence and the plasmid overlapping sequence were tested to ensure the expected RT-PCR reaction was taking place (Figure 4.4A in red and Figure 4.4B in cyan). PCR amplification with Platinum SuperFi II DNA polymerase gave a strong 3.5 kb band and a weaker 0.5 kb band and the no-enzyme controls showed very weak bands relative to the SuperFi II lanes (Figure 4.4).

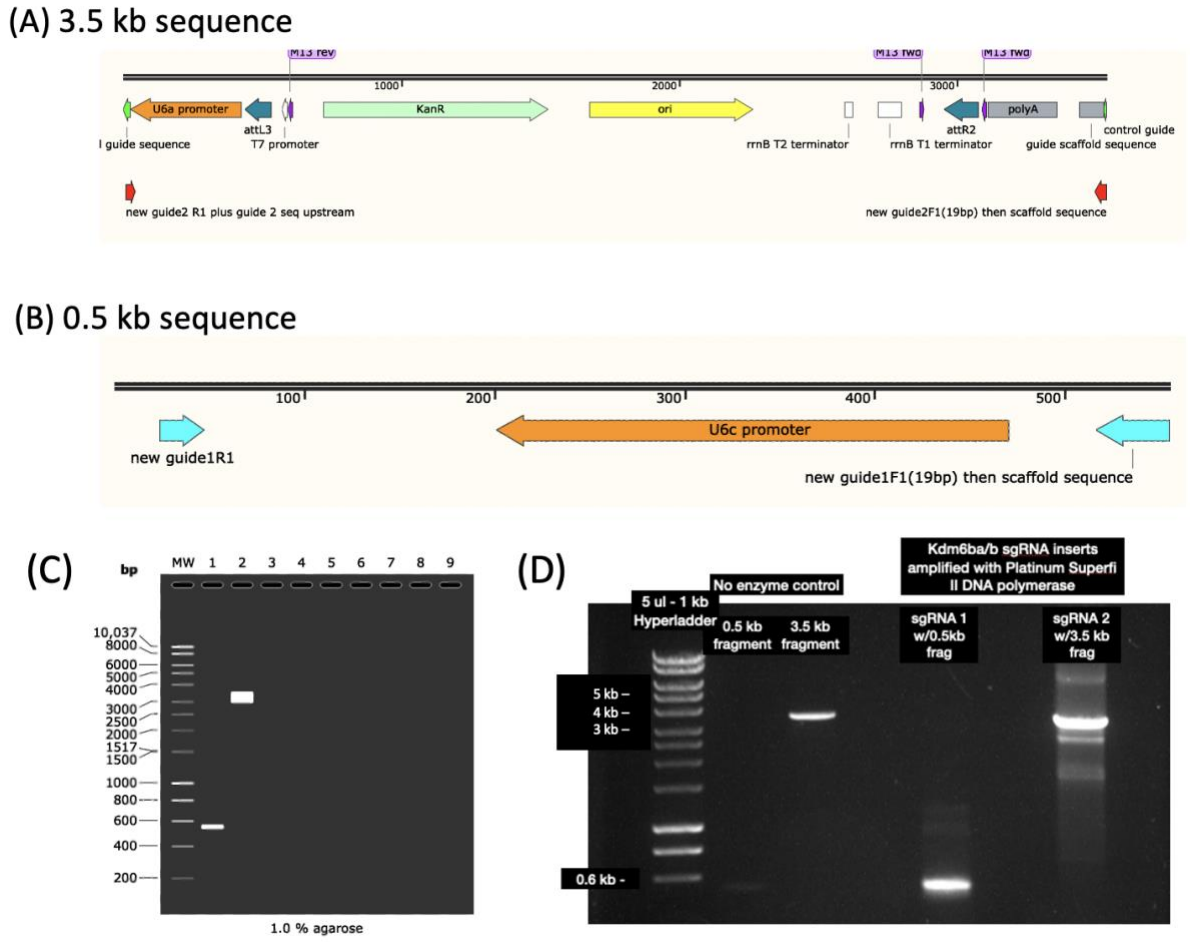

Figure 4.4. Testing DNA polymerase for neutrophil-specific knockdown guide RNA constructs

(A) SnapGene screenshot of the 3.5 kb 3' entry clone sequence showing forward and reverse primers in red (B) SnapGene screenshot of the 0.5 kb 3' entry clone sequence showing forward and reverse primers in cyan. (C) Screenshot of a simulated agarose gel using SnapGene, lane 1 shows the 0.5 kb fragment, lane 2 shows the 3.5 kb fragment, MW lane is Hyperladder 1 kb DNA ladder. (D) 1% Agarose gel showing 3'entry clone fragments amplified for *kdm6b* crRNA addition using Platinum SuperFi II DNA polymerase single technical replicate and a no DNA polymerase control. All gels use the Hyperladder 1 kb DNA ladder with the relevant ladder bands labelled.

4.3.3.b. RT-PCR to insert fragment into 3'Entry Clone

SuperFi II DNA Polymerase was used to insert the *kdm6ba* and *kdm6bb* crRNAs into the two digested fragments of the 3'Entry Clone (Materials and methods 2.3.7.d.i and ii). A 50 µl reaction was used for both RT-PCR reactions and the product digested by DpnI to remove any unwanted template and run on a 1% agarose TAE gel to confirm the presence of the correct fragments in line with those in Figure 4.4, a 0.5 kb fragment, and a 3.5 kb fragment. The 0.5 kb PCR amplification gave a solid, single band, and the 3.5 kb PCR amplification gave a 3.5 kb band (Figure 4.5).

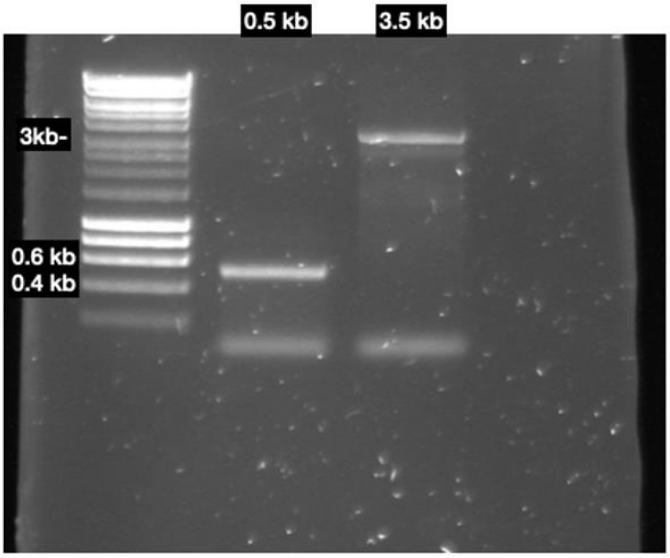

Figure 4.5. Confirmation of correct RT-PCR product following addition of *kdm6b* crRNA to 3'Entry clone

1% agarose TAE gel of the 0.5 kb and 3.5 kb fragments of the 3'Entry Clone following RT-PCR amplification with corresponding crRNA insertion primers and DpnI overnight digest at 37˚C. 5 ul of total 50 ul reaction run with NEB 6X loading buffer. Bioline 1 kb Hyperladder used and relevant ladder bands labelled.

4.3.3.c. Confirmation of correct In-Fusion reaction product.

In-Fusion HD reaction was performed to produce a circular plasmid (Figure 4.6C) made up of the 3.5 kb (Figure 4.6A) and 0.5 kb (Figure 4.6B) plasmids made in Results 4.3.3.b. This reaction product was transformed into Top 10 competent cells. A Midiprep was then used to extract the transformed plasmids. To test the In-Fusion HD reaction produced the required product, PstI and AvaI restriction digests were performed overnight on the extracted plasmids at serial dilutions. PstI produces a single cut to ensure the correct full-sized plasmid, whereas AvaI cuts in several sites to ensure the correct sequence is present (Figure 4.6.D). Due to the size of the plasmid, 4 kb, a single cut to linearise the fragment risks supercoiling of the product and that can be seen in the lanes Rest B, 1:100A and 1:100B of PstI digest product (Figure 4.6E). The AvaI digest does not show supercoiling, lanes Rest B, 1:100A, 1:100B and 1:10A all show the expected 2961, 638 and 383 bp bands, with the 52 bp band too small to resolve on a 1% gel (Figure 4.6F). A more dilute and shorter digest of the plasmid was performed with PstI on the product from the four lanes that showed supercoiling. This gel produced a 4 kb band in all sample lanes apart from the 1:10A (Figure 4.6G). This suggests the correct construct has been made, that construct will be referred to as p3e-U6akdm6bg1-U6c-kdm6bg2 and the Midiprep from the 1:100A lane was used first for LR reactions (Figure 4.7).

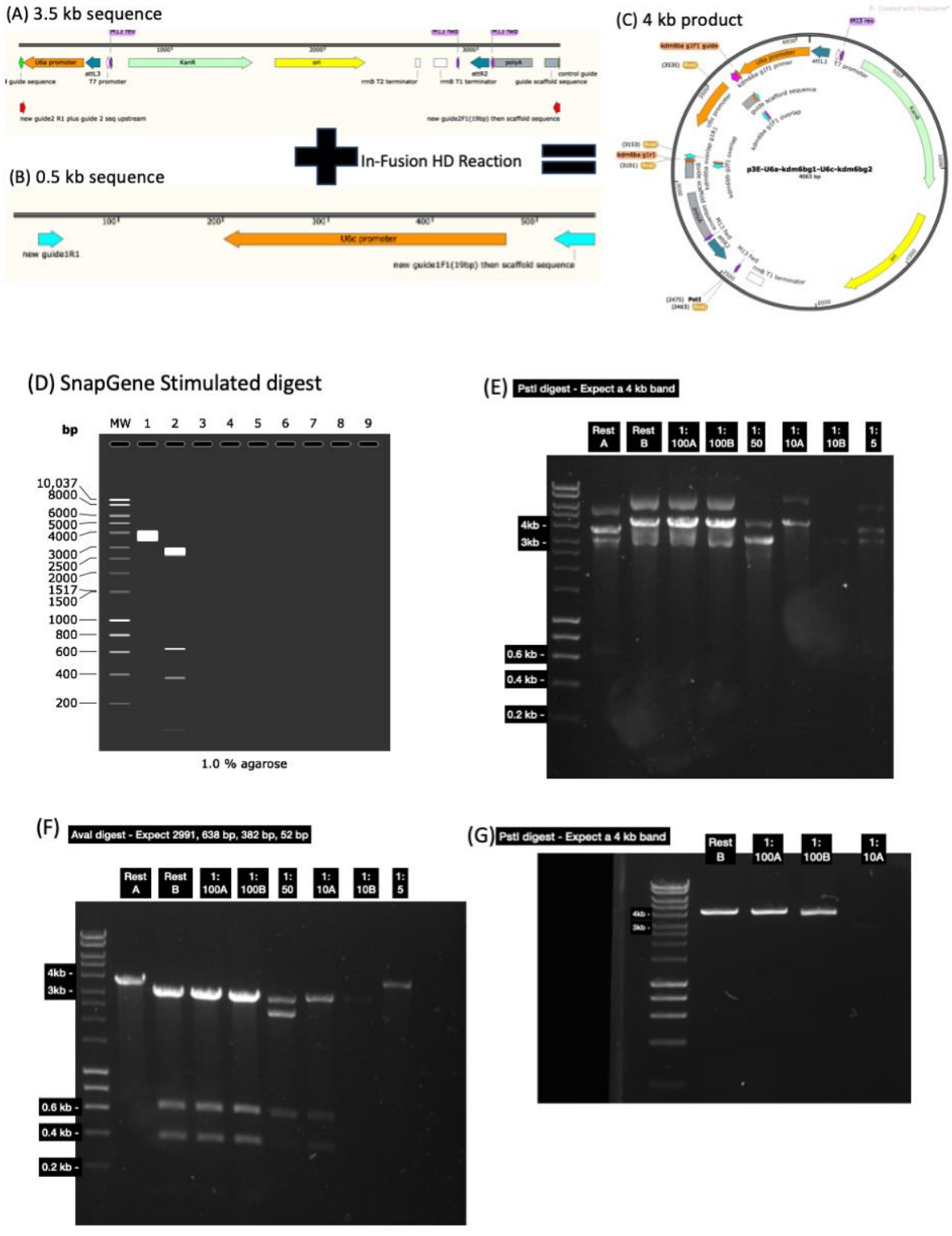

Figure 4.6. Digest of In-Fusion HD reaction product to confirm correct product.

(A) SnapGene screenshot of the 3.5 kb section of the 3' entry clone added to the In-Fusion HD reaction (B) Snapgene screenshot of the 0.5 kb section of the 3' entry clone added to the In-Fusion HD reaction (C) Snapgene screenshot of the expected In-Fusion HD reaction product

with AvaI restriction sites highlighted in gold and PstI restriction enzyme cut sight in bold (D) SnapGene screenshot of a simulate agarose gel of a restriction digest of the 4 kb 3' entry clone with PstI in lane 1 and AvaI in lane 2 with a Hyperladder 1 kb DNA ladder molecular weight ladder (E) Screenshot of Midipreps of overnight colony cultures diluted 1:5 and digested with PstI overnight and run on a 1% agarose TAE gel (dilution of transformed construct inoculated onto agar plate listed above each lane), expected product size shown above (F) Screenshot of Midipreps of overnight colony cultures diluted 1:5 and digested with AvaI overnight and run on a 1% agarose TAE gel (dilution of transformed construct inoculated onto agar plate listed above each lane). (G) Screenshot of Midipreps of overnight colony cultures diluted to 1:50 and digested with PstI for 15 mins and run on a 1% agarose TAE gel (dilution of transformed construct inoculated onto agar plate listed above each lane) All gels use a Hyperline 1 kb DNA ladder with relevant ladder bands labelled.

4.3.3.d. Confirmation of correct LR Clonase Reaction product

To make the full plasmid for microinjection, an attL and attR (LR) Clonase reaction was performed to combine the four major components required for the plasmid to function – using attL and attR sites within the vectors to perform recombination reactions catalysed by the LR Clonase enzyme. To confirm each of the components were present, four digests were performed targeting each of the key sites. These four digests were performed on two samples taken from Midipreps of the plasmid from transformed Top 10 competent cells (Figure 4.7). Midiprep 1 is shown in the first four lanes, lane 1 is the BamHI digest with the correct three bands, lane 2 shows the PflMI + StuI digest and shows perhaps a partial digestion with the 12,023 bp band but no 1080 bp band potentially due to issues with buffer compatibility. Lane 3 shows full digestion with StuI and NcoI with two bands at 12,358 bp and 1080 bp and lane 4 shows a digestion with BamHI, PflMI, StuI and NcoI giving all six correct bands. Sample 2 showed correct bands in lane 1 and lane 4 but some no specific bands in lane 2 and 4. For further work, sample 1 will be used as the full construct, pDest-Lyz-EGFP-U6akdm6bg1-U6c-kdm6bg2-Tol2-pA2 (Figure 4.8).

(A)

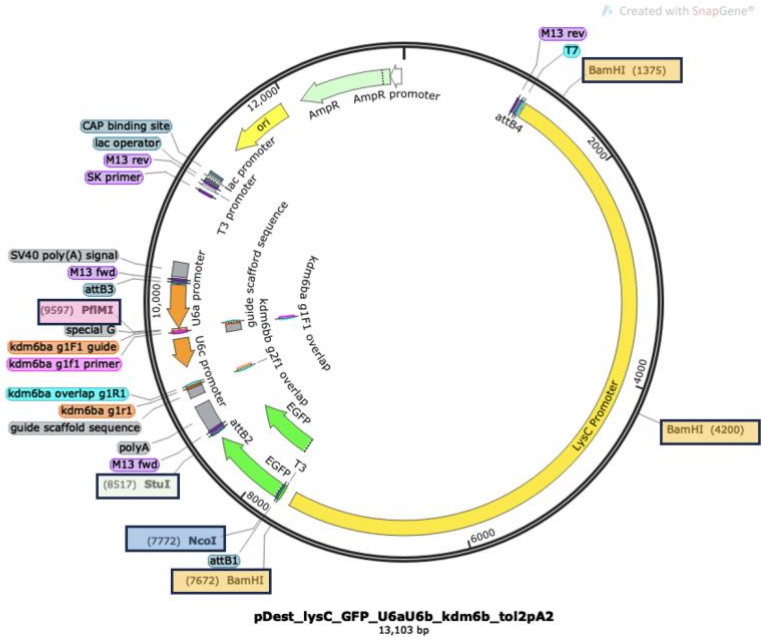

(B)

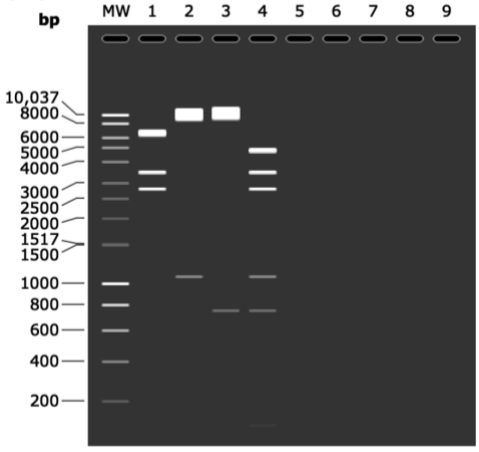

1.0 % agarose

MW: HyperLadder™ 1 kb

1: pDest_lysC_GFP_U6aU6b_kdm6b_tol2pA2 BamHI
   1. 6806 bp
   2. 3472 bp
   3. 2825 bp

2: pDest_lysC_GFP_U6aU6b_kdm6b_tol2pA2 PflMI + StuI
   1. 12,023 bp
   2. 1080 bp

3: pDest_lysC_GFP_U6aU6b_kdm6b_tol2pA2 StuI + NcoI
   1. 12,358 bp
   2. 745 bp

4: pDest_lysC_GFP_U6aU6b_kdm6b_tol2pA2 BamHI + StuI + NcoI + PflMI
   1. 4881 bp
   2. 3472 bp
   3. 2825 bp
   4. 1080 bp
   5. 745 bp
   6. 100 bp

(C)

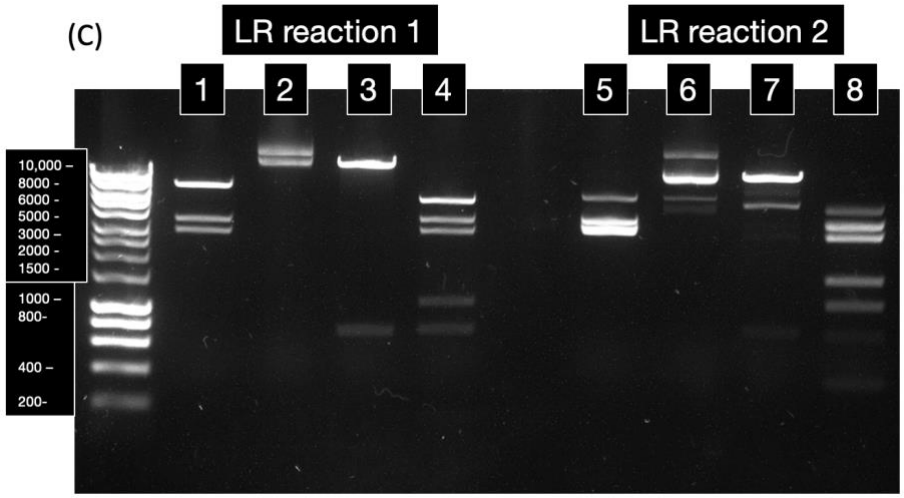

Figure 4.7. Confirmation of the correct LR reaction product by diagnostic digests

(A) Snapgene generated screenshot of the full pDest-LyzC-EGFP-U6akdm6bg1-U6c-kdm6bg2-Tol2-pA2 plasmid with notable features annotated. Restriction digest sites highlighted for testing of correct product, BamHI gold box with black outline, PflMI orange box with black outline, StuI green box with black outline, NcoI blue box with black outline (B) SnapGene simulation of restriction digests to test if the correct plasmid had been produced by the LR Clonase reaction, lane contents and band sizes listed on the righthand side (C) 1% agarose TAE gel of two Midipreps of overnight cultures from agar plates inoculated with transformed Top 10 competent cells digested to confirm the presence of the pDest-Lyz-EGFP-U6akdm6bg1-U6c-kdm6bg2-Tol2-pA2 construct. Lanes 1 and 5 are BamHI digest with expected bands at 6806, 3472 and 2825 bp, Lanes 2 and 6 are PflMI + StuI digest with expected bands of 12,023 and 1080 bp, lanes 3 and 7 are StuI + NcoI digestion with expected bands of 12,358 and 745 bp, and lanes 4 and 8 are BamHI, PflMI, StuI + NcoI digest with expected bands of 4881, 3472, 2825, 1080, 745 and 100 bp. Ladder is a Hyperline 1 kb ladder with relevant ladder bands labelled.

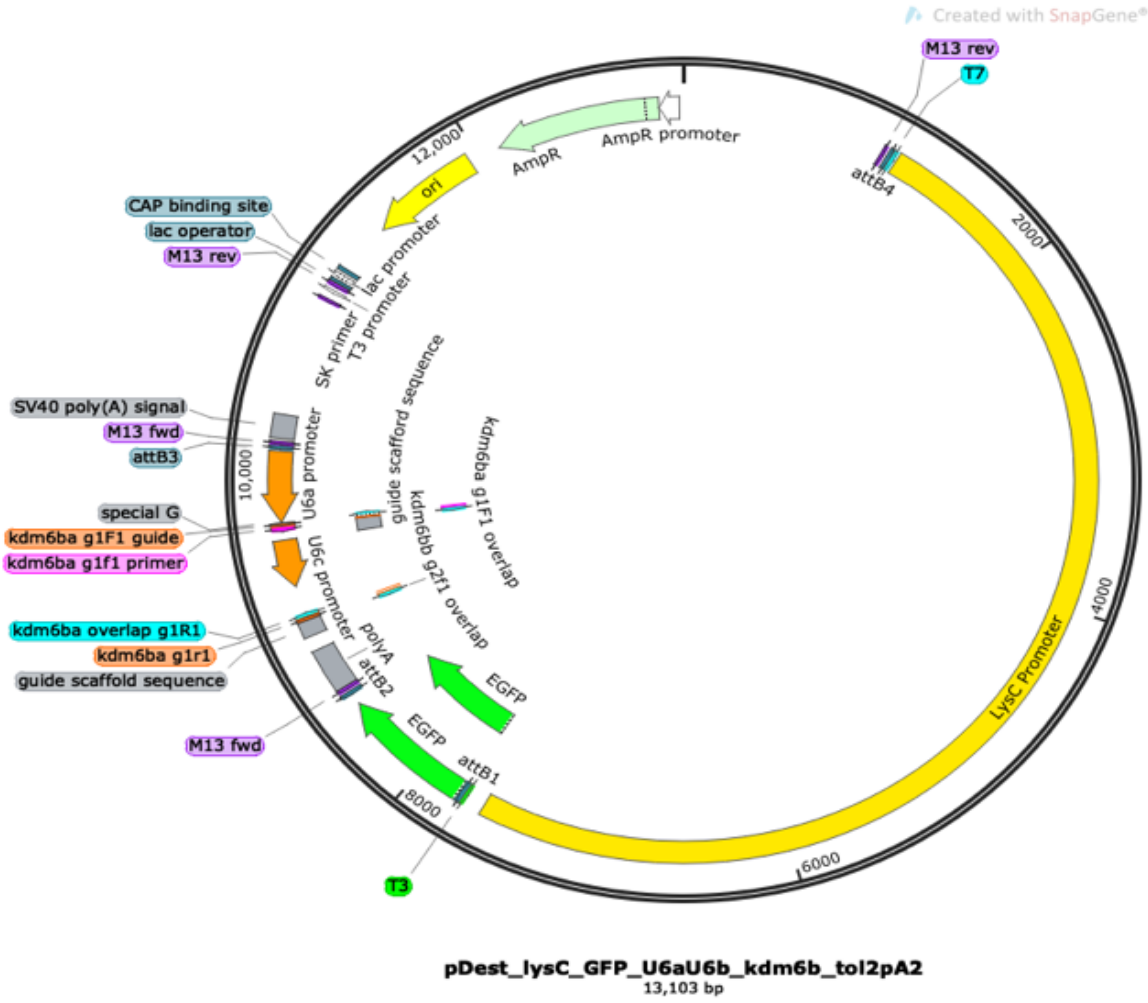

Figure 4.8. Plasmid of the *kdm6ba/b* guide RNA construct

Snapgene generated screenshot of the full pDest-LyzC-EGFP-U6akdm6bg1-U6c-kdm6bg2-Tol2-pA2 plasmid with notable features annotated.

4.3.3.e. Injection of pDest-Lyz-EGFP-U6akdm6bg1-U6c-kdm6bg2-Tol2-pA2 into *Tg(lyz:nfsβ-mCherry)sh260* embryos

To observe the percentage of neutrophils that take up the kdm6b crRNA construct, the construct was injected into single-cell stage embryos from an in-cross of the *Tg(lyz:nfsβ-mCherry)sh260* line. This line gives red neutrophils by the mCherry protein expression driven by the *lyz* promoter. The colocalisation of the red signal from the reporter line and the lyz-EGFP component of the construct can be used to quantify successful insertion of the construct into neutrophils. Tailfin injury was performed 3 dpf and the tailfin imaged using a Nikon wide-field fluorescent microscope. Images show that the number of $GFP^+mCherry^+$ neutrophils are relatively low (Figure 4.9A). In the representative image, there are 21 GFP^+ cells and 44 $mCherry^+$ cells, 19 cells are $GFP^+mCherry^+$ which is 43.2% of neutrophils (Figure 4.9B and C). This suggests that insertion into neutrophils is about 50% and for any experiments in the *Tg(Lyz:ntr-cas9)* line, this expression rate following transient injection of guides will have to be considered.

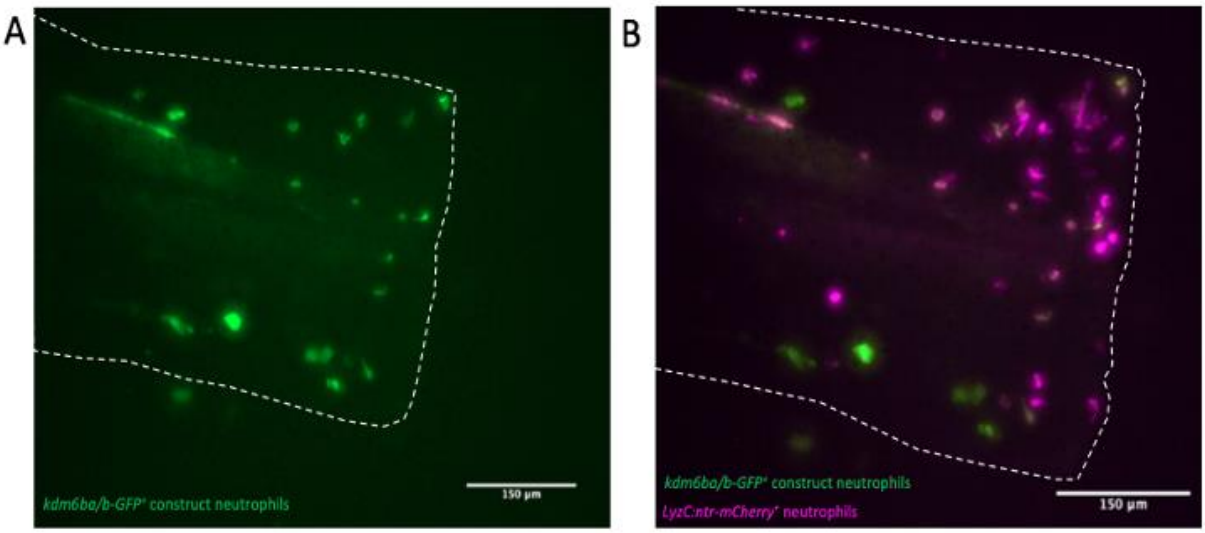

C

		Percentage of total neutrophils
Kdm6b sgRNA cells - GFP$^+$	22	n/a
Total neutrophils- mCherry+	44	n/a
Kdm6b sgRNA cells neutrophils - GFP$^+$mCherry$^+$	19	43.2%

Figure 4.9. Injection of *kdm6b* crRNA construct to *Tg(lyz:nfsβ-mCherry)sh260* zebrafish embryos produce GFP+ neutrophils.

(A) GFP (green) Fluorescent image of *Tg(lyz:nfsβ-mCherry)sh260* 3 dpf zebrafish larvae injured tailfin. Embryos injected with pDest-lyz-EGFP-U6akdm6bg1-U6c-kdm6bg2-Tol2-pA2 at the single-cell stage. Tailfin highlighted with white box. (B) GFP (green) and mCherry (magenta) fluorescent image of *Tg(lyz:nfsβ-mCherry)sh260* 3 dpf zebrafish larvae injured tailfin. Embryos injected with pDest-lyz-EGFP-U6akdm6bg1-U6c-kdm6bg2-Tol2-pA2 at the single-cell stage. Tailfin highlighted with white box. Both images taken used a Nikon wide-field fluorescent microscope at 20x magnification, 150 µm scale bars shown in bottom right. (C) Table showing number of GFP$^+$, mCherry$^+$ and GFP$^+$mCherry$^+$ cells at the highlighted wound site in the images. Percentage of double positive cells calculated by 100(double positive/mCherry+).

4.3.4. RT-PCR and qRT-PCR does not clearly show *kdm6b* transcript knockdown by 5'UTR guides.

In tandem with making the neutrophil-specific constructs, cDNA generated from larvae micro-injected with *kdm6ba/b* 5'UTR targeting guides was used to analyse gene expression post-knockdown. This was to test if the guides were suitable for neutrophil-specific knockdown as it would confirm whether mutations shown in Figure 4.3 generated loss of gene function as guides that target the 5'UTR of genes do not cause direct mutations in the coding sequence but cause changes in expression due to indirect changes to the open reading frame moving the ATG out of frame (Figure 4.10A). PCR was performed amplifying the coding sequence of *kdm6ba* and *kdm6bb* using *ef1a* as a house keeping gene and *hif1a*, a downstream target of KDM6B involved in neutrophilic inflammation (Shait Mohammed *et al.*, 2022). Injected/uninjected and injured/uninjured samples were compared to observe expression in all test scenarios, as *kdm6b* expression at baseline and in a homeostatic response to injury was unclear. Compared to the uninjected/uninjured controls and the tyrosinase injected/injured controls RT-PCR showed a decrease in *kdm6ba*, *kdm6bb* and *hif1a* expression based on the brightness of bands on a 2% Agarose gel (Figure 4.10B). qRT-PCR was then performed for more accuracy, adding injected/uninjured larvae cDNA to the panel. ΔCt values (Ct values normalised to the housekeeping gene Ct, with higher ΔCt meaning a lower concentration of amplified DNA) for *kdm6ba* and *hif1a* increased in the *kdm6ba/b* injected/uninjured and *kdm6ba/b* injected/injured samples relative to the controls, indicating less transcript present, however the ΔCt for *kdm6bb* was decreased in the *kdm6ba/b* injected/uninjured cDNA relative to uninjured controls and only showed small increases in ΔCt following injury relative to both the injured and uninjured controls (Figure 4.10C). ΔΔCt then compared relative expression of the target genes compared to the uninjected/uninjured control (higher ΔΔCt values mean lower expression). ΔΔCt for *kdm6ba* and *hif1a* were increased in both the *kdm6ba/b* treated groups, though increases following injury were not as high. *kdm6bb* was decreased following injection alone, but slightly increased following injury. Translating these findings to $2^{-\Delta\Delta Ct}$ to look at relative expression changes in the *kdm6ba/b* crRNA injected groups, *kdm6ba* expression was 0.14-fold lower in non-injured larvae and 0.63-fold lower in injured larvae relative to uninjured and uninjected, *kdm6bb* was 1.79-fold higher in uninjured and 0.78-fold lower in injured larvae relative to uninjured and uninjected and *hif1a* was 0.47-fold lower in uninjured and 0.97-fold lower in injured larvae

relative to uninjured and uninjected larvae (Figure 4.10D). Taken together these suggest that *kdm6ba* expression is partially knocked down by the guide but *kdm6bb* expression is not knocked down in the uninjured group and only partially knocked down in the injured group. Changes in *hif1a* expression does suggest some potential effects of kdm6b on downstream pathways though. Targeting the coding sequence rather than the 5'UTR may help deal with some of this ambiguity.

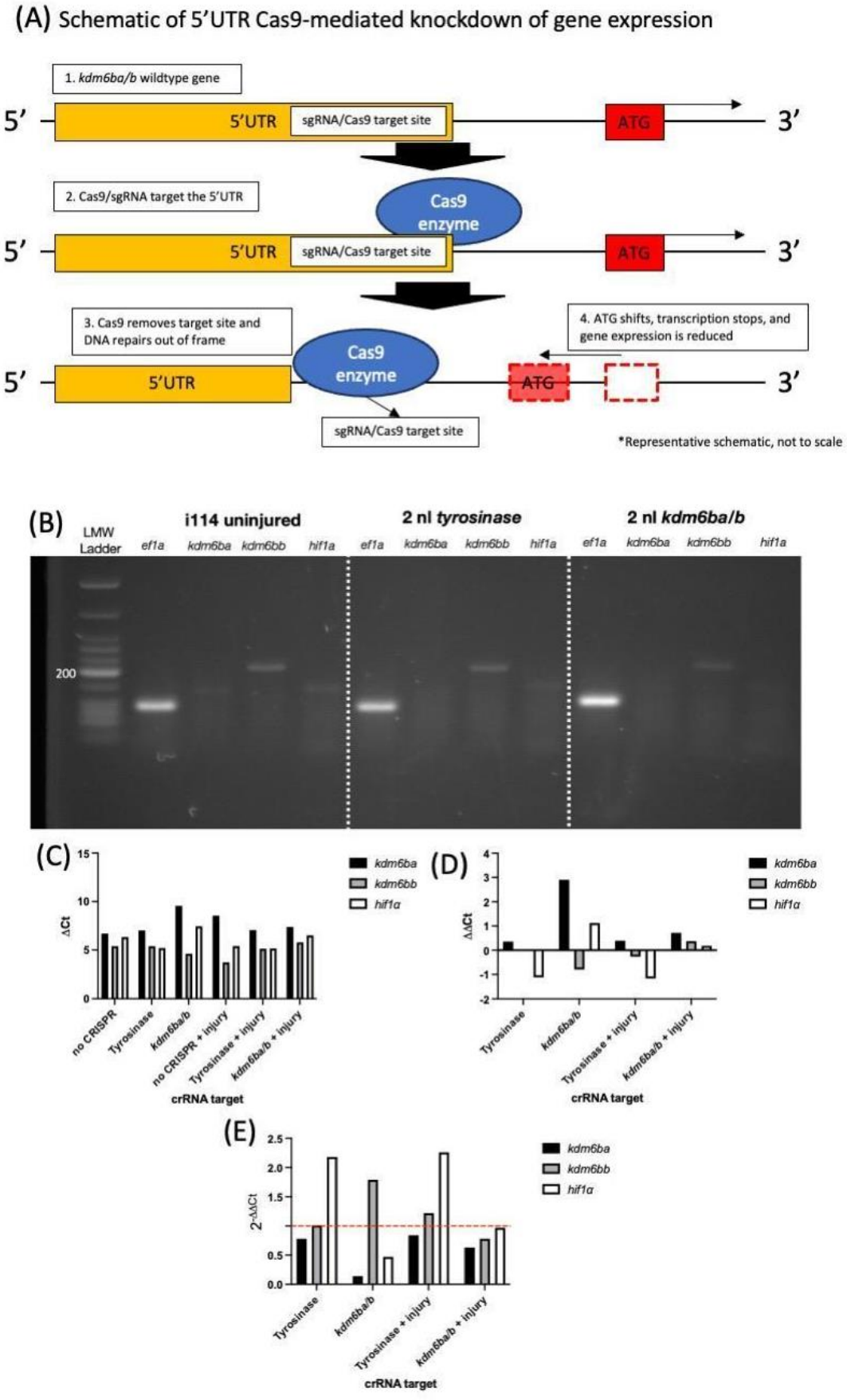
(A) Schematic of 5'UTR Cas9-mediated knockdown of gene expression
1. kdm6ba/b wildtype gene
5'
5'UTR
sgRNA/Cas9 target site
ATG
3'
2. Cas9/sgRNA target the 5'UTR
Cas9 enzyme
3. Cas9 removes target site and DNA repairs out of frame
4. ATG shifts, transcription stops, and gene expression is reduced
*Representative schematic, not to scale
(B)
LMW Ladder
i114 uninjured
2 nl tyrosinase
2 nl kdm6ba/b
ef1a
kdm6ba
kdm6bb
hif1a
200
(C)
ΔCt
kdm6ba
kdm6bb
hif1a
no CRISPR
Tyrosinase
kdm6ba/b
no CRISPR + injury
Tyrosinase + injury
kdm6ba/b + injury
crRNA target
(D)
ΔΔCt
(E)
2-ΔΔCt

Figure 4.10. PCR for *kdm6ba/b* expression following CRISPR/Cas9 targeting the 5'UTR

(A) Representative schematic of a 5'UTR targeting sgRNA/Cas9 system and why qRT-PCR is required to confirm gene expression changes post-injection of the guide as deletion does not directly alter transcription, but indirectly by altering the open reading frame. (B) 2% Agarose gel of cDNA *TgBAC(mpx:EGFP)i114s* in three treatment groups, uninjured and uninjected, injured and injected with 2 nl crRNA mix targeting tyrosinase and injured injected with 2 nl crRNA mix targeting the 5'UTR of *kdm6ba* and *kdm6bb. ef1a* was used as a housekeeping gene, *kdm6ba* and *kdm6bb* to look at the effect of the knockdown on gene expression and *hif1a* – a downstream target of *kdm6b*. NEB low molecular weight Quick-load ladder was used. (C) ΔCt values (target Ct – housekeeping Ct) for qRT-PCR to look at *kdm6b* and *hif1a* expression changes following targeted knockdown of *kdm6ba/b* or the tyrosinase control compared to uninjected controls. Injured and uninjured fish were compared. (D) ΔΔCt (Target ΔCt – no CRISPR/no injury Control ΔCt) showing gene expression change in target genes (E) $2^{-\Delta\Delta Ct}$ relative expression change of target genes.

4.3.5. Design and optimisation of crRNAs targeting the coding sequence of *kdm6ba* and *kdm6bb*.

New guides were designed targeting the coding sequences of prioritised chromatin remodelling enzymes following the ambiguity of qRT-PCR results for 5'UTR knockdown of *kdm6ba/b* (Results 4.4). *kdm6ba* and *b* were the first genes selected. Guides were designed using the IDT Custom Alt-R CRISPR/Cas9 guide design tool (https://eu.idtdna.com/site/order/designtool/index/CRISPR_SEQUENCE) with the aim of being as close to the translational start site as possible using gene sequences from ENSEMBL. Two guides were designed per paralog to microinject all four guides in combination for experiments. The number of base pairs between target sites was ensured not to be multiples of 3 to ensure deletions did not maintain the open reading frame required to produce a functioning protein. Primer pairs for diagnostic digest were designed so that the same pair of primers could be used for testing both guides in a single paralog and single cut site restriction enzymes were selected within the target sites (Appendix Figure 4.4A and B). Primers were tested using a gradient RT-PCR (Appendix Figure 4.4C and D). Microinjection of the single guides was then used to confirm knockdown for each guide. 2 nl were injected per embryo

into the *TgBAC(mpx:EGFP)i114* line and diagnostic digest of 3 dpf larvae gDNA performed (following the process in Figure 4.3.A). The crRNA targeting exon 5 of *kdm6ba* showed partial digestion of 7/8 larvae, suggesting a robust knockdown, with the eighth larvae showing full digestion to confirm the reaction was allowed to run to completion (Figure 4.11A). The guide targeting *kdm6ba* exon 6 also showed 7/8 larvae with partial digestion and one larva with full digestion, again suggesting good levels of knockdown (Figure 4.11B). Guides for *kdm6bb* targeted two parts of the same exon, exon 3. The guide targeting the 5' end of the exon, guide 3.1, showed partial digestion with the correct 697 and 183 bp bands across all 8 larvae (Figure 4.11C). The guide targeting the 3' end of the exon, guide exon 3.2, showed partial digestion with expected 637 and 243 bp bands in 7/8 larvae and full digestion in larva 2 (Figure 4.11D). While both *kdm6bb* guides gave the correct digested bands to suggest a robust knockdown, both diagnostic digests also produced several non-specific bands below the full 880 bp fragment. This is potentially due to the size of the amplified fragment being very large for the type of gDNA extraction performed, causing smaller fragments to be extracted and partially amplified in the PCR reaction. A cleaner gDNA preparation method may have reduced this. The four guides were then injected in a 2 nl combination mix of equal concentration into *TgBAC(mpx:EGFP)i114* single cell embryos and gDNA extracted 3 dpf for diagnostic digestion. For *kdm6ba* exon 5 crRNA, partial digestion with a bright undigested band was seen in 6/8 larvae, with the remaining two larvae showing partial digestion and the undigested control showing the correct 586 bp band (Figure 4.11E). *kdm6ba* exon 6 crRNA showed partial digestion in 7/8 guides and again the correct band in the undigested control (Figure 4.11F). *kdm6bb* exon 3.1 crRNA showed partial digestion in 5/8 larvae, no digestion in 2/8 and full digestion in 1/8 larvae showing a successful knockdown across 7/8 larvae and an 880 bp undigested control (Figure 4.11G). *kdm6bb* exon 3.2 crRNA gave partial digestion in 7/8 larvae and full digestion in the remaining larvae, again showing a good knockdown (Figure 4.11H). Amplification of the *kdm6bb* coding sequence fragment also removed the non-specific bands seen in Figure 4.11C and D. When combined, all 4 guides show good levels of knockdown in most larvae which gives a high probability of functional knockdown of both paralogs of *kdm6b,* suggesting diagnostic digestion is not required for post-injury genotyping. Larva 5 in all four PCRs showed complete digestion, perhaps suggesting this embryo was not injected effectively with the Cas9/crRNA mix but showing the restriction digest was given enough time

to run to completion in the absence of a digested control. This combination of guides was used for further *kdm6b* knockdown experiments.

(A)

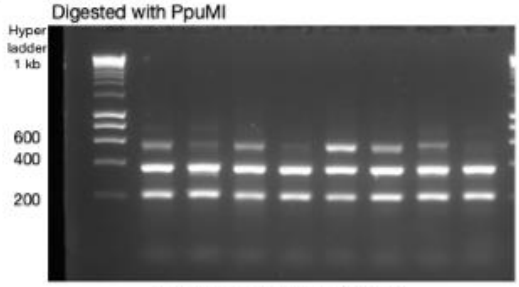

586 band = Successful knockdown
205 band and 381 band = Unsuccessful knockdown

(B)

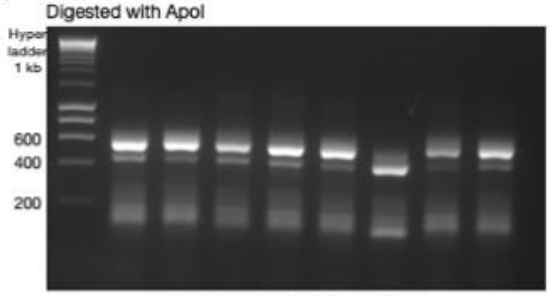

586 band = Successful knockdown
129 band and 457 band = Unsuccessful knockdown

(C)

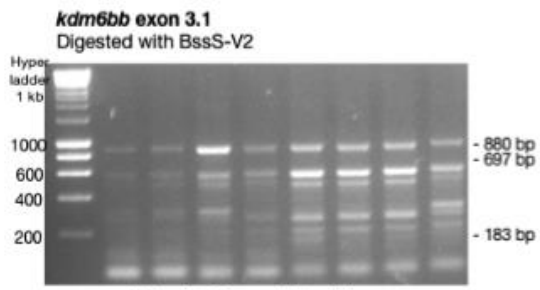

880 band = Successful knockdown
697 band and 183 band = Unsuccessful knockdown

(D)

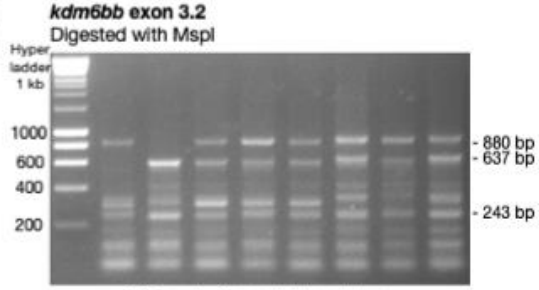

880 band = Successful knockdown
637 band and 243 band = Unsuccessful knockdown

(E)

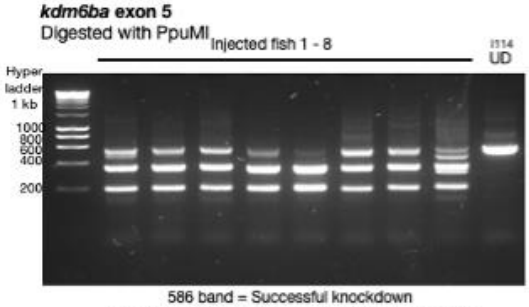

586 band = Successful knockdown
205 band and 381 band = Unsuccessful knockdown

(F)

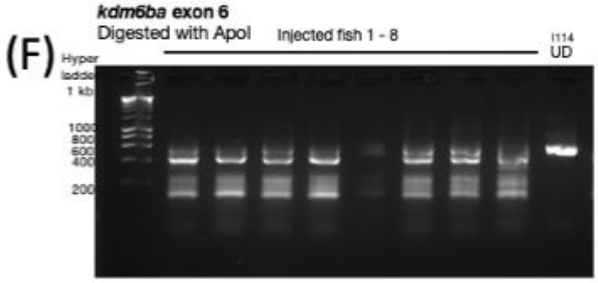

586 band = Successful knockdown
129 band and 457 band = Unsuccessful knockdown

(G)

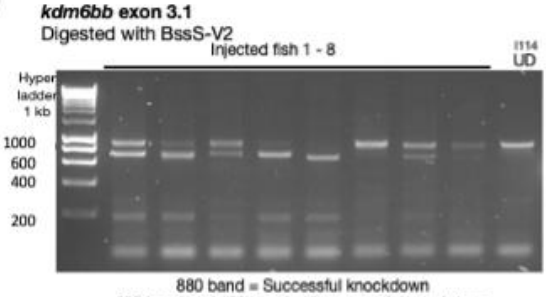

880 band = Successful knockdown
697 band and 183 band = Unsuccessful knockdown

(H)

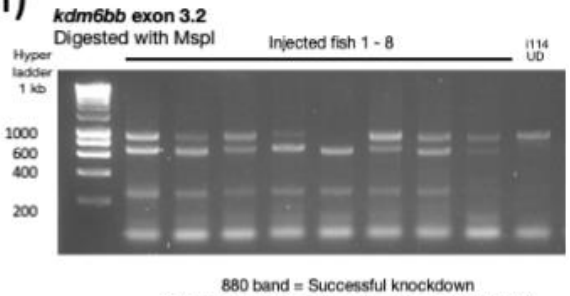

880 band = Successful knockdown
637 band and 243 band = Unsuccessful knockdown

Figure 4.11. Optimisation of injection of crRNAs for *kdm6ba* and *kdm6bb* coding sequences
(A-D) 2% Agarose + TAE gels showing diagnostic digest RT-PCR product from 8 injected zebrafish larvae gDNA. Larvae were injected with one of four crRNAs for *kdm6ba* or *kdm6bb* (Target gene, crRNA and restriction enzyme listed above gel). All gels were run with a Hyperline 1 kb ladder with the relevant ladder bands indicated. Required fragments for successful or unsuccessful digest listed below. (E-H) 2% Agarose gels showing diagnostic digest RT-PCR product from 8 injected zebrafish larvae gDNA. Larvae were injected with all four crRNAs targeting *kdm6ba* and *kdm6bb* (Target gene, crRNA and restriction enzyme listed above gel). All gels are run with a Hyperladder 1 kb ladder with the relevant ladder bands highlighted. Required fragments for successful or unsuccessful digestion listed below.

4.3.6. Whole-body knockdown of *kdm6ba* and *kdm6bb* using coding sequence targeting CRISPR/Cas9 results in decreased neutrophil inflammation resolution following tailfin injury

The crRNAs targeting the coding sequences of *kdm6ba* and *kdm6bb* were microinjected into the single cell stage of *TgBAC(mpx:EGFP)i114* zebrafish embryos to assess the effect of knockdown on neutrophil activity at a tailfin wound. Larvae were injured posterior to the caudal vein at 3 dpf and neutrophils counted under a fluorescent Leica microscope at 3, 6 and 24 hpi. A tyrosinase control was also used and counted – tyrosinase is involved in pigmentation of the larvae, and so tyrosinase knockdown produces unpigmented larvae, allowing for confirmation that the Cas9 enzyme is performing a knockdown. Larvae injected with *kdm6ba* and *kdm6bb* guides showed no significant changes in neutrophil recruitment at 3 and 6 hours (Figure 4.12B) and this was also reflected in the percentage change between 3 and 6 hpi relative to the tyrosinase knockdown control (Figure 4.12C). At 24 hpi, inflammation resolution is significantly decreased in the *kdm6ba/b* injected larvae (P=0.009) with the number of neutrophils at the wound averaging 20.8 compared to 16.6 in the tyrosinase knockdown control (Figure 4.12C). Percentage change in neutrophils between 6 and 24 hpi did not significantly change (Figure 4.12C) however, suggesting the effect may be due to overall increases in neutrophil number, rather than continued increase in recruitment at the later time points.

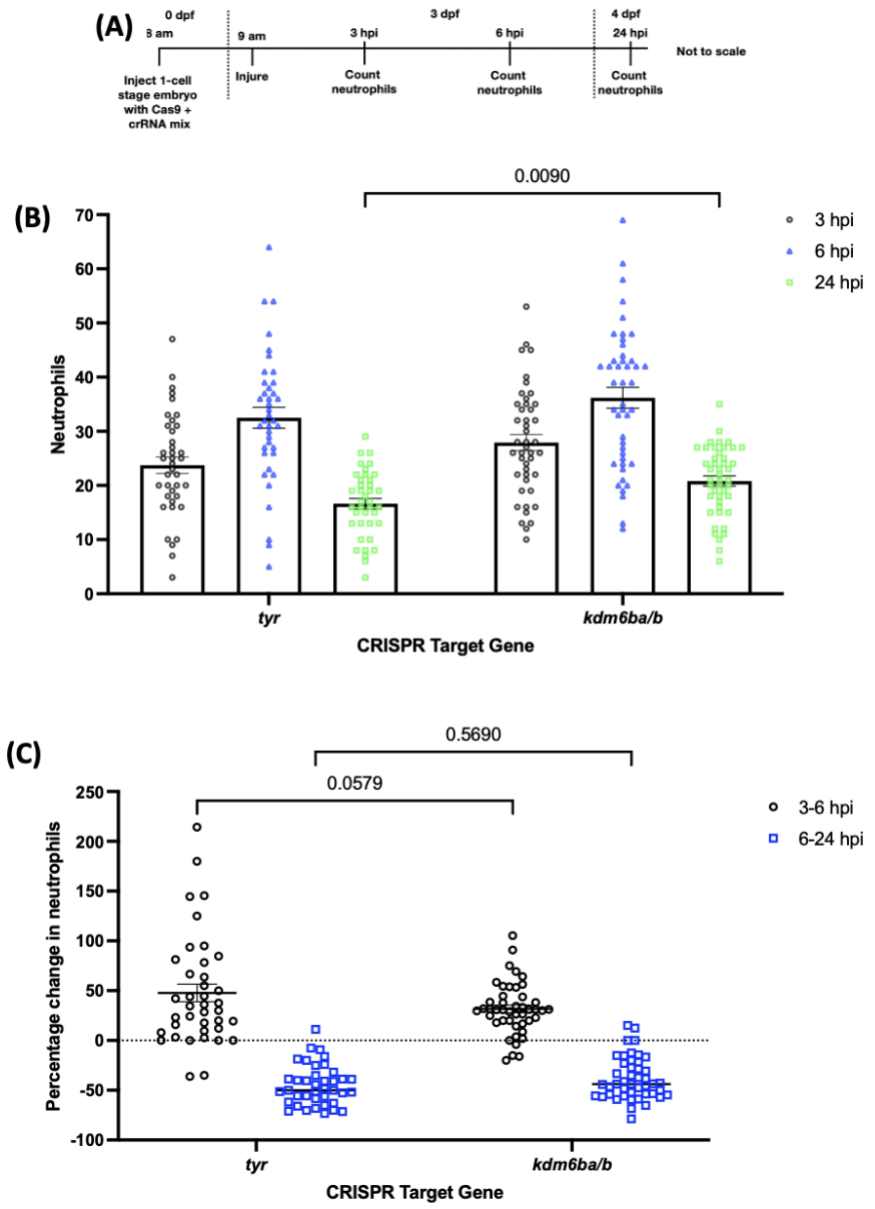

Figure 4.12. Whole-body knockdown of *kdm6ba* and *kdm6bb* targeting the coding sequence with CRISPR/Cas9 results in a significant reduction in inflammation resolution

(A) Time course for the experiment (B) Number of neutrophils recruited to the wound site posterior to the caudal vein in *TgBAC(mpx:EGFP)i114* 3 dpf zebrafish larvae injected with crRNAs targeting *tyr* as a control or *kdm6ba* and *kdm6bb* counted using a fluorescent microscope 3, 6 and 24 hpi (4 independent repeats, minimum 39 fish per group, mean ±SEM. Two-way ANOVA with Šídák's multiple comparisons test, significance $P \leq 0.05$). (B) Percentage change in the number of neutrophils at the wound site between 3 and 6 hpi and 6 and 24 hpi based on counts in panel A. (4 independent repeats, minimum 39 fish per group, mean ±SEM. Two-way ANOVA Šídák's multiple comparisons test)

4.3.7. Whole-body CRISPR/Cas9 knockdown targeting the coding sequence of *kdm6ba/b* causes a 1.58-fold increase in *hif1a* expression

HIF1α has been described as a gene involved in the KDM6B pathway, however the mechanism of action is unclear (Shait Mohammed *et al.*, 2022). To analyse the effect of *kdm6b* knockdown on *hif1a* expression, RNA was extracted from *TgBAC(mpx:EGFP)i114* larval zebrafish injected with *kdm6ba/b* coding sequence targeting crRNAs for Cas9 mediated knockdown. Larvae were injured 3 dpf and RNA extracted from 20 pooled embryos per group with TRIzol, at 3 hpi. qRT-PCR was performed to see whether whole-body expression of *hif1a* was altered in *kdm6b* knockdown following injury. Tyrosinase was used as the crRNA control and *ef1a* used as a housekeeping gene during qRT-PCR. Over 5 independent repeats, *hif1a* expression in *kdm6b* knockdown larvae showed no significant difference in raw expression – measured using ΔCt – compared to *tyr* knockdown (Figure 4.13A and B) but did show a relative expression change of a 1.58-fold increase in expression when compared to *hif1a* expression in the *tyr* knockdown group (Figure 4.13C). These data support a link between *kdm6b* and *hif1a* however the drivers of this change may be further revealed following RNAseq within knockdown neutrophils. An uninjured control was not used in this experiment, but further information about expression could be gained by further tests using one.

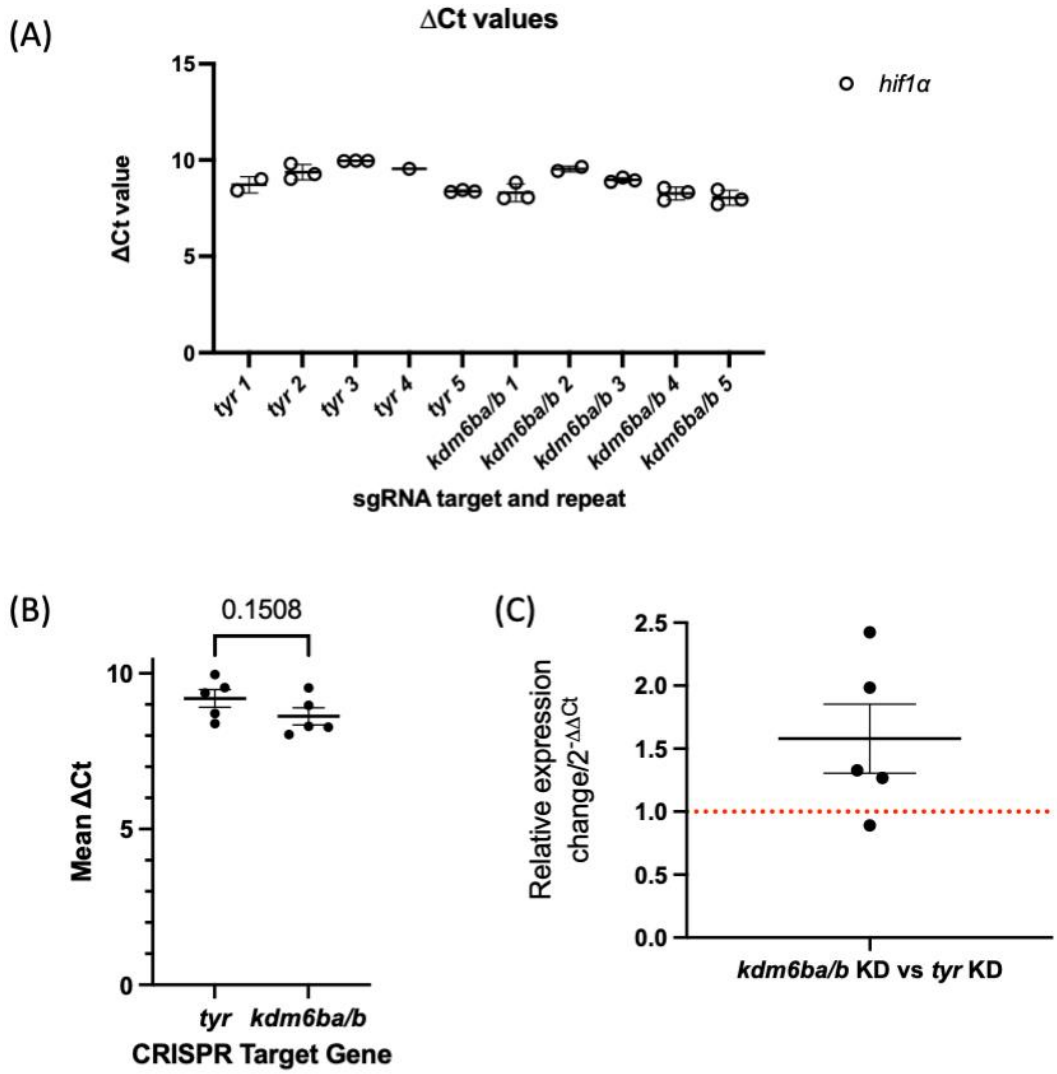

Figure 4.13. Whole-body knockdown of *kdm6ba/b* by CRISPR/Cas9 targeting the coding sequences causes a 1.58-fold increase in *hif1a* expression following tailfin injury

(A) ΔCt value for *hif1a* calculated by Ct(target) – Ct(Housekeeping) in each biological repeat from injured *tyr* injected and *kdm6b* crRNA injected larvae, 3 technical repeats per biological repeat, technical repeats removed if standard deviation >0.5. (Mean ±SEM) (B) Mean *hif1a* ΔCt value for *tyr* and *kdm6b* injected larvae (5 independent repeats, mean taken from technical repeats and plotted for each independent repeat, mean ±SEM, Mann-Whitney Test) (C) Relative expression change in *hif1a* between *kdm6ba*/b and *tyr* injected larvae calculated a $2^{-\Delta\Delta Ct}$, red line shows baseline of 1 = no expression change. (5 independent repeats, Mean ±SEM)

4.3.8. Design and optimisation of crRNAs targeting the coding sequence of *dot1l* and *ezh2*

Published work shows that *dot1l* knockdown is embryonic lethal when used for whole-body knockdown (Kara *et al.*, 2019). However, I designed a *dot1l* coding sequence guide to attempt to find a non-lethal Cas9 dose to optimise a guide for future neutrophil-specific knockdown in combination with the 5'UTR guide described in Results 4.3.2. The guide was designed using the IDT design tool as described in Results 4.3.7 (Figure 4.14A). Testing of the *dot1l* primers indicated that 56˚C was the optimum temperature (Figure 4.14C). However, microinjection of the *dot1l* guide in *TgBAC(mpx:EGFP)i114* embryos showed high levels of larval death at 4 hpf and RT-PCR of gDNA from surviving larvae showed full digestion of gDNA taken from suggesting any surviving larvae did not have successful knockdown (following the process in Figure 4.3.A) (Figure 4.14E). Previous work has shown whole-body dot1l knockdown to be lethal at the same time point (personal communication, Kara *et al.*, 2019). A guide targeting the *ezh2* coding sequence was designed using the IDT design tool and confirmed to match the coding sequence used ENSEMBL and SnapGene (Figure 4.14B). Optimisation of the primers by gradient RT-PCR showed the primer was most effective at 62˚C giving a single 219 bp band but lower temperatures produced non-specific bands (Figure 4.14D). Diagnostic digestion was performed with SacI and showed complete digestion (following the process in Figure 4.3.A) (Figure 4.14F). This confirmed the primers and restriction enzyme selection for *ezh2* were suitable for Cas9 injection.

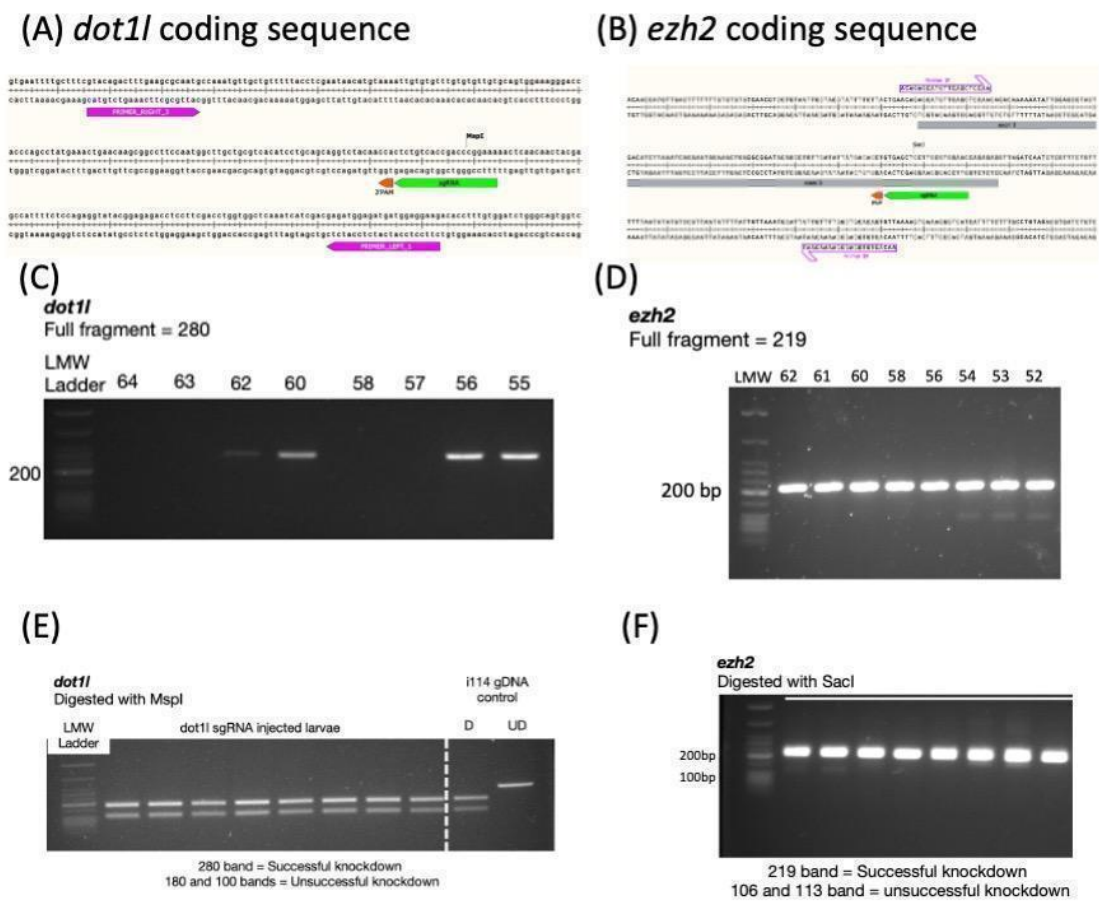

Figure 4.14. *dot1l* and *ezh2* coding sequence targeting crRNAs and primer optimisation.

(A) Sequence from the coding sequence of *dot1l* showing the crRNA target sites (green) and primers (purple) and restriction enzyme cut sites (label above crRNA target) used for diagnostic digest of knockdown (B) Sequence from the coding sequence of *ezh2* showing the crRNA target sites (green) and primers (purple) and restriction enzyme cut site (label above crRNA target) used for diagnostic digest of knockdown (C) Screenshot of a 2% Agarose gel showing samples from a temperature gradient (temperatures shown above lanes) RT-PCR to test the efficiency of the *dot1l* primers, 280 bp band required (D) Screenshot of a 2% Agarose gel showing samples from a temperature gradient (temperatures shown above lanes) RT-PCR to test the efficiency of the *ezh2* primers, 219 bp band required. (E) Screenshot of a 2% Agarose gel showing diagnostic digest RT-PCR product from 8 injected zebrafish larvae gDNA. Larvae were injected with crRNA for *dot1l* coding sequence (Target gene and restriction enzyme listed above gel). *TgBAC(mpx:EGFP)i114* uninjected gDNA used for digested and undigested control (F) 2% Agarose gels showing diagnostic digest RT-PCR product from 8 injected zebrafish larvae gDNA. Larvae were injected with crRNA for *ezh2* coding sequence

(Target gene restriction enzyme listed above gel). All gels are run with a NEB Quick-load low molecular weight DNA ladder with the relevant ladder bands highlighted. Required fragments for successful or unsuccessful digestion listed below the gel. *TgBAC(mpx:EGFP)i114* uninjected gDNA used for digested and undigested control.

4.3.9. Whole-body knockdown of *ezh2* leads to increased neutrophil recruitment 6 hpi and decreased neutrophil inflammation resolution 24 hpi.

The *ezh2* coding sequence targeting guide optimised in Results 4.3.8 was used for Cas9 mediated knockdown. The successful guide was micro-injected into *TgBAC(mpx:EGFP)i114* embryos at the one cell stage and a tailfin injury was performed at 3 dpf with neutrophils counted at 3, 6 and 24 hpi (Figure 4.15A). Counts were compared with tyrosinase crRNA injected controls (Figure 4.15B). There was no significant difference between the number of neutrophils at 3 hpi, with control larvae averaging 26.9 neutrophils and *ezh2* larvae averaging 32.5. At 6 hpi there was a significant increase in neutrophils in the *ezh2* larvae, with an average of 44.4 compared to 33.4 in the control (P=0.0156). There was also a significant increase in neutrophils at the wound at 24 hpi in the *ezh2* injected larva, averaging 26.1 neutrophils compared to 16.4 in the control (P<0.001). This suggests that recruitment is increased at 6 hpi and results in a delay to inflammation resolution as seen by the counts at 24 hpi. Successful *ezh2* knockdown therefore leads to increased neutrophil recruitment at 6 hpi and increased neutrophil numbers at 24 hpi, delaying inflammation resolution.

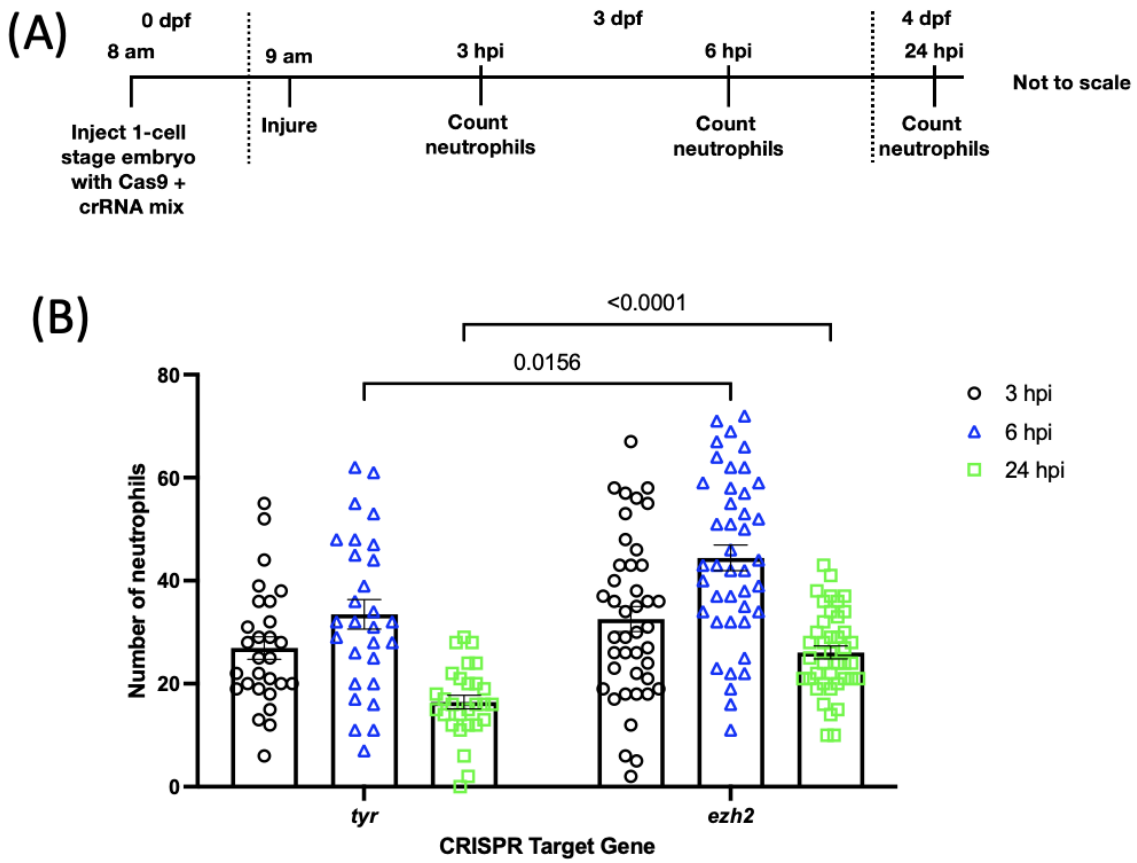

Figure 4.15. Whole-body CRISPR/Cas9 knockdown of *ezh2* results in a significant increase in neutrophils 6 hpi and 24 hpi

(A) Time course for experiment (B) Neutrophil counts at 3, 6 and 24 hpi comparing 3 dpf zebrafish larvae injected with Cas9 and guides targeting either *tyr* control or *ezh2* (3 independent repeats, 8-21 fish per group, Mean ±SEM, Mixed effects analysis with Sidaks multiple comparisons).

4.4. Discussion

Using published lists of chromatin remodelling enzymes, differentially expressed genes were identified in RNA sequencing datasets of activated neutrophils. These enzyme genes were sorted into a prioritised list based on differential expression, active chromatin states, and supporting literature to be used in both whole body and neutrophil specific CRISPR/Cas9 knockdown experiments. The identified enzymes were KDM6B, EZH2 and DOT1L.

The number of neutrophil RNA sequencing datasets used is limited compared to other systematic approaches perhaps due to the difficulty of working with this cell type. Sequencing of neutrophil RNA is very difficult and problematic. Neutrophils can apoptose during isolation leading to degradation of products before library preparation (Kim, Lu and Benayoun, 2022). Transcription of a gene may also not be the ultimate marker of chromatin remodelling enzyme activation and therefore an alternative approach may be more suitable, however it provides a starting point. Key chromatin remodelling enzymes could be transcribed and translated during neutrophil maturation and be activated by a secondary signal on detection of an immune threat. Cell surface receptor binding such as TLRs detecting a PAMP, or DAMP could trigger post-translational modifications of the enzyme, or co-factor binding as many enzymes work as part of a complex. A potential alternative would have been to use ChIP-seq for specific pro-transcriptional marks and pull out the marks associated with pro-inflammatory genes. The enzymes responsible for these modifications could then be searched for in both transcriptomic and proteomic datasets, with those with high expression likely to be involved in neutrophil regulation. However, there were not many freely available neutrophil chromatin or proteomic sequencing datasets when analysis was performed. Many of the datasets that did exist were available as raw data sets but were not pre-processed for analysis. Processing and analysing these datasets is complex and requires training that due to COVID-19 lockdowns was hard to obtain. RNA sequencing are therefore seen as the best option for this analysis based on the available pre-processed datasets at the time of analysis. If performed now, almost three years later, a larger variety of datasets are available, and a combined approach would help to narrow down the search for likely candidate genes. However, this was not possible due to competing wet-lab priorities.

Initial attempts to knockdown the target enzymes KDM6B, EZH2 and DOT1L used guide RNAs designed to target the 5'UTR of the enzyme genes. Successful deletion in the 5'UTR would cause a deletion that removed the promoter binding sites. These guides were also the preferred target site for a proposed model for neutrophil specific CRISPR interference (unpublished data). This CRISPR interference method was the original idea for how neutrophil specific knockdown would be performed in the project but was abandoned early in the project due to failures to implement the techniques in other laboratories. qRT-PCR showed *kdm6ba* presented a maximal 50% knockdown and no knockdown for *kdm6bb*. As a result, 5'UTR guide RNAs were no longer used and instead guides targeting the coding sequences of genes were prioritised.

Knockdown of *kdm6ba*/b with the coding sequence guides – two guide RNAs per paralog – resulted in a significant reduction in inflammation resolution, retaining neutrophils at the wound site for longer than the *tyr* control following caudal fin injury. KDM6B is a lysine demethylase that removes methyl groups from H3K27. Methylation of H3K27 is associated with gene silencing (Kruidenier *et al.*, 2012). Therefore, loss of KDM6B may result in genes remaining off when they need to be turned on. Based on the results of this knockdown, KDM6B may be involved in several processes in the neutrophil response to inflammation. KDM6B may be removing methylation at H3K27 in pro-inflammatory genes, so when KDM6B is not functional, neutrophils would not be able to perform roles such as phagocytosis or the respiratory burst, therefore the threat may not be cleared, and dysfunctional neutrophils continue to be recruited, and retained. Alternatively, KDM6B may be removing repressive marks at anti-inflammatory genes triggering the start of inflammation resolution. These may include genes that repress the inflammatory processes, such as genes that control apoptosis or reverse migration, or chemokine and cytokine genes that recruit macrophages to phagocytose dying neutrophils. Following *kdm6b* knockdown, these inflammation resolution processes may not be triggered, and neutrophils may be retained at the wound site. Identifying the inflammatory genes altered by *kdm6b* knockdown will help to answer these questions. KDM6B plays a role in macrophage activation and pro-inflammatory cytokine expression but it is unknown whether these processes are conserved between leukocytes (De Santa *et al.*, 2007, 2009; Kruidenier *et al.*, 2012; Yan *et al.*, 2014). Evidence for the role of KDM6B in neutrophil models is very limited. Using human peripheral blood neutrophils from

patients with sepsis, the membrane-bound proteinase 3 (mPR3)-dependent release of the pro-inflammatory cytokines IL-1β and TNFα were explored as these are major drivers in the onset of sepsis (Chen *et al.*, 2018). mPR3 is a serine protease stored in neutrophil granules and found on the plasma membrane following priming with pro-inflammatory cytokines that interacts with a variety of receptors and effector molecules (Hu, Westra and Kallenberg, 2009). Plasma from sepsis patients showed higher levels of IL-1β, TNFα and neutrophils showed increased *KDM6B* expression (referred to by its previous name JMJD3) relative to healthy controls. Isolated human neutrophils *in vitro* were then exposed to LPS with and without the KDM6B inhibitor, GSK-J4. LPS-treated neutrophils showed a decrease in H3K27me3, as well as a gene and protein increase in IL-1β and mPR3 relative to LPS + inhibitor-treated neutrophils. Chen *et al.*, (2018) show that KDM6B plays a major role in pro-inflammatory cytokine release from neutrophils following activation and provides a potential pathway how inflammation resolution may be altered in zebrafish following *kdm6b* knockdown. Therefore, zebrafish neutrophils without *kdm6b*, may lack proinflammatory *il1b* and *tnfa* transcription meaning that while neutrophils are recruited to the wound site, they will not secrete all the necessary cytokines or activate effector mechanisms required to deal with inflammatory threats leading to inflammation resolution.

The HIF1α pathway is also regulated by KDM6B. Shait Mohammed *et al.*, (2022) show, with increased *hif1a, kdm6b* also increases but they do not show a mechanism. In my *in vivo* knockdown model, qRT-PCR showed a non-significant increase in *hif1α* expression in *kdm6ba/b* knockdown relative to *tyr* knockdown control which translated to a non-significant 1.58-fold increase calculated by relative expression change, potentially contradicting Shait Mohammend's findings. While this change was not significant, it is perhaps interesting that the knockdown led to a 50% change in *hif1α* expression following injury relative to controls. From this, hypotheses can be drawn for further work to validate whether the change is biologically significant. Work studying KDM6B using the previous gene name of JMJD3, identifies that HIF1α is an activator of JMJD3/KDM6B in a murine model (Lee *et al.*, 2014). HIF1α drives *KDM6B* expression by binding hypoxia responsive elements present in the gene, as KDM6B requires oxygen to catalyse demethylation. So, under hypoxia, more KDM6B is required to be able to carry out essential functions to increase the chance of recruiting the necessary oxygen molecules. In the zebrafish *kdm6ba/b* knockdown, Kdm6b protein will not

be present and as a result, cells may be producing more HIF1α in an attempt to drive further *kdm6b* transcription, though the exact drivers of how this loop would be regulated are unknown. To test these hypotheses, quantification of genes that may be in the Kdm6b/Hif1α feedback loop following *kdm6b* knockdown will help to understand if KDM6B has the same targets as it does in humans. Neutrophil specific analysis is required as all these findings have been shown in whole body knockdowns and analysis performed on pooled whole embryo RNA, so it is unclear whether the effect is due to neutrophil specific changes or changes in the microenvironment.

EZH2 methylates histones as the catalytic subunit of polycomb repressor complex 2 (PRC2), specifically methylating H3K27 (Nutt *et al.*, 2020). Essentially, it has the inverse function to KDM6B, though not necessarily the same target genes regulating neutrophil function. Coding sequence targeting guides for *ezh2* showed increased neutrophil recruitment and kinetics and a decrease in inflammation resolution following caudal fin injury. These data suggest that EZH2 targets pro-inflammatory genes, which may prevent the wound site being overwhelmed by neutrophils and causing damage to healthy tissue, or genes that control movement of neutrophils to the wound site. EZH2 attaches repressive marks to the histones associated with its target genes, preventing transcription. Gunawan *et al.*, (2015) showed evidence for EZH2 being involved in chemotaxis during neutrophil recruitment. Work in a *Cre-Lox Ezh2* whole body deletion mouse models first showed that EZH2 is essential for sufficient extravasation of neutrophils out of the vasculature and into inflamed tissue (Gunawan *et al.*, 2015). Further work with *Cre-Lox Ezh2* knockout mice then showed that without EZH2, mouse neutrophils are not capable of properly performing chemotaxis and have reduced recruitment by counts in bronchoalveolar lavage following LPS exposure (Kitchen *et al.*, 2021). The authors hypothesised that EZH2 caused changes to cytoskeletal remodelling and not changes to chemokine responses. The findings presented in this thesis counter this idea, showing an increase in neutrophil recruitment 6 hours after immune challenge. Kitchen *et al.,* (2021) only looked at a single time point (4 hours post infection) whereas multiple time points are analysed here, though no change is seen at 3 hpi in the zebrafish data. These differences could be down to the model organism used or the method of analysis as neutrophil migration tracking was not performed in the zebrafish. A potentially different distribution of neutrophils at the tailfin wound was observed relative to *tyr* controls, however, this was not imaged or

quantified but could provide further interesting areas to investigate. The injury model will also be triggering different pathways to the infection model. Therefore Ezh2 could be carrying out different roles depending on the inflammatory stimuli as different stimuli trigger different conformational changes in neutrophil chromatin (Denholtz *et al.*, 2020). Kitchen *et al.,* (2021) also compared the phenotype seen in neutrophils to macrophages and showed that the role of chromatin remodelling enzymes does differ in different immune cells, with neutrophil-specific effects of *ezh2* deletion not seen in the macrophages. As well as looking at literature on chromatin remodelling enzyme function in neutrophils, part of the selection process for Kdm6b, Ezh2 and Dot1l was evidence for them playing roles in macrophage inflammatory processes and regulation due to overlap in function with neutrophils (Results 4.3.1.a. and b), but this new evidence may suggest that using these criteria was not the best approach (Yildirim-Buharalioğlu *et al.*, 2017; Chen *et al.*, 2020; Neele *et al.*, 2021). These data show why cell-specific studies are so important in understanding the role these chromatin remodelling enzymes play in regulating immune function as the role of the enzymes differ from cell to cell. The role of EZH2 in regulating cytokines in neutrophils is unknown and so further study is needed to make conclusions on the hypothesis that the increased recruitment is down to the lack of repression at pro-inflammatory cytokine loci as inflammation progresses.

Neutrophil-specific knockdown offers an excellent tool for studying the effect of genes in a single cell population. The technique used here inserts guide RNA sequences that target the 5'UTR of *kdm6ba* and *kdm6bb* into a single construct for injection into embryos that express a neutrophil specific Cas9 construct. While 5'UTR guides used in isolation did not provide the most efficient knockdown, this technique was developed in parallel with the whole-body knockdown analysis. The most optimal technique would be to combine guides that target sequences before the translational start site and within the coding sequence, as this has been shown to give efficient knockdown and could be utilised for future work (El-Brolosy *et al.*, 2019). This would be ideal to investigate the role of DOT1L in neutrophil function as whole-body knockdown was not possible due to the coding sequence guide leading to death as shown above and, in the literature, (Kara *et al.*, 2019). Preliminary work carried out in this thesis showed successful deletion within the guide target site in the 5'UTR and therefore combining both the 5'UTR and coding sequence guide could provide a potent neutrophil specific knockdown of *dot1l*.

A neutrophil specific Cas9 line has also been made using the Gal4-UAS system (Isiaku *et al.*, 2021). In this method, IDT guide RNAs were single cell microinjected into a neutrophil specific Cas9 line and validated to remain in the larval zebrafish until 3 dpf where caudal fin injuries can be performed. Using this method means that guides used for whole body knockdown can be used without the time-consuming process of making the guide specific constructs. Direct injection of the guides has not been tried in the Cas9 line we generated but using the same conditions as Isiaku *et al.*, (2021) provides no obvious hurdles. In this scenario, the neutrophils would not be fluorescently tagged, and another form of identification would have to be used. Examples include Sudan Black or TSA staining after fixation of the fish in 4% PFA, though this does not allow for continued analysis of neutrophil numbers in single larvae over a time course. Isiaku *et al.*, (2021) had mCherry^{+} neutrophils and maybe this could be explored for further work to easily observe neutrophil activity as the Cas9 line we have developed requires further validation to ensure there is functional Cas9 protein in neutrophils. Work carried out by Catherine Loynes to inject the Rac2 guide used by Wang *et al.,* (2021) showed no alteration in neutrophil recruitment number to a tailfin wound, however, further investigation is required using the kinetics experiments shown by Deng lab.

Work presented in this chapter shows how a method for identifying the potential chromatin remodelling enzymes responsible for regulating neutrophil function was developed and used to identify the target genes for a priority based CRISPR knockdown screen. This knockdown screen used whole body CRISPR/Cas9 to show that both KDM6B and EZH2 regulate neutrophil numbers at a tailfin wound and consequently are interesting targets for further investigation. Literature does suggest several pathways for how these enzymes may regulate neutrophil function and knockdown specifically in neutrophils followed by subsequent sequencing will help to identify the pathways these enzymes operate through. A neutrophil specific knockdown method was established but it was not possible to generate data in the time limits of the project, however suggestions have been made as to how this can be utilised and potentially improved for a rapid cell specific CRISPR/Cas9 knockdown screen of chromatin remodelling enzymes in the future. Overall, the field of chromatin remodelling in neutrophils has moved on rapidly since these enzymes were selected allowing for comparisons to be made to other model systems and sequencing datasets. Generating a sequencing dataset

from knockdown of *kdm6b* will allow us to add to this knowledge and further the understanding of how chromatin remodelling enzymes control neutrophil function.

Chapter 5: INTACT BirA/streptavidin pulldown of zebrafish neutrophils to understand how kdm6b regulates the neutrophil transcriptome.

5.1. Introduction

Chromatin remodelling enzymes play an essential role in defining cell type and function. We want to further the understanding of how these enzymes regulate neutrophil function. However, as previously discussed, neutrophils are challenging to work with especially in the context of next generation sequencing (NGS), though more datasets are now beginning to be produced (Kim, Lu and Benayoun, 2022). Consequently, we are only beginning to understand the role chromatin remodelling plays in neutrophil function, as well as identifying effector molecules of chromatin remodelling in neutrophils (Denholtz *et al.*, 2020).

To further study the role of chromatin remodelling enzymes in neutrophils, a method for neutrophil isolation and sequencing following CRISPR/Cas9 mediated knockdown of chromatin remodelling enzymes needed to be developed. Alone, *in vitro* CRISPR/Cas9 knockdown in neutrophils is challenging due to risks of rapid apoptosis or spontaneous activation making isolation of *in vitro* neutrophils for NGS technically difficult. Mammalian models do provide one option for isolating neutrophils for NGS, however that also remains challenging as neutrophils are often lost when isolating samples for sequencing using techniques such as FACS or specific kits from whole blood or bone marrow, again due to spontaneous activation and apoptosis and the extended timescales required before cells are ready for isolation (Kim, Lu and Benayoun, 2022). When the project started, these challenges meant there were no mammalian datasets for inflammatory neutrophils.

Using a zebrafish model allows us to overcome many of the challenges that arise when extracting neutrophil RNA for sequencing compared to *in vitro* and mammalian models. Previous chapters have discussed the ease at which CRISPR/Cas9 knockdown can be carried out in whole zebrafish embryos. This knockdown can easily target neutrophils allowing for downstream analysis. However, extraction of neutrophil RNA still provides some barriers. For this work, 3 dpf larvae are used due to the ease at which inflammatory processes can be

assessed following caudal fin injury. At 3 dpf, zebrafish larvae contain 150-200 neutrophils (Figure 3.2). This relatively low number means that any method for cell specific isolation needs to have a high yield both in terms of cell numbers/RNA concentration and RNA quality to prevent the use of excess larvae and to provide samples of high enough quality for sequencing. FACS does not provide a high yield relative to the number of fish used and RNA quality is often variable depending on how the flow cytometer is used and maintained. Second, FACS isolation may result in transcriptional alterations. A method with a higher yield and cleaner preparation would be ideal for neutrophil preparations.

A search was carried out for methods that would suit neutrophil isolation better than FACS with the aim to find a method that gives a high yield and high purity sample that could be used for transcriptomics. **I**solation of **n**uclei **ta**gged in specific **c**ell **t**ypes (abbreviated to INTACT) aligns to these goals as it was designed as a method to avoid the problems associated with FACS and other mechanical methods such as the need to use harsh procedures and expensive equipment (Deal and Henikoff, 2011). INTACT provides a bench top method for the isolation of nuclei from specific cell types from whole tissue samples that maintains nuclear integrity and allows for gene expression and epigenetic analysis. The method was initially developed using *Arabidopsis* root epidermis and uses transgenic constructs to isolate the nuclei, and as a result INTACT is possible in any transformable model organism (Deal and Henikoff, 2011). INTACT is achieved by biotagging the specific cell nuclei using specifically designed constructs allowing for highly specific isolation of cells for further analysis. Compared to FACS, the process uses minimal equipment and no specialised machines. The equipment is kept RNAse-free, and all work is carried out at 4˚C to prevent degradation of RNA. The process has been adapted for use in a zebrafish system including for the isolation of zebrafish neutrophils (Kenyon *et al.*, 2017; Trinh *et al.*, 2017). Synthetic DNA constructs facilitate the tagging of nuclei with an Avi-tagged Rangap fusion protein – a nuclear membrane protein – that allows for high-affinity binding of streptavidin dynabeads that ultimately allows from the isolation of the Avi-tagged nuclei. To allow for the streptavidin binding, a second synthetic construct drives the expression of cytoplasmic BirA by a cell specific promoter, that in the presence of biotin and ATP, biotinylate the Avi-tag and allows it to bind streptavidin (Figure 5.1A and B). To isolate the tagged nuclei, the zebrafish larvae are washed and homogenised in a series of RNAse free buffers to give a nuclear suspension

that is incubated with streptavidin bound magnetic beads. During this incubation period the streptavidin forms a high-affinity bond to the biotinylated Avi-tag to bind the tagged nuclei. The magnetic bead/nuclei suspension is then captured on a magnetic stand and washed with buffer, leaving a sample enriched for Avi-tagged, cell-specific nuclei. The nuclei are then lysed from the beads and RNA extracted for analysis.

For neutrophil isolation, the BirA protein is expressed by the neutrophil specific *mpx* promoter (Kenyon *et al.*, 2017). The INTACT protocol can then be combined with whole body CRISPR/Cas9 knockdown, and neutrophils from these larvae can be isolated by INTACT for gene expression analysis. Neutrophil specific CRISPR/Cas9 knockdown cannot be used due to the multiple fish transgenic lines needed reducing the number of tagged neutrophils and therefore reducing the yield significantly.

Overall, INTACT potentially provides a method for the isolation of cell specific RNA that is of high quality, high yield, and high purity relative to other isolation methods. When applied to a zebrafish model, INTACT can take advantage of the ease at which zebrafish can be genetical altered to perform cell specific differential gene expression analysis either by qRT-PCR or RNAseq comparing different treatment conditions such as caudal fin injury following gene knockdown.

5.2. Aims and hypothesis.

Chapter 4 established that knockdown of *kdm6ba/b* in zebrafish larvae leads to an increased retention of neutrophils at the wound site 24 hpi, when inflammation resolution would be expected to remove neutrophils from the wound (Figure 4.15). We hypothesise that knockdown of *kdm6b* using CRISPR/Cas9 leads to alterations to the neutrophil transcriptome. To understand how the neutrophil transcriptome is altered by *kdm6b* knockdown and how that may regulate neutrophil function I will:

- Optimise the INTACT pulldown method for isolating neutrophil nuclei for RNAseq.
- Knockdown *kdm6ba/b* using CRISPR/Cas9 in the INTACT zebrafish line, isolate the neutrophils by INTACT and perform whole transcriptome analysis (RNAseq).

- Carry out Bioinformatics analysis allowing for differential expression analysis of pro-inflammatory genes relative to controls.

This work will help to understand the downstream processes connected to *kdm6b* and how chromatin remodelling enzymes modulate neutrophil function.

5.3. Results

5.3.1. INTACT BirA/streptavidin pulldown extracts show enrichment for neutrophil nuclear RNA based on RT-PCR for neutrophil genes and adequate RNA quality using Agilent Bioanalyzer 2100 readouts.

To isolate neutrophil nuclear RNA for sequencing, the INTACT method first had to be optimised using local equipment and protocols and the quality of the nuclear extract confirmed. A stable, neutrophil specific mpx:BirA/ubiq:AviRangap zebrafish line containing both the required genetic constructs (Figure 5.1Ai and Aii) was generated with the help of Catherine Loynes by microinjection of the mpx:BirA construct and ubiq:AviRangap into separate fish lines then crossing the two transgenic lines to give a double transgenic line (Kenyon *et al.*, 2017; Trinh *et al.*, 2017). This produces a line that only contains Biotin-Rangap tagged neutrophil nuclei where no other cell type nuclei should be specifically extracted (Figure 5.1B).

Optimisation of the INTACT pulldown method proved challenging. First, adaptation of the original method was required due to issues acquiring the necessary equipment due to shortages brought on by the COVID-19 pandemic. The original work used a flow-through system, using a magnetic Miltenyi Biotec OctoMACS™ Separator rack to capture a nuclei-streptavidin bead suspension on the side of a pipette tip that sat within the rack. The correct P1000 pipette tips could not be acquired, meaning a tight seal could not be formed through the flow system. Due to this shortage in pipette tips, a stationary Stem Cell Technologies “Big Easy” EasySep magnet was used instead. This adapted system captured the bead/nuclei suspension on the sides of a 14 ml culture tube, attempting to capture as many nuclei as possible by multiple incubations of the buffer/nuclei-bead solution. This method proved capable of capturing a large quantity of beads and an optimal RNA concentration was confirmed using a Nanodrop 2000 to proceed to quality and purity assessment of the nuclear RNA using a Bioanalyzer 2100.

To extract nuclei for Bioanalyzer 2100 and RT-PCR analysis, non-injured 3 dpf larvae from the mpx:BirA/ubiq:AviRangap zebrafish line were washed and homogenised, incubated with streptavidin coated dynabeads, and the beads isolated on a magnetic stand before being

washed and RNA extracted (Figure 5.1C, step 3-6). The RNA concentration was measured using a Nanodrop 2000 and sent for further analysis using an Agilent Bioanalyzer 2100. Traces were compared to those in Materials and Methods 2.4.5.c. and Figure 2.5. Both the non-nuclear RNA and the neutrophil nuclei RNA show comparable traces to those in Figure 2.5 with the 25 nt peak representing the internal standard (Figure 5.2Ai and ii). Neutrophil nuclear RNA shows a prominent peak between 500 and 4000 nt representing most RNA fragments (Figure 5.2Aii), which the authors of Trinh *et al.*, (2017) confirmed was adequate as smaller nt peaks would suggest RNA degradation during the pulldown process. Further RNA was isolated using the INTACT technique and cDNA synthesised to analyse the content (Figure 5.2B). RT-PCR was used, and neutrophil nuclear cDNA compared to the cDNA from the supernatant excess flow-through from the pulldown system and age-matched whole larvae. Initial continued detection of non-neutrophil genes in the neutrophil nuclei RNA led to a refinement of the post-pulldown wash process (Appendix Figure 5.1). This was partly attributed to using the stationary magnet and not the flow-through system. Residual excess buffer/non-neutrophil nuclei mix was present in the bottom of the culture tube sitting on the magnet. Published flow-through methods used one wash following the pulldown process. The wash number was increased to five washes using the stationary magnet to reduce the excess in the culture tube and to dilute any excess that may be there. Neutrophil nuclei bound to streptavidin beads were retained on the side of the tube, so were not lost in the wash steps.

The final panel of genes used were: *ef1a* as a house keeping gene, *mpx* as a neutrophil-specific gene and *itga2b* used as a non-neutrophil gene. Neutrophil nuclear cDNA showed *ef1a* and *mpx* expression but not *itga2b* showing high specificity. The flow-through nuclei cDNA only showed *ef1a* confirming the flow-through was very low in contamination by neutrophils. Whole fish cDNA showed *ef1a, mpx* and *itg2b* confirming the primers work. The lack of *itg2ab* in the non-neutrophil nuclear RNA and weak band in the whole fish cDNA suggests *itg2ab* was only detectable at low levels in any of the samples. Other genes were used as non-neutrophil genes but proved difficult to optimise (Appendix Figure 5.1). Taken together, these data show that the INTACT method can isolate neutrophil nuclei as shown by enrichment of neutrophil genes for RNA sequencing.

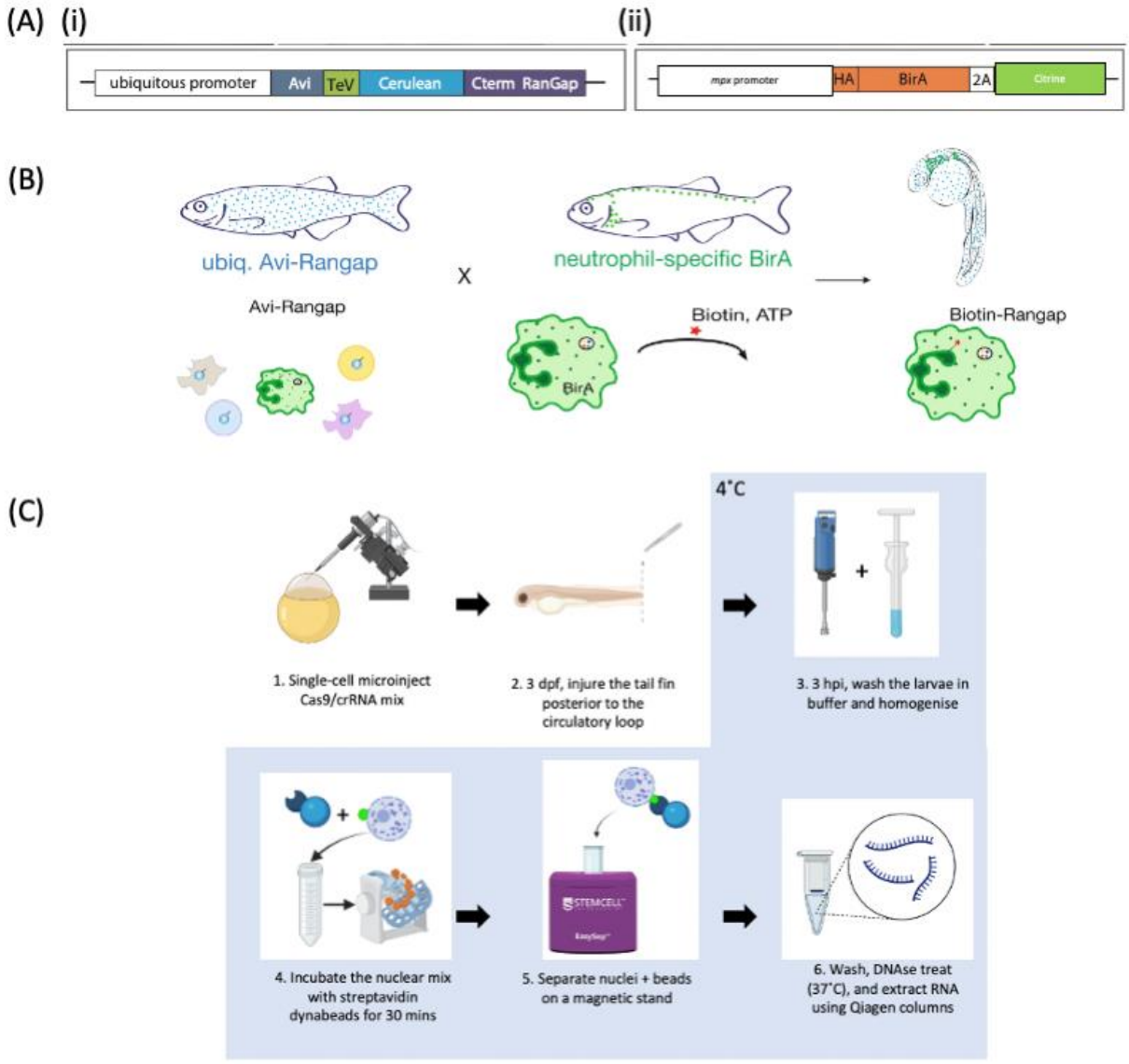

Figure 5.1. INTACT BirA/Streptavidin pulldown as a method for isolation of zebrafish neutrophil nuclei.

(A) The ubiquitously expressed (i) Avi-RanGap construct and (ii) mpx promoter driven BirA constructs adapted from Trinh *et al.*, (2017). (B) Schematic of how breeding of the Avi-RanGap and mpx-BirA zebrafish lines generate offspring with a Biotin-RanGap tagged neutrophil nuclei. (C) Workflow for extraction of RNA from biotagged neutrophil nuclei, blue background shows stages performed at 4˚C (made using BioRender and not to scale)

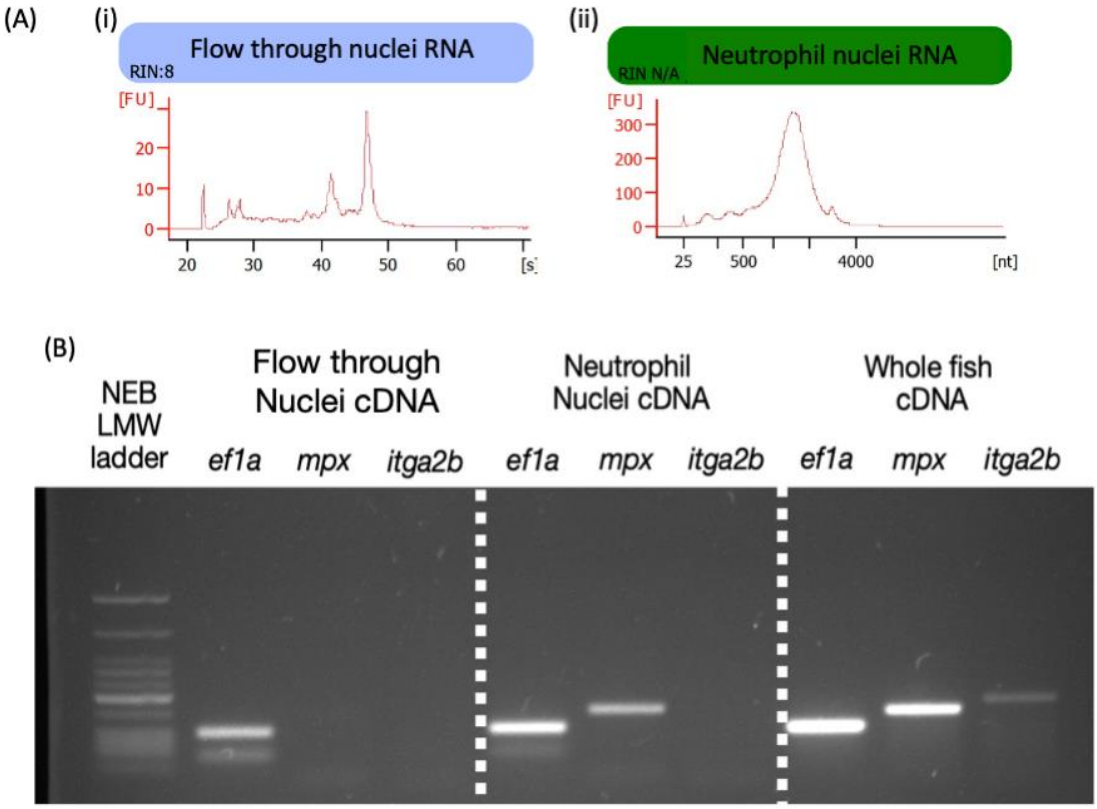

Figure 5.2. Analysis of INTACT extracted nuclear RNA samples shows enrichment for neutrophil genes and adequate RNA quality based on Agilent Bioanalyzer 2100 readouts.

(A) Agilent Bioanalyzer 2100 plots for RNA samples from (i) non-neutrophil nuclei RNA and (ii) neutrophil nuclear RNA. [nt] shows the number of bases for each peak and [FU] is the fluorescent units of those fragment sizes. (B) 2% Agarose gel of RT-PCR amplified genes to optimise the INTACT pulldown product. *ef1a* is used as a housekeeping gene, *mpx* is neutrophil specific and *itga2b* is not present in neutrophils. Flow-through nuclei cDNA is the excess of the pulldown, Neutrophil nuclei cDNA is the INTACT extracted product and Whole fish cDNA is taken from age-matched untreated mpx:BirA x Avi-RanGap larvae.

5.3.2. Quality control of INTACT pulldown *kdm6b* knockdown RNA sent for sequencing.

Three independent biological repeats of INTACT pulldown products using roughly 150 larvae per treatment per repeat – limited by how many embryos produced – were sent for sequencing by Source Biosciences. The aim was to analyse the neutrophil nuclear transcriptome following *kdm6b* knockdown with and without caudal fin injury (Figure 5.1B). A control group was created using crRNA for *tyr,* the gene encoding tyrosinase (as used in Chapter 4). Within each repeat, there were four RNA samples:

1. *tyr* CRISPR injected and no injury
2. *tyr* CRISPR injected and injury
3. *kdm6ba/b* CRISPR injected and no injury
4. *kdm6ba/b* CRISPR injected and injury

13 µl of RNA per sample was sent for sequencing to Source Biosciences. Source Biosciences prepared a pre-sequencing QC report, and the details are presented here (Figure 5.3). Concentrations were measured initially, and samples run on an Agilent Bioanalyzer 2100 with a RIN score produced. Concentrations ≥6 ng/µl and RIN scores ≥7 are recommended for sequencing (https://www.sourcebioscience.com/genomics/ngs/sample-requirements/). Samples for independent repeat 1 are labelled 1-4, repeat 2 are 5-8, and repeat 3 are 9-12. Several samples gave very low concentrations and RIN scores were mostly under 7 apart from samples 5 and 6 (Figure 5.3A). Samples 3 and 4 gave very low RIN scores of 2.6 and N/A respectively (Figure 5.3A). Referring to the Bioanalyzer plots, all samples apart from 3 and 4, showed traces that resemble Figure 2.5. with the 25 nt internal standard a 500-4000 nt peak for the RNA fragments (Figure 5.3B). It was decided to sequence repeat 2 and 3, but not repeat 1 due to the low concentrations, low RIN scores and Bioanalyzer plots for samples 3 and 4.

(A)

Generated by Source Biosciences

	External ID	Conc. (ng/µl)	RIN
Repeat 1	1	too low	4.1
	2	4.6	6.4
	3	too low	2.6
	4	too low	N/A
Repeat 2	5	63.2	7.7
	6	35	7.4
	7	too low	5
	8	5.52	5.2
Repeat 3	9	too low	4.8
	10	8.82	5.9
	11	too low	4.3
	12	5.7	5.9

(B)

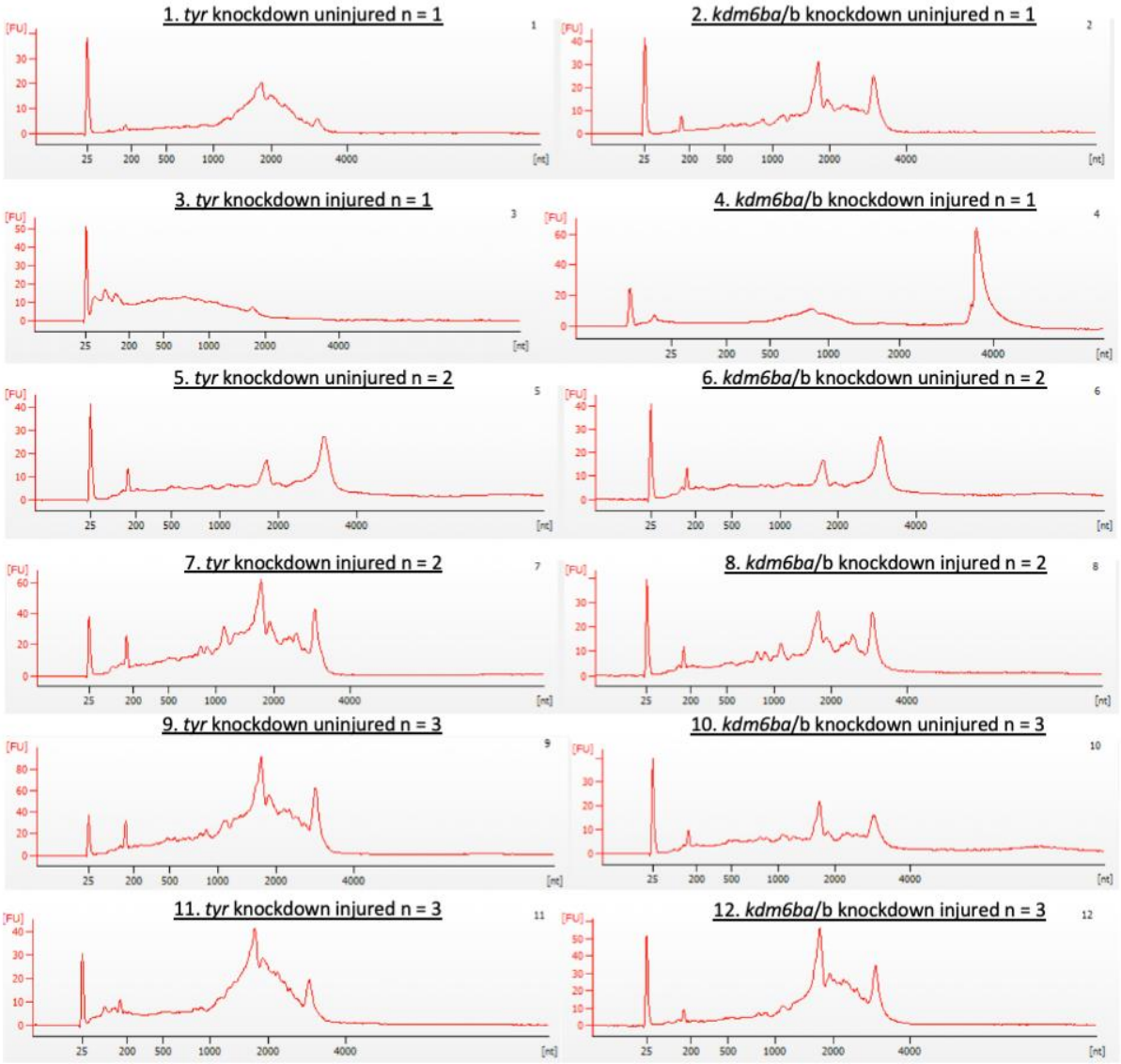

Figure 5.3. Quality control report from Source Biosciences

(A) Table of concentrations and RIN scores for RNA samples submitted for RNA sequencing to Source Biosciences measured by Invitrogen Qubit RNA assay and Agilent BioAnalyzer 2100 respectively. (B) Agilent BioAnalyzer 2100 plots for each of the 12 RNA samples submitted, labelled with the sample number and description above.

5.3.3. Post-sequencing bioinformatics report for the *kdm6b* knockdown RNAseq dataset shows the data set to be of sufficient quality for analysis.

Source Biosciences also produce a quality control report on the outputted sequencing data following the sequencing process. Presented here are the plots and scores associated with this data. The sequence quality of each base within a 150 bp read is generated and given a quality score between 0-40 based on the probability the base will be incorrect. A score of 40 is a 0.0001% chance of an incorrect base, 30 is a 0.001% and 20 a 0.01%. In the forward and reverse reads, the Q-score remains above 34 on average for all points, with some variation as shown by error bars down to 24 (Figure 5.4A and B). The percentage of missed bases within reads are also calculated for the forward and reverse reads and in both directions the score is 0% at every point (Appendix Figure 5.2A and B). These graphs show that despite initial issues with the RNA pre-sequencing (Figure 5.3), the output reads of detectable genes were of high quality and suitable for analysis.

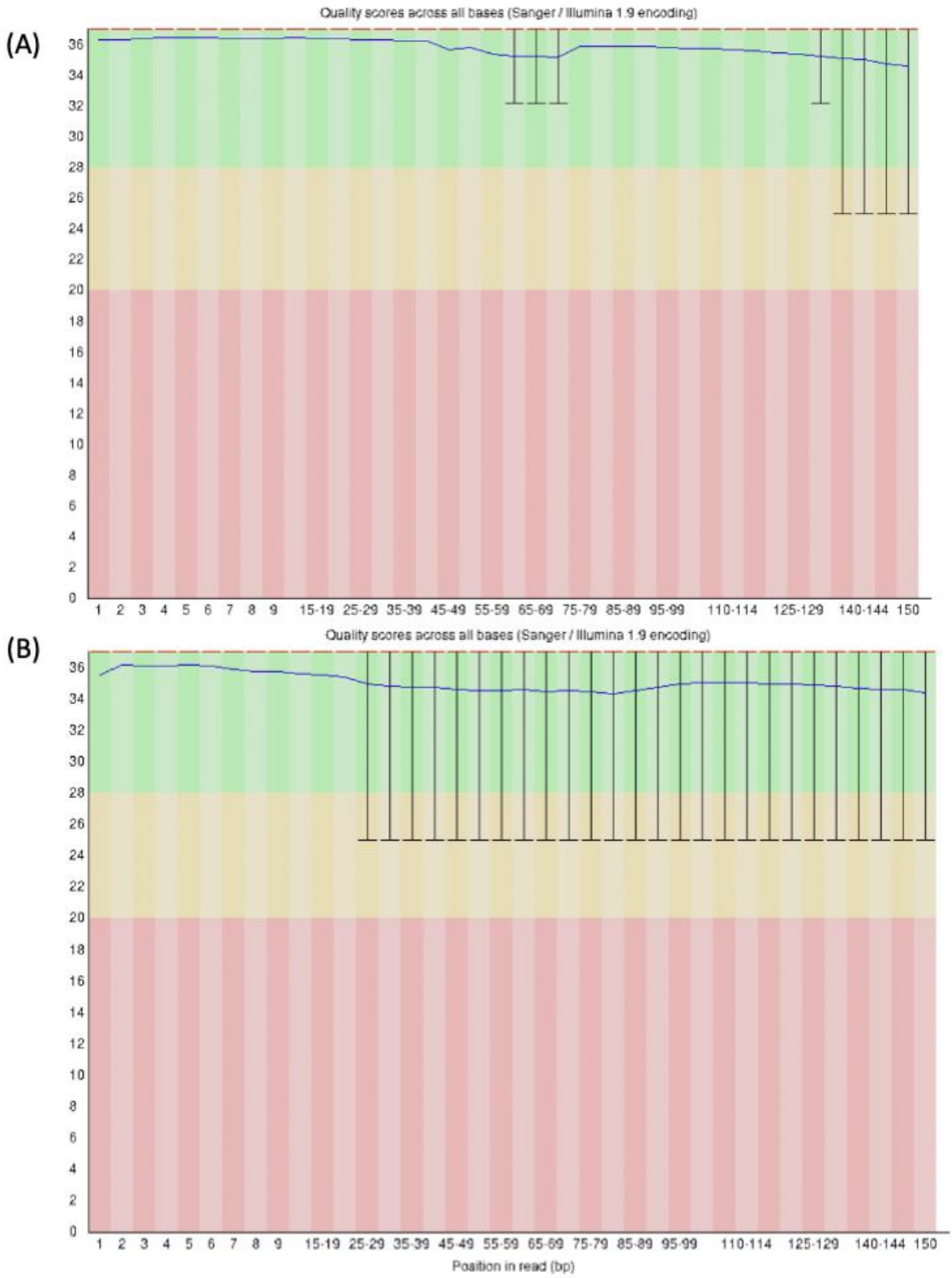

Figure 5.4. Bioinformatics Report from Source Biosciences

Graphs and legend content from Source Biosciences Bioinformatics QC report (A) Per base sequence quality plot generated for the forward read and (B) reverse read. Quality distribution is shown for every position in the read separately. Illumina sequencing data

shows a characteristic quality drop towards both ends. The longer the read length the lower the quality towards the 3’ end.

5.3.4. PCA plots and mean difference plots show the clustering and spread of the *kdm6b* knockdown RNAseq dataset.

5.3.4.a. PCA plots show clustering of groups based on knockdown/injury condition.

Raw sequencing files were mapped to the Danio rerio genome (danRer10) using HISAT2 and annotated using featureCounts in R, as described in Materials and Methods 2.4.6. Principal Component Analysis (PCA) was performed using R. PCA plots show clustering of datasets following dimensionality reduction to reduce input variables and analyse common features in a dataset. A PCA plot was produced based on the normalised counts per million (CPM) data generated using the edgeR package in RStudio from the normalised counts of genes detected in the dataset (Figure 5.5). The two repeats for *kdm6b* CRISPR injected and uninjured (green) and *tyr* CRISPR injected and injured (blue) show clustering on the PC2 axis, whereas *tyr* CRISPR injected and uninjured (purple) shows clustering on the PC1 axis. The *kdm6b* CRISPR injected and injured (orange) samples show most variation between sample repeats, with very little clustering on PC1 or PC2. This means repeats show common features in at least one of the PCA conditions apart from the *kdm6b* CRISPR injected and injured group. Given the differing conditions in each of the four groups, it is understandable why there may not be clustering between different treatment conditions as the neutrophil transcriptome following injury, will be very different than in non-injured samples.

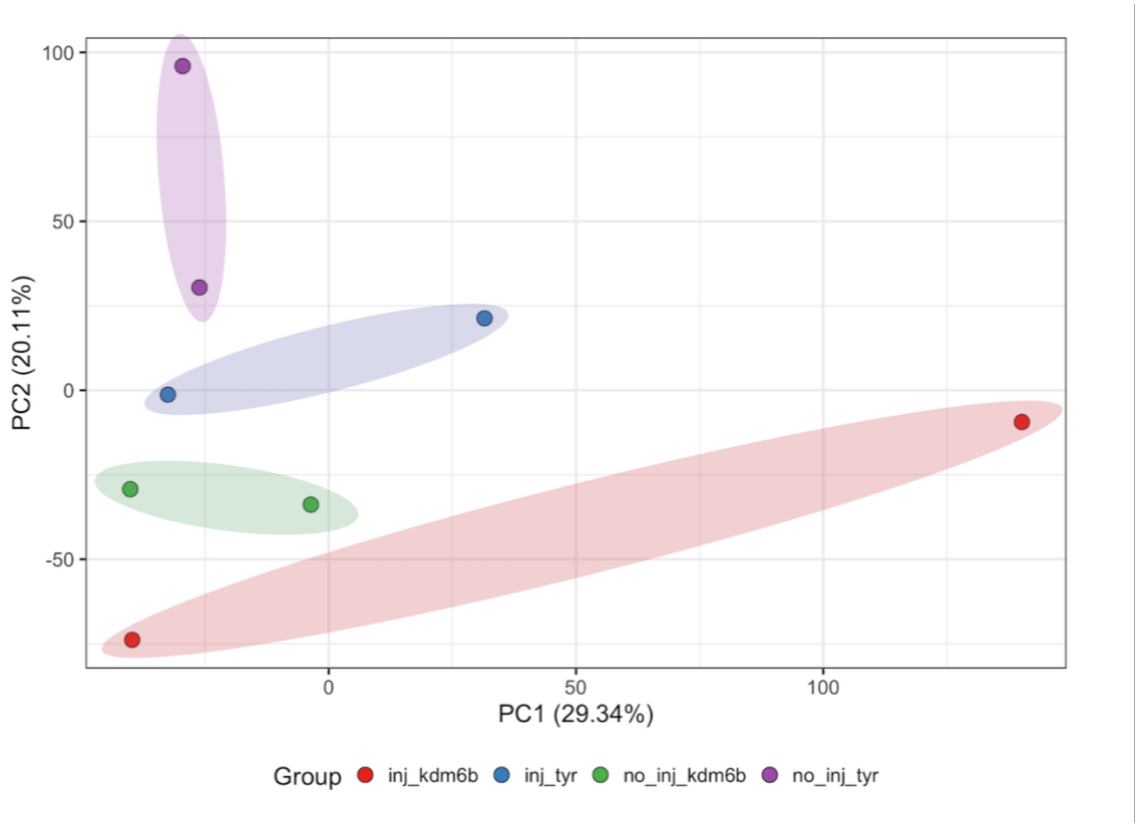

Figure 5.5. PCA plots show some clustering of groups based on sample type.

(A) PCA plot showing the clustering of the four samples sent for RNA sequencing. Groups are *kdm6b* guide injected and uninjured (green), *kdm6b* injected and injured (orange), *tyr* guide injected and uninjured (purple), and *tyr* guide injected and injured (blue). Two data points per group represent two independent repeats of up to 150 larvae per group.

5.3.4.b. Mean difference plots show a different distribution of differentially expressed genes depending on the knockdown/injury comparison.

Following generation of differential gene expression values between groups, mean difference plots were made using the limma package in RStudio plotting $\log_2$(average counts per million) against $\log_2$(differential gene expression fold change), individual points represent single genes (Figure 5.6A-D). The blue line on the y-axis is $\log_2(\pm 1.5)$, any genes with a 50% increase or decrease in expression any genes above the line show a change in expression pattern, though this is not statistically significant but may be biologically interesting. The *tyr* CRISPR injured was compared with *tyr* CRISPR uninjured to examine differentially expressed genes during neutrophil activation. This comparison shows a wider spread of genes that have increased expression, as points are seen above the top blue line of the y-axis (Figure 5.6A). The *kdm6b* CRISPR uninjured was compared with *tyr* CRISPR uninjured to look at differentially expressed genes in inactivated neutrophils following *kdm6b* knockdown. The *kdm6b* knockdown shows a greater spread and higher number of genes that are downregulated as seen by more points below the lower blue line on the y-axis (Figure 5.6B). The *kdm6b* CRISPR injured was compared with *kdm6b* CRISPR uninjured to look at differentially expressed genes during neutrophil activation relative to inactive neutrophils in the absence of *kdm6b*. This comparison showed a comparable spread in either direction compared to the *tyr* comparison with more positive differentially expressed genes than negative (Figures 5.6C and A). The *kdm6b* CRISPR injured was compared with *tyr* CRISPR injured to look at differentially expressed genes during neutrophil activation in the absence of *kdm6b* relative to the control. This comparison showed that the majority of differentially expressed genes were downregulated due to most points being below the lower blue line on the y-axis (Figure 5.6D). However, due to the gaps in the dataset, these changes may simply be down to lack of sequencing coverage and further validation either with further biological repeats, or downstream analysis using techniques such as qRT-PCR are required to draw meaningful conclusions.

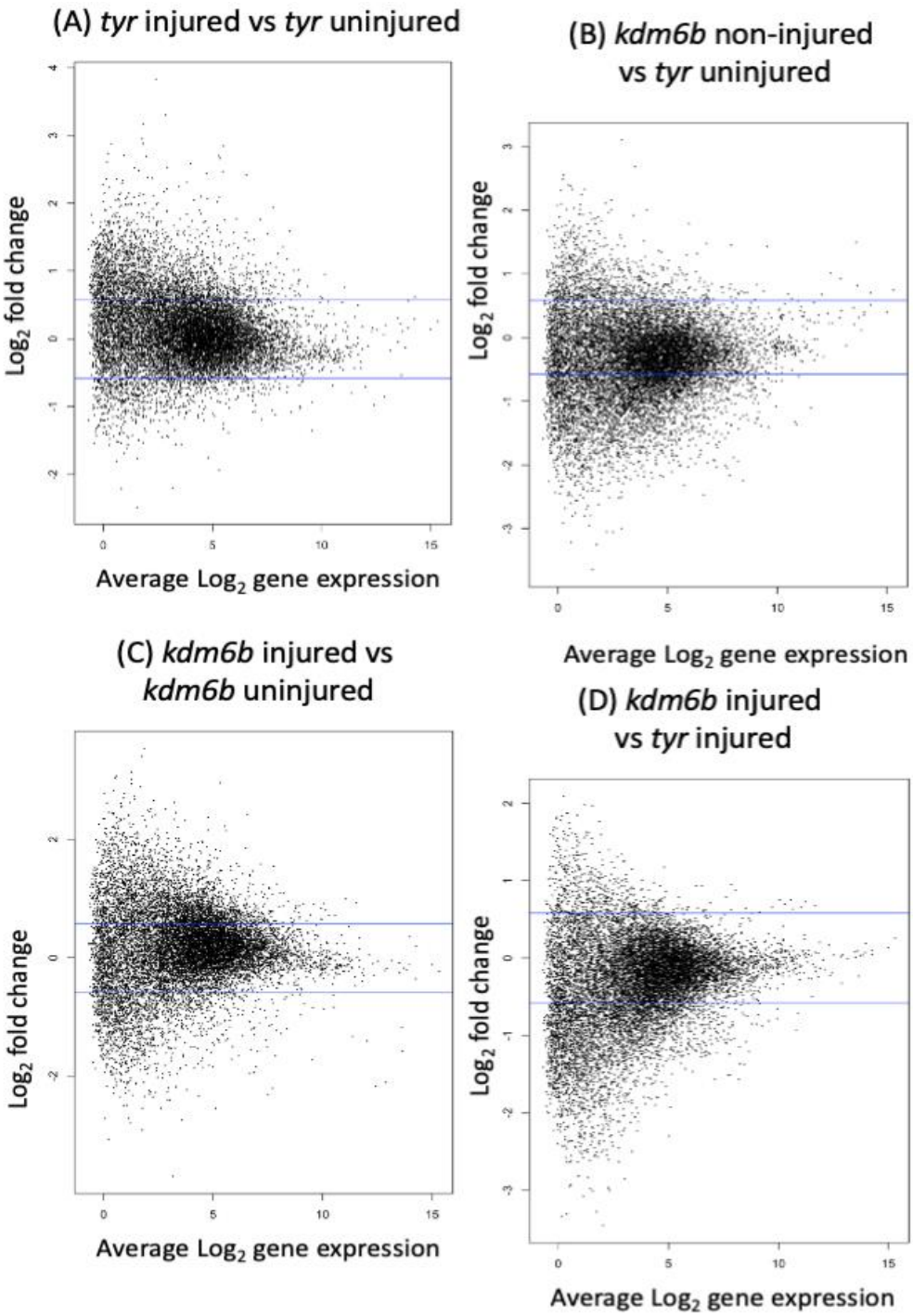

Figure 5.6. Mean difference plots show *kdm6b* knockdown and tailfin injury result in a different distribution of differentially expressed genes.

(A-D) Mean difference scatter plots comparing differential gene expression fold changes against from counts per million. Comparison condition listed above each graph. Y axis shows log_2 of fold change calculated between samples. X axis shows Log_2 of average expression value as counts per million. Blue lines on Y axis represents ±0.58, the $log_2(\pm 1.5)$, a 1.5-fold change, Y-axis aligned at 0.

5.3.5. *kdm6b* knockdown shows a different pattern of differentially expressed genes compared to the *tyr* control.

While the edgeR analysis and mean difference plots (Figure 5.6) show there are no significant differentially expressed genes between *tyr* and *kdm6b* knockdown with and without injury (likely due to low statistical power), it is still interesting to look at the genes with the largest fold-change in expression between treatments, to look for common genes and patterns, especially as this is a preliminary dataset as there are 2 independent repeats. For each comparison, genes were sorted based on $\log_2$(Fold change) and the top 10 genes with increased or decreased expression are presented here (Table 5.1). Overall, the four comparisons show one common gene, with *nr1d1* downregulated in *kdm6b* injured vs. *kdm6b* uninjured and *tyr* injured vs, *tyr* uninjured. This lack of common genes suggests the *kdm6b* knockdown conditions have caused considerable changes to the transcriptome both with and without injury. While these genes are varied, it is worth highlighting those with neutrophil linked processes.

5.3.5.a. Top 10 DEGs for *tyr* injected and injured vs. *tyr* injected and uninjured.

The *tyr* injured vs *tyr* uninjured comparison shows up-regulation of inflammatory genes such as *irf1b, cxcl18b, c3a.3* and *c3a.6* as expected due to the caudal fin injury triggering inflammatory signalling (Table 5.1). Down regulated genes include *nr1d1* and *per1b*, binding proteins implicated in circadian clocks and *wnt9b* implicated in enabling cytokine signalling. Transcriptional regulators *hoxc12a* and *med22* are also down-regulated (Table 5.1).

Gene	logFC	adj.P.Val
irf1b	3.82860602	0.99888924
cxcl18b	3.29854443	0.99888924
avl9	3.16812007	0.99888924
cyp2k18	2.94789031	0.99888924
scpp9	2.87909695	0.99888924
krt93	2.87569595	0.99888924
c3a.3	2.84051647	0.99888924
lepb	2.72807648	0.99888924
zgc:153968	2.70927951	0.99888924
c3a.6	2.69591785	0.99888924

Gene	logFC	adj.P.Val
he1a	-2.4847327	0.99888924
hoxc12a	-2.2096144	0.99888924
nr1d1	-2.202424	0.99888924
fabp11b	-1.9373045	0.99888924
si:dkey-245p14.4	-1.8024642	0.99888924
crygm5	-1.7633281	0.99888924
per1b	-1.7546686	0.99888924
med22	-1.6891838	0.99888924
mat2ab	-1.611721	0.99888924
wnt9b	-1.5671423	0.99888924

Table 5.1. Top 10 DEGs for *tyr* injected and injured vs. *tyr* injected and uninjured.

Gene names and Log_2 Fold Change values for the top 10 differentially expressed genes in comparisons listed above each Table. Positive values in the left-hand tables (orange) show

genes with increases in expression and negative values in right-hand tables (blue) show genes that decrease in expression. Non-coding RNAs have been removed.

5.3.5.b. Top 10 DEGs for *kdm6b* injected and uninjured vs. *tyr* injected and uninjured.

Comparing *kdm6b* uninjured vs *tyr* uninjured, inactive *kdm6b* knockdown neutrophils show up-regulation of *kmt2a* – a methyltransferase, *numb* – an endocytic adaptor protein, and *bnipl* – a BCL2 interacting protein involved in apoptosis (Table 5.2). Down-regulated genes include *sod3a* – a super oxide dismutase, and *jam2b* – a leukocyte adhesion molecule (Table 5.2).

Gene	logFC	adj.P.Val
kmt2a	3.10429995	0.44539498
rn7sk	2.677756	0.44539498
wtip	2.54864764	0.44539498
LOC795615	2.48037571	0.44962989
numb	2.39058671	0.48981299
dock5	2.37843525	0.46895088
si:dkey-46g23.5	2.32294246	0.47805468
zgc:172106	2.32158448	0.48981299
bnipl	2.30637258	0.46045435
LOC567622	2.23889145	0.45758201

Gene	logFC	adj.P.Val
zgc:173443	-3.6439633	0.44539498
si:dkey-10f21.4	-3.2514774	0.44539498
si:dkey-245p14.4	-3.2131615	0.44539498
fstl5	-3.0552149	0.44539498
zgc:153441	-3.0537822	0.44539498
aqp8a.2	-3.0053116	0.44539498
pomca	-2.9516323	0.48150047
sod3a	-2.9152642	0.44962989
jam2b	-2.800739	0.44539498
si:ch211-240l19.6	-2.7973565	0.44539498

Table 5.2. Top 10 DEGs for *kdm6b* injected and uninjured vs. *tyr* injected and uninjured.
Gene names and Log_2 Fold Change values for the top 10 differentially expressed genes in comparisons listed above each Table. Positive values in the left-hand tables (orange) show genes with increases in expression and negative values in right-hand tables (blue) show genes that decrease in expression. Non-coding RNAs have been removed.

5.3.5.c. Top 10 DEGs for *kdm6b* injected and injured vs. *kdm6b* injected and uninjured.

Comparing *kdm6b* injured vs. *kdm6b* uninjured, the activated (injured) neutrophils have increased expression of several inflammatory linked genes including *cfb* – part of the complement pathway, and *zgc:55413* also known as *ppt2a.*3 – a thiolester hydrolase in lysosome activity (Table 5.3). Up-regulation of myo6b and cep68 suggest potential changes to cytoskeletal structure too (Table 5.3). Down-regulated genes include *nr1d1* and *per3*, again suggesting dysregulation of circadian rhythms as seen in Table 5.1, and *baz2a* plays a part in heterochromatin structure, potentially altering chromatin confirmation and therefore gene expression (Table 5.3).

Gene	logFC	adj.P.Val
LOC564868	3.53598273	0.82967504
aqp7	3.40060988	0.82967504
si:dkey-175a17.4	3.13555231	0.82967504
ppfibp2b	3.06884072	0.82967504
zgc:55413	3.03939847	0.82967504
elna	3.01381918	0.82967504
cfb	2.95286426	0.82967504
pth1rb	2.93516967	0.82967504
myo6b	2.88549535	0.82967504
cep68	2.82733137	0.82967504

Gene	logFC	adj.P.Val
nr1d1	-3.6945119	0.82967504
LOC795615	-3.0711268	0.82967504
per3	-2.9132163	0.82967504
ca15a	-2.7468441	0.82967504
baz2a	-2.7093532	0.82967504
zgc:114200	-2.7086558	0.82967504
anxa5a	-2.5433039	0.82967504
dhrs13a.2	-2.5419112	0.82967504
zgc:86586	-2.5415629	0.82967504
zbtb16a	-2.4991375	0.82967504

Table 5.3. Top 10 DEGs for *kdm6b* injected and injured vs. *kdm6b* injected and uninjured.
Gene names and Log_2 Fold Change values for the top 10 differentially expressed genes in comparisons listed above each Table. Positive values in the left-hand tables (orange) show genes with increases in expression and negative values in right-hand tables (blue) show genes that decrease in expression. Non-coding RNAs have been removed.

5.3.5.d. Top 10 DEGs for *kdm6b* injected and injured vs. *tyr* injected and injured.

Comparing *kdm6b* injured vs *tyr* injured, up-regulated genes of interest include the histone protein component *hist2h3c, spa17* – a calmodulin binding protein, and *ralgps2* – a Ras binding protein (Table 5.4). Downregulated genes include the chemokine *ccl19b, krt93* – a cytoskeletal component and *vip* – a G-protein coupled receptor (Table 5.4).

Gene	logFC	adj.P.Val
pimr166	2.08979541	0.99598661
spa17	1.97669535	0.99598661
ralgps2	1.96782409	0.99598661
ankle2	1.86904241	0.99598661
agbl2	1.86695385	0.99598661
LOC569077	1.84445624	0.99598661
hist2h3c	1.83544208	0.99598661
vash2	1.82285299	0.99598661
slc26a4	1.77723053	0.99598661
zgc:194246	1.76422323	0.99598661

Gene	logFC	adj.P.Val
ccl19b	-3.4549003	0.99598661
cbln11	-3.3358065	0.99598661
krt93	-3.3061742	0.99598661
vip	-3.2765935	0.99598661
aldoca	-3.0761955	0.99598661
cntnap2a	-3.0064077	0.99598661
zgc:158494	-3.0023869	0.99598661
zdhhc7	-2.9803862	0.99598661
wdr89	-2.9725458	0.99598661
gck	-2.967789	0.99598661

Table 5.4. Top 10 DEGs for *kdm6b* injected and injured vs. *tyr* injected and injured.
Gene names and Log_2 Fold Change values for the top 10 differentially expressed genes in comparisons listed above each Table. Positive values in the left-hand tables (orange) show genes with increases in expression and negative values in right-hand tables (blue) show genes that decrease in expression. Non-coding RNAs have been removed.

5.3.5.e. Differentially expressed genes Top 10 summary.

These genes show that while there is not an overlap of genes between *tyr* and *kdm6b* knockdowns, there are several neutrophil/inflammation linked pathways represented in these differentially regulated genes such as calcium signalling, cytokine, chemokine and complement, and cell adhesion and cytoskeletal structure. Further investigation of these common pathways is required and expression of other genes within the pathways will help to understand how *kdm6b* knockdown is altering neutrophil function.

5.5.6 Ingenuity pathway analysis (IPA) shows trends toward down regulation of inflammatory canonical pathways following *kdm6b* knockout and injury

IPA software (Ingenuity® Systems, www.ingenuity.com) uses a library of known metabolic and signalling pathways, along with a knowledge base from peer-reviewed publications, to predict which canonical pathways are significantly activated or inhibited in user-provided datasets. IPA reports a Benjamini-Hochberg corrected p-value for canonical pathway enrichment in the user dataset (Krämer *et al.*, 2014). Zebrafish genes were converted to human orthologs prior to analysis by IPA. Using a ≥1.5-fold change in expression cut-off between datasets, the gene expression data for the *kdm6b* vs *tyr* knockdown/injury comparisons were input into the IPA software and the top 12 pathways overall and top 12 filtered for "Cellular Immune Response" presented with the red line denoting the p=0.05 threshold for significance. Orange shows an up-regulation of genes in the pathway, blue denotes down-regulation of genes and grey shows mixed differential expression with opacity of the bar showing a stronger signal.

5.5.6.a. IPA analysis of *tyr* injected and injured vs. *tyr* injected and uninjured

Looking at the canonical pathways for the *tyr* injured vs *tyr* uninjured comparison, significantly up-regulated pathways include several pathways in innate immunity such as Pattern recognition receptor signalling, antiviral innate immunity, and cytokine signalling (Figure 5.7A). There is also an upregulation of fibrosis signalling, an element of wound repair driven by transforming growth factor beta (TGF-β) signalling (Figure 5.7A) (Lichtman, Otero-Vinas and Falanga, 2016). The inflammatory terms show neutrophil specific terms expected to be involved in responses to caudal fin injury such as interferon and cytokine signalling including specifically IL-8 signalling, phagosome maturation and PAMP recognition (Figure 5.7B). These common pathways show that in control conditions, expected pathways are activated.

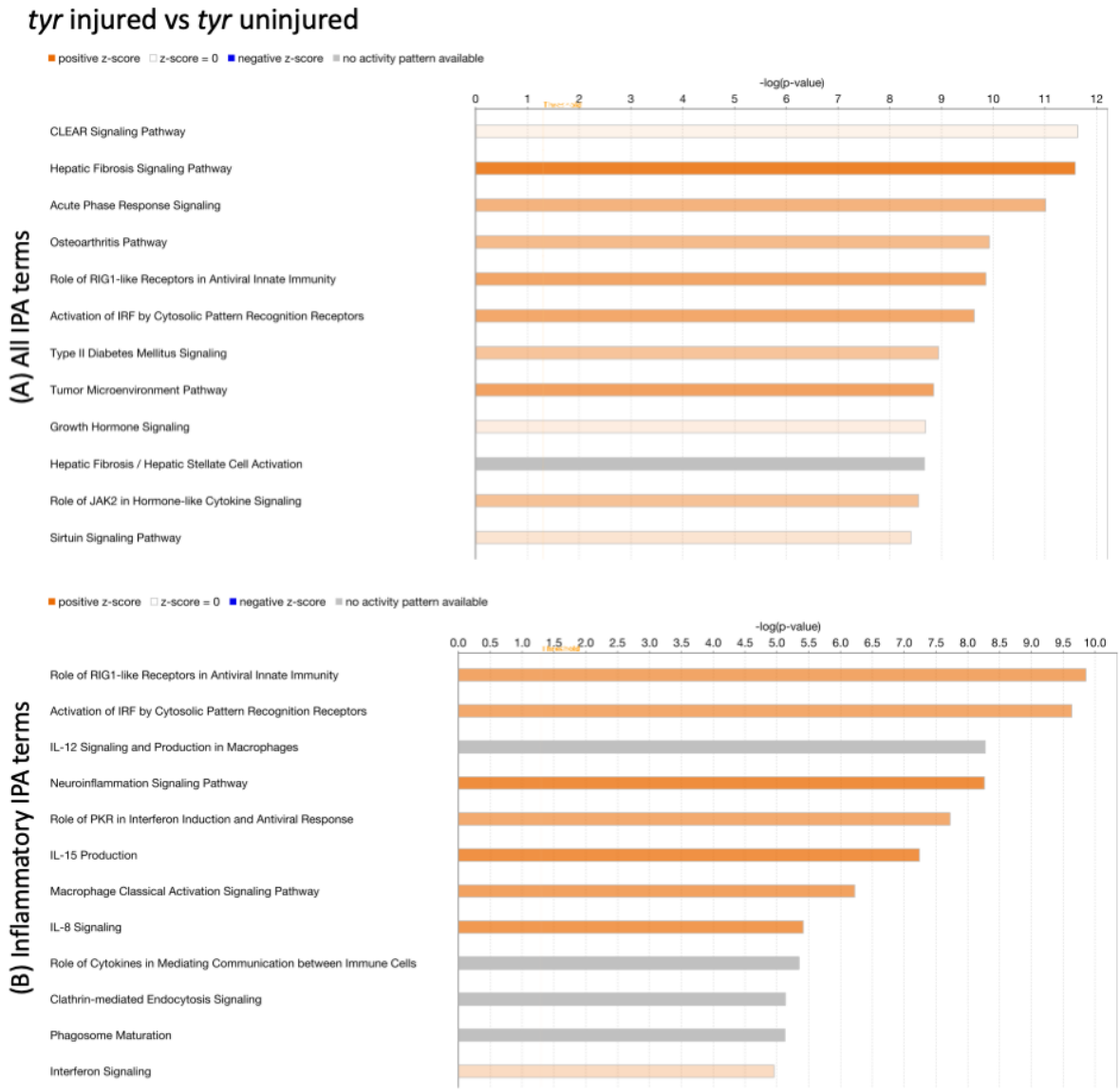

Figure 5.7. Ingenuity pathway analysis (IPA) shows trends in upregulation of pro-inflammatory pathways in *tyr* knockout control samples following and injury.

Canonical pathway analysis carried out using IPA software (Ingenuity® Systems, www.ingenuity.com). Comparing *tyr* injured vs *tyr* uninjured. Gene names converted to human orthologs from zebrafish using Babelgene package in RStudio. Bars show pathways with significant changes in expression of genes within the pathway shown as -Log_{10}(P-value), ±0.58 Log_2FC was set a threshold. Orange denotes positive changes in regulation of the pathway, grey shows both positive and negative changes and blue shows negative changes in the pathway. (A) The top 12 significant IPA canonical pathway terms based on –log_{10}(P-value), (B) top 12 significant IPA canonical pathway terms based on sorting for "Cellular Immune Response"

5.5.6.b. IPA analysis of *kdm6b* injected and uninjured vs. *tyr* injected and uninjured

Comparing *kd6mb* uninjured vs *tyr* uninjured to look at inactivated neutrophils, overall pathways show few inflammatory pathways but an overall downregulation in significant pathways. Of those pathways, neutrophil-specific phagosome maturation is significantly altered but in no clear direction, as well as circadian rhythm signalling, a pathway recently linked to neutrophil function (Figure 5.8A). Inflammatory pathways are also differentially regulated relative to the uninjured control with reductions in expression within CXCR4, IL-8, and fMLP signalling, as well up-regulation in the IL-7 pathways and nitric oxide production. Phagosome maturation and endocytosis signalling both show significant alterations in expression but with no clear direction (Figure 5.8B).

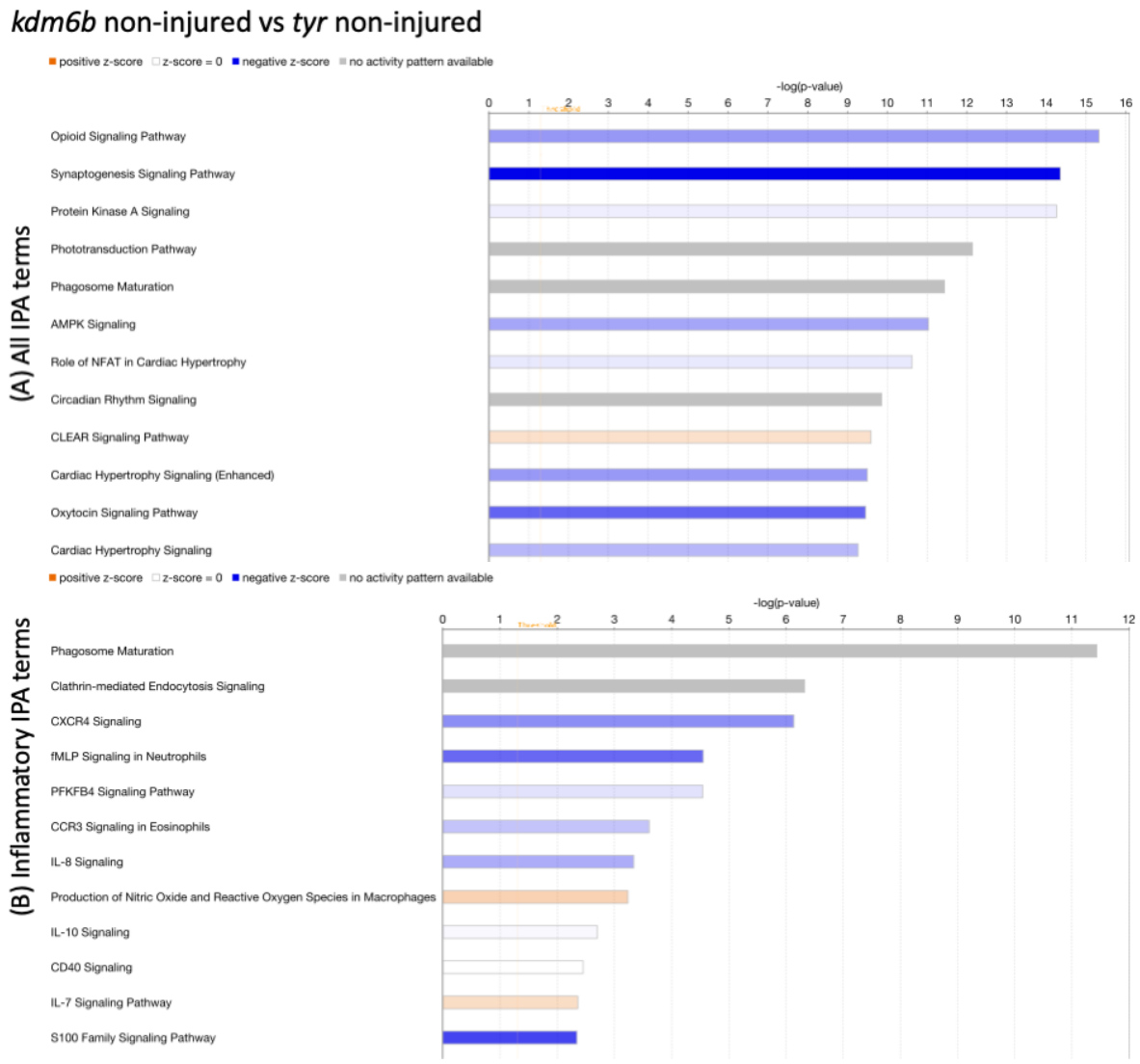

Figure 5.8. IPA shows trends of downregulation in inflammatory pathways in kdm6b knockout samples without injury relative to tyr control.

Canonical pathway analysis carried out using IPA software (Ingenuity® Systems, www.ingenuity.com). Comparing *kdm6b* injured vs *tyr* uninjured. Gene names converted to human orthologs from zebrafish using Babelgene package in RStudio. Bars show pathways with significant changes in expression of genes within the pathway shown as $-Log_{10}$ (P-value), ±0.58 Log_2FC was set a threshold. Orange denotes positive changes in regulation of the pathway, grey shows both positive and negative changes and blue shows negative changes in the pathway. (A) The top 12 significant IPA canonical pathway terms based on $-log_{10}$(P-value), (B) top 12 significant IPA canonical pathway terms based on sorting for "Cellular Immune Response"

5.5.6.c. IPA analysis of *kdm6b* injected and injured vs. *kdm6b* injected and uninjured.

Looking at *kdm6b* injured vs *kdm6b* uninjured, there are common pathways as seen in *tyr* injured vs *tyr* uninjured such as acute phase response and osteoarthritis pathway and additional pathways such as endocytosis and autophagy with many showing up-regulation (Figure 5.9A). Looking at inflammatory pathways, there is again an overlap with *tyr* injured vs *tyr* uninjured such as neuroinflammatory signalling, IL-8 signalling and RIG-1 antiviral response, but these pathways have either reduced increases in expression or down-regulation in the case of the RIG-1 response or PAMP recognition (Figure 5.9B). This begins to suggest an attenuation of inflammatory responses following *kdm6b* knockout.

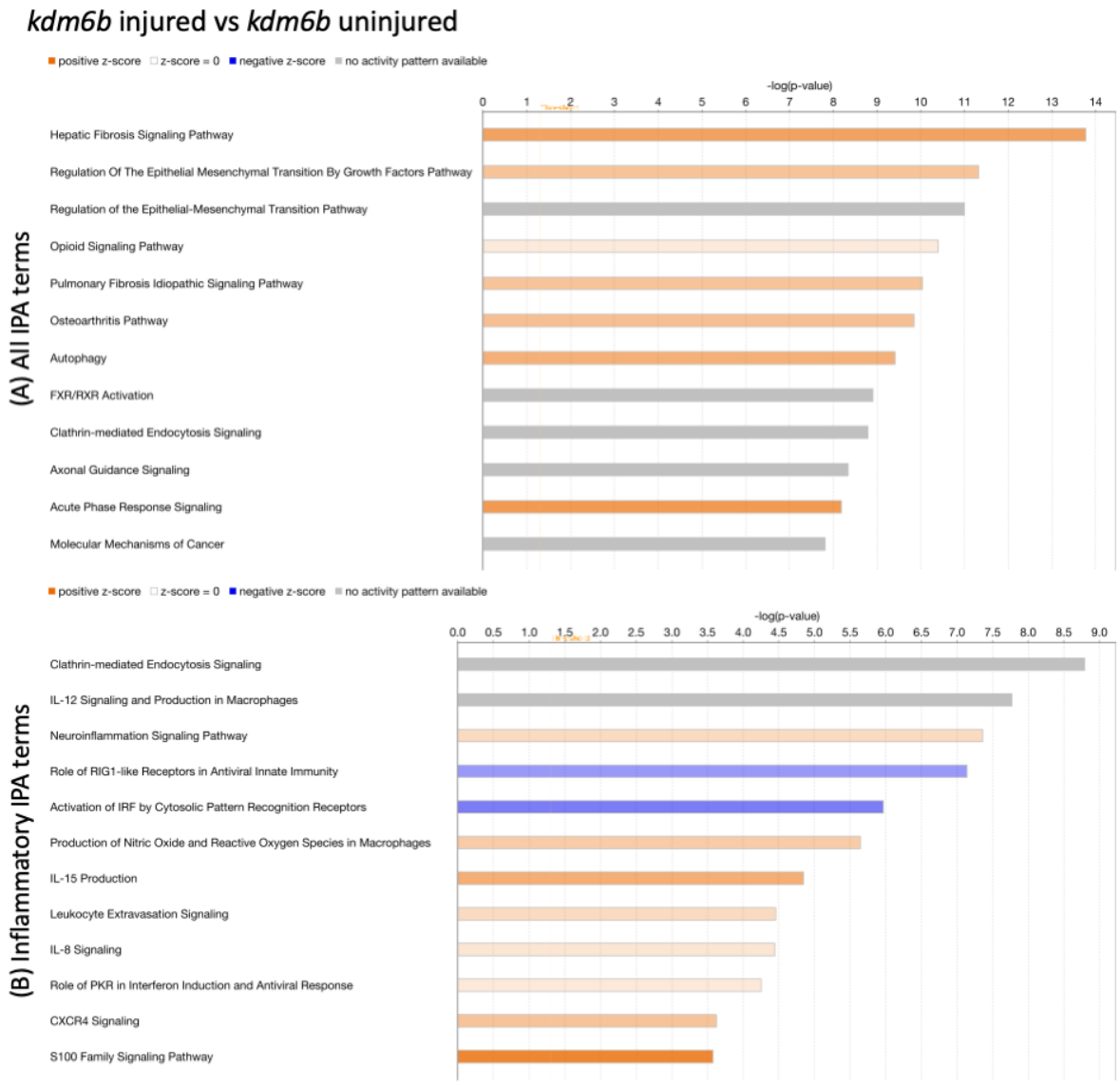

Figure 5.9. IPA shows trends of upregulation in pro-inflammatory pathways in *kdm6b* knockout samples with injury relative to *kdm6b* knockdown without injury.

Canonical pathway analysis carried out using IPA software (Ingenuity® Systems, www.ingenuity.com). Comparing *kdm6b* injured vs *kdm6b* uninjured. Gene names converted to human orthologs from zebrafish using Babelgene package in RStudio. Bars show pathways with significant changes in expression of genes within the pathway shown as -Log_{10}(P-value), ±0.58 Log_2FC was set a threshold. Orange denotes positive changes in regulation of the pathway, grey shows both positive and negative changes and blue shows negative changes in the pathway. (A) The top 12 significant IPA canonical pathway terms based on –log_{10}(P-value), (B) top 12 significant IPA canonical pathway terms based on sorting for "Cellular Immune Response"

5.5.6.d. IPA analysis of *kdm6b* injected and injured vs. *tyr* injected and injured.

The attenuation seen in 5.5.6c. is further supported by comparing *kdm6b* injured vs. *tyr* injured (Figure 5.10). When comparing all IPA terms, there is a general down-regulation of significant pathways with many interestingly overlapping with neurological pathways such as neurotransmitters and synapse pathways (Figure 5.10A). Looking at inflammation specific IPA terms, pathways previously shown to be upregulated following injury such as IL-8 signalling, CXCR4 signalling, nitric oxide production, and the anti-viral response are all downregulated further suggesting an attenuation of neutrophil effector mechanisms following *kdm6b* knockdown (Figure 5.10B).

5.5.6.e. Summary of IPA analysis

Knockdown of *kdm6b* shows an attenuation of pro-inflammatory pathways in both the injured and uninjured samples relative to *tyr* controls. Examining the most significantly altered pathways of all IPA terms the appearance of seemingly non-neutrophil terms in the IPA data may seem anomalous. However, this can be explained by differential expression of genes that are common to many signalling pathways such as G-protein coupled receptors, *nfkb* signalling, and *jak/stat* signalling. Manual inspection and curation of IPA results is vital to prevent false-positive reporting of pathways that pass the p-value cut-off based on expression of common genes alone.

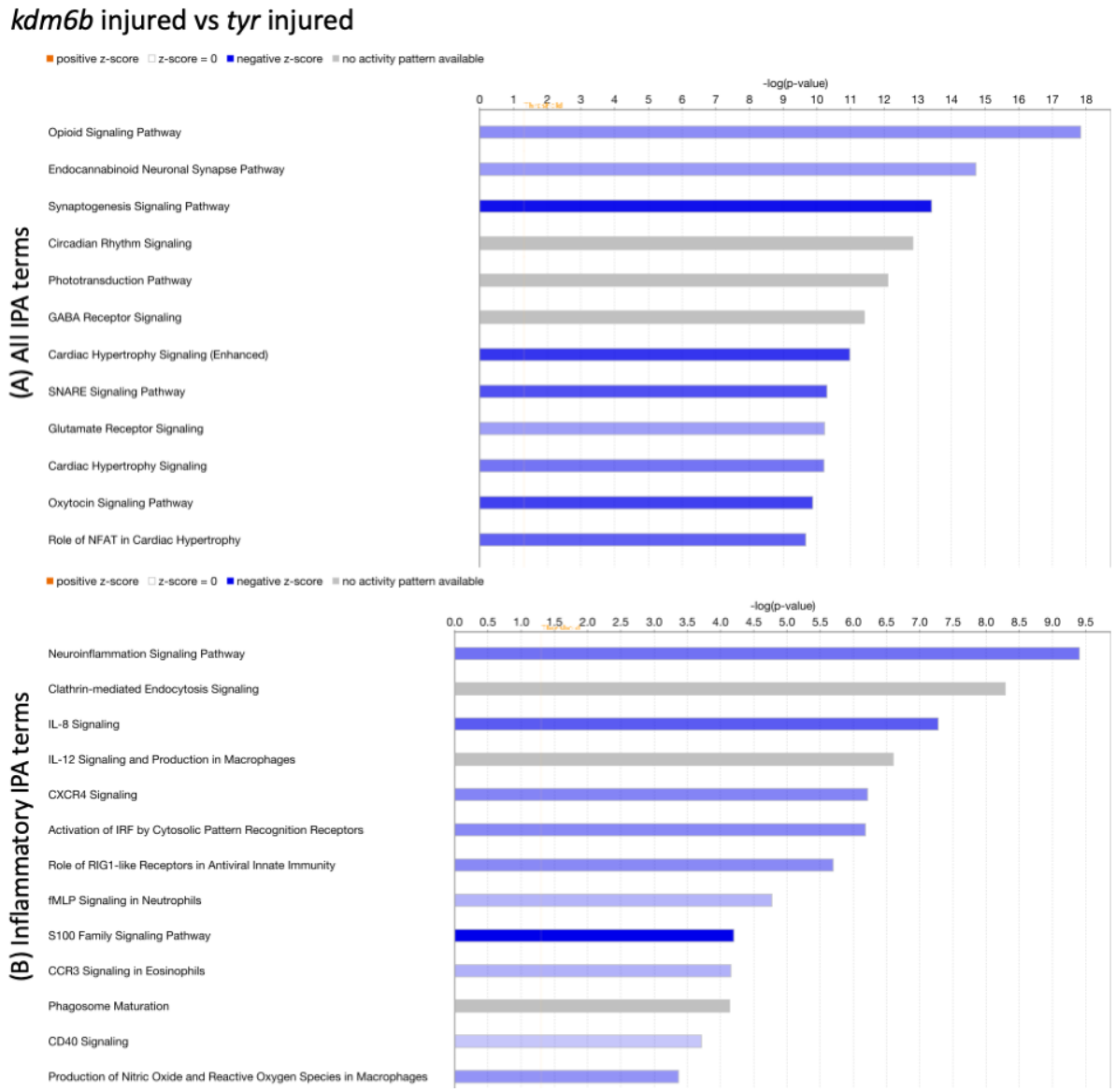

Figure 5.10. IPA shows trends in downregulation of pro-inflammatory pathways in *kdm6b* knockout samples with injury relative to *tyr* knockdown with injury.

Canonical pathway analysis carried out using IPA software (Ingenuity® Systems, www.ingenuity.com). Comparing *kdm6b* injured vs *tyr* injured. Gene names converted to human orthologs from zebrafish using Babelgene package in RStudio. Bars show pathways with significant changes in expression of genes within the pathway shown as -Log_{10}(P-value), ±0.58 Log_2FC was set a threshold. Orange denotes positive changes in regulation of the pathway, grey shows both positive and negative changes and blue shows negative changes in the pathway. (A) The top 12 significant IPA canonical pathway terms

based on $-\log_{10}$(P-value), (B) top 12 significant IPA canonical pathway terms based on sorting for “Cellular Immune Response”

5.3.7. IPA upstream analysis shows *kdm6b* knockdown significantly reduces trends in activation of pro-inflammatory pathways with and without injury.

The IPA software can also predict the upstream pathway activators (e.g. transcription factors, cell surface receptors, extracellular signalling molecules), again by applying a 1.5-fold change in gene expression cut-off and a Benjamini-Hochberg correction to p-values. Genes were converted to human orthologs from zebrafish and upstream regulator terms filtered for cytokines, G-protein coupled receptors, transcriptional regulators, and transmembrane receptors. First, comparisons of the controls *tyr* injured vs *tyr* uninjured predicts significant activation of gene expression following injury by pro-inflammatory cytokines TNF, IFNγ, IL-6, and IL-1β, and transcription factors such as STAT3, JUN and RELA (Table 5.5A). Looking at changes in inactive neutrophils by comparing *kdm6b* uninjured vs *tyr* uninjured, there is an inhibition to transcriptional regulators though none are directly linked to neutrophil function (Table 5.5B). However, this still suggests large changes in transcriptional regulation following knockdown of *kdm6b*. Comparing *kdm6b* injured vs. *kdm6b* uninjured, there is still a predicted upstream regulation of gene expression by many of the cytokines seen in the control comparison such as TNF, IFN and IL-6, though the activation z-score is lower than in the control (Table 5.5C). There is also activation of several transcription factors including CREB, FOXO1, SP1 and CREBBP. The reduced z-score suggests an attenuation of pathways relative to the control much like in the canonical pathways (Figure 5.5). This reduction in neutrophil effector activity is further shown in the *kdm6b* injured vs *tyr* injured, with inhibition of pro-inflammatory extracellular signalling regulators including IFNγ, TNF and IL1β all seen to be activated in the control (Table 5.5D). Within the *kdm6b* injured vs *tyr* injured comparison, transcriptional regulators are also inhibited, including pathways that were activated in the *tyr* controls such as TP53 and RELA. Overall, these data show that while pro-inflammatory pathways are activated following *kdm6b* knockdown, these pathways are significantly reduced relative to the *tyr* controls, potentially reducing the ability of neutrophils to clear infectious threats relative to in *tyr* controls. Further investigation of specific genes in these pathways are now required to identify where the changes are occurring and validate the bioinformatics analysis.

(A) *tyr* injured vs *tyr* uninjured

Upstream Regulator	Expr Log Ratio	Molecule Type	Predicted Activation State	Activation z-score	p-value of overlap
TNF		cytokine	Activated	5.226	3.57E-29
IFNG		cytokine	Activated	5.997	6.93E-21
IL1B	1.974	cytokine	Activated	5.047	1.26E-19
OSM		cytokine	Activated	4.556	7.54E-19
IL6		cytokine	Activated	6.234	4.36E-18
STAT3	1.119	transcription regulator	Activated	4.681	7.09E-18
RELA	0.799	transcription regulator	Activated	4.262	1.19E-17
TP53	0.083	transcription regulator	Activated	2.178	4.16E-16
TNFSF11		cytokine	Activated	3.444	4.93E-16
JUN	0.575	transcription regulator	Activated	2.935	2.22E-15

(B) *kdm6b* uninjured vs *tyr* uninjured

Upstream Regulator	Expr Log Ratio	Molecule Type	Predicted Activation State	Activation z-score	p-value of overlap
HNF4A	-1.691	transcription regulator	Inhibited	-2.953	7.71E-34
CREB1	-0.723	transcription regulator	Inhibited	-3.06	3.11E-23
FEV	-0.559	transcription regulator	Inhibited	-4.783	6.06E-20
SMARCA4	-0.226	transcription regulator	Inhibited	-4.847	2.84E-16
NEUROG3	0.296	transcription regulator	Inhibited	-4.44	4.05E-15
NEUROD1	-1.121	transcription regulator	Inhibited	-4.03	1.72E-13
FOXO1	1.716	transcription regulator	Inhibited	-2.464	2.5E-13
SP1	0.334	transcription regulator	Inhibited	-3.418	4.58E-13
OTX2		transcription regulator	Inhibited	-2.375	5.19E-13
NFE2L2	1.378	transcription regulator	Inhibited	-5.091	1.63E-12

(C) *kdm6b* injured vs *kdm6b* uninjured

Upstream Regulator	Expr Log Ratio	Molecule Type	Predicted Activation State	Activation z-score	p-value of overlap
TNF		cytokine	Activated	3.157	2.11E-23
HNF4A	0.84	transcription regulator	Activated	3.375	4.06E-20
IFNG		cytokine	Activated	2.439	1.32E-19
SP1	0.456	transcription regulator	Activated	2.248	2.4E-16
OSM		cytokine	Activated	2.367	1.88E-15
FOXO1	2.304	transcription regulator	Activated	2.964	1.07E-13
IL6		cytokine	Activated	3.4	2.06E-12
CREBBP		transcription regulator	Activated	2.075	2.91E-12
CREB1	0.639	transcription regulator	Activated	2.135	2.72E-11
TWIST1	0.458	transcription regulator	Activated	2.516	1.03E-10

(D) *kdm6b* injured vs *tyr* injured

Upstream Regulator	Expr Log Ratio	Molecule Type	Predicted Activation State	Activation z-score	p-value of overlap
IFNG		cytokine	Inhibited	-4.387	4.5E-21
TNF		cytokine	Inhibited	-3.786	5.24E-21
SP1	0.188	transcription regulator	Inhibited	-4.775	1.19E-14
TP53	0.112	transcription regulator	Inhibited	-3.735	1.72E-12
IL1B	-2.211	cytokine	Inhibited	-3.244	6.71E-12
REST		transcription regulator	Activated	4.691	7.69E-12
FEV	-0.484	transcription regulator	Inhibited	-3.787	1.8E-11
NEUROG3	0.182	transcription regulator	Inhibited	-3.578	3.59E-11
NEUROD1	-1.207	transcription regulator	Inhibited	-3.97	4.46E-11
RELA	-0.427	transcription regulator	Inhibited	-3.53	5.51E-11

Table 5.5. IPA Upstream pathways shows trends of inhibition in pro-inflammatory pathways in *kdm6b* knockdown and injury.

(A-D) Tables of upstream gene pathways predicted by IPA to be altered following *kdm6b* knockdown relative to tyr knockdown controls. Comparisons shown above each Table. Gene names converted to human from zebrafish using Babelgene in RStudio. P values calculated by IPA based on overlap of common downstream pathways. Pathways sorted for Inflammatory terms - transcriptional regulators, cytokines, G-protein coupled receptors and transmembrane receptors. Orange shows activated pathways and blue shows inhibited pathways.

5.3.8. Genes shown to be up regulated in neutrophil activation trend toward differential expressed in *kdm6b* knockouts.

To further investigate the genes involved in the pathways shown to be dysregulated using IPA, published panels of genes implicated in neutrophil lifecycle and activation were analysed. During the neutrophil lifecycle, several transcription factors were implicated to control specific stages in a murine model including maturation, activation, and survival (Khoyratty *et al.*, 2021). Secondly, Khoyratty *et al.,* (2021) identified genes that are differentially regulated following activation and identified the chromatin states of these genes. These genes were converted from murine to zebrafish orthologs and box plots generated from the *kdm6b* knockdown RNAseq dataset using CPM values. No statistics were performed due to the data only being two independent repeats. Several genes were lost either due to lack of zebrafish orthologs or a lack of coverage in the dataset.

5.3.8.a. Expression of genes regulating neutrophil maturation do not change in *kdm6b* knockdown.

Maturation is the process where neutrophils migrate from the bone marrow and into the circulation where they can monitor the body for threats. Runx1 and Klf6 were identified as regulators of neutrophil maturation (Khoyratty *et al.*, 2021). In the *kdm6b* knockdown RNAseq data set, *klf6a* was the only maturation gene identified. *klf6a* was seen to have relatively similar expression across the 4 treatment conditions ranging between 140 and 160 CPM on average without injury, and 125 and 130 on average with injury (Figure 5.11A).

5.3.8.b. Genes regulating neutrophil activation present a varied expression pattern following *kdm6b* knockdown.

When neutrophils sense a threat, they are activated to carry out pro-inflammatory action to clear the threat. To drive this change in neutrophil activity, Relb, Irf5, Junb were shown to be essential transcription factor genes (Khoyratty *et al.*, 2021). Overall, these activation related genes also showed little change due to the knockdown with and without injury (Figure 5.11B). Gene expression did increase with injury as expected due to activation of neutrophils. Looking at specific genes, Junb paralogs *junba* and *junbb* both showed similar CPM between control and *kdm6b* knockout without injury and *junbb* showed little change with injury. With injury *junba* showed a reduction of 40 CPM to 30 CPM in injury when *kdm6b* was knocked down.

irf5 also showed little change with and without injury between *kdm6b* knockdown and control.

5.3.8.c. Expression of genes regulating neutrophil survival is altered in *kdm6b* knockdown.

Neutrophil survival pathways delay spontaneous apoptosis and allow neutrophils to continue pro-inflammatory function. Genes implicated as regulators of survival include *relb* and *rfx*2 (Khoyratty *et al.*, 2021). *rfx2* was present in the *kdm6b* knockdown dataset and showed little change in *tyr* with and without injury and *kdm6b* without injury (Figure 5.11C). In *kdm6b* injured there was a small drop in *rfx2* expression, but the two repeats had a lot of variation, however this may suggest potential small changes to neutrophil survival such as increased neutrophil apoptosis in the *kdm6b* knockdown following activation due to lower levels of *rfx2* to maintain survival pathways, instead triggering pro-apoptotic pathways.

5.3.8.d. Expression of genes upregulated with open chromatin in neutrophil activation show trends towards reduction in *kdm6b* knockdown.

When neutrophils are activated, there is a change in cell phenotype to allow for neutrophil effector function to be carried out. To do this, the transcriptome of the neutrophil is changed and chromatin at key genes is opened to allow for transcription of previously repressed genes. Khoyratty *et al,* (2021) identified up-regulated genes with open chromatin in neutrophil activation using a combination of assay for transposase-accessible chromatin with sequencing (ATAC-seq) and RNAseq, I cross-referenced these genes with the *kdm6b* knockdown RNAseq data. Of the up-regulated genes identified by Khoyratty *et al.,* (2021) , *il1b, tnfb* and *abca1a* and *abca1b* were present in the *kdm6b* knockdown dataset and CPM counts were plotted (Figure 5.11D). CPM values for *il1b* and *tnfb* were relatively low, but in the *kdm6b* knockdown the increase in CPM seen with injury in the *tyr* knockdown was lost, remaining at baseline for both *il1b* and *tnfb*. Both IL-1β and TNF are essential pro-inflammatory cytokines, being released to signal to other neutrophils (and other leukocytes) and to promote inflammation by activating genes such as *nfkb*. A reduction of expression of *il1b* and *tnf* in the *kdm6b* knockdown will therefore have important consequences for the inflammatory process following tail fin injury. Of the other up-regulated genes in neutrophil activation identified by Khoyratty *et al.,* (2021), *Abca1* has two zebrafish paralogs, both of which were present in the *kdm6b* knockdown dataset. *abca1a* does not increase following

injury in the *kdm6b* samples but does in the control, whereas *abca1b* shows no change between *kdm6b* knockdown and control following injury. ABCA1 is an ATP-binding cassette that regulates lipid transport across the plasma membrane and potentially formation of the inflammasome and NETosis in atherosclerosis (Westerterp *et al.*, 2018).

5.3.8.e. Genes downregulated with closed chromatin in neutrophil activation show trends of differential regulated in *kdm6b* knockdown.

Downregulated genes with closed chromatin were also identified following neutrophil activation by Khoyratty *et al.*, (2021). Of these downregulated genes, 6 were found in the *kdm6b* knockdown dataset *rdh14a, stard4, polr3k, fam20a, rdh14b* and *chst12a* (Figure 5.11E). Out of the six genes, *rdh14a, polr3k* and *fam20a* showed little difference between each sample. After activation through injury in the zebrafish model, the published data suggests these genes would be downregulated (Khoyratty *et al.*, 2021). Examining the other down regulated and closed chromatin genes (Khoyratty *et al.*, 2021), *stard4,* shows a small increase in expression following *kdm6b* knockdown with and without injury. There is also a loss of the increase in expression seen in *rdh14b* following injury in *kdm6b* knockdown. In the *kdm6b* knockdown, *chst12a* expression is much higher without injury but that increase is lost following injury which would be expected as neutrophils become activated, though the CPM values are particularly low. Of the three differentially regulated genes, two are upregulated and one is downregulated with very small changes, whether these changes are biologically relevant remains unanswered. STARD4 is a lipid transporter, RDH14 is a retinol dehydrogenase and CHST12 is a sulfotransferase, understanding how these relate to neutrophil function will help to understand if these changes alter neutrophil activation.

5.3.8.f. Summary: Genes associated with neutrophil activation show trends towards downregulated following *kdm6b* knockdown and tailfin injury.

These data further support the IPA data showing a reduction in pro-inflammatory genes following neutrophil activation (Figure 5.11.D). Across the neutrophil lifecycle though, there is little difference in the genes that regulate the three stages maturation, activation, and survival (Figure 5.11.A-C). However, without statistical analysis conclusions cannot be drawn and the quality of the dataset limits the genes present. Instead, further validation should be carried out by performing qRT-PCR but there was not time for this in this project.

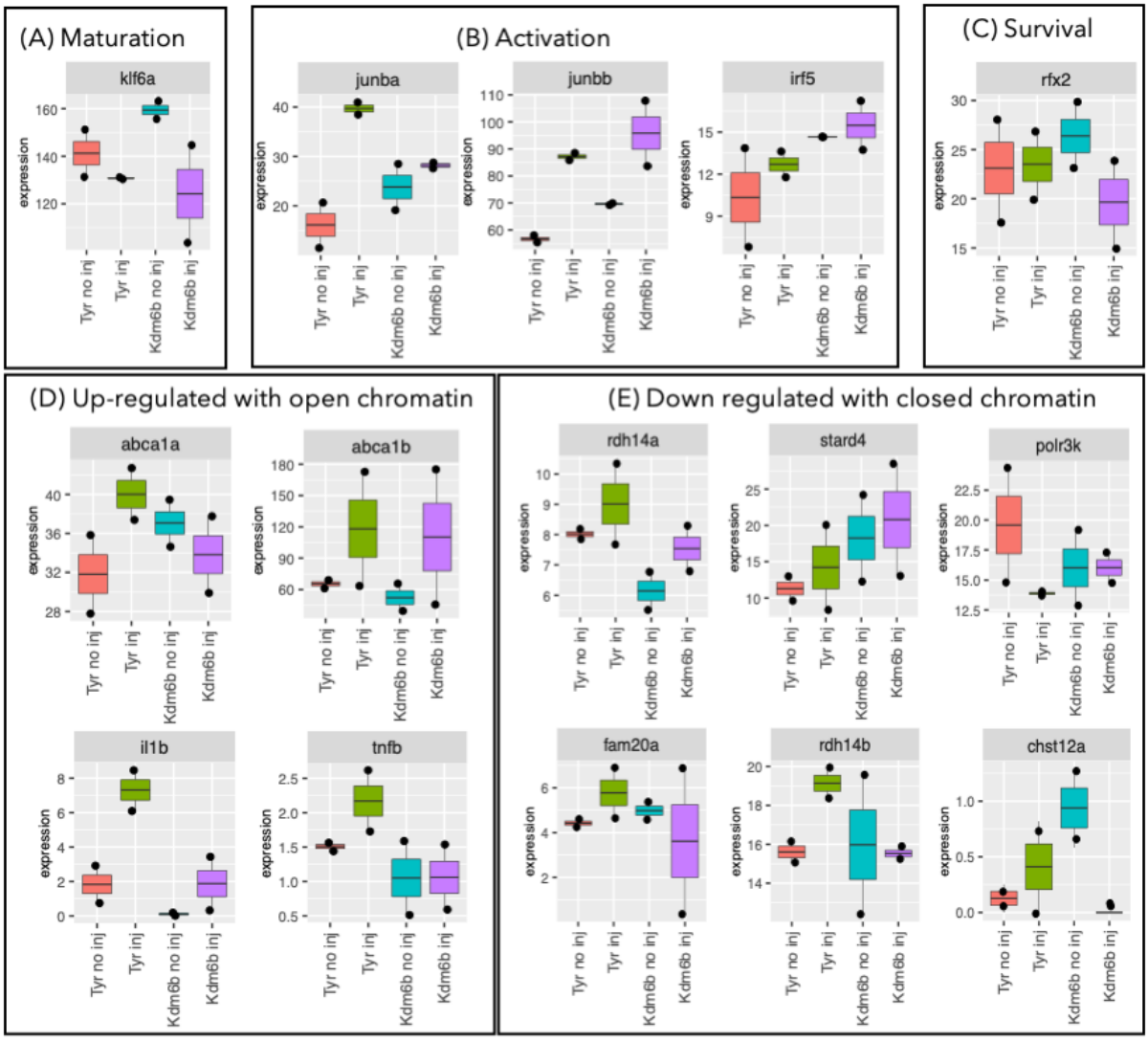

Figure 5.11. Genes shown to be up regulated with open chromatin during the neutrophil life cycle and activation trend towards differential expression following *kdm6b* knockdown and tailfin injury.

Khoyratty *et al.*, (2021) identified genes essential to specific stages of the neutrophil life cycle using a murine model. These genes were converted to zebrafish orthologs, and CPM values presented in box plots in each of the treatment conditions. (A) Genes essential to maturation (B) Genes essential to activation (C) Genes essential to survival. During activation of neutrophils Khoyratty *et al.,* (2021) also analysed gene expression and chromatin confirmation by RNAseq and ATAC-seq respectively. (D) shows CPM values in box plots in each treatment condition of genes identified to have open chromatin and increased expression by Khoyratty *et al.,* (2021) during neutrophil activation. (E) Shows CPM values in box plots in each treatment condition of genes identified to have closed chromatin and decreased

expression by Khoyratty *et al.,* (2021) during neutrophil activation. Some genes were excluded due to lack of zebrafish orthologs or low counts in the dataset. All murine genes converted to zebrafish genes using Babelfish in RStudio. 2 independent repeats.

5.3.9. Transcription factors up regulated following bacterial exposure may also be up-regulated following injury following *kdm6b* knockdown.

Following either PMA treatment or *E. coli* treatment, *in vitro* human neutrophils undergo a series of chromatin remodelling events (Denholtz *et al.*, 2020). These findings were incredibly important in the field, proving that even when neutrophils are terminally differentiated, they are dynamic cells capable of altering their chromatin profile to alter the transcriptome depending on the immune challenge the cell encounters to return the body to homeostasis. These events occur at the loci of proinflammatory genes and transcription factor elements. Of the loci identified following PMA treatment or E. coli treatment, *spi1b, fosl2, cebpb* and *jund* were identified as zebrafish orthologs of these genes in the *kdm6b* knockdown RNAseq dataset. These were transcription factors implicated with the activation of neutrophils following *E. coli* treatment (Figure 5.12). In *kdm6b* knockdown, *spi1b* – the gene that encodes PU.1 – was increased without injury and showed increased average expression in injury while in the control injury caused a decrease in *spi1b* (Figure 5.12A). In *kdm6b* knockdown, *cebpb* showed no difference compared to the control with or without injury (Figure 5.12B). Without injury, *fosl2* showed no difference between *kdm6b* and control, but following injury showed a 50% attenuation to the increase in expression seen in the control (Figure 5.12C). The final transcription factor *jund* showed very low CPM values but showed an increase in expression in the *kdm6b* knockdown both with and without injury (Figure 5.12D). These data suggest little change to the activation pattern seen with *kdm6b* knockdown compared to published data on *E. coli* infection, with a pattern of increasing expression following injury as expected due to neutrophil activation. Again, the lack of statistics due to only providing two independent repeats means further validation is required to draw true conclusions as well as investigation of genes not detected in the *kdm6b* knockdown RNAseq.

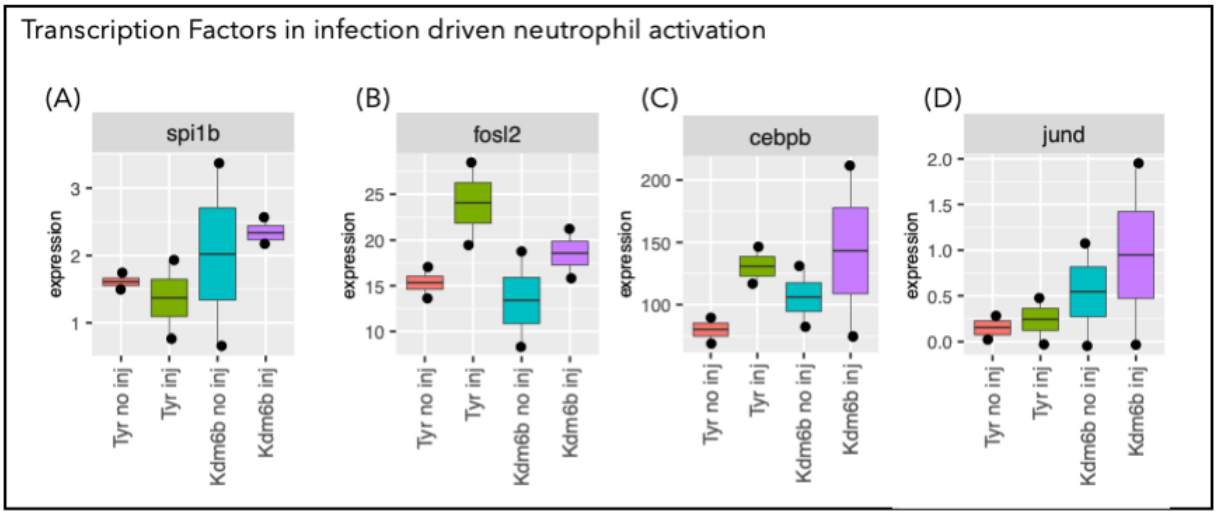

Figure 5.12. Transcription factors up-regulated following bacterial exposure may also be up-regulated following injury following *kdm6b* knockdown.

Denholtz *et al.,* (2020) identified genes with altered chromatin following neutrophil activation following PMA and *E. coli* treatment *in vitro*. These genes were converted to zebrafish orthologs using the Babelgene package for RStudio and CPM values presented in box plots in each of the treatment conditions. Only *E. coli* genes were extracted from the dataset and are (A) spi1b – the gene that encodes PU.1, (B) fosl2, (C) cebpb, and (D) jund. All human genes converted to zebrafish genes using Babelfish in RStudio. 2 independent repeats.

5.3.10. Genes associated with R848 treatment of neutrophils show some trends in differential regulation following *kdm6b* knockdown.

Chapter 3 discusses the role the drug R848 plays on *in vitro* human neutrophils and explores the role R848 plays on neutrophils *in vivo*. A panel of genes was produced based on the genes implicated in R848 dependent activation of neutrophils *in vitro* (Zimmermann *et al.*, 2015). The expression of these genes was analysed in the *kdm6b* knockdown RNAseq dataset to look for overlapping pathways with the aim to discover common pathways that could further explore how neutrophil chromatin remodelling can be altered by pharmacological interventions. KDM6B is a demethylase that targets H3K27me3, removing repressive enhancer marks. R848 dependent activation of EP300 and CREBBP can result in addition of the active enhancer acetylation mark H3K27 in *in vitro* human neutrophils (Zimmermann *et al.*, 2015). R848 may therefore be able to be used in combination with KDM6B modulation to promote reactivation of pathways related to KDM6B deficiency. To test if this is possible, R848 associated gene expression was analysed in the kdm6b knockdown dataset. Genes were subcategorised into receptors (*tlr4, tlr7* and *tlr8*), cytokines (*il6, tnf, il12b, il10, il1ra* and *csf3*), transcription factors (*nfkb1, nfkb2, rela, sp1b, cebpb* and *mapk11*), and chromatin remodelling enzymes (*ep300, crebbp* and *brd4*) and converted to zebrafish orthologs and searched for in the *kdm6b* knockdown RNAseq dataset to produce boxplots of CPM values. Where cytokines were not detectable, receptors were used as an estimated measure of expression.

5.3.10.a. Expression of receptors agonised by R848 does not change or genes are not detectable in the *kdm6b* dataset.

R848 signals through TLR7 and TLR8 with some action through TLR4. Looking at the receptors, *tlr4ba* was the only detectable receptor, but showed very little expression (Figure 5.13A). In *kdm6b* knockdown, *tlr4* expression did not increase following injury in the *kdm6b* knockdown but did in the control. As TLR8 is the main receptor for R848 signalling in neutrophils, this does not reveal a lot about the signalling pathway in *kdm6b* knockdown as *tlr8* paralog expression was not detected in the dataset.

5.3.10.b. Expression of several cytokines linked to R848 activation of TLR8 are altered by *kdm6b* knockdown.

From the selected cytokine panel, four were detectable (Figure 5.13B). Most interesting of those was *tnfb*, a major inflammatory regulator. *tnfb* was lower in the *kdm6b* knockdown and did not increase with injury suggesting *kdm6b* alters pro-inflammatory activity. IL-12B is a cytokine in T-cell and natural killer cell activation linked to the R848 pathway. In the *kdm6b* knockdown dataset, *il12ba* was higher in the *kdm6b* knockdown overall but did not increase with injury, but in both instances, CPM was very low. No change was seen between control and *kdm6b* knockdown for *il6r* (receptor gene used in place of *il6*) and *csf3b*.

5.3.10.c. Expression of transcription factors activated by R848 binding TLR8 are trend towards reduction following *kdm6b* knockdown.

Five transcription factors known to be activated by R848 were detected (Figure 5.13C). Minimal change was seen in the *nfkb2* and *cebpb* expression between *kdm6b* knockdown and *tyr* control with and without injury, the only difference being that the *nfkb2* expression increase was smaller in the *kdm6b* injury. This reduction could be connected to decreases in *tnf* expression. There was a decrease in expression of *mapk11* following *kdm6b* knockdown in both the uninjured and injured relative to the control. With *kdm6b* knockdown, *spi1b* showed increased expression relative to the *tyr* control and an increase following injury whereas the *tyr* control shows a decrease. *kdm6b* knockdown shows an increase in *rela* expression without injury relative to control, but that change is lost with injury. This shows that several pro-inflammatory transcription factors are altered by *kdm6b* knockdown.

5.3.10.d. Expression of the chromatin remodelling enzyme *brd4* is altered by *kdm6b* knockdown.

Out of the chromatin remodelling enzymes identified to play a role in the downstream actions of R848, *brd4* was identified in the *kdm6b* knockdown dataset and showed increased expression following *kdm6b* knockdown with and without injury (Figure 5.13D). The lack of *crebbp* and *ep300* paralogs in the dataset limit the conclusions that can be drawn, however analysis of *crebbp* and *ep300* targets are more interesting in the context of *kdm6b* activity.

5.3.10.e. Summary: Genes involved in the R848 driven activation of neutrophils may be dysregulated by kdm6b knockdown.

Taken as a whole, these data show some dysregulation of R848 related pathways, but the changes are very small and only affect certain genes. There is a suggestion that *kdm6b* knockdown regulates R848-driven genes such as *tnf* and *il1b.* Perhaps there is some overlap in pathways, but further work is needed to identify potential druggable targets with R848 or other chromatin remodelling chemical compounds.

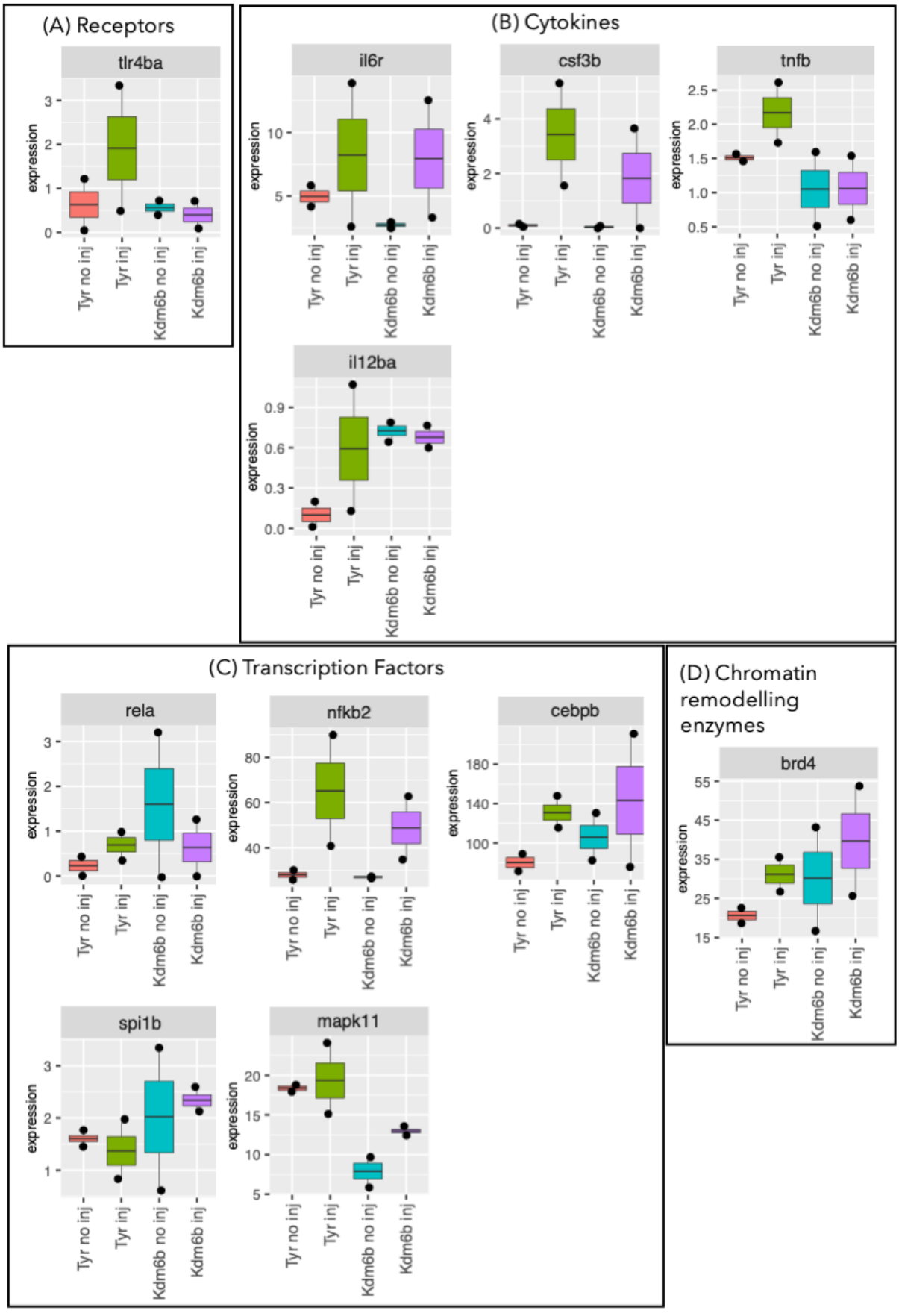
(A) Receptors
tlr4ba
(B) Cytokines
il6r
csf3b
tnfb
il12ba
(C) Transcription Factors
rela
nfkb2
cebpb
spi1b
mapk11
(D) Chromatin remodelling enzymes
brd4
expression
Tyr no inj
Tyr inj
Kdm6b no inj
Kdm6b inj

Figure 5.13. Expression of genes in *kdm6b* knockdown RNAseq previously shown by Zimmerman *et al.,* (2015) to be involved in neutrophil activation of R848.

Gene expression shown as counts per million. Treatment shown on the x-axis (A) Transmembrane receptors for R848 - TLR7 and 8 not in this dataset (B) Cytokines and chemokines released by neutrophils following R848 treatment – cytokine receptors used if cytokines are not in the dataset (C) Transcription factors linked to R848 activated genes and loci (D) Chromatin remodelling enzymes in R848 driven signalling. All human genes converted to zebrafish genes using Babelfish in RStudio. 2 independent repeats.

5.4. Discussion

INTACT BirA/Streptavidin pulldown was used to extract neutrophil nuclear RNA for RNA sequencing following the CRISPR/Cas9 targeted knockdown of the chromatin remodelling KDM6B from injured and uninjured 3 dpf zebrafish larvae. Analysis of the neutrophil-specific transcriptome by gene differential expression analysis following enzyme knockdown and injury produced the first available dataset of its type for neutrophils to increase the knowledge of how chromatin remodelling regulates neutrophil function.

To confirm a pure sample of neutrophils and lack of contamination with other cell types, RT-PCR consistently showed the neutrophil nuclei to have high *mpx* gene expression and the excess flow-through to have low *mpx* expression, confirming an enrichment for neutrophils. *itga2b* was used as a non-neutrophil marker and no transcript was detected in the neutrophil nuclear RNA. Identification of a non-neutrophil gene proved difficult, with many of the initially attempted genes giving positive readouts due to low level expression in neutrophils as shown by published datasets and may prove an issue if adapting the method to poorly classified cell types (Rougeot *et al.*, 2019). While small amounts of excess non-neutrophil nuclei may be retained, this was determined to be adequate for RNAseq extraction for library preparation.

Overall, the INTACT method does not necessarily provide a straightforward alternative to isolating specific zebrafish cell populations compared to techniques such as FACS as suggested by previous work. However, here in Sheffield, preparation of neutrophils for RNAseq from zebrafish has not been possible at the FACS facility and therefore INTACT would still be the preferred method for such a complex experiment in the future. Setting up the INTACT method is complicated and requires specific equipment and conditions but is manageable once optimised. For example, a cold room must be close to the wet lab space and optimising the protocol to get to the stage of preparing samples for RNA sequencing took over a year. However, once the experimental set up is fully optimised, RNA extraction can be completed in 1-2 days. It is also worth noting that injection of the guide/Cas9 mix was into the yolk of the embryo at the single-cell stage. While this method can lead to efficient knockdown, it would be recommended that in future experiments, an effort should be made to inject into the single cell of the embryo to increase the chances of edits being made at the single-cell

stage, before the first cell division, and mutations being maintained in the animal (Terzioglu *et al.*, 2020).

Quality control (QC) reports of the RNA submitted for sequencing showed low RNA concentrations and poor RNA quality for several samples. Some of these scores meant that one of the three independent repeats was discarded from the sequencing run rather than preparing another repeat. The decision not to attempt another repeat was made due to several factors. The main factor was the time it had taken to generate the initial three repeats relative to the time left on the project. The adult zebrafish crossed to produce the embryos for the experiment did not always lay enough eggs to reliably generate enough knockdown embryos for the four groups in each independent repeat. 100+ embryos per group are recommended in published work but at times the number used was closer to 50 with these repeats reflected in the concentrations retrieved (Trinh *et al.*, 2017). As neutrophils have relatively low quantities of RNA this becomes even more of an issue compared to other cell types. Low concentrations often generate lower RIN scores and so may explain the correlation in the QC reports between low concentration samples and RIN scores. If the fish laid sufficient eggs each time, three repeats could be prepared in 2-3 weeks, instead this took 2-3 months – potentially due to zebrafish line or aquarium conditions at the time of the work. RNA sequencing data from two repeats can still produce preliminary data that can be validated by methods such as qRT-PCR and a final repeat can be added later if required (although this may include batch variation into the down-stream analysis). Despite the issues, post-sequencing QC showed good quality reads with very few errors.

Despite the pre-sequencing reports, bioinformatics analysis of *kdm6b* knockdown neutrophils did generate interesting data. Analysis of the data in PCA plots showed clustering based on the sample type. Spread of differentially expressed genes in mean difference plots showed the spread of differentially expressed genes was dependent on knockdown and injury but no significant genes due to the use of only 2 independent repeats for the sequencing run. Ranking differentially expressed genes based on fold-change between treatments showed few genes of interest but did show a very different pattern of differentially expressed genes between *kdm6b* and *tyr* controls with and without injury, suggesting that *kdm6b* knockdown without injury caused a global change in the neutrophil transcriptome which then led to

further alterations following injury. However, in this case looking at altered pathways may present more insight than looking at specific genes as an overall goal of the project is to look at how chromatin remodelling alters neutrophil activity and effector functions, not just gene expression.

Pathway analysis using IPA software showed a significant down regulation of many pathways in the *kdm6b* knockdown with and without injury relative to *tyr* controls. Of most interest here are the inflammatory pathways, though other pathways were also analysed. Comparing *kdm6b* uninjured to *tyr* uninjured neutrophils, notable differentially regulated pathways including phagosome maturation, ROS generation, and cytokine signalling including fMLP, IL-7, 8 and 10. This suggests that before activation or exposure to an inflammatory stimulus, *kdm6b* knockdown downregulates pathways essential to neutrophil function meaning that these neutrophils could be less prepared to deal with immune challenge than control neutrophils. Comparing *kdm6b* injured to *tyr* injured neutrophils, there is a significant downregulation of inflammatory pathways. Again, notable differentially regulated pathways include phagosome maturation, ROS generation, and chemokine cytokine signalling including fMLP and IL-8. Other notably altered pathways are downstream responses of PAMP signalling and RIG-1 receptor signalling, and endocytosis. These pathways suggest that in *kdm6b* knockdown, neutrophil responses to inflammation are reduced with cells unable to return the body back to homeostasis. Previous data using CRISPR/Cas9 knockdown showed that *kdm6b* knockdown neutrophils were recruited to the wound as normal but showed a reduction in inflammation resolution. These data support the hypothesis that the retention of neutrophils seen *in vivo* was due to an attenuation of neutrophil effector mechanisms preventing the initiation of inflammation resolution (Chapter 4). If *kdm6b* knockdown results in a reduction in endocytosis and a reduction in PAMP sensing, uptake of threats may be reduced. If then ROS production is reduced and phagosome maturation altered, neutrophils may not be able to break down the infectious threats that are phagocytosed, reducing clearance of infection, and maintaining inflammation. Injection of fluorescent beads or bacteria into *kdm6b* knockdown zebrafish larvae and analysis of both engulfment and bacterial killing will help to answer these questions.

Further use of IPA identified the IL-1β and TNF pathways had significantly reduced activity upstream of differentially expressed genes in the *kdm6b* knockdown and injury compared to *tyr* knockdown controls. Both are essential to neutrophil activation and effector functions, but also shown to be regulated by KDM6B in neutrophils (Chen *et al.*, 2018). Upstream analysis also identified RELA/NF-κBp65 transcription factor pathways to be reduced. RELA acts as a potent pro-inflammatory transcription factor as part of the NF-κB family and so reduction in the pathway will reduce processes such as cytokine release and even promote anti-inflammatory pathways (Marwick *et al.*, 2018). Reduction in these pathways further supports the hypothesis that a reduction in neutrophil effector function driven by the loss of *kdm6b* contributes to a decrease in neutrophil inflammation resolution. IPA does have some limitations as it is predictive analysis based on differentially expressed genes in the dataset, and so validation of specific genes and processes is required before definitive conclusions are drawn.

To analyse expression of genes essential to neutrophil function and pathways highlighted by previous analysis, several panels of genes were identified based on the literature. Choosing published lists prevented bias that could be created by cherry picking genes from the data set. Genes involved in the key phases of neutrophil maturation, activation, and survival were shown to be largely unchanged following *kdm6b* knockdown compared to controls. It was only when looking at genes that are upregulated following activation when changes were seen, showing a decrease in *il1b* and *tnfb* expression following *kdm6b* knockdown and injury relative to *tyr* controls. This supports published work in *in vitro* human neutrophils where inhibiting KDM6B lead to a reduction in *il1b* and *tnfb* expression and matches the IPA upstream pathways analysis that predicts a down regulation of both pathways based on gene expression changes across the whole data set (Chen *et al.*, 2018). It also further supports the hypothesis that *kdm6b* knockdown leads to a reduction in pro-inflammatory pathways.

Denholtz *et al.*, (2020) identified that neutrophils alter their chromatin confirmation depending on the stimuli they are exposed to. This allows the neutrophils at a site of immune challenge to be specifically equipped to fight the threat, whether that's bacterial or sterile inflammation, opening the chromatin at key gene loci. KDM6B has been implicated in driving inflammatory cytokine release in sepsis patients and also to be increased in LPS treatment of

in vitro neutrophils and so has been shown to play a part in multiple inflammatory states (Chen *et al.*, 2018). Denholtz *et al.*, (2020) implicated pathways by gene ontology terms associated with PMA exposure to mimic sterile inflammation, the main GO terms gave several hundred genes, 75 of which came up in the *kdm6b* knockdown dataset and too much information to be shown here. Bacterial infection was explored using *E. coli* and a panel of four transcription factors were found in the *kdm6b* dataset. Analysis of the expression of these genes showed only small differences in expression in *kdm6b* knockdown with or without injury relative controls, many of which could be accounted for due to activation of neutrophils as genes such as *sp1* are implicated in general neutrophil activation regardless of the stimuli. These results were expected due to the type of stimuli. A sterile inflammatory event such as a tailfin wound would be unlikely to trigger the *E. coli* pathways shown by Denholtz *et al.*, (2020). It would be ideal to generate a smaller panel of genes based on the PMA treatment data from Denholtz *et al.*, (2020) to get a better idea of how *kdm6b* alters genes implicated in chromatin remodelling events in sterile activation of neutrophils. This could also be compared to a second set of sequencing data generated from knockdown of *kdm6b* and an INTACT pulldown following infection.

Evidence on how chromatin remodelling directly affects inflammatory pathways in neutrophils are limited. R848 – the TLR8 agonist explored in Chapter 3 – has allowed for us to understand how chromatin remodelling driven by TLR8 activation promotes the release of inflammatory cytokines such as IL-6 and TNFα from neutrophils (Zimmermann *et al.*, 2015). Genes implicated in the R848–TLR8–IL-6 pathway were explored in the *kdm6b* knockdown dataset to attempt to find how KDM6B may alter the release of specific cytokines. While several of the key genes such as *tlr8* and *il6* were not expressed in the dataset, notable reductions were seen in *tlr4*, *tnf* and *rela* following *kdm6b* knockdown, the latter of which have been highlighted and discussed in the context of previous panels based on the literature. The reduction in both *rela* and *tnf* continue to strengthen the idea that *kdm6b* knockdown reduces the pro-inflammatory environment, meaning neutrophils cannot function efficiently following loss of the enzyme. The reduction in *tlr4* expression also suggests an alteration to the ability of neutrophils to sense pathogens. TLR4 plays a major role in bacterial sensing in humans, but its role in zebrafish immunity is unknown (Chen *et al.*, 2021). The reduction of the expression of these genes raises an interesting prospect for R848 to treat potential *kdm6b*

related deficiencies in neutrophil function associated with ageing and disease as the drug may be able to drive processes otherwise lost due to *kdm6b* loss. KDM6B has been linked to promoting cellular senescence with the aim of preventing severe age-related decline and to maintain homeostasis (Salminen *et al.*, 2014). KDM6B has been shown in mouse models to play a role in cellular senescence by regulating p53 translocation to the nuclei (Salminen *et al.*, 2014). KDM6B can also promote senescence by demethylating the INK4 box – a tumour suppressor locus – in cancer cell lines (Salminen *et al.*, 2014). If KDM6B function is lost in ageing neutrophils, there may be a reduction in senescence, promoting survival of dysfunctional neutrophils. R848 could be used to recover some of these pathways. While a crossover between the pathways is unknown, KDM6B demethylates H3K27 and R848 driven activation of TLR8 drives modifications at key loci by EP300/CREBBP that is capable of also modifying H3K27 by adding acetyl marks to promote gene transcription. KDM6B could therefore be priming these genes for additional marks from enzymes such as EP300. Interestingly, *brd4* expression is increased in the *kdm6b* dataset. BRD4 is a reader of histone acetylation and expression could be increased to compensate for a loss of H3K27ac due to the removal of H3K27 priming by KDM6B. Further exploration of these pathways is required to answer this. Investigation of other known agonist pathways could also help us to understand how KDM6B is regulating further inflammatory processes.

While the analyses of specific gene expression begin to show some of the pathways that KDM6B may be operating in, there are some limitations. The main limitation is the missing genes in the dataset that limited the number of genes analysed in the panels based on published work. This is likely due to the low concentration of some of the samples combined with some of the samples having low RIN scores before sequencing meaning key genes may not have been present at detectable levels. While at times attempts have been made to adjust for this – such as using cytokines receptors when cytokines were not available – several key inflammatory regulators are missing including several interleukins, toll like receptors, and inflammatory transcription factors. Another limitation is the capturing of only neutrophil nuclei. This means that cytoplasmic mRNA is ignored and so only a partial picture of the transcriptome may be being captured as cytoplasmic mRNA being shuttled to the ribosome or operating in a signalling capacity is missed (Berger *et al.*, 2012). Finally, the lack of a third independent repeat meant statistics could not be performed on the differential expression

analysis of specific genes between groups represented in box plots and so definitive conclusions cannot be drawn from the dataset. Instead, qRT-PCR analysis needs to be performed targeting the genes for validation of the results. However, now that the method has been established and the requirements for sequencing pulldown products are better understood, the third repeat or a full sequencing run can be produced a lot more easily than it was here.

Overall, these data suggest that *kdm6b* may be important in regulating several pro-inflammatory pathways following tailfin injury, however the lack of statistics in the RNAseq data mean a definitive conclusion cannot be drawn. As a lysine demethylase, KDM6B normally functions by removing methylation marks at H3K27 that suppress transcription by promoting heterochromatin formation. These data propose the hypothesis that when neutrophils are activated by tailfin injury, KDM6B demethylates pro-inflammatory gene loci such as those for *il1b* and *tnf,* allowing for the addition of pro-transcriptional acetylation marks to be added at H3K27 by other chromatin remodelling enzymes that drive inflammation and return the wound site to homeostasis. In *kdm6b* knockdown, the removal of methylation does not occur and instead these genes remain repressed, resulting in delayed inflammation and a lack of inflammatory effector mechanisms. In the future, identifying the next steps of the cascade will be key, such as finding the exact loci that are being altered, the enzymes that add further pro-transcriptional acetylation marks, and finding the exact processes that are lost due to *kdm6b* loss.

The work within this thesis has shown the suitability of a pipeline of investigation for chromatin remodelling in neutrophils using an *in vivo* model. The pipeline generated uses chemical probes, bioinformatic approaches and genetic knockdown to dissect the epigenetic regulation of inflammation. I have shown proof of principle that this approach can work based on R848 data, Cas9 knockdown of *kdm6b* and *ezh2* and the generation of a preliminary RNAseq dataset. This approach could be scaled up to examine all chromatin remodelling enzymes and then the data pulled together using a major bioinformatic push to show how chromatin remodelling regulates neutrophil function. This would, as a by-product, show which genes were common to important regulators of function, leading to a fuller understanding of how neutrophil functions are regulated.

Chapter 6. General Discussion and Future Work

6.1. Summary of the major findings of this work

We are just beginning to understand chromatin remodelling in neutrophil function. Changes in conformation of DNA by the addition of chemical modifications to histones by chromatin remodelling enzymes is a clear driver for neutrophilic responses to specific stimuli, with specific conformational changes associated with different threats (Denholtz *et al.*, 2020). However, the actual chromatin remodelling enzymes responsible for these changes are unclear with only a handful of publications exploring the role they play (Chen *et al.*, 2018; Kitchen *et al.*, 2021). Chromatin remodelling enzymes, however, provide a potential druggable target in inflammatory conditions and so further exploration would be beneficial.

Age-related changes to the immune system and many chronic inflammatory conditions are characterised by neutrophil dysfunction. As shown by Denholtz *et al.,* (2020), chromatin remodelling controls neutrophil function and so it is reasonable to hypothesise that changes in neutrophil function in ageing and disease might be partly explained by changes in chromatin conformation. Therefore, altering the chromatin of disease state neutrophils may return them to homeostatic function and thereby help to treat the disease. If these chromatin changes can be targeted to premature neutrophils in the bone marrow, they can be inherited, and changes be made to populations compared to treatments that specifically target downstream pathways and may only alter fully mature neutrophils, meaning a patient may require long term treatment. However, this must be approached with caution as off-target changes to chromatin remodelling may alter healthy pathways in both neutrophils and other cell types. Chromatin remodelling enzymes must therefore be carefully identified and methods that specially target neutrophils developed. To know what to target in disease, the enzymes controlling neutrophil chromatin during healthy inflammation need to be identified using a suitable model. The overall aim of this thesis was to identify the chromatin remodelling enzymes responsible for regulating neutrophil function. This was attempted by taking advantage of the zebrafish model and in particular the ease at which larval zebrafish

can be chemically and genetically altered and neutrophil function observed using transgenic lines and neutrophils isolated for transcriptomic sequencing.

Across the three results chapters the key findings are as follows. Chapter 3 aimed to use chemicals shown to regulate neutrophil chromatin remodelling *in vitro* to attempt to alter in *vivo* neutrophil activity. Work used R848, a TLR8 agonist that alters chromatin conformation at the *il6* locus, to test whether zebrafish neutrophils display similar behaviour to human neutrophils when exposed to chromatin remodelling compounds and it was shown that *in vivo* inflammation resolution could be modulated by R848. However, exact chromatin remodelling events were not identified, and further work is needed to address this.

Chapter 4 aimed to identify chromatin remodelling enzymes that regulated neutrophil function *in vivo* using a whole-body and neutrophil-specific CRISPR/Cas9 knockdown approach. Initial work identified potential chromatin remodelling enzymes in human *in vitro* neutrophil function using *in silico* screening of RNAseq data with KDM6B, EZH2 and DOT1L presenting as the most likely targets. CRISPR/Cas9 knockdown was then used to show that in the absence of *kdm6b*, inflammation resolution was reduced following a tailfin wound. CRISPR/Cas9 knockdown of *ezh2* led to increased recruitment of neutrophils to the tailfin wound and an attenuation of inflammation resolution. Knockdown of *dot1l* lead to embryonic death before the development of neutrophils so no observations could be made. Neutrophil-specific knockdown analysis was not achieved but the system was developed, and optimisation started.

Finally, in Chapter 5, the aim was to establish downstream gene expression changes following *kdm6b* knockdown in inflammatory neutrophils. *kdm6b* was knocked down using CRISPR/Cas9 technology and neutrophil nuclear RNA was extracted and sequenced. Sequencing produced preliminary data suggesting an attenuation of pro-inflammatory pathways in *kdm6b* knockdown neutrophils following injury compared to control guide injected and injured controls. Further analysis of specific genes found that expression of both *il1b* and *tnf*, two key inflammatory cytokines were reduced relative to controls in the *kdm6b* knockdown larvae both with and without injury. As only a preliminary dataset was generated, statistical analysis could not be performed so comparisons cannot be made without further

validation. Secondly, bioinformatics analysis was limited and analysis of gene ontology and how pathways identified by IPA software overlap with diseases was not performed.

Taken as a whole, this work supports the view that chromatin remodelling enzymes dictate neutrophil function and has produced the first known *in vivo* RNA sequencing dataset of the neutrophil transcriptome following CRISPR/Cas9 mediated knockdown of a chromatin remodelling enzyme – in this case *kdm6b* – though the dataset is preliminary due to the lack of statistics. Furthermore, it shows how zebrafish can act as a model for the study of neutrophil epigenetics and sets out a selection of techniques for a systematic approach to such study.

6.2. Implications for the understanding of neutrophil chromatin remodelling *in vivo*.

The work presented in this thesis adds to the understanding of how chromatin remodelling enzymes act in neutrophils and especially expands on the knowledge of *in vivo* behaviour in neutrophil models.

The workflow for the R848 exposure not only shows that zebrafish neutrophils are epigenetically modifiable in a similar process to human neutrophils but provides a workflow for the study of other chromatin remodelling modifying compounds in zebrafish models creating a potential screening method for the quick identification of further enzymes responsible for neutrophil function. It also strengthens the case for being able to use zebrafish neutrophils as a model for neutrophil chromatin remodelling to partially mimic human activity, a useful tool in the laboratory.

Work utilising the CRISPR/Cas9 knockdown of chromatin remodelling enzymes builds on what little information is known about chromatin remodelling enzymes and their roles in neutrophil function. It is the first work observing neutrophil function following depletion of chromatin remodelling using an *in vivo* zebrafish model and provides a simple workflow for it to be performed in the future using other enzymes.

The CRISPR/Cas9 work targeted *kdm6b* and *ezh2*. Both enzymes have been previously implicated in neutrophil activity but details on functional pathways are limited with KDM6B work only looking at neutrophil pro-inflammatory gene and protein expression and EZH2 work only looking at neutrophil recruitment (Chen *et al.*, 2018; Kitchen *et al.*, 2021). This thesis provides to my knowledge the most detailed information yet on the role Kdm6b plays in neutrophil activity and shows the first details of how Kdm6b affects neutrophil recruitment and inflammation recruitment at wounds in an *in vivo* sterile inflammation model. The generation of the *kdm6b* knockdown RNA sequencing dataset, even as a piece of preliminary data as it only has two independent repeats, provides a valuable resource for the neutrophil research community, and allows for searches to be carried out for genes of interest in complex processes specific to individual research questions. The change in expression of *il1b* and tnf seen in the RNAseq data also helps to further validate zebrafish as a model for *in vivo* modelling of neutrophil chromatin remodelling as it matches changes seen in (Chen *et al.*, 2018).

The neutrophil recruitment and inflammation resolution experiments in *ezh2* knockdown zebrafish larvae provided information on how Ezh2 may regulate neutrophil response to sterile injury. These data lay the groundwork for the further study of Ezh2 in neutrophil function using the pipeline generated by the *kdm6b* work in the zebrafish in hand with data already available on EZH2's role in a murine model (Kitchen *et al.*, 2021).

Overall, KDM6B and EZH2 have been identified as chromatin remodelling enzymes that regulate neutrophil movement to and from the wound site in a zebrafish model and provide a new area of study for how these enzymes function in regulating neutrophilic inflammation. Techniques have been presented to research the role of chromatin remodelling enzymes in zebrafish neutrophils and the techniques can be transferred to other enzymes for further study. Here, the process of identification of targets, functional observation of neutrophils in an *in vivo* system, and downstream analysis of gene expression through cell-specific sequencing have been demonstrated. These are all valuable tools for expanding on our knowledge of chromatin remodelling.

6.3. Future work

Throughout Chapter Discussions, specific experiments have been outlined to further explore the research aims of each chapter.

Chapter 3 aimed to chemically target neutrophil chromatin remodelling to test *in vitro* findings on chromatin remodelling. R848 was identified to play a role in neutrophil inflammation resolution, but the exact chromatin remodelling pathways were not examined. Injury experiments using inhibitors to the chromatin remodelling enzymes implicated in the pathway such as Ep300, Crebbp and Brd4 will help to understand if the pathways are directly homologous to *in vitro* neutrophils. Further work can also exam chromatin conformation and modification changes at the loci of pro-inflammatory genes implicated in the R848 pathway such as *il6* and *tnf*.

In Chapter 4, the work aimed to identify chromatin remodelling enzymes in neutrophil function using a CRISPR/Cas9 knockdown approach. Initial bioinformatics analysis identified 20 enzymes to target but only 3 of those enzymes progressed to the Cas9 knockdown stage, *kdm6b, ezh2* and *dot1l*. Future work could examine more of the 20-enzyme list in a whole-body knockdown. *kdm6b* and *ezh2* knockdown could also be performed to examine potential changes in neutrophil functions such as changes to phagocytosis and NETosis. Furthermore, the neutrophil-specific knockdown techniques presented in Chapter 4 provide an opportunity for the study of chromatin remodelling enzymes in zebrafish neutrophils. A targeted knockdown of *kdm6b* and *ezh2* can help to distinguish whether the effects seen in the whole-body knockdown of the enzymes in neutrophil phenotype and kinetics are down to changes specifically in the neutrophils or changes to the microenvironment acting on the neutrophils. The neutrophil specific system needs optimising before it can be used to generate data. Preliminary injections of the construct into the *Tg(lyz:nfsβ-mCherry)sh260* line showed co-localised signal of the construct GFP signal in the mCherry neutrophils but effective knockdown within neutrophils needs to be confirmed using validated control guide RNAs with known effects in neutrophils. Once developed the technique presents a great tool for studying the role of many enzymes in a screen.

Chapter 5 aimed to find genes regulated by the knockdown of kdm6b in neutrophils. This was achieved by the generation of a neutrophil-specific RNA sequencing dataset of inflammatory neutrophils following *kdm6b* knockdown. However, this dataset was only preliminary as only two independent repeats on RNA samples were sequenced. Generation of a full dataset with three independent repeats would allow for statistical analysis to be performed on differential gene expression and for genes to be identified for validation by qRT-PCR. Further future work would examine gene expression changes in inflammatory neutrophils following the CRISPR/Cas9 mediated knockdown of *ezh2* based on the neutrophil recruitment data generated in Chapter 4. EZH2 is a histone methyltransferase that adds methyl groups to H3K27 to repress transcription. This methyltransferase activity is the inverse to the demethylase activity of *kdm6b*, which demethylates H3K27me2/3 to drive gene transcription. An *ezh2* knockdown sequencing dataset would therefore provide a complementary dataset to the KDM6B work. It would be reasonable to hypothesise that many of the inflammatory processes altered by *kdm6b* knockdown, would see inverse regulation in an *ezh2* knockdown scenario.

6.4. New research questions

New research questions have also arisen from the work presented in this thesis. KDM6B has been identified as the main gene of interest and finding further roles for KDM6B in healthy neutrophils is the logical next step. Neutrophils carry out a range of effector functions and finding how altering *kdm6b* expression may alter can form the backbone of future experiments. Using zebrafish transgenic reporters can allow for analysis of several processes, especially when combined with fluorescent staining and imaging. Based on the findings in Chapters 4 and 5 concerning neutrophil activity and gene expression following *kdm6b* knockdown, there is a suggestion that neutrophils are maturing as expected, being recruited to the wound site, but then not being activated as needed and being retained at the wound. Experiments into functions associated with activity and inflammation resolution would be appropriate to answer this hypothesis. Questions arising therefore include:

- How is phagocytosis and intracellular killing altered? This question can be addressed by injection of fluorescent bacteria or beads and using *in vivo* imaging to measure

uptake of bacteria/beads. Use of pH sensitive fluorescent reporters can also be used to assess intracellular killing within the phagosome.

- What is the effect on NETosis? NETosis can be measured in neutrophils using a fluorescent reporter for H2A, a component of the NET structure. These structures can be counted following an injury experiment across time lapse fluorescent imaging.
- How is inflammation resolution altered?
    - What are the effects on reverse migration? Use fluorescent time lapse imaging of the *TgBAC(mpx:EGFP)i114* neutrophil zebrafish reporter line following tailfin injury to trace neutrophil migration away from the wound using tracking software.
    - How is apoptosis and clearance by macrophages altered? Combine imaging of the neutrophil and macrophage reporter lines to monitor engulfment of neutrophils at inflammation resolution time points. Use TUNEL assay to stain for apoptotic neutrophils at inflammation resolution time points.

Functional knock-in of *kdm6b* could then be attempted in knockdowns to recover any of the functions seen to be altered to confirm they are *kdm6b* dependent. Furthermore, generation of a stable *kdm6b* knockout zebrafish line using the *TgBAC(mpx:EGFP)i114* as a background to give green neutrophils will enable for many of these observations to be made without CRISPR/Cas9 microinjection in the experimental timeline.

The aim of this thesis was to first test whether zebrafish neutrophils could model *in vitro* observations on neutrophil chromatin remodelling and then to identify chromatin remodelling enzymes that regulate neutrophil function. These were achieved by showing R848 action and identifying *kdm6b* and *ezh2* as potential targets, however questions are left unanswered. Part of my hypothesis was that alterations in chromatin remodelling in neutrophils drives ageing and disease pathologies. Moving forward, addressing this part of the hypothesis provides interesting areas to investigate as that has not been addressed here. The role of the *kdm6b*, *ezh2* and other enzymes identified from the *in silico* work here can be examined in neutrophils from inflammatory diseases and ageing. One day, these enzymes could be targeted for therapies against inflammatory ageing and chronic inflammatory conditions. Using inflammatory disease patients and elderly donor neutrophils to look for alterations in KDM6B expression will help to understand if it plays a role in such conditions.

This can be done using qRT-PCR and western blotting and functional analysis can be performed using chromatin immunoprecipitation targeting KDM6B specific modifications. If changes are seen, sequencing experiments can be performed to look at not only changes in gene expression but also changes in chromatin conformation using ATAC-seq. Much of this workflow could then be transferred to exploring the role of EZH2 and DOT1L, and eventually other chromatin remodelling enzymes.

Overall, this thesis has identified that zebrafish neutrophils provide an appropriate model for chromatin remodelling in neutrophils and that *kdm6b* and *ezh2* provide interesting candidates for further investigation into regulation of neutrophil function *in vivo*. Identifying the pathways regulated by these enzymes provides further research questions to be tackled in the future. The data presented in this work has shown the suitability of a pipeline of investigation for the role of chromatin remodelling enzymes in neutrophil function in a zebrafish model. The pipeline uses chemical probes, bioinformatic approaches and genetic knockdown to dissect the epigenetic regulation of inflammation. This thesis has shown proof of principle that this approach can work using R848 as a chemical approach and Cas9 knockdown of *kdm6b* and *ezh2* as a genetic approach. This approach could be scaled up to examine all the chromatin remodelling enzymes and the data pulled together using a major bioinformatic push to show how chromatin remodelling regulates neutrophil function. This would, as a by-product, show which genes were common to important regulators of function, leading to a fuller understanding of how neutrophil functions are regulated.

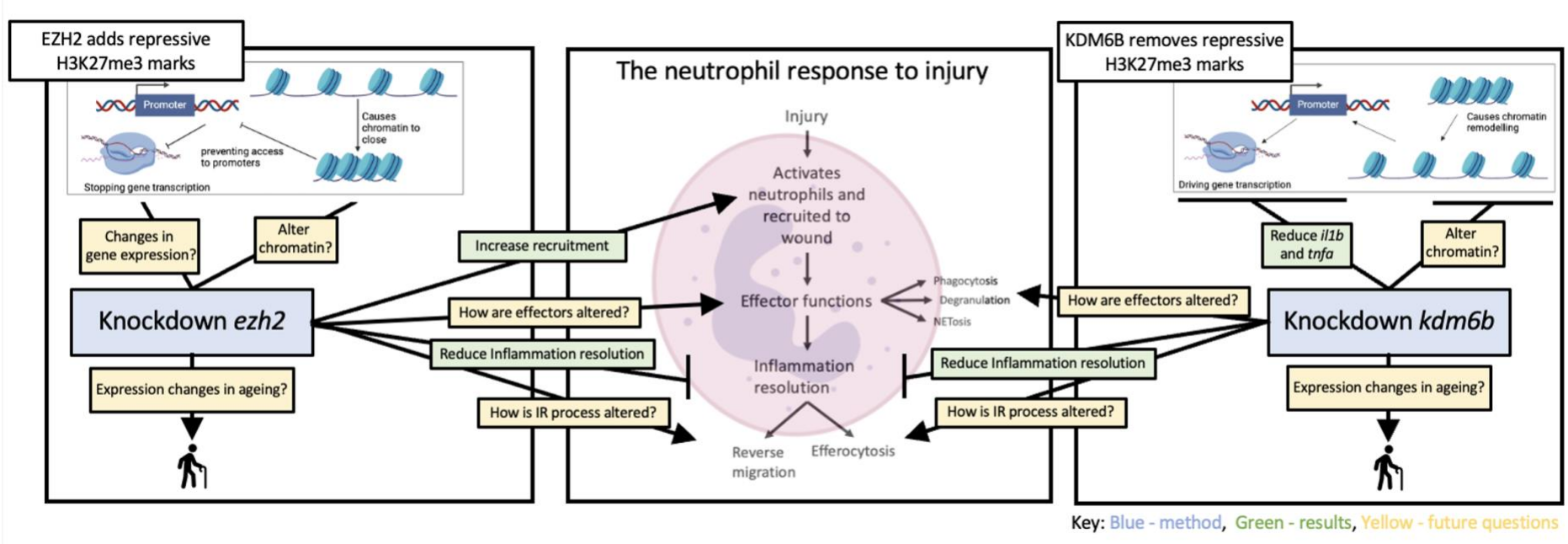

Figure 6.1. Summary of the major findings and future directions for this work

Diagram created using assets from BioRender showing the main finding of this thesis concerning the roles of KDM6B and EZH2 in neutrophil response to injury. Blue boxes show experimental methods, green boxes show findings, and yellow boxes show future questions to be answered.

7. References

Abbasi, M. *et al.* (2019) 'Strategies toward rheumatoid arthritis therapy; the old and the new', *Journal of cellular physiology*. J Cell Physiol, 234(7), pp. 10018–10031. doi: 10.1002/JCP.27860.

Abdulaziz, K. *et al.* (2016) 'National Survey of Geriatricians to Define Functional Decline in Elderly People with Minor Trauma', *Canadian Geriatrics Journal*. Canadian Geriatrics Society, 19(1), p. 2. doi: 10.5770/CGJ.19.192.

Abete, I. *et al.* (2019) 'Association of lifestyle factors and inflammation with sarcopenic obesity: data from the PREDIMED-Plus trial', *Journal of Cachexia, Sarcopenia and Muscle*, XXX, p. jcsm.12442. doi: 10.1002/jcsm.12442.

Ablain, J. *et al.* (2015) 'A CRISPR/Cas9 Vector System for Tissue-Specific Gene Disruption in Zebrafish Developmental Cell Resource A CRISPR/Cas9 Vector System for Tissue-Specific Gene Disruption in Zebrafish'. doi: 10.1016/j.devcel.2015.01.032.

Aitcheson, S. M. *et al.* (2021) 'Skin Wound Healing: Normal Macrophage Function and Macrophage Dysfunction in Diabetic Wounds', *Molecules (Basel, Switzerland)*. Molecules, 26(16). doi: 10.3390/MOLECULES26164917.

Alves-Fernandes, D. K. and Jasiulionis, M. G. (2019) 'The Role of SIRT1 on DNA Damage Response and Epigenetic Alterations in Cancer', *International journal of molecular sciences*. Int J Mol Sci, 20(13). doi: 10.3390/IJMS20133153.

Amulic, B. *et al.* (2012) 'Neutrophil Function: From Mechanisms to Disease', *Annual Review of Immunology*, 30(1), pp. 459–489. doi: 10.1146/annurev-immunol-020711-074942.

Andersson, M. *et al.* (2022) 'Low Holding Densities Increase Stress Response and Aggression in Zebrafish', *Biology*. Biology (Basel), 11(5). doi: 10.3390/BIOLOGY11050725.

Aslam, M. A. *et al.* (2021) 'Histone methyltransferase DOT1L controls state-specific identity during B cell differentiation', *EMBO reports*. EMBO Rep, 22(2). doi: 10.15252/EMBR.202051184.

Babu, A. *et al.* (2018) 'Chemical and genetic rescue of an ep300 knockdown model for Rubinstein Taybi Syndrome in zebrafish', *Biochimica et Biophysica Acta (BBA) - Molecular Basis of Disease*. Elsevier, 1864(4), pp. 1203–1215. doi: 10.1016/J.BBADIS.2018.01.029.

Ballesteros, I. *et al.* (2020) 'Co-option of Neutrophil Fates by Tissue Environments', *Cell*, 183(5), pp. 1282-1297.e18. doi: 10.1016/j.cell.2020.10.003.

Barkaway, A. *et al.* (2021) 'Age-related changes in the local milieu of inflamed tissues cause aberrant neutrophil trafficking and subsequent remote organ damage', *Immunity*, 54(7), pp. 1494-1510.e7. doi: 10.1016/j.immuni.2021.04.025.

Barnett, K. *et al.* (2012) 'Epidemiology of multimorbidity and implications for health care, research, and medical education: a cross-sectional study', *The Lancet*. Elsevier, 380(9836), pp. 37–43. doi: 10.1016/S0140-6736(12)60240-2.

Bass, D. A. *et al.* (1986) 'Subpopulations of neutrophils with increased oxidative product formation in blood of patients with infection - PubMed', *J Immunol*, 136(3), pp. 860–866. Available at: https://pubmed.ncbi.nlm.nih.gov/3001188/ (Accessed: 22 November 2022).

Bates, J. M. *et al.* (2007) 'Intestinal Alkaline Phosphatase Detoxifies Lipopolysaccharide and Prevents Inflammation in Response to the Gut Microbiota', *Cell host & microbe*. NIH Public Access, 2(6), p. 371. doi: 10.1016/J.CHOM.2007.10.010.

Benayoun, B. A. *et al.* (2019) 'Remodeling of epigenome and transcriptome landscapes with aging in mice reveals widespread induction of inflammatory responses', *Genome Research*, 29(4), pp. 697–709. doi: 10.1101/gr.240093.118.

Benayoun, B. A., Pollina, E. A. and Brunet, A. (2015) 'Epigenetic regulation of ageing: linking environmental inputs to genomic stability', *Nat Rev Mol Cell Biol*, 16(10), pp. 593–610. doi: 10.1038/nrm4048.

Berger, M. *et al.* (2012) 'Neutrophils Express Distinct RNA Receptors in a Non-canonical Way', *The Journal of Biological Chemistry*. American Society for Biochemistry and Molecular Biology, 287(23), p. 19409. doi: 10.1074/JBC.M112.353557.

Bird, A. P. (1986) 'CpG-Rich islands and the function of DNA methylation', *Nature*, 321(6067), pp. 209–213. doi: 10.1038/321209a0.

Blaes, A. *et al.* (2017) 'Cardio-oncology Related to Heart Failure: Common Risk Factors Between Cancer and Cardiovascular Disease.', *Heart failure clinics*. NIH Public Access, 13(2), pp. 367–380. doi: 10.1016/j.hfc.2016.12.006.

Borghesi, L. and Milcarek, C. (2006) 'From B cell to plasma cell: regulation of V(D)J recombination and antibody secretion', *Immunologic research*. Immunol Res, 36(1–3), pp. 27–32. doi: 10.1385/IR:36:1:27.

Bournazos, S. *et al.* (2017) 'Signaling by Antibodies: Recent Progress', *https://doi.org/10.1146/annurev-immunol-051116-052433*. Annual Reviews , 35, pp. 285–311. doi: 10.1146/ANNUREV-IMMUNOL-051116-052433.

Brinkmann, V. *et al.* (2004) 'Neutrophil extracellular traps kill bacteria', *Science (New York, N.Y.)*. Science, 303(5663), pp. 1532–1535. doi: 10.1126/SCIENCE.1092385.

Brubaker, A. L. *et al.* (2013) 'Reduced Neutrophil Chemotaxis and Infiltration Contributes to Delayed Resolution of Cutaneous Wound Infection with Advanced Age', *The Journal of Immunology*. American Association of Immunologists, 190(4), pp. 1746–1757. doi: 10.4049/JIMMUNOL.1201213.

Brubaker, S. W. *et al.* (2015) 'Innate immune pattern recognition: a cell biological perspective', *Annual review of immunology*. Annu Rev Immunol, 33, pp. 257–290. doi: 10.1146/ANNUREV-IMMUNOL-032414-112240.

Brummelman, J., Pilipow, K. and Lugli, E. (2018) 'The Single-Cell Phenotypic Identity of Human CD8+ and CD4+ T Cells', *International review of cell and molecular biology*. Int Rev Cell Mol Biol, 341, pp. 63–124. doi: 10.1016/BS.IRCMB.2018.05.007.

Burgener, S. S. and Schroder, K. (2020) 'Neutrophil Extracellular Traps in Host Defense', *Cold Spring Harbor Perspectives in Biology*. Cold Spring Harbor Laboratory Press, 12(7), p. a037028. doi: 10.1101/CSHPERSPECT.A037028.

Burger, A. *et al.* (2016) 'Maximizing mutagenesis with solubilized CRISPR-Cas9 ribonucleoprotein complexes'. doi: 10.1242/dev.134809.

Burn, G. L. *et al.* (2021) 'The Neutrophil'. doi: 10.1016/j.immuni.2021.06.006.

Butcher, S. K. *et al.* (2001) 'Senescence in innate immune responses: reduced neutrophil phagocytic capacity and CD16 expression in elderly humans', *Journal of Leukocyte Biology*. John Wiley & Sons, Ltd, 70(6), pp. 881–886. doi: 10.1189/JLB.70.6.881.

Cancro, M. P. and Tomayko, M. M. (2021) 'Memory B cells and plasma cells: The differentiative continuum of humoral immunity', *Immunological reviews*. Immunol Rev, 303(1), pp. 72–82. doi: 10.1111/IMR.13016.

Candel, S. *et al.* (2014) 'Tnfa signaling through tnfr2 protects skin against oxidative stress-induced inflammation', *PLoS biology*. PLoS Biol, 12(5). doi: 10.1371/JOURNAL.PBIO.1001855.

Chazaud, B. (2016) 'Inflammation during skeletal muscle regeneration and tissue remodeling: Application to exercise-induced muscle damage management', *Immunology and Cell Biology*, 94(2), pp. 140–145. doi: 10.1038/icb.2015.97.

Chen, H. *et al.* (2021) 'Genome-wide analysis of Toll-like receptors in zebrafish and the effect of rearing temperature on the receptors in response to stimulated pathogen infection', *Journal of Fish Diseases*. Blackwell Publishing Ltd, 44(3), pp. 337–349. doi:

10.1111/JFD.13287.

Chen, L. *et al.* (2016) 'Genetic Drivers of Epigenetic and Transcriptional Variation in Human Immune Cells.', *Cell*. Cell, 167(5), pp. 1398-1414.e24. doi: 10.1016/j.cell.2016.10.026.

Chen, Xiang *et al.* (2020) 'Methyltransferase Dot1l preferentially promotes innate IL-6 and IFN-β production by mediating H3K79me2/3 methylation in macrophages', *Cellular & molecular immunology*. Cell Mol Immunol, 17(1), pp. 76–84. doi: 10.1038/S41423-018-0170-4.

Chen, Yang *et al.* (2018) 'JMJD3 is involved in neutrophil membrane proteinase 3 overexpression during the hyperinflammatory response in early sepsis.', *International immunopharmacology*, 59, pp. 40–46. doi: 10.1016/j.intimp.2018.03.027.

Chen, Z. *et al.* (2017) 'Epigenetic Regulation: A New Frontier for Biomedical Engineers', *Annual Review of Biomedical Engineering*. Annual Reviews, 19(1), pp. 195–219. doi: 10.1146/annurev-bioeng-071516-044720.

Cheung, P. *et al.* (2018) 'Single-Cell Chromatin Modification Profiling Reveals Increased Epigenetic Variations with Aging.', *Cell*. Elsevier, 173(6), pp. 1385-1397.e14. doi: 10.1016/j.cell.2018.03.079.

Chin, J. S. R. *et al.* (2019) 'Behavioral Approaches to Studying Innate Stress in Zebrafish', *JoVE (Journal of Visualized Experiments)*. Journal of Visualized Experiments, 2019(147), p. e59092. doi: 10.3791/59092.

Christoffersson, G. *et al.* (2012) 'VEGF-A recruits a proangiogenic MMP-9-delivering neutrophil subset that induces angiogenesis in transplanted hypoxic tissue', *Blood*. Blood, 120(23), pp. 4653–4662. doi: 10.1182/BLOOD-2012-04-421040.

Ciupe, S. M. *et al.* (2021) 'Bistable Mathematical Model of Neutrophil Migratory Patterns After LPS-Induced Epigenetic Reprogramming', *Frontiers in Genetics*, 12(February). doi: 10.3389/fgene.2021.633963.

Coombs, C. *et al.* (2019) 'Chemokine receptor trafficking coordinates neutrophil clustering and dispersal at wounds in zebrafish', *Nature Communications*, 10(1). doi: 10.1038/s41467-019-13107-3.

Coussens, L. M. and Werb, Z. (2002) 'Inflammation and cancer', *Nature*. Nature, 420(6917), pp. 860–867. doi: 10.1038/NATURE01322.

Covre, L. P. *et al.* (2020) 'The role of senescent T cells in immunopathology', *Aging Cell*. Wiley-Blackwell, 19(12). doi: 10.1111/ACEL.13272.

Crainiciuc, G. *et al.* (2022) 'Behavioural immune landscapes of inflammation', *Nature*. Springer US, 601(7893), pp. 415–421. doi: 10.1038/s41586-021-04263-y.

Cusanovich, D. A. *et al.* (2018) 'A Single-Cell Atlas of In Vivo Mammalian Chromatin Accessibility', *Cell*. Cell Press, 174(5), pp. 1309-1324.e18. doi: 10.1016/J.CELL.2018.06.052.

Dang, W. *et al.* (2009) 'Histone H4 lysine 16 acetylation regulates cellular lifespan', *Nature 2009 459:7248*. Nature Publishing Group, 459(7248), pp. 802–807. doi: 10.1038/nature08085.

Deal, R. B. and Henikoff, S. (2011) 'The INTACT method for cell type–specific gene expression and chromatin profiling in Arabidopsis thaliana', *Nature Protocols*, 6(1), pp. 56–68. doi: 10.1038/nprot.2010.175.

Denholtz, M. *et al.* (2020) 'Upon microbial challenge, human neutrophils undergo rapid changes in nuclear architecture and chromatin folding to orchestrate an immediate inflammatory gene program', *Genes and Development*, 34(3–4), pp. 149–165. doi: 10.1101/gad.333708.119.

Dolgalev, I. (2022) 'babelgene: Gene Orthologs for Model Organisms in a Tidy Data Format.' Available at: https://igordot.github.io/babelgene/.

Domcke, S. *et al.* (2020) 'A human cell atlas of fetal chromatin accessibility', *Science*. American Association for the Advancement of Science, 370(6518). doi: 10.1126/SCIENCE.ABA7612/SUPPL_FILE/ABA7612_DOMCKE_TABLE-S7.XLSX.

Doudna, J. A. and Charpentier, E. (2014) 'Genome editing. The new frontier of genome engineering with CRISPR-Cas9', *Science (New York, N.Y.)*. Science, 346(6213). doi: 10.1126/SCIENCE.1258096.

Drew, W., Wilson, D. V. and Sapey, E. (2018) 'Inflammation and neutrophil immunosenescence in health and disease: Targeted treatments to improve clinical outcomes in the elderly', *Experimental Gerontology*, 105, pp. 70–77. doi: 10.1016/j.exger.2017.12.020.

Eisenberg, T. *et al.* (2009) 'Induction of autophagy by spermidine promotes longevity', *Nature Cell Biology 2009 11:11*. Nature Publishing Group, 11(11), pp. 1305–1314. doi: 10.1038/ncb1975.

El-Brolosy, M. A. *et al.* (2019) 'Genetic compensation triggered by mutant mRNA degradation', *Nature*. Nature, 568(7751), pp. 193–197. doi: 10.1038/S41586-019-1064-Z.

Ellett, F. *et al.* (2011) 'mpeg1 promoter transgenes direct macrophage-lineage expression in zebrafish', *Blood*. The American Society of Hematology, 117(4), p. e49. doi: 10.1182/BLOOD-

2010-10-314120.

Ellett, F. *et al.* (2015) 'Defining the phenotype of neutrophils following reverse migration in zebrafish', *Journal of Leukocyte Biology*, 98(6), pp. 975–981. doi: 10.1189/jlb.3MA0315-105R.

Emanuelli, G. *et al.* (1986) 'Influence of Age on Polymorphonuclear Leukocytes in vitro: Phagocytic Activity in Healthy Human Subjects', *Gerontology*. Karger Publishers, 32(6), pp. 308–316. doi: 10.1159/000212809.

Evrard, M. *et al.* (2018) 'Developmental Analysis of Bone Marrow Neutrophils Reveals Populations Specialized in Expansion, Trafficking, and Effector Functions', *Immunity*. Cell Press, 48(2), pp. 364-379.e8. doi: 10.1016/J.IMMUNI.2018.02.002.

Fabbri, E. *et al.* (2016) 'Association Between Accelerated Multimorbidity and Age-Related Cognitive Decline in Older Baltimore Longitudinal Study of Aging Participants without Dementia', *Journal of the American Geriatrics Society*, 64(5), pp. 965–972. doi: 10.1111/jgs.14092.

Fadok, V. A. *et al.* (1998) 'Macrophages that have ingested apoptotic cells in vitro inhibit proinflammatory cytokine production through autocrine/paracrine mechanisms involving TGF-beta, PGE2, and PAF', *The Journal of clinical investigation*. J Clin Invest, 101(4), pp. 890–898. doi: 10.1172/JCI1112.

Fagiolo, U. *et al.* (1993) 'Increased cytokine production in mononuclear cells of healthy elderly people', *European Journal of Immunology*. John Wiley & Sons, Ltd, 23(9), pp. 2375–2378. doi: 10.1002/EJI.1830230950.

Fahy, G. M. *et al.* (2019) 'Reversal of epigenetic aging and immunosenescent trends in humans', *Aging Cell*, (May), pp. 1–12. doi: 10.1111/acel.13028.

Feldman, N., Rotter-Maskowitz, A. and Okun, E. (2015) 'DAMPs as mediators of sterile inflammation in aging-related pathologies', *Ageing Research Reviews*, 24, pp. 29–39. doi: 10.1016/j.arr.2015.01.003.

Ferrari, L. *et al.* (2019) 'Extracellular vesicles released by colorectal cancer cell lines modulate innate immune response in zebrafish model: The possible role of human endogenous retroviruses', *International Journal of Molecular Sciences*. MDPI AG, 20(15). doi: 10.3390/IJMS20153669.

Feser, J. *et al.* (2010) 'Elevated histone expression promotes life span extension', *Molecular cell*. Mol Cell, 39(5), pp. 724–735. doi: 10.1016/J.MOLCEL.2010.08.015.

Filardy, A. A. *et al.* (2010) 'Proinflammatory Clearance of Apoptotic Neutrophils Induces an IL-

12lowIL-10high Regulatory Phenotype in Macrophages', *The Journal of Immunology*. American Association of Immunologists, 185(4), pp. 2044–2050. doi: 10.4049/JIMMUNOL.1000017.

Fortin, C. F. *et al.* (2007) 'GM-CSF activates the Jak/STAT pathway to rescue polymorphonuclear neutrophils from spontaneous apoptosis in young but not elderly individuals', *Biogerontology*. Biogerontology, 8(2), pp. 173–187. doi: 10.1007/S10522-006-9067-1.

Franceschi, C. *et al.* (2000) 'Inflamm-aging An Evolutionary Perspective on Immunosenescence INTRODUCTION: THE NETWORK HYPOTHESIS OF AGING', *Ann. N Y Acad. Sci.*, 908, pp. 244–254. Available at: https://nyaspubs.onlinelibrary.wiley.com/doi/pdf/10.1111/j.1749-6632.2000.tb06651.x (Accessed: 5 June 2019).

François, S. *et al.* (2005) 'Inhibition of neutrophil apoptosis by TLR agonists in whole blood: involvement of the phosphoinositide 3-kinase/Akt and NF-kappaB signaling pathways, leading to increased levels of Mcl-1, A1, and phosphorylated Bad', *Journal of immunology (Baltimore, Md. : 1950)*. J Immunol, 174(6), pp. 3633–3642. doi: 10.4049/JIMMUNOL.174.6.3633.

Freire, M. O. and Van Dyke, T. E. (2013) 'Natural resolution of inflammation', *Periodontology 2000*. NIH Public Access, 63(1), p. 149. doi: 10.1111/PRD.12034.

Fuchs, T. A. *et al.* (2007) 'Novel cell death program leads to neutrophil extracellular traps', *The Journal of Cell Biology*. The Rockefeller University Press, 176(2), p. 231. doi: 10.1083/JCB.200606027.

Fulop, T. *et al.* (2004) 'Signal transduction and functional changes in neutrophils with aging', *Aging Cell*. John Wiley & Sons, Ltd, 3(4), pp. 217–226. doi: 10.1111/J.1474-9728.2004.00110.X.

Fulop, T. *et al.* (2020) 'Immunosenescence is both functional/adaptive and dysfunctional/maladaptive', *Seminars in Immunopathology*. Springer Science and Business Media Deutschland GmbH, 42(5), pp. 521–536. doi: 10.1007/S00281-020-00818-9/FIGURES/1.

Fülöp, T. *et al.* (1985) 'Age-dependent alterations of Fc gamma receptor-mediated effector functions of human polymorphonuclear leucocytes.', *Clinical and experimental immunology*, 61(2), pp. 425–32. Available at: http://www.ncbi.nlm.nih.gov/pubmed/2994926 (Accessed: 12 October 2022).

Fülöp, T. *et al.* (1997) 'Changes in apoptosis of human polymorphonuclear granulocytes with aging', *Mechanisms of ageing and development*. Mech Ageing Dev, 96(1–3), pp. 15–34. doi: 10.1016/S0047-6374(96)01881-7.

Futosi, K., Fodor, S. and Mócsai, A. (2013) 'Neutrophil cell surface receptors and their intracellular signal transduction pathways', *International Immunopharmacology*, 17, pp. 638–650. doi: 10.1016/j.intimp.2013.06.034.

Gagnon, J. A. *et al.* (2014) 'Efficient Mutagenesis by Cas9 Protein-Mediated Oligonucleotide Insertion and Large-Scale Assessment of Single-Guide RNAs'. doi: 10.1371/journal.pone.0098186.

Galkina, E. and Ley, K. (2009) 'Immune and inflammatory mechanisms of atherosclerosis (*)', *Annual review of immunology*. Annu Rev Immunol, 27, pp. 165–197. doi: 10.1146/ANNUREV.IMMUNOL.021908.132620.

Gavrilov, L. A. and Gavrilova, N. S. (2002) 'Evolutionary Theories of Aging and Longevity', *The Scientific World JOURNAL*, 2, pp. 339–356. doi: 10.1100/tsw.2002.96.

Gomez, C. R., Boehmer, E. D. and Kovacs, E. J. (2005) 'The aging innate immune system', *Current Opinion in Immunology*. Elsevier Current Trends, 17(5), pp. 457–462. doi: 10.1016/J.COI.2005.07.013.

Gonzalez-Freire, M. *et al.* (2018) 'Skeletal muscle ex vivo mitochondrial respiration parallels decline in vivo oxidative capacity, cardiorespiratory fitness, and muscle strength: The Baltimore Longitudinal Study of Aging', *Aging cell*. Aging Cell, 17(2). doi: 10.1111/ACEL.12725.

Greer, E. L. *et al.* (2010) 'Members of the Histone H3 Lysine 4 Trimethylation Complex Regulate Lifespan in a Germline-dependent Manner in C. elegans', *Nature*. NIH Public Access, 466(7304), p. 383. doi: 10.1038/NATURE09195.

Grentzinger, T. *et al.* (2012) 'piRNA-mediated transgenerational inheritance of an acquired trait', *Genome research*. Genome Res, 22(10), pp. 1877–1888. doi: 10.1101/GR.136614.111.

Grigg, J. M. *et al.* (1991) 'Neutrophil apoptosis and clearance from neonatal lungs', *Lancet (London, England)*. Lancet, 338(8769), pp. 720–722. doi: 10.1016/0140-6736(91)91443-X.

Grimm, A. and Eckert, A. (2017) 'Brain aging and neurodegeneration: from a mitochondrial point of view.', *Journal of neurochemistry*. J Neurochem, 143(4), pp. 418–431. doi: 10.1111/jnc.14037.

Gunawan, M. *et al.* (2015) 'The methyltransferase Ezh2 controls cell adhesion and migration through direct methylation of the extranuclear regulatory protein talin', *Nature Immunology*

2015 16:5. Nature Publishing Group, 16(5), pp. 505–516. doi: 10.1038/ni.3125.

Guo, X. *et al.* (2015) 'Regulation of histone demethylase KDM6B by hypoxia-inducible factor-2α', *Acta biochimica et biophysica Sinica*. Acta Biochim Biophys Sin (Shanghai), 47(2), pp. 106–113. doi: 10.1093/ABBS/GMU122.

Haithcock, E. *et al.* (2005) 'Age-related changes of nuclear architecture in Caenorhabditis elegans', *Proceedings of the National Academy of Sciences of the United States of America*. Proc Natl Acad Sci U S A, 102(46), pp. 16690–16695. doi: 10.1073/PNAS.0506955102.

Hamilton, N. *et al.* (2020) 'The failure of microglia to digest developmental apoptotic cells contributes to the pathology of RNASET2-deficient leukoencephalopathy', *Glia*. John Wiley & Sons, Ltd, 68(7), pp. 1531–1545. doi: 10.1002/GLIA.23829.

Handy, D. E., Castro, R. and Loscalzo, J. (2011) 'Epigenetic modifications: Basic mechanisms and role in cardiovascular disease', *Circulation*, 123(19), pp. 2145–2156. doi: 10.1161/CIRCULATIONAHA.110.956839.

Harbort, C. J. *et al.* (2015) 'Neutrophil oxidative burst activates ATM to regulate cytokine production and apoptosis', *Blood*, 126(26), pp. 2842–2851. doi: 10.1182/blood-2015-05-645424.

Hastings, S. N. and Heflin, M. T. (2005) 'A systematic review of interventions to improve outcomes for elders discharged from the emergency department', *Academic emergency medicine : official journal of the Society for Academic Emergency Medicine*. Acad Emerg Med, 12(10), pp. 978–986. doi: 10.1197/J.AEM.2005.05.032.

Hato, T. and Dagher, P. C. (2015) 'How the Innate Immune System Senses Trouble and Causes Trouble', *Clinical Journal of the American Society of Nephrology : CJASN*. American Society of Nephrology, 10(8), p. 1459. doi: 10.2215/CJN.04680514.

Hattermann, K. *et al.* (2007) 'The Toll-like receptor 7/8-ligand resiquimod (R-848) primes human neutrophils for leukotriene B4, prostaglandin E2 and platelet-activating factor biosynthesis', *FASEB journal : official publication of the Federation of American Societies for Experimental Biology*. FASEB J, 21(7), pp. 1575–1585. doi: 10.1096/FJ.06-7457COM.

Hawkins, P. G. *et al.* (2009) 'Promoter targeted small RNAs induce long-term transcriptional gene silencing in human cells.', *Nucleic acids research*. Oxford University Press, 37(9), pp. 2984–95. doi: 10.1093/nar/gkp127.

Hayashi, F., Means, T. K. and Luster, A. D. (2003) 'Toll-like receptors stimulate human neutrophil function', *Blood*. Blood, 102(7), pp. 2660–2669. doi: 10.1182/BLOOD-2003-04-

1078.

Hayflick, L. and Moorhead, P. S. (1961) 'The serial cultivation of human diploid cell strains', *Experimental Cell Research*. Academic Press, 25(3), pp. 585–621. doi: 10.1016/0014-4827(61)90192-6.

Hazeldine, J. *et al.* (2014) 'Impaired neutrophil extracellular trap formation: A novel defect in the innate immune system of aged individuals', *Aging Cell*, 13(4), pp. 690–698. doi: 10.1111/acel.12222.

Hébert, R. (1997) 'Functional decline in old age', *CMAJ: Canadian Medical Association Journal*. Canadian Medical Association, 157(8), p. 1037. Available at: /pmc/articles/PMC1228259/?report=abstract (Accessed: 6 October 2022).

Henry, K. M. *et al.* (2013) 'Zebrafish as a model for the study of neutrophil biology', *Journal of Leukocyte Biology*, 94(4), pp. 633–642. doi: 10.1189/jlb.1112594.

Hidalgo, A. *et al.* (2019) 'The Neutrophil Life Cycle', *Trends in Immunology*, 40(7), pp. 584–597. doi: 10.1016/j.it.2019.04.013.

Hoshijima, K. *et al.* (2019) 'Highly Efficient CRISPR-Cas9-Based Methods for Generating Deletion Mutations and F0 Embryos that Lack Gene Function in Zebrafish', *Developmental cell*. Dev Cell, 51(5), pp. 645-657.e4. doi: 10.1016/J.DEVCEL.2019.10.004.

Hruscha, A. *et al.* (2013) 'Efficient CRISPR/Cas9 genome editing with low off-target effects in zebrafish', *Development*. The Company of Biologists, 140(24), pp. 4982–4987. doi: 10.1242/DEV.099085.

Hu, N., Westra, J. and Kallenberg, C. G. M. (2009) 'Membrane-bound proteinase 3 and its receptors: relevance for the pathogenesis of Wegener's Granulomatosis', *Autoimmunity reviews*. Autoimmun Rev, 8(6), pp. 510–514. doi: 10.1016/J.AUTREV.2008.01.003.

Hu, W. *et al.* (2021) 'A Novel Function of TLR2 and MyD88 in the Regulation of Leukocyte Cell Migration Behavior During Wounding in Zebrafish Larvae', *Frontiers in Cell and Developmental Biology*, 9(February), pp. 1–18. doi: 10.3389/fcell.2021.624571.

Hu, Z. *et al.* (2014) 'Nucleosome loss leads to global transcriptional up-regulation and genomic instability during yeast aging', *Genes & development*. Genes Dev, 28(4), pp. 396–408. doi: 10.1101/GAD.233221.113.

Hwang, W. Y. *et al.* (2013) 'Efficient In Vivo Genome Editing Using RNA-Guided Nucleases', *Nature biotechnology*. NIH Public Access, 31(3), p. 227. doi: 10.1038/NBT.2501.

Imperatore, F. *et al.* (2017) 'SIRT1 regulates macrophage self-renewal', *The EMBO Journal*, 36,

pp. 2353–2372. doi: 10.15252/embj.201695737.

Isiaku, A. I. *et al.* (2021) 'Transient, flexible gene editing in zebrafish neutrophils and macrophages for determination of cell-autonomous functions', *Disease Models & Mechanisms*, 14(7). doi: 10.1242/dmm.047431.

Isles, H. M. *et al.* (2019) 'The CXCL12/CXCR4 Signaling Axis Retains Neutrophils at Inflammatory Sites in Zebrafish', *Frontiers in immunology*, 10(July), p. 1784. doi: 10.3389/fimmu.2019.01784.

Jao, L. E., Wente, S. R. and Chen, W. (2013) 'Efficient multiplex biallelic zebrafish genome editing using a CRISPR nuclease system', *Proceedings of the National Academy of Sciences of the United States of America*. National Academy of Sciences, 110(34), pp. 13904–13909. doi: 10.1073/PNAS.1308335110/-/DCSUPPLEMENTAL.

Jasper, A. E. *et al.* (2019) 'Understanding the role of neutrophils in chronic inflammatory airway disease [version 1; peer review: 2 approved] 1 2'. doi: 10.12688/f1000research.18411.1.

Jenuwein, T. and Allis, C. D. (2001) 'Translating the histone code', *Science*. Science, pp. 1074–1080. doi: 10.1126/science.1063127.

Jin, C. *et al.* (2011) 'Histone demethylase UTX-1 regulates C. elegans life span by targeting the insulin/IGF-1 signaling pathway', *Cell metabolism*. Cell Metab, 14(2), pp. 161–172. doi: 10.1016/J.CMET.2011.07.001.

Juss, J. K. *et al.* (2016) 'Acute respiratory distress syndrome neutrophils have a distinct phenotype and are resistant to phosphoinositide 3-kinase inhibition', *American Journal of Respiratory and Critical Care Medicine*, 194(8), pp. 961–973. doi: 10.1164/rccm.201509-1818OC.

Kalliolias, G. D. and Ivashkiv, L. B. (2016) 'TNF biology, pathogenic mechanisms and emerging therapeutic strategies', *Nature reviews. Rheumatology*. NIH Public Access, 12(1), p. 49. doi: 10.1038/NRRHEUM.2015.169.

Kanther, M. *et al.* (2011) 'Microbial Colonization Induces Dynamic Temporal and Spatial Patterns of NF-κB Activation in the Zebrafish Digestive Tract', *Gastroenterology*, 141(1), pp. 197–207. doi: 10.1053/j.gastro.2011.03.042.

Kao, H. Y. *et al.* (2000) 'Isolation of a novel histone deacetylase reveals that class I and class II deacetylases promote SMRT-mediated repression.', *Genes & development*. Genes Dev, 14(1), pp. 55–66. Available at: http://www.ncbi.nlm.nih.gov/pubmed/10640276 (Accessed: 19

February 2020).

Kara, N. *et al.* (2019) 'The miR-216a-Dot1l Regulatory Axis Is Necessary and Sufficient for Müller Glia Reprogramming during Retina Regeneration', *Cell reports*. Cell Rep, 28(8), pp. 2037-2047.e4. doi: 10.1016/J.CELREP.2019.07.061.

Karvelis, T. *et al.* (2013) 'crRNA and tracrRNA guide Cas9-mediated DNA interference in Streptococcus thermophilus', *RNA Biology*. Taylor & Francis, 10(5), p. 841. doi: 10.4161/RNA.24203.

Kaur, J., Daoud, A. and Eblen, S. T. (2019) 'Targeting Chromatin Remodeling for Cancer Therapy', *Current molecular pharmacology*. Curr Mol Pharmacol, 12(3), pp. 215–229. doi: 10.2174/1874467212666190215112915.

Kawai, T. and Akira, S. (2010) 'The role of pattern-recognition receptors in innate immunity: update on Toll-like receptors', *Nature immunology*. Nat Immunol, 11(5), pp. 373–384. doi: 10.1038/NI.1863.

Kenyon, A. *et al.* (2017) 'Active nuclear transcriptome analysis reveals inflammasome-dependent mechanism for early neutrophil response to Mycobacterium marinum', *Scientific Reports*. Springer US, 7(1), pp. 1–14. doi: 10.1038/s41598-017-06099-x.

Keppler, B. R. and Archer, T. K. (2008) 'Chromatin-modifying enzymes as therapeutic targets - Part 1', *Expert Opinion on Therapeutic Targets*, 12(10), pp. 1301–1312. doi: 10.1517/14728222.12.10.1301.

Khoyratty, T. E. *et al.* (2021) 'Distinct transcription factor networks control neutrophil-driven inflammation', *Nature Immunology*. Nature Research, 22(9), pp. 1093–1106. doi: 10.1038/S41590-021-00968-4.

Kim, D. *et al.* (2019) 'Graph-based genome alignment and genotyping with HISAT2 and HISAT-genotype', *Nature Biotechnology 2019 37:8*. Nature Publishing Group, 37(8), pp. 907–915. doi: 10.1038/s41587-019-0201-4.

Kim, D. H. *et al.* (2006) 'Argonaute-1 directs siRNA-mediated transcriptional gene silencing in human cells.', *Nature structural & molecular biology*. Nat Struct Mol Biol, 13(9), pp. 793–7. doi: 10.1038/nsmb1142.

Kim, D. H. *et al.* (2008) 'MicroRNA-directed transcriptional gene silencing in mammalian cells.', *Proceedings of the National Academy of Sciences of the United States of America*. Proc Natl Acad Sci U S A, 105(42), pp. 16230–5. doi: 10.1073/pnas.0808830105.

Kim, D. H. *et al.* (2019) 'Knockout of longevity gene Sirt1 in zebrafish leads to oxidative injury,

chronic inflammation, and reduced life span', *PloS one*. PLoS One, 14(8). doi: 10.1371/JOURNAL.PONE.0220581.

Kim, M., Lu, R. J. and Benayoun, B. A. (2022) 'Single-cell RNA-seq of primary bone marrow neutrophils from female and male adult mice', *Scientific Data*, 9(1), p. 442. doi: 10.1038/s41597-022-01544-7.

KIM, M., MOON, H.-B. and SPANGRUDE, G. J. (2003) 'Major Age-Related Changes Of Mouse Hematopoietic Stem/Progenitor Cells', *Annals of the New York Academy of Sciences*, 996(1), pp. 195–208. doi: 10.1111/j.1749-6632.2003.tb03247.x.

Kim, S., Yu, N. K. and Kaang, B. K. (2015) 'CTCF as a multifunctional protein in genome regulation and gene expression', *Experimental & Molecular Medicine 2015 47:6*. Nature Publishing Group, 47(6), pp. e166–e166. doi: 10.1038/emm.2015.33.

Kirkwood, T. B. (1977) 'Evolution of ageing.', *Nature*. Nature, 270(5635), pp. 301–4. doi: 10.1038/270301a0.

Kitchen, G. B. *et al.* (2021) 'The histone methyltransferase Ezh2 restrains macrophage inflammatory responses', *The FASEB Journal*. Wiley-Blackwell, 35(10). doi: 10.1096/FJ.202100044RRR.

Kotas, M. E. and Medzhitov, R. (2015) 'Homeostasis, Inflammation, and Disease Susceptibility', *Cell*. NIH Public Access, 160(5), p. 816. doi: 10.1016/J.CELL.2015.02.010.

Krämer, A. *et al.* (2014) 'Causal analysis approaches in Ingenuity Pathway Analysis', *Bioinformatics (Oxford, England)*. Bioinformatics, 30(4), pp. 523–530. doi: 10.1093/BIOINFORMATICS/BTT703.

Krishnamoorthy, N. *et al.* (2018) 'Neutrophil cytoplasts induce TH17 differentiation and skew inflammation toward neutrophilia in severe asthma', *Science Immunology*. American Association for the Advancement of Science, 3(26). doi: 10.1126/SCIIMMUNOL.AAO4747/SUPPL_FILE/AAO4747_SM.PDF.

Kruidenier, L. *et al.* (2012) 'A selective jumonji H3K27 demethylase inhibitor modulates the proinflammatory macrophage response', *Nature 2012 488:7411*. Nature Publishing Group, 488(7411), pp. 404–408. doi: 10.1038/nature11262.

Kubes, P. (2018) 'The enigmatic neutrophil: what we do not know', *Cell and Tissue Research*. Springer Verlag, 371(3), pp. 399–406. doi: 10.1007/S00441-018-2790-5/FIGURES/1.

Kumar, B. V., Connors, T. J. and Farber, D. L. (2018) 'Human T cell development, localization, and function throughout life', *Immunity*. NIH Public Access, 48(2), p. 202. doi:

10.1016/J.IMMUNI.2018.01.007.

Kumar, V. and Sharma, A. (2010) 'Neutrophils: Cinderella of innate immune system', *International Immunopharmacology*. Elsevier, 10(11), pp. 1325–1334. doi: 10.1016/J.INTIMP.2010.08.012.

Lacy, P. (2006) 'Mechanisms of degranulation in neutrophils', *Allergy, Asthma and Clinical Immunology*, 2(3), pp. 98–108. doi: 10.2310/7480.2006.00012.

Lämmermann, T. *et al.* (2013) 'Neutrophil swarms require LTB4 and integrins at sites of cell death in vivo', *Nature 2013 498:7454*. Nature Publishing Group, 498(7454), pp. 371–375. doi: 10.1038/nature12175.

Laphanuwat, P., Gomes, D. C. O. and Akbar, A. N. (2023) 'Senescent T cells: Beneficial and detrimental roles', *Immunological reviews*. Immunol Rev. doi: 10.1111/IMR.13206.

Lapinet, J. A. *et al.* (2000) 'Gene expression and production of tumor necrosis factor alpha, interleukin-1beta (IL-1beta), IL-8, macrophage inflammatory protein 1alpha (MIP-1alpha), MIP-1beta, and gamma interferon-inducible protein 10 by human neutrophils stimulated with group B meningococcal outer membrane vesicles', *Infection and immunity*. Infect Immun, 68(12), pp. 6917–6923. doi: 10.1128/IAI.68.12.6917-6923.2000.

Larson, K. *et al.* (2012) 'Heterochromatin formation promotes longevity and represses ribosomal RNA synthesis', *PLoS genetics*. PLoS Genet, 8(1). doi: 10.1371/JOURNAL.PGEN.1002473.

Lee, G. R. (2018) 'The Balance of Th17 versus Treg Cells in Autoimmunity', *International Journal of Molecular Sciences*. Multidisciplinary Digital Publishing Institute (MDPI), 19(3). doi: 10.3390/IJMS19030730.

Lee, H. Y. *et al.* (2014) 'HIF-1-Dependent Induction of Jumonji Domain-Containing Protein (JMJD) 3 under Hypoxic Conditions', *Molecules and Cells*. Korean Society for Molecular and Cellular Biology, 37(1), p. 43. doi: 10.14348/MOLCELLS.2014.2250.

Lewis, A. and Elks, P. M. (2019) 'Hypoxia induces macrophage tnfa expression via cyclooxygenase and prostaglandin E2 in vivo', *Frontiers in Immunology*, 10(SEP), pp. 1–14. doi: 10.3389/fimmu.2019.02321.

Liao, Y., Smyth, G. K. and Shi, W. (2019) 'The R package Rsubread is easier, faster, cheaper and better for alignment and quantification of RNA sequencing reads', *Nucleic acids research*. Nucleic Acids Res, 47(8). doi: 10.1093/NAR/GKZ114.

Lichtman, M. K., Otero-Vinas, M. and Falanga, V. (2016) 'Transforming growth factor beta

(TGF-β) isoforms in wound healing and fibrosis', *Wound repair and regeneration : official publication of the Wound Healing Society [and] the European Tissue Repair Society*. Wound Repair Regen, 24(2), pp. 215–222. doi: 10.1111/WRR.12398.

Lieschke, G. J. and Currie, P. D. (2007) 'Animal models of human disease: zebrafish swim into view', *Nature Reviews Genetics 2007 8:5*. Nature Publishing Group, 8(5), pp. 353–367. doi: 10.1038/nrg2091.

Liew, P. X. and Kubes, P. (2019) 'The Neutrophil's Role During Health and Disease', *Physiological Reviews*. American Physiological Society Bethesda, MD , 99(2), pp. 1223–1248. doi: 10.1152/physrev.00012.2018.

Liu, J. *et al.* (2019) 'Roles of Telomere Biology in Cell Senescence, Replicative and Chronological Ageing.', *Cells*. Cells, 8(1). doi: 10.3390/cells8010054.

Lo, M. W. and Woodruff, T. M. (2020) 'Complement: Bridging the innate and adaptive immune systems in sterile inflammation', *Journal of Leukocyte Biology*. John Wiley and Sons Inc., 108(1), pp. 339–351. doi: 10.1002/JLB.3MIR0220-270R.

Loh, W. and Vermeren, S. (2022) 'Anti-Inflammatory Neutrophil Functions in the Resolution of Inflammation and Tissue Repair', *Cells*. Cells, 11(24). doi: 10.3390/CELLS11244076.

López-Otín, C. *et al.* (2013) 'The hallmarks of aging', *Cell*. Cell, p. 1194. doi: 10.1016/j.cell.2013.05.039.

López-Otín, C. *et al.* (2023) 'Hallmarks of aging: An expanding universe', *Cell*. Elsevier B.V., 186(2), pp. 243–278. doi: 10.1016/J.CELL.2022.11.001.

Loynes, C. A. *et al.* (2010) 'Pivotal Advance: Pharmacological manipulation of inflammation resolution during spontaneously resolving tissue neutrophilia in the zebrafish', *Journal of leukocyte biology*. J Leukoc Biol, 87(2), pp. 203–212. doi: 10.1189/JLB.0409255.

Loynes, C. A. *et al.* (2018) 'PGE 2 production at sites of tissue injury promotes an anti-inflammatory neutrophil phenotype and determines the outcome of inflammation resolution in vivo', *Science Advances*, 4(9). doi: 10.1126/sciadv.aar8320.

Lu, A. T. *et al.* (2019) 'DNA methylation GrimAge strongly predicts lifespan and healthspan', *Aging*, 11(2), pp. 303–327. doi: 10.18632/aging.101684.

Luger, K., Dechassa, M. L. and Tremethick, D. J. (2012) 'New insights into nucleosome and chromatin structure: An ordered state or a disordered affair?', *Nature Reviews Molecular Cell Biology*. Nature Publishing Group, 13(7), pp. 436–447. doi: 10.1038/nrm3382.

Makki, F. (2017) *Effects of Chromatin Remodelling on Neutrophil Gene Expression*. University

of Liverpool.

Manda-Handzlik, A. *et al.* (2018) 'The influence of agents differentiating HL-60 cells toward granulocyte-like cells on their ability to release neutrophil extracellular traps', *Immunology and cell biology*. Immunol Cell Biol, 96(4), pp. 413–425. doi: 10.1111/IMCB.12015.

Mariño-Ramírez, L. *et al.* (2005) 'Histone structure and nucleosome stability', *Expert Review of Proteomics*, pp. 719–729. doi: 10.1586/14789450.2.5.719.

Marjoram, L. *et al.* (2015) 'Epigenetic control of intestinal barrier function and inflammation in zebrafish', *Proceedings of the National Academy of Sciences of the United States of America*. National Academy of Sciences, 112(9), pp. 2770–2775. doi: 10.1073/PNAS.1424089112/SUPPL_FILE/PNAS.201424089SI.PDF.

Marwick, J. A. *et al.* (2018) 'Neutrophils induce macrophage anti-inflammatory reprogramming by suppressing NF-κB activation', *Cell Death & Disease*. Nature Publishing Group, 9(6). doi: 10.1038/S41419-018-0710-Y.

Maures, T. J. *et al.* (2011) 'The H3K27 demethylase UTX-1 regulates C. elegans lifespan in a germline-independent, insulin-dependent manner', *Aging cell*. Aging Cell, 10(6), pp. 980–990. doi: 10.1111/J.1474-9726.2011.00738.X.

McColl, G. *et al.* (2008) 'Pharmacogenetic analysis of lithium-induced delayed aging in Caenorhabditis elegans', *The Journal of biological chemistry*. J Biol Chem, 283(1), pp. 350–357. doi: 10.1074/JBC.M705028200.

Millerand, M., Berenbaum, F. and Jacques, C. (2019) 'Danger signals and inflammaging in osteoarthritis', *Clinical and experimental rheumatology*, 37(5), pp. 48–56.

Minciullo, P. L. *et al.* (2016) 'Inflammaging and Anti-Inflammaging: The Role of Cytokines in Extreme Longevity', *Arch. Immunol. Ther. Exp.*, 64, pp. 111–126. doi: 10.1007/s00005-015-0377-3.

Mócsai, A., Walzog, B. and Lowell, C. A. (2015) 'Intracellular signalling during neutrophil recruitment', *Cardiovascular Research*. Oxford Academic, 107(3), pp. 373–385. doi: 10.1093/CVR/CVV159.

Moorlag, S. J. C. F. M. *et al.* (2020) 'BCG Vaccination Induces Long-Term Functional Reprogramming of Human Neutrophils', *Cell Reports*. ElsevierCompany., 33(7), p. 108387. doi: 10.1016/j.celrep.2020.108387.

Muire, P. J. *et al.* (2017) 'Differential gene expression following TLR stimulation in rag1-/- mutant zebrafish tissues and morphological descriptions of lymphocyte-like cell populations.',

PloS one. Public Library of Science, 12(9), p. e0184077. doi: 10.1371/journal.pone.0184077.

Nasevicius, A. and Ekker, S. C. (2000) 'Effective targeted gene "knockdown" in zebrafish', *Nature Genetics 2000 26:2*. Nature Publishing Group, 26(2), pp. 216–220. doi: 10.1038/79951.

Nathan, C. and Ding, A. (2003) 'Leading Edge Review Nonresolving Inflammation'. doi: 10.1016/j.cell.2010.02.029.

Neefjes, J. *et al.* (2011) 'Towards a systems understanding of MHC class I and MHC class II antigen presentation', *Nature reviews. Immunology*. Nat Rev Immunol, 11(12), pp. 823–836. doi: 10.1038/NRI3084.

Neele, A. E. *et al.* (2021) 'Myeloid Ezh2 Deficiency Limits Atherosclerosis Development', *Frontiers in Immunology*, 11(January), pp. 1–9. doi: 10.3389/fimmu.2020.594603.

Newman, A. B. *et al.* (2016) 'Trajectories of function and biomarkers with age: the CHS All Stars Study', *International journal of epidemiology*. Int J Epidemiol, 45(4), pp. 1135–1145. doi: 10.1093/IJE/DYW092.

Ni, S. *et al.* (2021) 'EZH2 Mediates miR-146a-5p/HIF-1 α to Alleviate Inflammation and Glycolysis after Acute Spinal Cord Injury', *Mediators of inflammation*. Mediators Inflamm, 2021. doi: 10.1155/2021/5591582.

Nordenfelt, P. and Tapper, H. (2011) 'Phagosome dynamics during phagocytosis by neutrophils', *Journal of Leukocyte Biology*. Wiley, 90(2), pp. 271–284. doi: 10.1189/JLB.0810457.

Nourshargh, S., Renshaw, S. A. and Imhof, B. A. (2016) 'Reverse Migration of Neutrophils: Where, When, How, and Why?', *Trends in Immunology*. Elsevier Ltd, 37(5), pp. 273–286. doi: 10.1016/j.it.2016.03.006.

Nutt, S. L. *et al.* (2020) 'EZH2 function in immune cell development', *Biological chemistry*. Biol Chem, 401(8), pp. 933–943. doi: 10.1515/HSZ-2019-0436.

O'Connell, M. R. *et al.* (2014) 'Programmable RNA recognition and cleavage by CRISPR/Cas9', *Nature 2014 516:7530*. Nature Publishing Group, 516(7530), pp. 263–266. doi: 10.1038/nature13769.

O'Sullivan, R. J. *et al.* (2010) 'Reduced histone biosynthesis and chromatin changes arising from a damage signal at telomeres', *Nature structural & molecular biology*. NIH Public Access, 17(10), p. 1218. doi: 10.1038/NSMB.1897.

Ogryzko, N. V *et al.* (2014) 'Zebrafish tissue injury causes upregulation of interleukin-1 and caspase-dependent amplification of the inflammatory response.', *Disease models &*

mechanisms. Company of Biologists, 7(2), pp. 259–64. doi: 10.1242/dmm.013029.

de Oliveira, S. *et al.* (2013) 'Cxcl8 (IL-8) Mediates Neutrophil Recruitment and Behavior in the Zebrafish Inflammatory Response', *The Journal of Immunology*, 190(8), pp. 4349–4359. doi: 10.4049/jimmunol.1203266.

Ou, H.-L. and Schumacher, B. (2018) 'DNA damage responses and p53 in the aging process', *Blood*, 131(5), pp. 488–495. doi: 10.1182/blood-2017-07-746396.

Palikaras, K., Lionaki, E. and Tavernarakis, N. (2015) 'Coordination of mitophagy and mitochondrial biogenesis during ageing in C. elegans.', *Nature*. Nature, 521(7553), pp. 525–8. doi: 10.1038/nature14300.

Pardo, P. S. and Boriek, A. M. (2020) *SIRT1 Regulation in Ageing and Obesity*, *Mechanisms of Ageing and Development*. Elsevier Ireland Ltd. doi: 10.1016/j.mad.2020.111249.

Parker, D. C. (1993) 'T cell-dependent B cell activation', *Annual review of immunology*. Annu Rev Immunol, 11, pp. 331–360. doi: 10.1146/ANNUREV.IY.11.040193.001555.

Peiró, T. *et al.* (2018) 'Neutrophils drive alveolar macrophage IL-1β release during respiratory viral infection Respiratory infection', *Thorax*, 73, pp. 546–556. doi: 10.1136/thoraxjnl-2017-210010.

Pilsczek, F. H. *et al.* (2010) 'A novel mechanism of rapid nuclear neutrophil extracellular trap formation in response to Staphylococcus aureus.', *Journal of Immunology (Baltimore, Md. : 1950)*. The American Association of Immunologists, 185(12), pp. 7413–7425. doi: 10.4049/JIMMUNOL.1000675.

Portela, A. *et al.* (2013) 'DNA methylation determines nucleosome occupancy in the 5'-CpG islands of tumor suppressor genes', *Oncogene 2013 32:47*. Nature Publishing Group, 32(47), pp. 5421–5428. doi: 10.1038/onc.2013.162.

Progatzky, F. *et al.* (2019) 'Induction of innate cytokine responses by respiratory mucosal challenge with R848 in zebrafish, mice, and humans', *Journal of Allergy and Clinical Immunology*, 144(1), pp. 342-345.e7. doi: 10.1016/j.jaci.2019.04.003.

Rabe, K. F. and Watz, H. (2017) 'Chronic obstructive pulmonary disease', *The Lancet*. Lancet Publishing Group, 389(10082), pp. 1931–1940. doi: 10.1016/S0140-6736(17)31222-9.

Rahman, A. *et al.* (2019) 'Inhibition of ErbB kinase signalling promotes resolution of neutrophilic inflammation', *eLife*. Elife, 8. doi: 10.7554/ELIFE.50990.

Ramanathan, K. *et al.* (2018) 'Neutrophil activation signature in juvenile idiopathic arthritis indicates the presence of low-density granulocytes', *Rheumatology (United Kingdom)*, 57(3),

pp. 488–498. doi: 10.1093/rheumatology/kex441.

Ravetch, J. V. and Bolland, S. (2003) 'IgG Fc Receptors', *https://doi.org/10.1146/annurev.immunol.19.1.275*. Annual Reviews 4139 El Camino Way, P.O. Box 10139, Palo Alto, CA 94303-0139, USA , 19, pp. 275–290. doi: 10.1146/ANNUREV.IMMUNOL.19.1.275.

Renshaw, S. A. *et al.* (2006) 'A transgenic zebrafish model of neutrophilic inflammation', *Blood*, 108(13), pp. 3976–3978. doi: 10.1182/blood-2006-05-024075.

Renshaw, S. A. and Trede, N. S. (2012) 'A model 450 million years in the making: Zebrafish and vertebrate immunity', *DMM Disease Models and Mechanisms*. Company of Biologists, 5(1), pp. 38–47. doi: 10.1242/DMM.007138/-/DC1.

Rincón, E., Rocha-Gregg, B. L. and Collins, S. R. (2018) 'A map of gene expression in neutrophil-like cell lines.', *BMC genomics*. BMC Genomics, 19(1), p. 573. doi: 10.1186/s12864-018-4957-6.

Robertson, A. L. *et al.* (2014) 'A Zebrafish Compound Screen Reveals Modulation of Neutrophil Reverse Migration as an Anti-Inflammatory Mechanism', *Sci Transl Med*, 6(225). doi: 10.1126/scitranslmed.3007672.

Robertson, A. L. *et al.* (2016) 'Identification of benzopyrone as a common structural feature in compounds with anti-inflammatory activity in a zebrafish phenotypic screen', *Disease Models & Mechanisms*, 9(6), pp. 621–632. doi: 10.1242/dmm.024935.

Robinson, M. D., McCarthy, D. J. and Smyth, G. K. (2009) 'edgeR: A Bioconductor package for differential expression analysis of digital gene expression data', *Bioinformatics*. Bioinformatics, 26(1), pp. 139–140. doi: 10.1093/bioinformatics/btp616.

Rørvig, S. *et al.* (2013) 'Proteome profiling of human neutrophil granule subsets, secretory vesicles, and cell membrane: correlation with transcriptome profiling of neutrophil precursors', *Journal of Leukocyte Biology*. Wiley, 94(4), pp. 711–721. doi: 10.1189/JLB.1212619.

Rossi, D. J. *et al.* (2005) 'Cell intrinsic alterations underlie hematopoietic stem cell aging.', *Proceedings of the National Academy of Sciences of the United States of America*. Proc Natl Acad Sci U S A, 102(26), pp. 9194–9. doi: 10.1073/pnas.0503280102.

Rougeot, J. *et al.* (2019) 'RNAseq profiling of leukocyte populations in zebrafish larvae reveals a cxcl11 chemokine gene as a marker of macrophage polarization during mycobacterial infection', *Frontiers in Immunology*. Frontiers Media S.A., 10(MAR), p. 832. doi:

10.3389/FIMMU.2019.00832/BIBTEX.

Sabroe, I. *et al.* (2004) 'What can we learn from highly purified neutrophils?', *468 Biochemical Society Transactions*, 32.

Salminen, A. *et al.* (2014) 'Histone demethylase Jumonji D3 (JMJD3/KDM6B) at the nexus of epigenetic regulation of inflammation and the aging process', *Journal of Molecular Medicine*. Springer Verlag, 92(10), pp. 1035–1043. doi: 10.1007/S00109-014-1182-X/FIGURES/2.

Sander, J. D. *et al.* (2011) 'Targeted gene disruption in somatic zebrafish cells using engineered TALENs', *Nature biotechnology*. NIH Public Access, 29(8), p. 697. doi: 10.1038/NBT.1934.

De Santa, F. *et al.* (2007) 'The Histone H3 Lysine-27 Demethylase Jmjd3 Links Inflammation to Inhibition of Polycomb-Mediated Gene Silencing', *Cell*. Cell Press, 130(6), pp. 1083–1094. doi: 10.1016/J.CELL.2007.08.019.

De Santa, F. *et al.* (2009) 'Jmjd3 contributes to the control of gene expression in LPS-activated macrophages', *The EMBO Journal*. John Wiley & Sons, Ltd, 28(21), pp. 3341–3352. doi: 10.1038/EMBOJ.2009.271.

Santoro, A., Bientinesi, E. and Monti, D. (2021) 'Immunosenescence and inflammaging in the aging process: age-related diseases or longevity?', *Ageing Research Reviews*. Elsevier Ireland Ltd, 71. doi: 10.1016/J.ARR.2021.101422.

Sapey, E. *et al.* (2014) 'Phosphoinositide 3-kinase inhibition restores neutrophil accuracy in the elderly: toward targeted treatments for immunosenescence', *Blood Journal*, 123(2), pp. 239–248. doi: 10.1182/blood-2013-08.

Sauce, D. *et al.* (2017) 'Reduced Oxidative Burst by Primed Neutrophils in the Elderly Individuals Is Associated With Increased Levels of the CD16bright/CD62Ldim Immunosuppressive Subset', *The Journals of Gerontology: Series A*. Oxford Academic, 72(2), pp. 163–172. doi: 10.1093/GERONA/GLW062.

Savill, J. S. *et al.* (1989) 'Macrophage phagocytosis of aging neutrophils in inflammation. Programmed cell death in the neutrophil leads to its recognition by macrophages.', *The Journal of clinical investigation*. J Clin Invest, 83(3), pp. 865–75. doi: 10.1172/JCI113970.

Sayed, N. *et al.* (2021) 'An inflammatory aging clock (iAge) based on deep learning tracks multimorbidity, immunosenescence, frailty and cardiovascular aging', *Nature Aging 2021 1:7*. Nature Publishing Group, 1(7), pp. 598–615. doi: 10.1038/s43587-021-00082-y.

Scaffidi, P. and Misteli, T. (2006) 'Lamin A-dependent nuclear defects in human aging', *Science*. Cold Spring Harbor Laboratory Press, 312(5776), pp. 1059–1063. doi:

10.1126/SCIENCE.1127168.

Scalabrino, G. and Ferioli, M. E. (1984) 'Polyamines in mammalian ageing: an oncological problem, too? A review', *Mechanisms of ageing and development*. Mech Ageing Dev, 26(2–3), pp. 149–164. doi: 10.1016/0047-6374(84)90090-3.

Scheer, S. *et al.* (2020) 'The Methyltransferase DOT1L Controls Activation and Lineage Integrity in CD4 + T Cells during Infection and Inflammation', *Cell reports*. Cell Rep, 33(11). doi: 10.1016/J.CELREP.2020.108505.

Schrempft, S. and Stringhini, S. (2023) 'Socioeconomic inequalities in the Pace of Aging', *Aging (Albany NY)*. Impact Journals, LLC, 15(6), p. 1706. doi: 10.18632/AGING.204595.

Schroeder, H. W. and Cavacini, L. (2010) 'Structure and Function of Immunoglobulins', *The Journal of allergy and clinical immunology*. NIH Public Access, 125(2 0 2), p. S41. doi: 10.1016/J.JACI.2009.09.046.

Schultze, M. (1865) 'Ein heizbarer Objecttisch und seine Verwendung bei Untersuchungen des Blutes', *Archiv für mikroskopische Anatomie*, 1(1), pp. 1–42. doi: 10.1007/BF02961404.

Servant, G. *et al.* (2000) 'Polarization of Chemoattractant Receptor Signaling During Neutrophil Chemotaxis', *Science (New York, N.Y.)*. NIH Public Access, 287(5455), p. 1037. doi: 10.1126/SCIENCE.287.5455.1037.

Shah, A. N. *et al.* (2015) 'Rapid reverse genetic screening using CRISPR in zebrafish', *Nature methods*. NIH Public Access, 12(6), p. 535. doi: 10.1038/NMETH.3360.

Shait Mohammed, M. R. *et al.* (2022) 'The Histone H3K27me3 Demethylases KDM6A/B Resist Anoikis and Transcriptionally Regulate Stemness-Related Genes', *Frontiers in Cell and Developmental Biology*. Frontiers Media S.A., 10, p. 83. doi: 10.3389/FCELL.2022.780176/BIBTEX.

Shimizu, Y. and Kawasaki, T. (2021) 'Histone acetyltransferase EP300 regulates the proliferation and differentiation of neural stem cells during adult neurogenesis and regenerative neurogenesis in the zebrafish optic tectum', *Neuroscience letters*. Neurosci Lett, 756. doi: 10.1016/J.NEULET.2021.135978.

Sonninen, T. M. *et al.* (2020) 'Proteostasis Disturbances and Inflammation in Neurodegenerative Diseases', *Cells*. Multidisciplinary Digital Publishing Institute (MDPI), 9(10). doi: 10.3390/CELLS9102183.

Srinivas, N., Rachakonda, S. and Kumar, R. (2020) 'Telomeres and Telomere Length: A General Overview', *Cancers*. Multidisciplinary Digital Publishing Institute, 12(3), p. 558. doi:

10.3390/cancers12030558.

Stackowicz, J., Jönsson, F. and Reber, L. L. (2019) 'Mouse Models and Tools for the in vivo Study of Neutrophils.', *Frontiers in immunology*. Front Immunol, 10, p. 3130. doi: 10.3389/fimmu.2019.03130.

Sun, L. *et al.* (2020) 'Innate-adaptive immunity interplay and redox regulation in immune response', *Redox biology*. Redox Biol, 37. doi: 10.1016/J.REDOX.2020.101759.

Sun, N., Youle, R. J. and Finkel, T. (2016) 'The Mitochondrial Basis of Aging.', *Molecular cell*. Mol Cell, 61(5), pp. 654–666. doi: 10.1016/j.molcel.2016.01.028.

Sutton, M., Grimmer-Somers, K. and Jeffries, L. (2008) 'Screening tools to identify hospitalised elderly patients at risk of functional decline: a systematic review', *International journal of clinical practice*. Int J Clin Pract, 62(12), pp. 1900–1909. doi: 10.1111/J.1742-1241.2008.01930.X.

Taggart, C. *et al.* (2000) 'Oxidation of either Methionine 351 or Methionine 358 in α1-Antitrypsin Causes Loss of Anti-neutrophil Elastase Activity', *Journal of Biological Chemistry*. Elsevier BV, 275(35), pp. 27258–27265. doi: 10.1016/s0021-9258(19)61505-x.

Tamassia, N. *et al.* (2019) 'Human neutrophils activated via TLR8 promote Th17 polarization through IL-23', *Journal of Leukocyte Biology*, 105(6), pp. 1155–1165. doi: 10.1002/JLB.MA0818-308R.

Tamassia, N. *et al.* (2021) 'Induction of OCT2 contributes to regulate the gene expression program in human neutrophils activated via TLR8', *Cell reports*. Cell Rep, 35(7). doi: 10.1016/J.CELREP.2021.109143.

Teixeira, C. F. P. *et al.* (2005) 'Effects of neutrophil depletion in the local pathological alterations and muscle regeneration in mice injected with Bothrops jararaca snake venom.', *International journal of experimental pathology*. Int J Exp Pathol, 86(2), pp. 107–15. doi: 10.1111/j.0959-9673.2005.00419.x.

Terzioglu, M. *et al.* (2020) 'Improving CRISPR/Cas9 mutagenesis efficiency by delaying the early development of zebrafish embryos', *Scientific Reports*. Nature Publishing Group, 10(1). doi: 10.1038/S41598-020-77677-9.

Todd, J. A. (2010) 'Etiology of Type 1 Diabetes', *Immunity*, pp. 457–467. doi: 10.1016/j.immuni.2010.04.001.

Traver, D. *et al.* (2003) 'The Zebrafish as a Model Organism to Study Development of the Immune System', *Advances in Immunology*. Academic Press Inc., 81, pp. 253–330. doi:

10.1016/S0065-2776(03)81007-6.

Trinh, L. A. *et al.* (2017) 'Biotagging of Specific Cell Populations in Zebrafish Reveals Gene Regulatory Logic Encoded in the Nuclear Transcriptome', *Cell Reports*, 19(2), pp. 425–440. doi: 10.1016/j.celrep.2017.03.045.

Valcarce, D. G. *et al.* (2023) 'Stress decreases spermatozoa quality and induces molecular alterations in zebrafish progeny', *BMC biology*. BMC Biol, 21(1), p. 70. doi: 10.1186/S12915-023-01570-W.

Vallabhapurapu, S. and Karin, M. (2009) 'Regulation and function of NF-kappaB transcription factors in the immune system', *Annual review of immunology*. Annu Rev Immunol, 27, pp. 693–733. doi: 10.1146/ANNUREV.IMMUNOL.021908.132641.

Varshney, G. K. *et al.* (2015) 'High-throughput gene targeting and phenotyping in zebrafish using CRISPR/Cas9', *Genome research*. Genome Res, 25(7), pp. 1030–1042. doi: 10.1101/GR.186379.114.

Verdijk, L. B. *et al.* (2014) 'Satellite cells in human skeletal muscle; From birth to old age', *Age*, 36(2), pp. 545–557. doi: 10.1007/s11357-013-9583-2.

Vilchez, D., Saez, I. and Dillin, A. (2014) 'The role of protein clearance mechanisms in organismal ageing and age-related diseases', *Nature Communications*, 5(1), p. 5659. doi: 10.1038/ncomms6659.

Villeponteau, B. (1997) 'The heterochromatin loss model of aging.', *Experimental gerontology*. Exp Gerontol, 32(4–5), pp. 383–94. doi: 10.1016/s0531-5565(96)00155-6.

Visnes, T. *et al.* (2018) 'Small-molecule inhibitor of OGG1 suppresses proinflammatory gene expression and inflammation', *Science*, 362(6416), pp. 834–839. doi: 10.1126/science.aar8048.

Vogt, K. L. *et al.* (2018) 'Priming and de-priming of neutrophil responses in vitro and in vivo', *European Journal of Clinical Investigation*. Blackwell Publishing Ltd, 48. doi: 10.1111/ECI.12967.

Vono, M. *et al.* (2017) 'Neutrophils acquire the capacity for antigen presentation to memory CD4+ T cells in vitro and ex vivo', *Blood*. Content Repository Only!, 129(14), pp. 1991–2001. doi: 10.1182/BLOOD-2016-10-744441.

Voynow, J. A. and Shinbashi, M. (2021) 'Neutrophil Elastase and Chronic Lung Disease', *Biomolecules*. Multidisciplinary Digital Publishing Institute (MDPI), 11(8). doi: 10.3390/BIOM11081065.

Walmsley, S. R. *et al.* (2005) 'Hypoxia-induced neutrophil survival is mediated by HIF-1α–dependent NF-κB activity', *The Journal of Experimental Medicine*. The Rockefeller University Press, 201(1), p. 105. doi: 10.1084/JEM.20040624.

Wang, J. *et al.* (2017) 'Visualizing the function and fate of neutrophils in sterile injury and repair', *Science*. American Association for the Advancement of Science, 358(6359), pp. 111–116. doi: 10.1126/SCIENCE.AAM9690/SUPPL_FILE/AAM9690S9.MP4.

Wang, Y. *et al.* (2021) 'A robust and flexible CRISPR/Cas9-based system for neutrophil-specific gene inactivation in zebrafish', *Journal of Cell Science*. Company of Biologists Ltd, 134(8). doi: 10.1242/jcs.258574.

Wang, Y. and Jönsson, F. (2019) 'Expression, role, and regulation of neutrophil Fcγ receptors', *Frontiers in Immunology*. Frontiers Media S.A., 10(AUG), p. 1958. doi: 10.3389/FIMMU.2019.01958/BIBTEX.

Watanabe, Y. *et al.* (2019) 'Bidirectional crosstalk between neutrophils and adipocytes promotes adipose tissue inflammation', *FASEB Journal*, 33(11), pp. 11821–11835. doi: 10.1096/fj.201900477RR.

Weber, F. C. *et al.* (2015) 'Neutrophils are required for both the sensitization and elicitation phase of contact hypersensitivity', *Journal of Experimental Medicine*. The Rockefeller University Press, 212(1), pp. 15–22. doi: 10.1084/JEM.20130062.

Wenisch, C. *et al.* (2000) 'Effect of age on human neutrophil function', *Journal of Leukocyte Biology*. Federation of American Societies for Experimental Biology, 67(1), pp. 40–45. doi: 10.1002/JLB.67.1.40.

Westerterp, M. *et al.* (2018) 'Cholesterol Efflux Pathways Suppress Inflammasome Activation, NETosis, and Atherogenesis', *Circulation*. Circulation, 138(9), pp. 898–912. doi: 10.1161/CIRCULATIONAHA.117.032636.

Williams, G. C. (1957) 'Pleiotropy, Natural Selection, and the Evolution of Senescence', *Evolution*. Society for the Study of Evolution, 11(4), p. 398. doi: 10.2307/2406060.

Williams, S. Y. and Renquist, B. J. (2016) 'High Throughput Danio Rerio Energy Expenditure Assay', *Journal of Visualized Experiments : JoVE*. MyJoVE Corporation, 2016(107), p. 53297. doi: 10.3791/53297.

Willis, A. R. *et al.* (2018) 'Shigella-Induced Emergency Granulopoiesis Protects Zebrafish Larvae from Secondary Infection'. doi: 10.1128/mBio.00933-18.

Wilson, D. *et al.* (2017) 'Frailty and sarcopenia: The potential role of an aged immune system',

Ageing Research Reviews. Elsevier B.V., 36, pp. 1–10. doi: 10.1016/j.arr.2017.01.006.

Wilson, D. *et al.* (2020) 'Frailty Is Associated with Neutrophil Dysfunction Which Is Correctable with Phosphoinositol-3-Kinase Inhibitors', *Journals of Gerontology - Series A Biological Sciences and Medical Sciences*, 75(12), pp. 2320–2325. doi: 10.1093/gerona/glaa216.

Wong, S. L. *et al.* (2015) 'Diabetes primes neutrophils to undergo NETosis, which impairs wound healing', *Nature medicine*. Nat Med, 21(7), pp. 815–819. doi: 10.1038/NM.3887.

Woodfin, A. *et al.* (2011) 'The junctional adhesion molecule JAM-C regulates polarized transendothelial migration of neutrophils in vivo', *Nature immunology*. Nat Immunol, 12(8), pp. 761–769. doi: 10.1038/NI.2062.

Wright, H. L. *et al.* (2013) 'RNA-Seq Reveals Activation of Both Common and Cytokine-Specific Pathways following Neutrophil Priming', *PLoS ONE*, 8(3). doi: 10.1371/journal.pone.0058598.

Wright, H. L. *et al.* (2017) 'Low-density granulocytes: functionally distinct, immature neutrophils in rheumatoid arthritis with altered properties and defective TNF signalling', *Journal of Leukocyte Biology*, 101(2), pp. 599–611. doi: 10.1189/jlb.5a0116-022r.

Wu, S.-Y. and Chiang, C.-M. (2007) 'The double bromodomain-containing chromatin adaptor Brd4 and transcriptional regulation.', *The Journal of biological chemistry*. J Biol Chem, 282(18), pp. 13141–5. doi: 10.1074/jbc.R700001200.

Wu, Z. *et al.* (2016) 'Heterogeneity of Human Neutrophil CD177 Expression Results from CD177P1 Pseudogene Conversion.', *Plos Genetics*. Public Library of Science, 12(5), pp. e1006067–e1006067. doi: 10.1371/JOURNAL.PGEN.1006067.

Xie, X. *et al.* (2020) 'Single-cell transcriptome profiling reveals neutrophil heterogeneity in homeostasis and infection', *Nature Immunology 2020 21:9*. Nature Publishing Group, 21(9), pp. 1119–1133. doi: 10.1038/s41590-020-0736-z.

Yan, B. *et al.* (2018) 'Histone deacetylase 6 modulates macrophage infiltration during inflammation', *Theranostics*. Theranostics, 8(11), pp. 2927–2938. doi: 10.7150/THNO.25317.

Yan, Q. *et al.* (2014) 'Jmjd3-mediated epigenetic regulation of inflammatory cytokine gene expression in serum amyloid A-stimulated macrophages', *Cellular Signalling*. Pergamon, 26(9), pp. 1783–1791. doi: 10.1016/J.CELLSIG.2014.03.025.

Yanagisawa, S. *et al.* (2009) 'Oxidative stress augments toll-like receptor 8 mediated neutrophilic responses in healthy subjects', *Respiratory Research*. BioMed Central, 10(1), p. 50. doi: 10.1186/1465-9921-10-50.

Yasuda, T. *et al.* (2021) 'Inflammation-driven senescence-associated secretory phenotype in

cancer-associated fibroblasts enhances peritoneal dissemination', *Cell reports*. Cell Rep, 34(8). doi: 10.1016/J.CELREP.2021.108779.

Yatim, K. M. and Lakkis, F. G. (2015) 'A brief journey through the immune system.', *Clinical journal of the American Society of Nephrology : CJASN*. American Society of Nephrology, 10(7), pp. 1274–81. doi: 10.2215/CJN.10031014.

Yildirim-Buharalioğlu, G. *et al.* (2017) 'Regulation of Epigenetic Modifiers, Including KDM6B, by Interferon-γ and Interleukin-4 in Human Macrophages', *Frontiers in immunology*. Front Immunol, 8(FEB). doi: 10.3389/FIMMU.2017.00092.

Yipp, B. G. *et al.* (2012) 'Infection-induced NETosis is a dynamic process involving neutrophil multitasking in vivo', *Nature medicine*. Nat Med, 18(9), pp. 1386–1393. doi: 10.1038/NM.2847.

Yoshizaki, T. *et al.* (2010) 'SIRT1 inhibits inflammatory pathways in macrophages and modulates insulin sensitivity', *American Journal of Physiology - Endocrinology and Metabolism*. American Physiological Society, 298(3), p. E419. doi: 10.1152/AJPENDO.00417.2009.

Zhang, P. *et al.* (2016) 'An Overview of Chromatin-Regulating Proteins in Cells', *Current protein & peptide science*. NIH Public Access, 17(5), p. 401. doi: 10.2174/1389203717666160122120310.

Zhang, Q. and Cao, X. (2019) 'Epigenetic regulation of the innate immune response to infection', *Nature Reviews Immunology 2019 19:7*. Nature Publishing Group, 19(7), pp. 417–432. doi: 10.1038/s41577-019-0151-6.

Zhang, T., Pilko, A. and Wollman, R. (2020) 'Loci specific epigenetic drug sensitivity', *Nucleic Acids Research*, 48(9), p. 4810. doi: 10.1093/nar/gkaa210.

Zheng, Y. *et al.* (2020) 'A human circulating immune cell landscape in aging and COVID-19', *Protein and Cell*, 11(10), pp. 740–770. doi: 10.1007/s13238-020-00762-2.

Zhou, G. X. and Liu, Z. J. (2017) 'Potential roles of neutrophils in regulating intestinal mucosal inflammation of inflammatory bowel disease', *Journal of digestive diseases*. J Dig Dis, 18(9), pp. 495–503. doi: 10.1111/1751-2980.12540.

Zhou, W. *et al.* (2018) *Neutrophil-specific knockout demonstrates a role for mitochondria in regulating neutrophil motility in zebrafish*, *Disease Models & Mechanisms*. doi: 10.1242/dmm.033027.

Zhu, S. *et al.* (2017) 'LMO1 Synergizes with MYCN to Promote Neuroblastoma Initiation and

Metastasis', *Cancer Cell*. Cell Press, 32(3), pp. 310-323.e5. doi: 10.1016/J.CCELL.2017.08.002.
Zimmermann, M. *et al.* (2015) 'Chromatin remodelling and autocrine TNFα are required for optimal interleukin-6 expression in activated human neutrophils', *Nature Communications*. Nature Publishing Group, 6, pp. 1–14. doi: 10.1038/ncomms7061.
Zimmermann, M. *et al.* (2016) 'IFNα enhances the production of IL-6 by human neutrophils activated via TLR8', *Scientific Reports*. Nature Publishing Group, 6. doi: 10.1038/SREP19674.

8. Appendix

8.1. Chapter 3 Appendix

Appendix 3.1. Optimisation of IL-6 RT-qPCR primers by gradient PCR, efficiency curve and melt curve analysis

R848 has been shown *in vitro* to cause chromatin remodelling at the neutrophil *il6* locus to increase production of IL-6 (Zimmerman et al., 2015). Before investigating the chromatin remodelling involved when zebrafish neutrophils are exposed to R848, altered IL-6 expression needed to be confirmed via RT-qPCR when zebrafish are treated with R848. Four pairs of forward and reverse primers for *il6* were designed and first used to amplify *il6* in wild type, untreated zebrafish larval cDNA. Gradient RT-PCR using annealing temperatures based around the primers' T_M value was performed to ensure the primers produced a single amplicon (Figure 3.12A). Primer pairs 2 and 3 produced no bands so were discarded. Primer pair 1 produced a single amplicon and the strongest band was at 57^OC. This annealing temperature was used for the RT-qPCR. RT-qPCR was optimised by performing, in triplicate, five dilutions of cDNA (1:5, 1:10, 1:20, 1:50 and 1:100) and an efficiency curve and melt curve generated (Figure 3.12D(i) and 3.12D(ii)). This produced an efficiency curve with a score of 80% and a melt curve with several consistent peaks. Due to the several peaks on the melt curve, primer pair 4 was also tested as above as it produced a single amplicon which showed the strongest band at 55^OC annealing temperature (Figure 3.12C). Primer pair 4 was tested by RT-qPCR which gave an efficiency score of 128% and multiple inconsistent peaks on the melt curve (Figure 3.12E(i) and (ii)) For both primer pairs, rsp29 was used as a housekeeping gene. Melt curve analysis shows a consistent single peak showing the cDNA was suitable for the experiment (Figures 4.12F(i) and (ii)). The multiple consistent peaks in Figure 4.13E(ii) and F(ii) are likely due to high G-C content causing the amplicon to denature in stages during melt curve analysis, especially when taken with the single amplicon shown by RT-PCR in Figure 4.12B, rather than non-specific primer pairing. IL-6 primer pair 1 was chosen as the most reliable and consistent primer pair.

A

	Forward	Reverse
IL-6 primer pair 1	ATCCGCTCAGAAAACAGTGCT	CCATACTGCTGAACACGGGG
IL-6 primer pair 2	GACGGCATTTGAAGGGGTCA	GCGTTAGACATCTTTCCGTGCT
IL-6 primer pair 3	ATGCCATCCGCTCAGAAAACA	CCCATACTGCTGAACACGGG
IL-6 primer pair 4	TCCGCTCAGAAAACAGTGCTAT	TCCGCTCAGAAAACAGTGCTAT

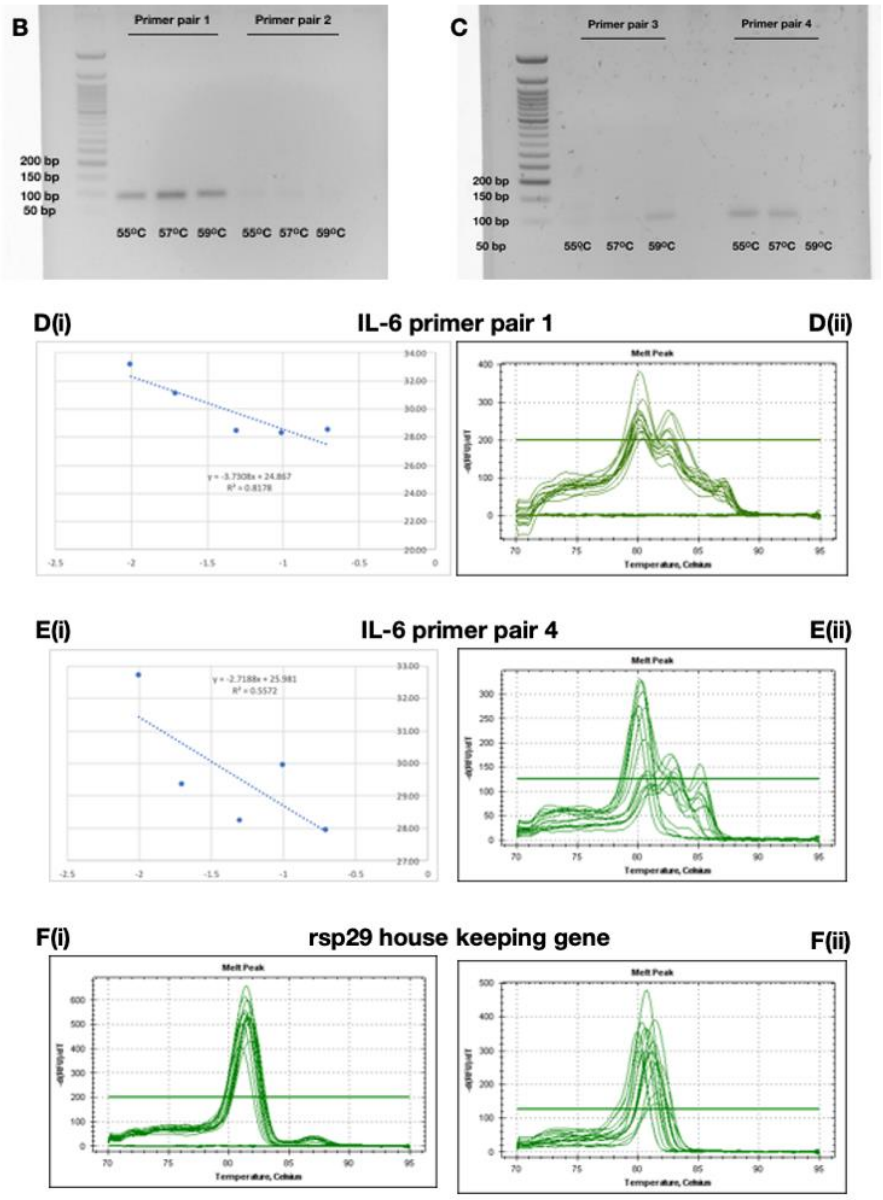

Appendix Figure 3.1: Optimisation of IL-6 qPCR primers pairs for quantification of IL-6 expression

(A) Forward and reverse primer sequences designed using primer3 shown 5'-3' (B,C) 1% agarose gel of PCR products run at gradient temperatures (listed below the blots) to optimise primer pairs 1, 2, 3 and 4. (D(i)) Efficiency graph for primer pair 1 plotting the Ct value against the Log_{10}(dilution cDNA) (Dii) Melt curve for primer pair 1 (E(i)) Efficiency graph for primer pair 4 plotting the Ct value against the Log_{10}(dilution cDNA) (E(ii) Melt curve for primer pair

1. (F(i)) Melt curve analysis for the housekeeping gene rsp29 used for primer pair 1. (F(ii)) Melt curve analysis for housekeeping gene rsp29 used for primer pair 4

Appendix 3.2. Incubation with C646 and R848 in combination significantly reduces inflammation resolution

The previous experiments have confirmed that R848 can act on zebrafish neutrophils by several of the same pathways seen *in vitro*. However, the effects of R848 on zebrafish neutrophil chromatin remodelling enzymes has not yet been explored. To investigate what chromatin remodelling pathways may be involved, 3 dpf zebrafish larvae were injured at the tailfin and treated with C646 (an EP300/ CREBBP inhibitor) 4 hpi and neutrophil inflammation resolution observed 8 and 24 hpi. EP300 and CREBPP were shown by Zimmermann *et al.*, (2015) to be essential chromatin remodelling enzymes in R848 dependent transcriptional changes in human neutrophils. Inhibition of the EP300/ CREBBP pathway and consequential changes in neutrophil phenotype would further confirm that R848 acted on zebrafish neutrophils by the same pathways as human neutrophils *in vitro*. Treatment of injured zebrafish larvae with C646 in isolation, showed no significant changes compared to the control (Figure 3.14A). On the other hand, treatment with R848 showed a significant increase in the number of neutrophils at the wound site 8 hpi from 30 to 36 ($p=0.0496$, two-way ANOVA with Tukey's multiple comparison test). Treatment with C646 and R848 in combination showed a significant increase in the number of neutrophils present at the wound site relative to the control from 16 to 21 ($p=0.0115$, two-way ANOVA with Tukey's multiple comparison test), suggesting a delay in inflammation resolution. These data suggest that the EP300/ CREBBP pathway is only contributing to neutrophil phenotype when exposed to R848 and not in homeostatic function in these assays. This is further supported by the neutrophil kinetics data presented by the percentage change in neutrophils between 8 and 24 hpi (Figure 3.14B). Combination treatment of R848 and C646 shows a significant decrease in percentage change to 28.2% compared to the control of 47.5% ($p=0.0087$) and treatment with R848 and C646 in isolation, 46.5% ($p=0.0122$)and 44.4% ($p=0.0429$) respectively (Two-way ANOVA with Sidak's multiple comparison test). Taken in combination, these data tentatively suggest that R848 operates in zebrafish neutrophils to accelerate inflammation resolution via the EP300/ CREBBP pathway. However, as the R848 dependent changes seen in Figure 3.4 are not confirmed in these experiments, this needs further investigation to make a definitive conclusion.

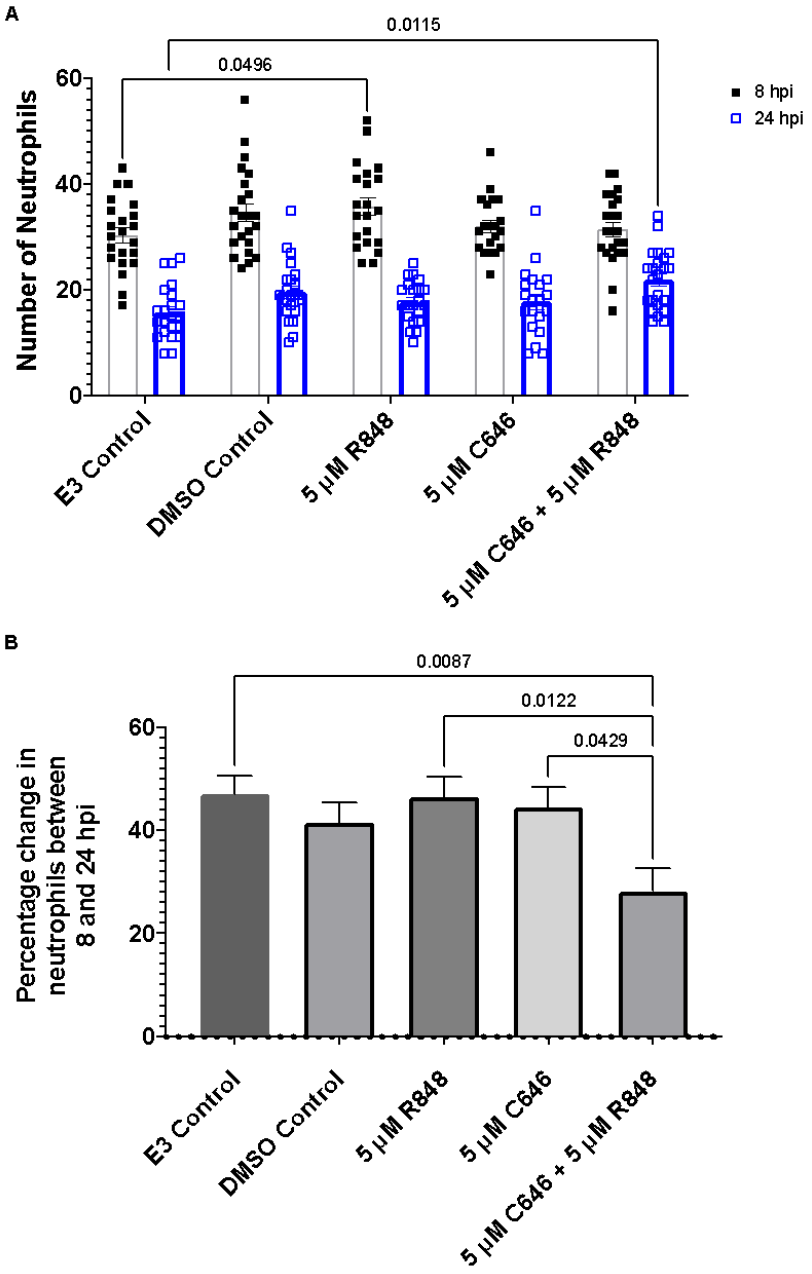

Appendix Figure 3.2. In combination with R848, inhibition of EP300 and CREBBP by C646 significantly reduces neutrophil inflammation resolution and neutrophil kinetics 24 hpi

(A) Number of neutrophils at the wound 8 and 24 hpi in injured zebrafish larvae with combinations of 5 µM of R848 and 5 µM C646 and an E3 only control (3 independent repeats, ±SEM, minimum 19 fish per group, Two-way ANOVA with Tukey's multiple comparison test). (E) Percentage change in neutrophils at the wound between 8 and 24 hpi comparing larvae treated with combinations of 5 µM of R848 and 5 µM C646 and an E3 only control (3 independent repeats, ± SEM, minimum 19 fish per group, Two-way ANOVA with Sidak's multiple comparison test)

Appendix 3.3. SIRT1 inhibition significantly increases neutrophil recruitment to the tailfin 3 hpi

The chromatin remodelling enzyme, SIRT1, is a histone deacetylase associated with ageing and inflammation related functions including macrophage function, DNA-damage signalling, cancer, and in a zebrafish model chronic inflammation and regeneration (Yoshizaki *et al.*, 2010; Imperatore *et al.*, 2017; Alves-Fernandes and Jasiulionis, 2019; D. H. Kim *et al.*, 2019; Pardo and Boriek, 2020). EX527 is a SIRT1 inhibitor, which has been shown to alter chromatin remodelling enzymes, but has not been used *in vivo* in zebrafish to observe changes in neutrophil phenotype. These compounds are of interest here as they may hold the key to the pathways that control neutrophil function. Here, neutrophil recruitment to a tailfin injury in 3 dpf *TgBAC(mpx:EGFP)i114* zebrafish larvae was observed following treatment with 50 µM EX527. Neutrophils at the wound were counted 3 and 6 hpi using a fluorescent wide-field microscope by SSC placement student Samuel Evans under my supervision. EX527 significantly increased the number of neutrophils at the wound 3 hpi with an average number of neutrophils at 33 compared to 25 in the control ($p=0.0226$, Mixed effects analysis with Sidak's multiple comparisons) (Figure 3.15A). These data suggest that inhibitors of SIRT1 increase either the speed that neutrophils are recruited to the wound following initial injury or can recruit larger numbers over a shorter period, potentially by increasing pro-inflammatory signalling. This effect is only short lived however, as the increase is not significant 6 hpi and there is no change in neutrophil kinetics between 3 and 6 hpi (Figure 3.15B).

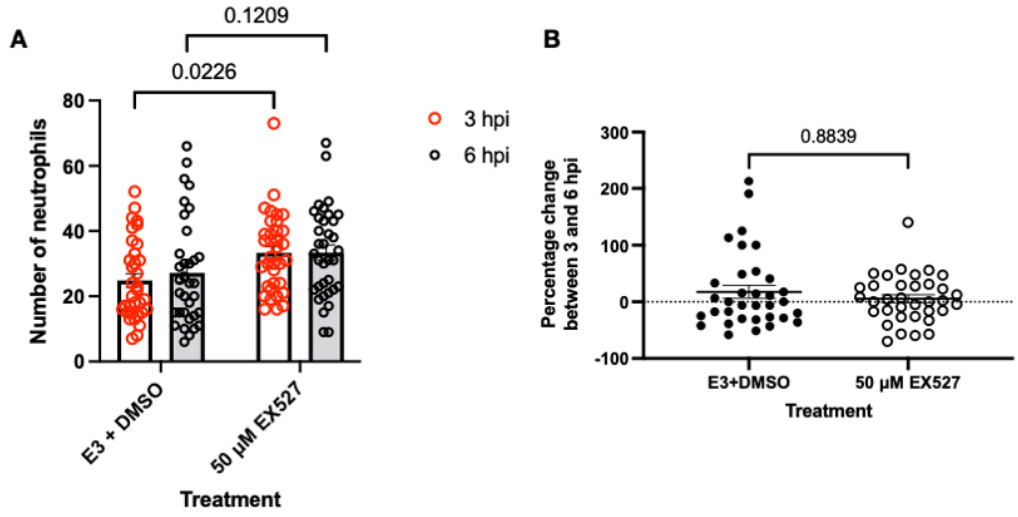

Appendix Figure 3.3. The SIRT1 inhibitor, EX527, significantly increases the recruitment of neutrophils to the injured zebrafish tailfin, 3 hpi

(A) Number of neutrophils at the wound 3 and 6 hpi in injured zebrafish larvae with 50 µM of EX527 and an E3 only control (3 independent repeats, ±SEM, minimum 34 fish per group, Mixed effects analysis with Sidak's multiple comparisons). (B) Percentage change in neutrophils at the wound 3 and 6 hpi in injured zebrafish larvae with 50 µM of EX527 and an E3 only control (3 independent repeats, ±SEM, minimum 34 fish per group, Mann-Whitney test following Shapiro-Wilks test for normality)

Appendix 3.4. R848/C646 Discussion

The mechanism of action of R848 involves chromatin remodelling enzymes adding modifications to histones that alter the conformation of the *il6* locus to allow for transcription factor binding and gene transcription (Zimmermann *et al.*, 2015). C646 inhibits both histone acetyltransferases EP300 and CREBBP, which are recruited to the IL-6 locus on stimulation with R848. Zimmerman *et al.,* (2015) used C646 to attenuate the effects of R848 on *in vitro* human neutrophils. *In vivo*, where zebrafish larvae were incubated with C646 and R848, the combined treatment only significantly reduced inflammation resolution relative to the untreated control and had no effect relative to single drug treatment. Combined treatment however did have a significant effect on neutrophil kinetics relative to the larvae treated with the single drugs. These data therefore cannot confirm that changes to neutrophil number when larvae are treated with R848 are down to chromatin remodelling events but do confirm that changes to neutrophil kinetics seen during inflammation resolution are dependent on EP300 and CREBBP. It is also worth highlighting that previously observed R848 effects on inflammation resolution have not been reproducible here. Because of the genome duplication in zebrafish causing TLR8 to have three zebrafish paralogs and combined with the fact the *in vivo* ligand for zebrafish TLR8 is unknown the exact interactions that relate to EP300/CREBBP are unclear (Chen *et al.*, 2021). R848 may only bind one TLR8 paralog and how TLRs interact with EP300/CREBBP is unknown. Zebrafish also have two paralogs of *ep300* and *crebbp*, and it has not been confirmed that C646 can target both or either, however, previous studies have shown that C646 can alter other processes in zebrafish (Babu *et al.*, 2018; Shimizu and Kawasaki, 2021) but not in the context of zebrafish immunity. The specificity of TLR/enzyme paralog interactions could explain why a change in kinetics, but not neutrophil number, is seen as a specific paralog may modify the loci of genes associated with kinetics and alter recruitment/inflammation resolution. Further characterisation of both TLR paralogs and chromatin remodelling enzyme paralogs including receptor sites and binding sequences can help to answer these questions. The lack of understanding of these interactions shows why increased study of chromatin remodelling in neutrophil function using a zebrafish model is required. Continuing work has furthered the understanding of how TLR8 activation by R848 in human neutrophils alters gene expression, chromatin remodelling and transcription factor binding, recently identifying OCT2 as another transcription factor of interest, binding crucial enhancers along with known factors AP-1, PU.1 and NF-κB (Tamassia *et al.*, 2021). The RNA

sequencing produced allows for increased panels of genes to investigate by qRT-PCR in zebrafish neutrophils, modifications to investigate using ChIP, and finally, CRISPR targets for knockdown – a technique that cannot be used in human neutrophils.

Appendix 3.5. Sirt1 discussion

To further explore other chromatin remodelling enzymes and pathways, the SIRT1 inhibitor EX527 was added to larval zebrafish Inhibition of *sirt1* caused a significant increase in the number of neutrophils recruited to the wound during the initiation phase of inflammation. Little is known about the role of SIRT1 in neutrophils and particularly in zebrafish neutrophils. As this was a drug treatment and not a targeted knockdown, the changes in neutrophil number may not be down to neutrophil-specific changes. However, work using a *sirt1* homozygous mutant zebrafish line may be able to explain why changes in neutrophil recruitment are seen (D. H. Kim *et al.*, 2019). qRT-PCR analysis of the knockout larvae showed a whole-body up regulation of pro-inflammatory genes including *il1b, tnfa, il6* and *il8*. This would explain why neutrophils are recruited at a higher number in the drug treated group, as the *sirt1*$^{-/-}$ pro-inflammatory environment would promote this, though there may be some alterations on directed recruitment if the whole body is showing systemic inflammation. Performing qRT-PCR on larvae treated with the inhibitor will help answer this and specific analysis of the neutrophils from these larvae will help to determine whether the changes are due to neutrophil-specific changes or changes to the neutrophil microenvironment. Collectively, it enhances the case for the ability to alter zebrafish neutrophil using chemical epigenetic modifiers.

8.2. Chapter 4 Appendix

Appendix 4.1. CRISPR/Cas9 targeting chromatin remodelling enzymes in the R848 pathway

CRISPR/Cas9 presents a quick and easy way to alter gene expression in zebrafish larvae. Published literature can provide easily selectable targets for knockdown that can be quickly optimised and injected into embryos. As part of their work with R848, Zimmerman *et al.* (2015) identified several chromatin remodelling enzymes that were involved in the process of remodelling at the *il6* locus on addition of R848. These were CRB and P300 – now more widely referred to as CREPPB and EP300, and BRD4. crRNAs to target these genes were designed using the website CHOPCHOP. CREBBP and EP300 both have paralogues in the zebrafish genome, for this work *crebbpa* and *ep300a* were chosen. The 5'UTR and promoter sequences of the genes were chosen as the target regions with the view to set up a cell-specific CRISPR interference, a project that was later abandoned in favour of neutrophil-specific CRISPR. Figure 4.1A-C shows the target sites of the crRNAs, primer pairs and restriction enzymes selected for diagnostic digest. Confirmation of primer action was tested using uninjected, 3 dpf *TgBAC(mpx:EGFP)i114* larvae gDNA amplifying the target sequence via RT-PCR at 52˚C annealing temperature. Bright bands were seen for all three primer pairs and primers were deemed to be suitable for a test digest (Figure 4.1D). The test digest was performed for 4 hours and showed full digest for the *ep300a* amplicon and *crebbpa* amplicon and almost full digest for the brd4 amplicon, with a 224 bp band visible (Figure 4.1E, smaller bands in the digest are highlighted with black boxes). The primers and restriction enzymes were efficient enough to be used for diagnostic digest following single-cell injection.

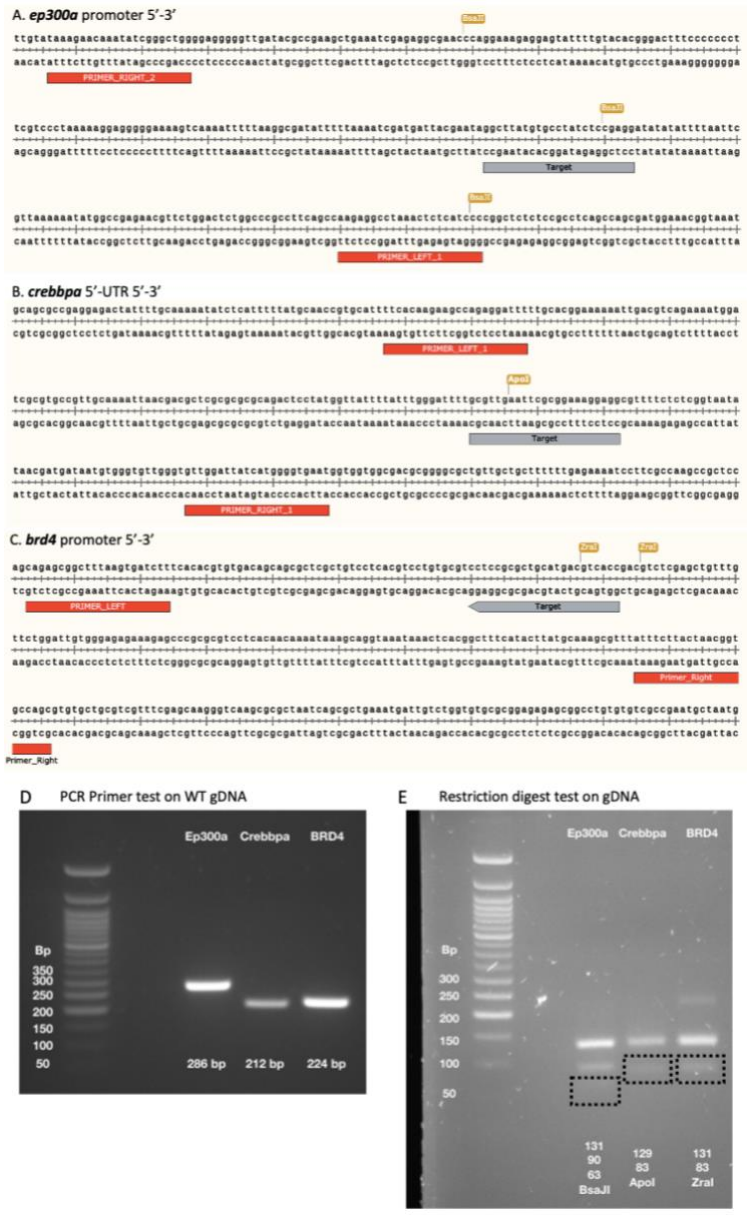

Appendix Figure 4.1. Sequences and primer tests for R848 pathway associated chromatin remodelling enzymes

(A-C) Cropped crRNA target sequences with 5'-3' sense strand on top created in Snapgene with enzyme and site above, crRNA target in grey, primers in red and digest sites above sequence (D) 2% agarose gel showing gDNA amplified by PCR from 3 dpf zebrafish larvae (E) 3% agarose gel showing gDNA digested for 4 hours at enzyme specific temperatures Both D and E use NEB Quick-load 50 bp DNA ladder, labels show enzymes targeted for amplification and expected product sizes including restriction enzyme and sizes with small bands highlighted in black

Appendix 4.2. Single-cell injection of CRISPR targeting the R848 chromatin remodelling enzymes *crebbpa*, *ep300a* and *brd4*

Single-cell injection was optimised by diagnostic digest following injection of 0.5, 1 and 2 nl of crRNA mix. Diagnostic digest was performed with the addition of non-injected *TgBAC(mpx:EGFP)i114* controls for just the RT-PCR and the PCR and digest. The diagnostic digest for the *ep300a* amplicon showed full digest of all eight injected larvae gDNA with a clear 256 bp band in the uninjected/undigested control showing correct amplification of the target fragment, however no amplicon was seen in the digested control (Figure 4.2A). Injection of the crebbpa crRNA lead to a large rate of larval death and only one larva could be saved for gDNA extraction. This larva showed full digestion, but that may be because all larvae with successful knockdown died. Controls showed a correct but faint 192 bp band in the uninjected/undigested control and faint full digestion bands in the digested control (Figure 4.2B). Digest of the *brd4* crRNA injected larvae showed partial digestion across all 7/8 larvae, with the final larvae showing no bands. However, in the digested control, there is also partial digestion, suggesting this is due to a short incubation time and not successful knockdown of the *brd4* target fragment. The uninjected/undigested control has the correct 224 bp band. Overall, these guides seem to be ineffective and new targets need to be found to continue.

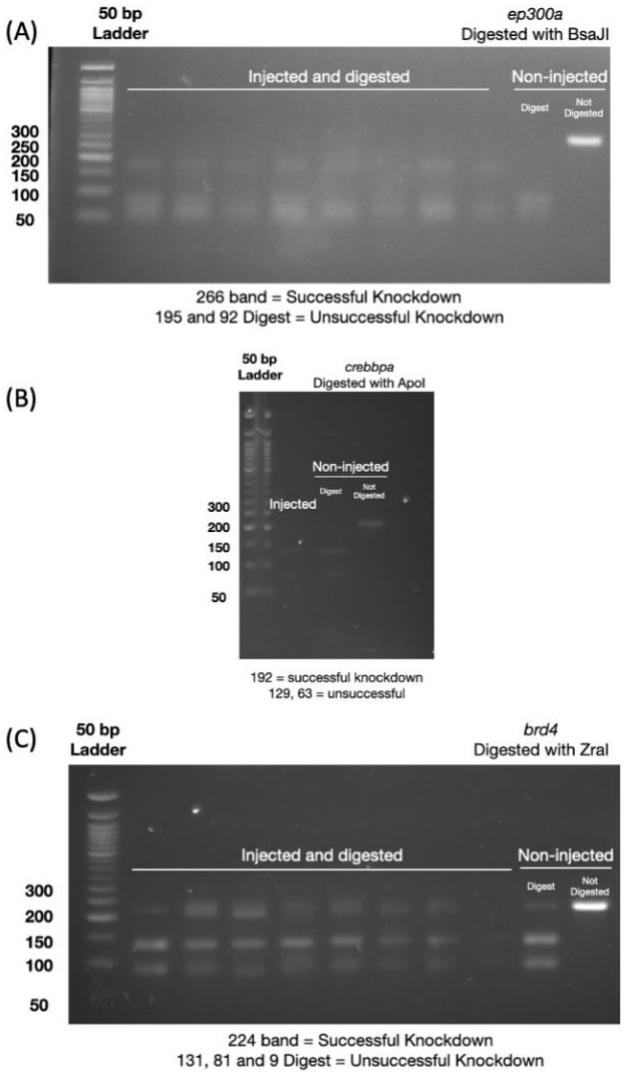

Appendix Figure 4.2. Diagnostic digest for efficiency of crRNAs for chromatin remodelling enzymes implemented in the R848 pathways

2% Agarose gels of gDNA from 3 dpf larvae injected with 2 nl crRNA mixes targeting (A) *ep300a* digested with BsaJI (B) *crebbpa* digested with ApoI and (C) *brd4* digested with ZraI, all with an uninjected TgBAC(mpx:EGFP)i114 control with and without digest. Fragment sizes for knockdown vs. no knockdown listed below each gel.

Appendix 4.3. Optimisation of CRISPR/Cas9 guides for newly selected chromatin remodelling enzymes

From the list of nine chromatin remodelling enzymes initially selected, five were selected for initial attempts at knockdown. Again, guides were designed in the 5'UTR with a view to future attempt cell specific CRISPRi. The zebrafish a and b paralogs for brd2 were both chosen but only the b paralog of *kdm6b* due to the annotation of the datasets making it hard to distinguish between a and b (A problem resolved for later analysis and reflected in the presentation of RPKM values for *kdm6ba* and *kdm6bb* in Figure 4.4C). Primer pairs were designed around the target site and restriction enzymes that cut in the crRNA target site chosen from diagnostic digest (Figure 4.5A-F). Primers were tested on uninjected 3 dpf *TgBAC(mpx:EGFP)i114* gDNA and digests performed using the corresponding restriction enzyme All primer pairs showed full digestion, apart from the hdac6 primer pair that showed a full 275 bp band only and sit6, that showed partial digestion only (Figure 4.5F). Amplification of the hdac6 sequence was performed again and digest performed again, a full-size band was seen in the undigested and faint digest bands shown in the AluI treated sample (Figure 4.5G). Diagnostic digest of gDNA from injected embryos showed full digestion, and therefore unsuccessful knockdown in brd2b, hdac6, dot1l, sirt6 and kdm6b targeting guides (Figure 4.6B-E). The brd2a guide showed partial digestion but due to the lack of a digested control, it is difficult to tell if that is due to weak knockdown, or insufficient digest (Figure 4.6A).

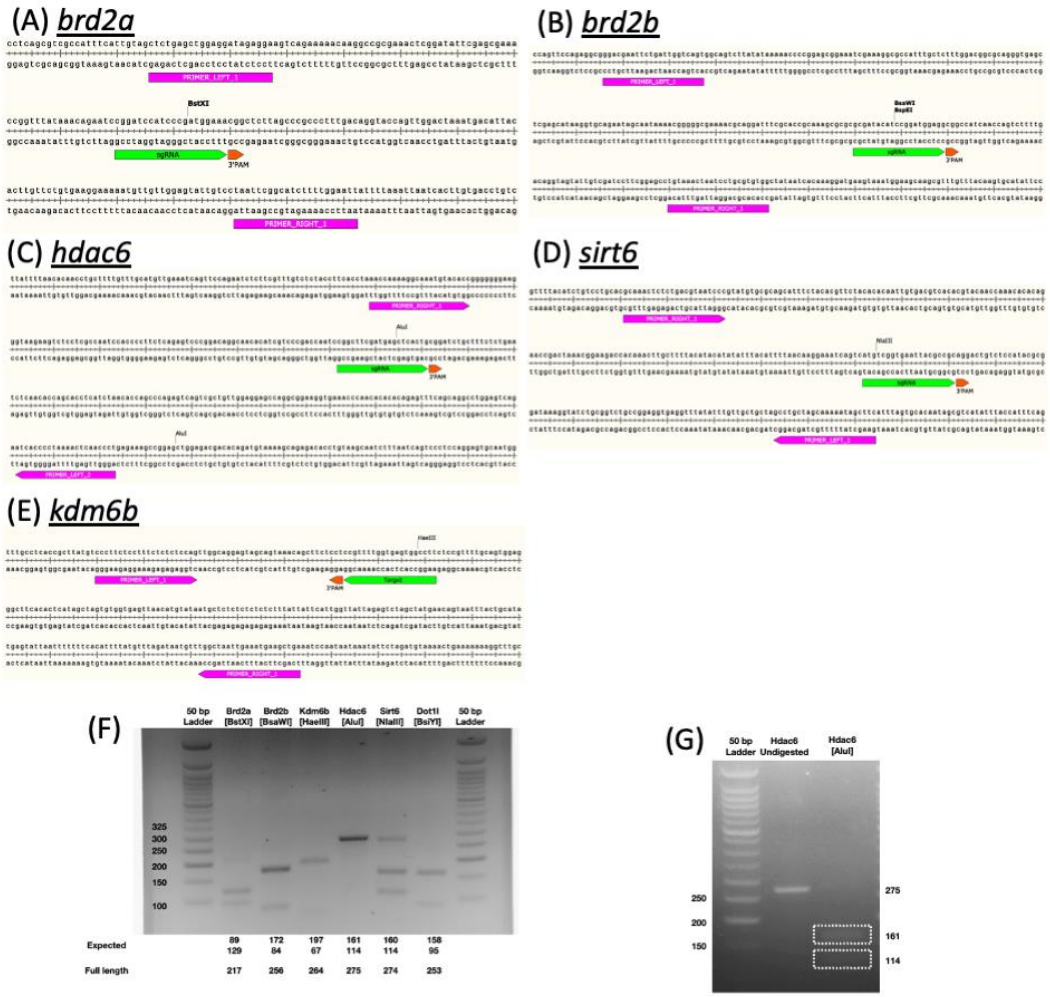

Appendix Figure 4.3. crRNA target sites for promoters or 5'UTRs of chromatin remodelling enzymes and testing of primers

(A-E) Target sequences of crRNAs designed by CHOPCHOP transferred to SnapGene and annotated with crRNA in green, 3'UTR in orange and primer sequences in magenta, arrows show direction and restriction digest cut site labelled. (F) 2% Agarose gel of PCR and digest product from uninjected TgBAC(mpx:EGFP)i114 embryos to test primer and enzymatic digest. Enzymes show in square brackets and product sizes below. NEB 50 bp Quick-load ladder used and annotated for relevant sizes. Colours inverted on the gel for better resolution. (G) 2% Agarose gel of PCR PCR and digest product from uninjected TgBAC(mpx:EGFP)i114 embryos to test primer and enzymatic digest for hdac6 with AluI, as the digest was not successful in F. NEB 50 bp Quick-load ladder used and annotated for relevant sizes and expected band sizes shown on the right side. Faint digested bands highlighted with white boxes.

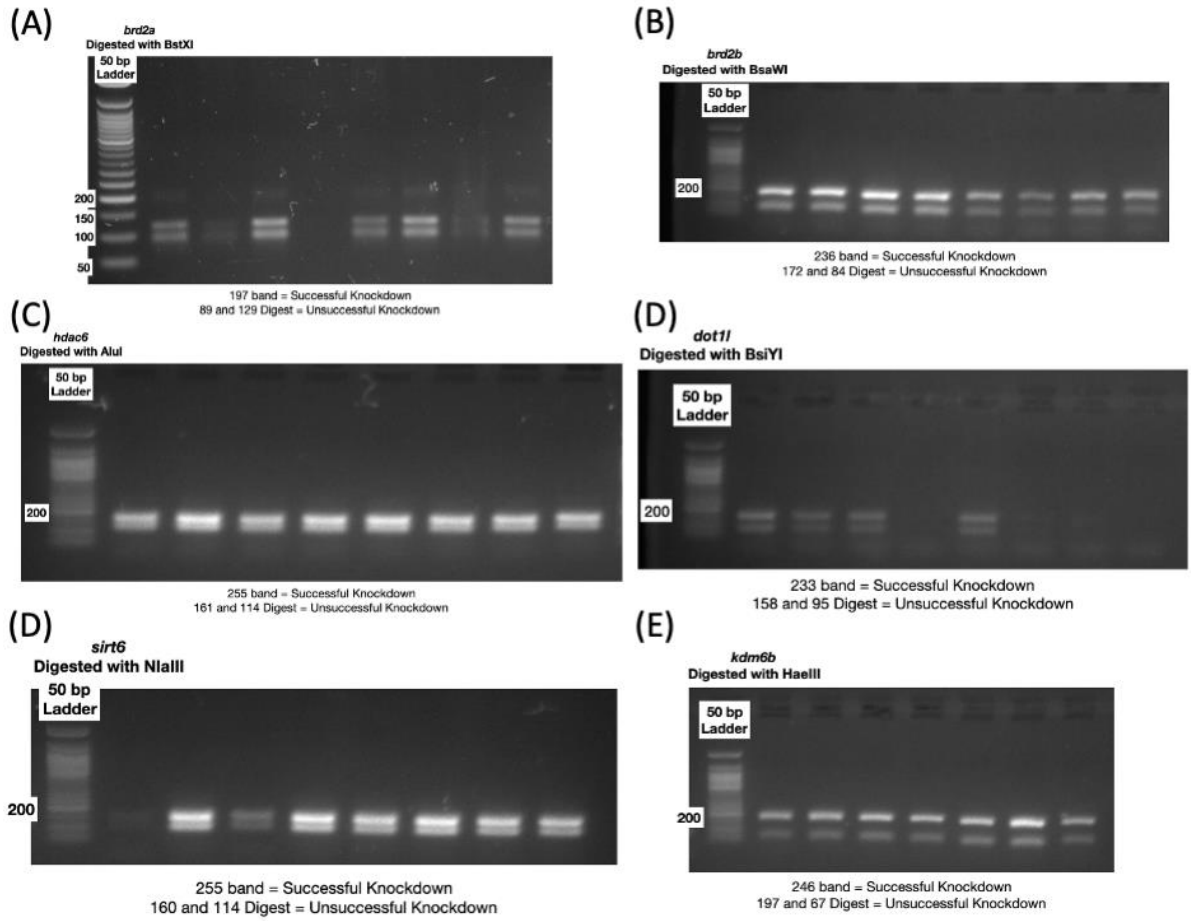

Appendix Figure 4.4. Diagnostic digest of PCR product from gDNA of embryos injected with 5'UTR/promoter crRNAs

(A-F) 2% Agarose gels of digested PCR product from 8 individual embryos injected with 2 nl single crRNA/Cas9 mixture. crRNA target and restriction enzyme listed above each gel. Expected band sizes shown below each gel, PCR product digested overnight at restriction enzyme specific temperature. All ladders are NEB Quick-load 50 bp DNA ladder, 200 bp band annotated.

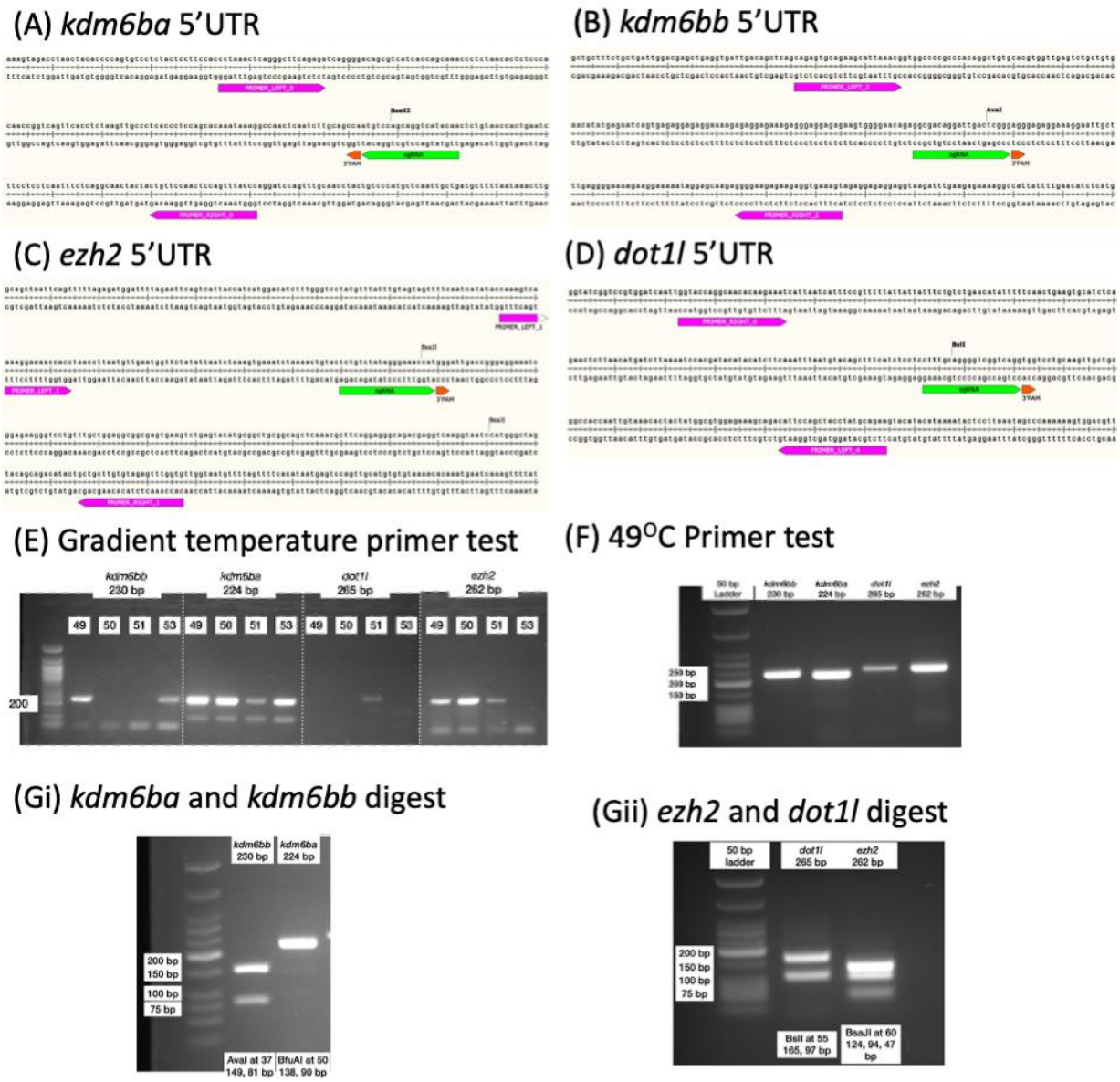

Appendix Figure 4.5. crRNA target sites for 5'UTRs of chromatin remodelling enzymes and testing of primers

(A-D) Target sequences of crRNAs designed by CHOPCHOP transferred to SnapGene and annotated with crRNA in green, 3'UTR in orange and primer sequences in magenta, arrows show direction and restriction digest cut site labelled. (E) 2% Agarose gel of TgBAC(mpx:EPF)i114 3 dpf embryo gDNA amplified by gradient temperature RT-PCR to test primer action. Amplified 5'UTR shown above the with expected band sizes, temperature shown above each lane. Ezh2 samples added from separate image. (F) 2% Agarose gel of TgBAC(mpx:EPF)i114 3 dpf embryo gDNA amplified by 49^{O}C RT-PCR. Amplified 5'UTR shown above the with expected band sizes above each lane. NEB Quick-load 50 bp ladder with

relevant bands labelled. (G) 2% Agarose gel showing products of test digests for restrictions enzymes to perform diagnostic digest. (I) Shows digests for kdm6ba and kdm6bb crRNA diagnostic digest (ii) shows digests for ezh2 and dot1l diagnostic digests. Labels above each lane shows corresponding gene to the targeted 5'UTR and undigested band sizes. Labels below show the restriction enzyme, digestion temperature and expected band sizes. All gels used the NEB Quick-load 50 bp ladder with relevant bands labelled.

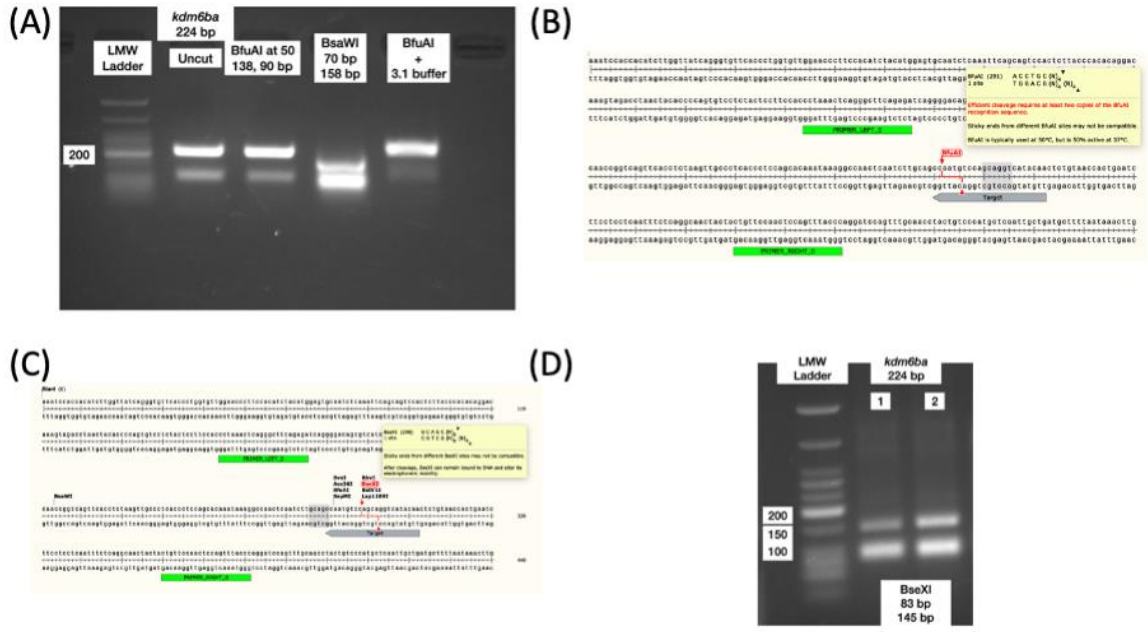

Appendix Figure 4.6. Optimising a diagnostic digest for the *kdm6ba* 5'UTR crRNA

(A) 2% Agarose gel of RT-PCR products of digests to confirm for correct product amplification and digestion. Uncut product was used to confirm the reaction was occurring. BfuAI was used as before and with NEB 3.1 reaction buffer to see if a change in reaction conditions could rectify the issue, and BsaWI used as an enzyme that can cut in the PCR fragment to ensure a digest can occur (B) SnapGene screen shot showing BfuAI as a Type II restriction enzyme (C) SnapGene screenshot showing BSexI is an alternative for diagnostic digest. (D) 2% Agarose gel of RT-PCR products amplifying the kdm6ba 5'UTR in 3 dpf *TgBAC(mpx:EPF)i114* embryo gDNA digested with BSexI, two technical repeats shown. Undigested fragment size shown above lanes and digested fragments shown below. NEB Quick-load LMW ladder used, and relevant bands labelled.

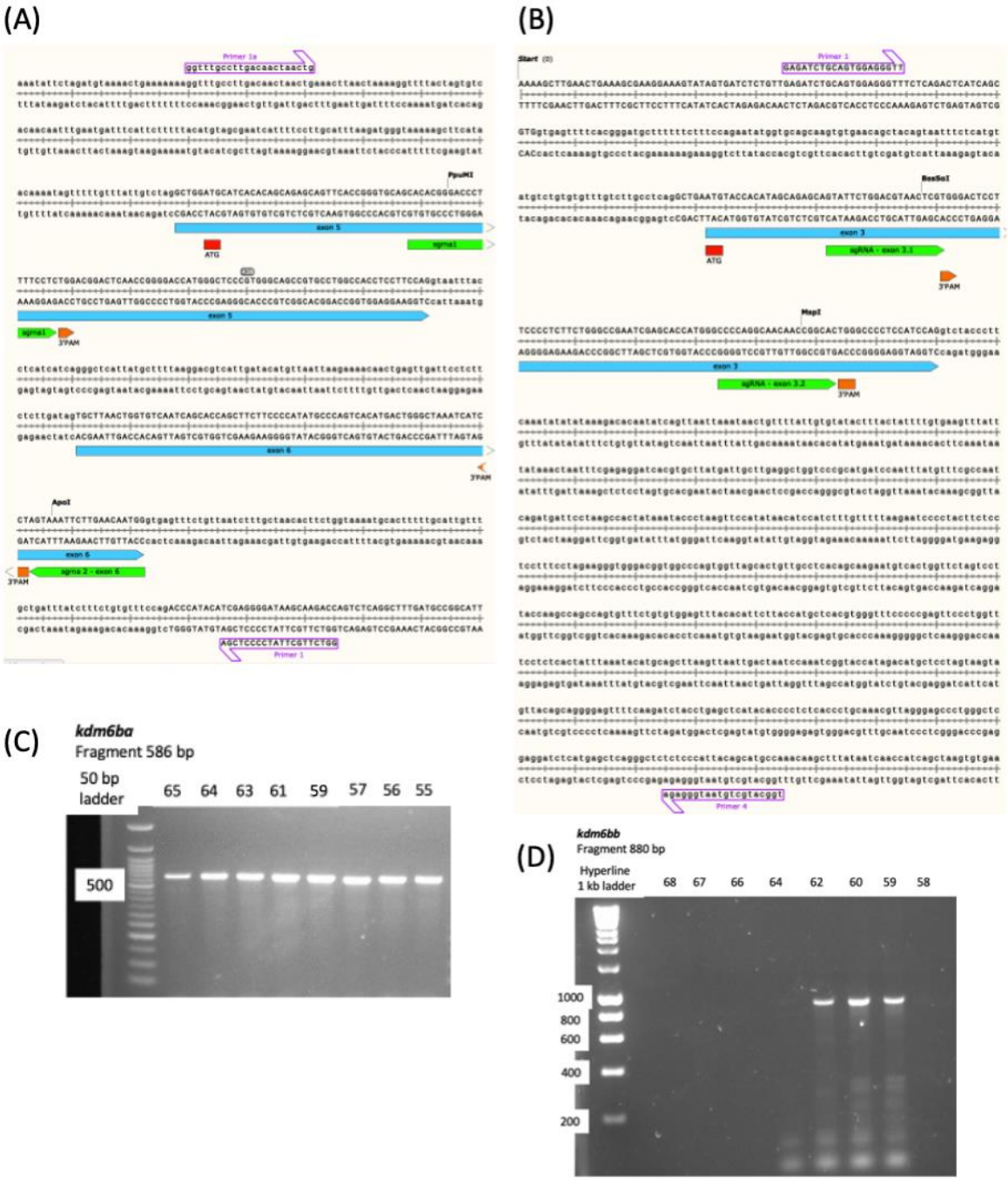

Appendix Figure 4.7. kdm6ba and kdm6bb coding sequence targeting crRNAs and primer optimisation

(A) Sequence from the 5'UTR, transcriptional start site (ATG red) and first two coding exons (blue) of kdm6ba showing the two crRNA target sites (green) and primers (purple) and restriction enzyme cut sites (label above crRNA target) used for diagnostic digest of knockdown (B) Sequence from the 5'UTR, transcriptional start site (ATG red) and first coding exon of kdm6ba showing the two crRNA target sites (green) and primers (purple) and

restriction enzyme cut site (label above crRNA target) used for diagnostic digest of knockdown (C) 2% Agarose gel showing samples from a temperature gradient (temperatures shown above lanes) RT-PCR to test the efficiency of the kdm6ba primers using a NEB Quick-load 50 bp DNA ladder with relevant ladder bands shown, 586 bp band required (D) 2% Agarose gel showing samples from a temperature gradient (temperatures shown above lanes) RT-PCR to test the efficiency of the kdm6bb primers using a Hyperline 1 kb ladder with relevant ladder bands labelled, 880 bp band required.

8.3. Chapter 5 Appendix

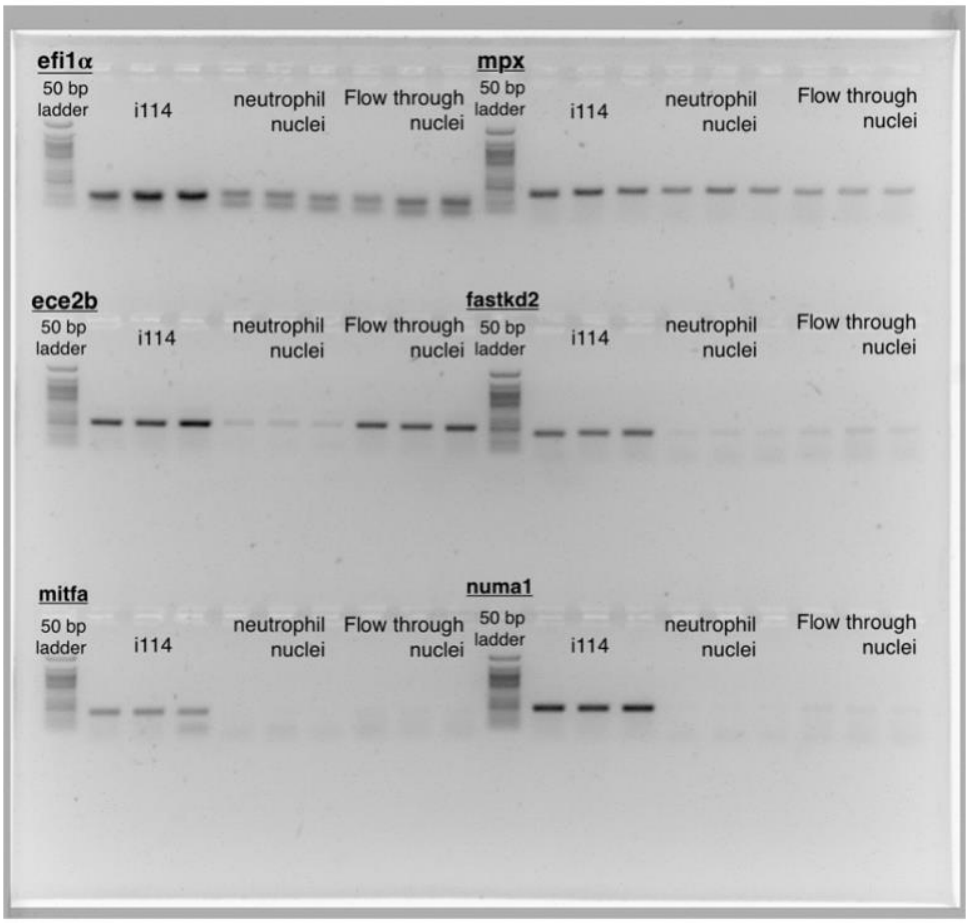

Appendix Figure 5.1. Optimisation of primers for analysis of INTACT pulldown products

2% Agarose gel of RT-PCR amplified genes to optimise the INTACT pulldown product. *ef1a* is used as a housekeeping gene, *mpx* is neutrophil specific, and *ece2b, fastkd2, mitfa* and *numa1* are not present in neutrophils. Flow-through nuclei cDNA is the flow-through excess of the pulldown, Neutrophil nuclei cDNA is the INTACT extracted product and i114 denotes cDNA is taken from age-matched untreated TgBAC(mpx:EGFP)i114 larvae. All samples were amplified and run on the gel as three technical replicates.

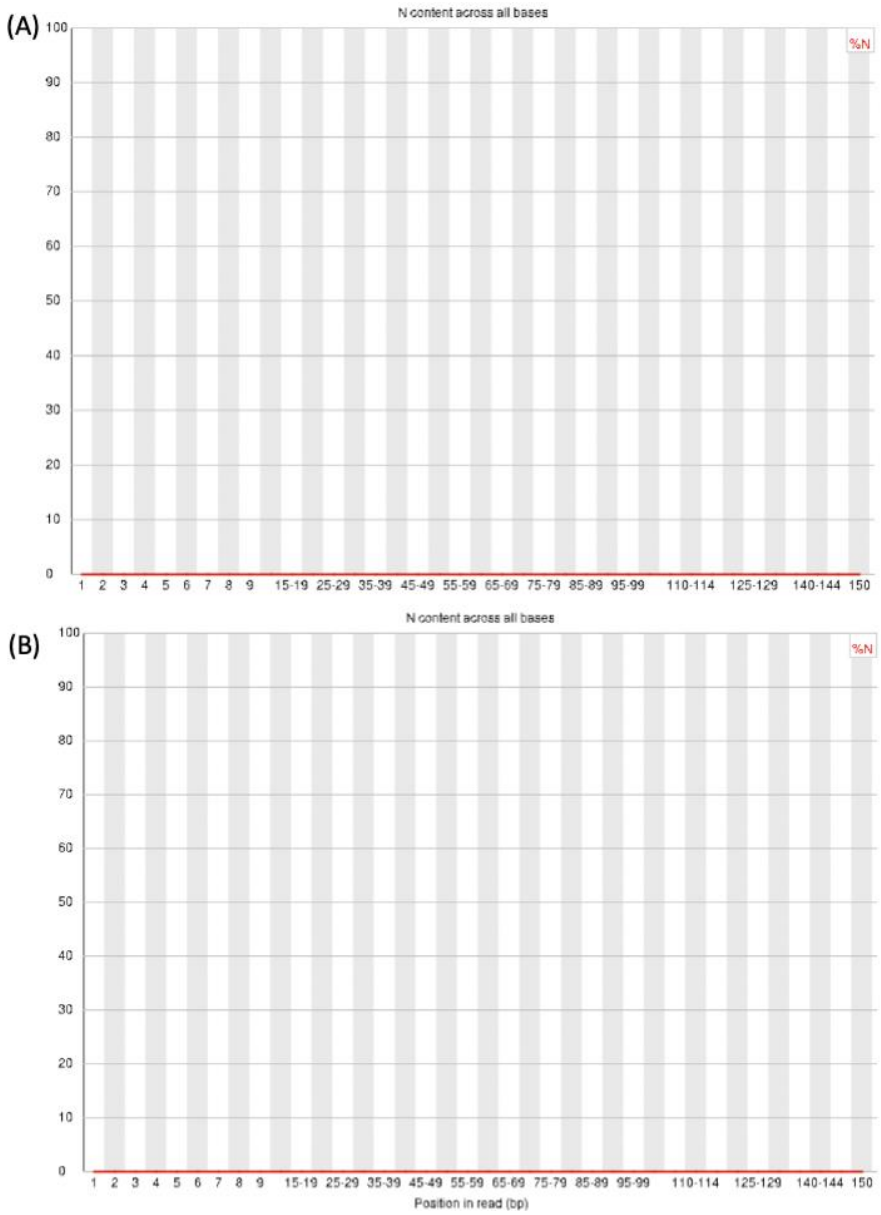

Appendix Figure 5.2. Missed reads in bioinformatics.

(A) If the sequencing instrument was unable to determine a base it substitutes it with an N instead of a conventional base. The plot shows the relative number of Ns compared to the overall number of bases called along each position in the reads derived from the forward primer and (B) reverse primer. The proportion of Ns is usually very low < 5%. Higher numbers might indicate a problem with the sample/library or sequencing reagents.